

Twenty years of structure research on quasicrystals. Part I. Pentagonal, octagonal, decagonal and dodecagonal quasicrystals

Walter Steurer*

Laboratory of Crystallography, Department of Materials, ETH Zurich and MNF, University of Zurich, CH-8092 Zurich, Switzerland

Received November 11, 2003; accepted February 6, 2004

*Pentagonal quasicrystals / Octagonal quasicrystals /
Decagonal quasicrystals / Dodecagonal quasicrystals /
Quasicrystal structure analysis*

Contents

1 Introduction	391
2 Occurrence of axial quasicrystals	392
3 Crystallographic description of axial quasicrystals	393
3.1 Pentagonal phases	395
3.2 Octagonal phases	395
3.3 Decagonal phases	396
3.4 Dodecagonal phases	397
4 Limits and potentialities of methods for quasicrystal structure analysis	398
5 The structure of axial quasicrystals	401
5.1 Octagonal phases	402
5.2 Decagonal phases	403
5.2.1 4 Å and 8 Å periodicity	406
5.2.1.1 Al–Co	406
5.2.1.2 Al–Ni	407
5.2.1.3 Al–Co–Cu	408
5.2.1.4 Al–Co–Ni	411
5.2.1.5 Al–Co–Pd	421
5.2.1.6 Al–Fe–Ni	422
5.2.1.7 Al–Me1–Me2 (Me1 = Cu, Ni, Me2 = Rh, Ir)	423
5.2.1.8 Zn–Mg–RE (RE = Y, Dy, Ho, Er, Tm, Lu)	423
5.2.2 12 Å periodicity	424
5.2.2.1 d–Al–Mn	424
5.2.2.2 d–Al–Mn–Pd	426
5.2.3 16 Å periodicity	430
5.2.3.1 d–Al–Pd	431
5.2.3.2 Al–Fe	432
5.2.3.3 d–Al–Me–Pd (Me = Fe, Mg, Mn, Os, Ru)	432
5.2.3.4 d–Al–Ni–Ru	434

5.2.4 High-pressure experiments on decagonal phases	434
5.2.5 Surface studies of decagonal phases	434
5.3 Dodecagonal phases	435
6 Conclusions	437
References	437

Abstract. Is quasicrystal structure analysis a never-ending story? Why is still not a single quasicrystal structure known with the same precision and reliability as structures of regular periodic crystals? What is the state-of-the-art of structure analysis of axial quasicrystals? The present comprehensive review summarizes the results of almost twenty years of structure analysis of axial quasicrystals and tries to answer these questions as far as possible. More than 2000 references have been screened for the most reliable structural models of pentagonal, octagonal, decagonal and dodecagonal quasicrystals. These models, mainly based on diffraction data and/or on bulk and surface microscopic images are critically discussed together with the limits and potentialities of the respective methods employed.

1 Introduction

At the end of 2003 more than 22 million different chemical substances were known¹. For approximately 400.000 of them the crystal structure was determined². Apart from the existence of a few hundred incommensurately modulated structures (IMS) and composite structures (CS)³, there was no reason to doubt that the ground state (i.e. the thermodynamic equilibrium state at 0 K) of all these compounds and of condensed matter in general is represented by a periodic crystal structure.

¹ see CASTM at <http://www.cas.org/>

² see data bases: organic and metalorganic structures, CSDTM at <http://www.ccdc.cam.ac.uk/>; inorganic structures, ICSDTM at <http://www.fiz-informationsdienste.de/en/DB/icsd/>; intermetallic phases, CRYSTMETTM at <http://www.tothcanada.com/>; Pauling FileTM at <http://www.paulingfile.ch/>

³ partly contained in the data base ICSDB at <http://www.cryst.ehu.es/icsdb/>

* e-mail: steurer@mat.ethz.ch

On April 8th, 1982, D. Shechtman discovered a novel phase with icosahedral diffraction symmetry in rapidly solidified $\text{Al}_{86}\text{Mn}_{14}$. This was the discovery of quasicrystals, which fundamentally changed our understanding of structural order on atomic scale. Quasicrystals (QC) rang in a paradigm change (Kuhn, 1962) in crystallography.

The completely new thing on QC is that they cannot be described properly by a periodic basis structure and a periodic modulation with incommensurate ratio of length scales such as IMS, or as an incommensurate intergrowth of two or more mutually modulated periodic structures such as CS. However, QC, IMS and CS have in common that they can be described as three-dimensional (3D) irrational sections of nD ($n > 3$) translationally periodic hypercrystal structures (see Steurer, Haibach, 2001, and references therein). All three of them form the class of known aperiodic crystals.

Even twenty years after the first publication on icosahedral Al–Mn (Shechtman, Blech, Gratias, Cahn, 1984) and more than 8000 publications later, there is still not a single QC structure known with the reliability that is normal in standard structure analysis. This is reflected, for instance, in the long-lasting and still ongoing discussion about the structure of decagonal Al–Co–Ni, the best studied decagonal QC model system so far (see chapter 5.2.1.4).

Despite the more than 2000 papers on structural problems of QC, only a few out of the approximately 50 stable ternary and binary QC structures have been studied quantitatively so far. The accurate knowledge of the structure and dynamical properties of at least one QC as a function of temperature and pressure, however, is one of the prerequisites for answering fundamental questions such as:

- What governs formation and stability of QC?
- Are QC entropy-stabilized high-temperature phases or are they a ground state of matter (thermodynamically stable at zero K)?
- Is the structure of QC quasiperiodic in the strict sense?
- Why only 5-, 8-, 10-, and 12-fold symmetries have been observed in QC (so far)?

What makes QC structure analysis so demanding is that it comprises the determination on atomic scale of both the short-range order (SRO) and long-range-order (LRO). SRO mainly refers to the atomic arrangement inside a unit tile or cluster (i.e. a recurrent structural building unit), LRO to the ordering of the unit tiles or clusters themselves. The LRO of 3D periodic structures can definitely be described by one of the 14 Bravais lattice types. In case of QC, there are infinitely many different “quasilattices”, i.e. strictly quasiperiodic arrangements of unit tiles or clusters, not to speak about other types of aperiodic structures (see, for instance, Axel, Gratias, 1995). Another problem is that the inherent (?) disorder has to be considered in structure analyses as well. A satisfactory QC structure solution will be based on experimental data from electron microscopy, spectroscopy, surface imaging methods, high-resolution diffraction methods and will include quantum-mechanical calculations as well.

Based on the structural studies published to date one can summarize that:

- The degree of perfection of several QC is comparable to that of silicon (i.e. several micrometer correlation length).

- Structures of real QC (i.e. the experimentally studied samples) closely resemble quasiperiodic structures at least at high temperatures and on time/space average.
- The structure of some QC can be quite well described by cluster decorated quasiperiodic tilings, coverings and/or by the higher-dimensional approach.
- Many QC seem to be thermodynamically stable at least at high temperature.

The present review updates the article “The structure of quasicrystals” published in *Zeitschrift für Kristallographie* fourteen years ago (Steurer, 1990). Since then the number of publications on QC raised from approximately 1800 to more than 8000. Several books have been published as well either focusing on physical properties of QC (Goldman, Sordet, Thiel, Dubois, 1997; Stadnik, 1999; Dubois, Thiel, Urban, 1999; Belin-Ferre, Berger, Quiquandon, 2000; Suck, Schreiber, Häussler, 2002; Trebin, 2003) or on mathematical aspects (Axel, Gratias, 1995; Axel, Denoyer, Gazeau, 1999; Baake, Moody, 2000; Kramer, Papadopolos, 2003). A number of comprehensive review articles appeared in the last years on general aspects of QC (Yamamoto, 1996b), decagonal QC (Ranganathan, Chattopadhyay, Singh, Kelton, 1997), surface studies on QC (Diehl, Ledieu, Ferralis, Szmodis, McGrath, 2003; McGrath, Ledieu, Cox, Diehl 2002), electron-microscopic studies of QC (Hiraga, 2002), and many more. However, there was never a review since Steurer (1990) critically discussing the progress in structure analysis of QC in a comprehensive way.

The review on QC structures will be published in two parts. The present part I is dedicated to axial QC. In part II the structure of icosahedral QC will be reviewed. These two reviews are aimed at taking stock of two decades of combined effort of the QC community to solve the structure of QC and to understand their formation and stability.

2 Occurrence of axial quasicrystals

QC, i.e. phases with diffraction patterns closely resembling those of quasiperiodic structures in the strict sense, have been found in approximately one hundred metallic systems. According to their diffraction (Fourier space) symmetry, they are classified as icosahedral (i-), pentagonal (p-), octagonal (o-), decagonal (d-) or dodecagonal (dd-) phases. Also a few QC with crystallographic symmetry, such as cubic, are known (Feng, Lu, Ye, Kuo, Withers, van Tendeloo, 1990; Donnadiu, Su, Proult, Harmelin, Effenberg, Aldinger, 1996; Donnadiu, Harmelin, Su, Seifert, Effenberg, Aldinger, 1997). Quite a few QC were found to be stable at least at high temperature as far as it can be experimentally proved. Besides, there is a large number of metastable binary and ternary QC known, which can only be prepared by rapid solidification techniques. Stable QC can reach a very high degree of perfection (several micrometers correlation length). Large, millimeter- or even centimeter-sized single crystals have been grown of i-Al–Mn–Pd, i-Al–Pd–Re, i-Cd–Yb, i-Zn–Mg–Dy, i-Zn–Mg–Ho, d-Al–Co–Cu and d-Al–Co–Ni. The elements known to be involved in QC formation are marked in the periodic table of elements (Fig. 2-1).

1	2	3	4	5	6	7	8	9	10	11	12	13	14	15	16	17	18
1																	2
H																	He
3	4											5	6	7	8	9	10
Li	Be											B	C	N	O	F	Ne
11	12											13	14	15	16	17	18
Na	Mg											Al	Si	P	S	Cl	Ar
19	20	21	22	23	24	25	26	27	28	29	30	31	32	33	34	35	36
K	Ca	Sc	Ti	V	Cr	Mn	Fe	Co	Ni	Cu	Zn	Ga	Ge	As	Se	Br	Kr
37	38	39	40	41	42	43	44	45	46	47	48	49	50	51	52	53	54
Rb	Sr	Y	Zr	Nb	Mo	Tc	Ru	Rh	Pd	Ag	Cd	In	Sn	Sb	Te	I	Xe
55	56	57	72	73	74	75	76	77	78	79	80	81	82	83	84	85	86
Cs	Ba	La	Hf	Ta	W	Re	Os	Ir	Pt	Au	Hg	Tl	Pb	Bi	Po	At	Rn
87	88	89	104														
Fr	Ra	Ac	Ku														

* Lanthanide metals	58	59	60	61	62	63	64	65	66	67	68	69	70	71
	Ce	Pr	Nd	Pm	Sm	Eu	Gd	Tb	Dy	Ho	Er	Tm	Yb	Lu
* Actinide metals	90	91	92	93	94	95	96	97	98	99	100	101	102	103
	Th	Pa	U	Np	Pu	Am	Cm	Bk	Cf	Es	Fm	Md	No	Lr

Fig. 2-1. Elements involved in the formation of binary, ternary or quaternary stable or metastable quasicrystals with icosahedral, pentagonal, octagonal, decagonal or dodecagonal diffraction symmetry (shaded cells).

To date, stable axial QC have been found in more than twenty ternary and quaternary systems (see Tables 5.2-1 and 5.3-1). Metastable axial QC are known in approximately forty binary and ternary systems (see Tables 5.1-1, 5.2-2, 5.3-1). Most of the stable QC were found under the assumption that they are electronically stabilized (Hume-Rothery phases), i.e. that they are stable only at a particular valence electron concentration such as $e/a = 1.75$ or 2 (Tsai, 2003). This approach was particularly successful in metallic systems where already approximants were known. (Crystalline) approximants are phases with periodic structures, which are locally similar to that of QC.

Several chances were missed to identify novel intermetallic phases as QC long before D. Shechtman's discovery. As early as 1939, the aluminum rich part of the Al–Cu–Fe system was studied and a new phase, denoted ψ , reported (Bradley, Goldschmidt, 1939). Since at that time only X-ray powder diffraction was used for phase characterization, the icosahedral symmetry of this quasicrystalline phase could not be seen. The same happened in the system Al–Cu–Li, where Hardy, Silcock (1956) found a phase T_2 with weak, “fairly simple”, but not cubic powder pattern, later identified as QC (Saintfort, Dubost, Dubus, 1985; Ball, Lloyd, 1985). Lemmerz, Grushko, Freiburg, Jansen (1994) identified the unknown stable phase $Al_{10}FeNi_3$, discovered in a study of the phase diagram Al–Fe–Ni (Khaidar, Allibert, Driole, 1982), as decagonal phase. The Z phase in the system Mg–Zn–Y (Padezhnova, Melnik, Miliyevskiy, Dobatkina, Kinzhibalo, 1982) also corresponds to a quasicrystalline phase (Luo, Zhang, Tang, Zhao, 1993). Recently, the “unknown” compounds $Cd_{5.7}Y$ (Palenzona, 1971) and $Cd_{17}Ca_3$ (Bruzzone, 1972) in the binary systems Cd–Y and Cd–Ca, respectively, have also been identified as QC (Tsai, Guo, Abe, Takakura, Sato, 2000; Guo, Abe, Tsai, 2000b).

There are only a very few QC for which there is some experimental evidence for thermodynamic stability at least at high temperature (d-Al–Fe–Ni, d-Al–Co–Ni, i-Al–Cu–Li, i-Al–Cu–Fe, d- and i-Al–Mn–Pd). In the case of most other QC, their stability has not been studied sufficiently or not at all. It is certainly not sufficient to check X-ray powder diffraction patterns because high-order approximants or 1D QC cannot be distinguished from

decagonal QC in this way due to reflection-profile overlapping and limited resolution. It is also not sufficient to check electron diffraction patterns of annealed samples (low resolution, only a few grains are investigated, the sample may be in an intermediate transformation state). The best proof of the stability of any phase is to study reversible phase transformations by all techniques available, from thermal analysis and dilatometry to *in situ* high-resolution electron microscopy and X-ray or neutron diffraction methods.

3 Crystallographic description of axial quasicrystals

Pentagonal, octagonal, decagonal and dodecagonal QC possess structures being quasiperiodic in two dimensions and periodic in the third one. Their symmetry can be equally well described in 3D reciprocal space (Rabson, Mermin, Rokhsar, Wright, 1991) and 5D direct space (Janssen, 1988; Yamamoto, 1996b, and references therein), respectively. For the detailed description of quasiperiodic structures (“where are the atoms?”), however, the nD description in direct space is more appropriate. In the following a short introduction is given into the 5D crystallographic description of pentagonal, octagonal, decagonal and dodecagonal QC based on Steurer, Haibach (1999a, 2001, and references therein).

Indexing

The set of all diffraction vectors \mathbf{H} forms a Fourier module M^* of rank five in physical (parallel) space,

$$M^* = \left\{ \mathbf{H}^{\parallel} = \sum_{i=1}^5 h_i \mathbf{a}_i^* \mid h_i \in \mathbb{Z} \right\},$$

which can be decomposed into two submodules $M^* = M_1^* \oplus M_2^*$. $M_1^* = \{h_1 \mathbf{a}_1^* + h_2 \mathbf{a}_2^* + h_3 \mathbf{a}_3^* + h_4 \mathbf{a}_4^*\}$ corresponds to a Z-module of rank four in a 2D subspace, $M_2^* = \{h_5 \mathbf{a}_5^*\}$ corresponds to a Z-module of rank one in a 1D subspace. Consequently, the first submodule can be considered as a projection of a 4D reciprocal lattice, $M_1^* = \pi^{\parallel}(\Sigma^*)$, while the second submodule is of the form of a regular 1D reciprocal lattice, $M_2^* = \mathcal{A}^*$.

Due to scaling symmetry, indexing is not unique (cf. Mukhopadhyay, Lord, 2002; Lord, 2003). Nevertheless an optimum basis (low indices are assigned to strong reflections) can be derived: not the metrics, as for regular periodic crystals, but the intensity distribution (related to the Patterson peaks in direct space) characterizes the best choice of indexing (see, e.g., Cervellino, Haibach, Steurer, 1998). An appropriate set of reciprocal basis vectors can be identified experimentally in the following way:

- Find directions of systematic absences or pseudoabsences determining the possible orientations of the reciprocal basis vectors (cf. Rabson, Mermin, Rokhsar, Wright, 1991);
- Find pairs of strong reflections whose physical space diffraction vectors are related to each other by the scaling factor;
- Index these reflections by assigning an appropriate

3D point group	order of the group	conditions	$n = 5$ trigonal type	$n = 8$ tetragonal type	$n = 10$ hexagonal type	$n = 12$ dodecagonal type
$\frac{n}{m} \frac{2}{m} \frac{2}{m}$	$4n$	n even		$\frac{8}{m} \frac{2}{m} \frac{2}{m}$	$\frac{10}{m} \frac{2}{m} \frac{2}{m}$	$\frac{12}{m} \frac{2}{m} \frac{2}{m}$
$\bar{n} 2 m$	$2n$	n even		$\bar{8} 2 m$	$\bar{10} 2 m$	$\bar{12} 2 m$
$\bar{n} \frac{2}{m}$	$4n$	n odd	$\bar{5} \frac{2}{m}$			
$n m m$	$2n$	n even		$8 m m$	$10 m m$	$12 m m$
$n m$	$2n$	n odd	$5 m$			
$n 22$	$2n$	n even		$8 22$	$10 22$	$12 22$
$n 2$	$2n$	n odd	$5 2$			
$\frac{n}{m}$	$2n$	n even		$\frac{8}{m}$	$\frac{10}{m}$	$\frac{12}{m}$
\bar{n}	n	n even		$\bar{8}$	$\bar{10}$	$\bar{12}$
	$2n$	n odd	$\bar{5}$			
n	n		5	8	10	12

Table 3-1. Point group symmetry in reciprocal space for the general case as well as for pentagonal, octagonal, decagonal and dodecagonal quasicrystals (see Rabson, Mermin, Rokhsar, Wright, 1991). The corresponding (if any) periodic crystal symmetry type is given as well.

Table 3-2. 3D decagonal point groups of order k and corresponding 5D decagonal space groups with reflection conditions (cf. Rabson, Mermin, Rokhsar, Wright, 1991).

3D point group	Order k	5D space group	reflection condition
$\frac{10}{m} \frac{2}{m} \frac{2}{m}$	40	$P \frac{10}{m} \frac{2}{m} \frac{2}{m}$	no condition
		$P \frac{10}{m} \frac{2}{c} \frac{2}{c}$	$h_1 h_2 h_3 h_4 h_5 : h_5 = 2n$
		$P \frac{10_5}{m} \frac{2}{m} \frac{2}{c}$	$h_1 h_2 \bar{h}_2 \bar{h}_1 h_5 : h_5 = 2n$
		$P \frac{10_5}{m} \frac{2}{c} \frac{2}{m}$	$h_1 h_2 h_3 h_4 h_5 : h_5 = 2n$
$\frac{10}{m}$	20	$P \frac{10}{m}$	no condition
		$P \frac{10_5}{m}$	$0000h_5 : h_5 = 2n$
$10 2 2$	20	$P 10 2 2$	no condition
		$P 10_j 2 2$	$0000h_5 : jh_5 = 10n$
$10 m m$	20	$P 10 m m$	no condition
		$P 10 c c$	$h_1 h_2 h_3 h_4 h_5 : h_5 = 2n$
			$h_1 h_2 \bar{h}_2 \bar{h}_1 h_5 : h_5 = 2n$
		$P 10_5 m c$	$h_1 h_2 \bar{h}_2 \bar{h}_1 h_5 : h_5 = 2n$
		$P 10_5 c m$	$h_1 h_2 h_3 h_4 h_5 : h_5 = 2n$
$\bar{10} m 2$	20	$P \bar{10} m 2$	no condition
		$P \bar{10} c 2$	$h_1 h_2 h_3 h_4 h_5 : h_5 = 2n$
		$P \bar{10} 2 m$	no condition
		$P \bar{10} 2 c$	$h_1 h_2 \bar{h}_2 \bar{h}_1 h_5 : h_5 = 2n$
$\bar{10}$	10	$P \bar{10}$	no condition
10	10	$P 10$	no condition
		$P 10_j$	$0000h_5 : jh_5 = 10n$

value to a^* . This value should be derived from the shortest interatomic distance and the edge length of the unit tiles expected in the structure;

- A reciprocal basis is appropriate if all observable Bragg reflections can be indexed with integers.

Diffraction symmetry

The diffraction symmetry of pentagonal, octagonal, decagonal and dodecagonal QC can be described by the Laue groups $\bar{5}m$ or $\bar{5}$ and n/mmm or n/m with $n = 8, 10$ and 12 , respectively. The axial point groups are listed in Tab. 3-1, the decagonal space groups in Tab. 3-2 (for pentagonal, octagonal and dodecagonal space groups see Rabson, Mermin, Rokhsar, Wright, 1991). These space groups are a subset of all 5D space groups that fulfill the condition that their 5D point groups are isomorphous to the 3D point groups describing the diffraction symmetry. The orientation of the symmetry elements in the 5D space is defined by the isomorphism of the 3D and 5D point groups. However, the action of the n -fold rotation is different in the subspaces \mathbf{V}^{\parallel} and \mathbf{V}^{\perp} : a rotation by $2\pi/n$ in \mathbf{V}^{\parallel} is correlated to a rotation by $2\pi k/n$ in \mathbf{V}^{\perp} (coupling factor $k = 2$ for $n = 5$, $k = 3$ for $n = 8$ and 10 , $k = 5$ for $n = 12$). The reflection and inversion operations are equivalent in both subspaces.

Structure factor

The structure factor of a QC in the 5D description corresponds to the Fourier transform of the content of the 5D unit cell

$$F(\mathbf{H}) = \sum_{k=1}^N f_k(\mathbf{H}^{\parallel}) T_k(\mathbf{H}^{\parallel}, \mathbf{H}^{\perp}) g_k(\mathbf{H}^{\perp}) e^{2\pi i \mathbf{H} \mathbf{r}_k}$$

with 5D diffraction vectors $\mathbf{H} = \sum_{i=1}^5 h_i \mathbf{d}_i^*$, N hyperatoms per 5D unit cell, parallel space atomic scattering factor $f_k(\mathbf{H}^{\parallel})$, temperature factor $T_k(\mathbf{H}^{\parallel}, \mathbf{H}^{\perp})$, and perpendicular space geometrical form factor $g_k(\mathbf{H}^{\perp})$. $T_k(\mathbf{H}^{\parallel}, \mathbf{0})$ is equivalent

lent to the conventional Debye-Waller factor, $T_k(\mathbf{0}, \mathbf{H}^\perp)$ describes random fluctuations along the perpendicular space coordinate. These fluctuations cause in physical space characteristic jumps of vertices (*phason flips*). All phason flips map the vertices on positions, which can be described by physical space vectors of the type $\mathbf{r}^\parallel = \sum_{i=1}^5 n_i \mathbf{a}_i$.

The set $M = \left\{ \mathbf{r}^\parallel = \sum_{i=1}^5 n_i \mathbf{a}_i \mid n_i \in \mathbb{Z} \right\}$ of all possible vectors forms a \mathbb{Z} -module. The shape of the atomic surfaces corresponds to a selection rule for the actually occupied positions out of the infinite number given by M (de Bruijn, 1981). The geometrical form factor $g_k(\mathbf{H}^\perp)$ is equivalent to the Fourier transform of the *atomic surface*, i.e. the 2D perpendicular space component of the 5D *hyperatoms*.

Point density

The point density ρ_{PD} (number of vertices per unit area) of a tiling with edge length a_r can be calculated from the ratio of the relative number of unit tiles in the tiling to their area or from the 5D description

$$\rho_{\text{PD}} = \frac{\sum_i \Omega_{\text{AS}}^i}{\Omega_{\text{UC}}}$$

with Ω_{AS}^i and Ω_{UC} the areas of the atomic surfaces and the volume of the unit cell, respectively.

3.1 Pentagonal phases

An axial QC with pentagonal diffraction symmetry is called pentagonal phase. Its holohedral Laue symmetry group is $K = \bar{5}m$. The set M^* of all reciprocal space vectors \mathbf{H}^\parallel remains invariant under the action of the symmetry operators of the point group $\bar{5}m$ and its subgroups (Table 3-1). M^* is also invariant under scaling $\mathbf{S}^m M^* = s^m M^*$ with $s = (1 \pm \sqrt{5})/2$. The scaling matrix reads

$$\mathbf{S} = \begin{pmatrix} 0 & 1 & 0 & -1 & 0 \\ 0 & 1 & 1 & -1 & 0 \\ -1 & 1 & 1 & 0 & 0 \\ -1 & 0 & 1 & 0 & 0 \\ 0 & 0 & 0 & 0 & 1 \end{pmatrix}.$$

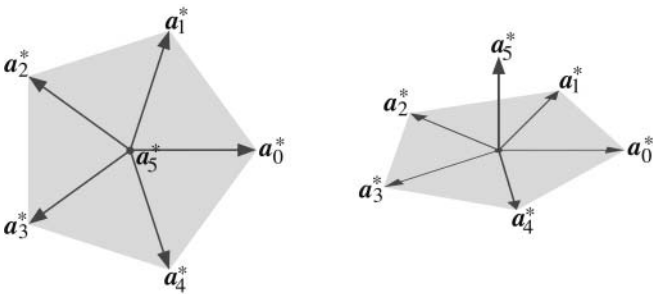


Fig. 3.1-1. Star of reciprocal basis vectors of the pentagonal quasicrystal and the decagonal quasicrystal (setting I), respectively. At left, the projection along \mathbf{a}_5^* is shown, at right, a perspective view is given.

All vectors $\mathbf{H}^\parallel \in M^*$ can be represented as $\mathbf{H}^\parallel = \sum_{i=1}^5 h_i \mathbf{a}_i^*$ on the basis (V-basis) $\mathbf{a}_i^* = a_i^* (\cos 2\pi i/5, \sin 2\pi i/5, 0)$, $i = 1, \dots, 4$ and $\mathbf{a}_5^* = a_5^* (0, 0, 1)$ (**Fig. 3.1-1**). The components of \mathbf{a}_i^* refer to a Cartesian coordinate system in physical space. The reciprocal basis \mathbf{d}_i^* , $i = 1, \dots, 5$, in the 5D embedding space (D -space) reads

$$\mathbf{d}_i^* = a_i^* \mathbf{e}_i, \quad \text{with} \quad \mathbf{e}_i = \begin{pmatrix} \cos(2\pi i/5) \\ \sin(2\pi i/5) \\ 0 \\ c \cos(6\pi i/5) \\ c \sin(6\pi i/5) \end{pmatrix}_V,$$

$$i = 1 \dots 4 \quad \text{and} \quad \mathbf{d}_5^* = a_5^* \begin{pmatrix} 0 \\ 0 \\ 1 \\ 0 \\ 0 \end{pmatrix}_V.$$

The coupling factor can be $k = 2$ or $k = 3$ without changing the metric tensor. With the condition $\mathbf{d}_i^* \cdot \mathbf{d}_j^* = \delta_{ij}$ a basis in direct 5D space is obtained

$$\mathbf{d}_i = \frac{2}{5a_i^*} (\mathbf{e}_i - \mathbf{e}_0), \quad \text{with} \quad \mathbf{e}_0 = \begin{pmatrix} 1 \\ 0 \\ 0 \\ 1 \\ 0 \end{pmatrix}_V,$$

$$i = 1 \dots 4 \quad \text{and} \quad \mathbf{d}_5 = \frac{1}{a_5^*} \begin{pmatrix} 0 \\ 0 \\ 1 \\ 0 \\ 0 \end{pmatrix}_V.$$

Without loss of generality c can be set to 1. The metric tensors G , G^* are of the type

$$\begin{pmatrix} A & B & B & B & 0 \\ B & A & B & B & 0 \\ B & B & A & B & 0 \\ B & B & B & A & 0 \\ 0 & 0 & 0 & 0 & C \end{pmatrix}$$

with $A = 2a_1^{*2}$, $B = -1/2 a_1^{*2}$, $C = a_5^{*2}$ and $A = 4/(5a_1^{*2})$, $B = 2/(5a_1^{*2})$, $C = 1/a_5^{*2}$ for the reciprocal and direct space, respectively. Therewith we obtain $d_i^* = a_i^* \sqrt{2}$, $i = 1 \dots 4$, $d_5^* = a_5^*$, $\alpha_{ij}^* = 104.47^\circ$, $i, j = 1 \dots 5$ and $d_i = 2/(\sqrt{5} a_i^*)$, $i = 1 \dots 4$, $d_5 = 1/a_5^*$, $\alpha_{ij}^* = 60^\circ$, $\alpha_{i5}^* = 90^\circ$, $i, j = 1 \dots 4$ for the magnitudes of the lattice parameters in reciprocal and direct space, respectively. The volume of the 5D unit cell amounts to $V = \sqrt{|G|} = 4/(5\sqrt{5} a_1^{*4} a_5^*)$.

3.2 Octagonal phases

An axial QC with octagonal diffraction symmetry is called octagonal phase. Its holohedral Laue symmetry group is $K = 8/mmm$. The set M^* of all reciprocal space vectors \mathbf{H}^\parallel remains invariant under the action of the symmetry

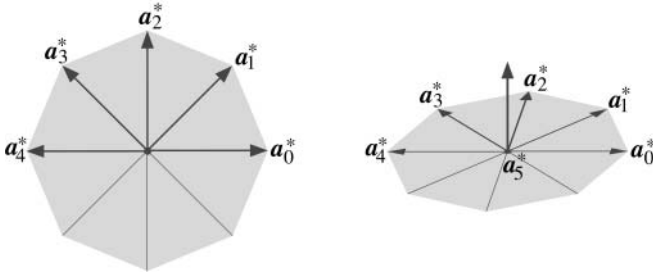


Fig. 3.2-1. Star of reciprocal basis vectors of the octagonal quasicrystal. At left, the projection along a_5^* is shown, at right, a perspective view is given.

operators of the point group $8/mmm$ and its subgroups (Table 3-1). M^* is also invariant under scaling $S^m M^* = s^m M^*$ with $s = 1 \pm \sqrt{2}$. The scaling matrix reads

$$S = \begin{pmatrix} 1 & 1 & 0 & -1 & 0 \\ 1 & 1 & 1 & 0 & 0 \\ 0 & 1 & 1 & 1 & 0 \\ -1 & 0 & 1 & 1 & 0 \\ 0 & 0 & 0 & 0 & 1 \end{pmatrix}.$$

All vectors $\mathbf{H} \in M^*$ can be represented as $\mathbf{H} = \sum_{i=1}^5 h_i \mathbf{a}_i^*$ on the basis (V-basis) $\mathbf{a}_i^* = a_i^* (\cos 2\pi i/8, \sin 2\pi i/8, 0)$, $i = 1, \dots, 4$ and $\mathbf{a}_5^* = a_5^* (0, 0, 1)$ (Fig. 3.2-1). The components of \mathbf{a}_i^* refer to a Cartesian coordinate system in physical space. The reciprocal basis \mathbf{d}_i^* , $i = 1, \dots, 5$, in the 5D embedding space (D -space) reads

$$\mathbf{d}_i^* = a_i^* \mathbf{e}_i, \quad \text{with} \quad \mathbf{e}_i = \begin{pmatrix} \cos(2\pi i/8) \\ \sin(2\pi i/8) \\ 0 \\ c \cos(6\pi i/8) \\ c \sin(6\pi i/8) \end{pmatrix}_V, \\ i = 1 \dots 4 \quad \text{and} \quad \mathbf{d}_5^* = a_5^* \begin{pmatrix} 0 \\ 0 \\ 1 \\ 0 \\ 0 \end{pmatrix}_V.$$

The coupling factor amounts to $k = 3$. With the condition $\mathbf{d}_i \cdot \mathbf{d}_j^* = \delta_{ij}$ a basis in direct 5D space is obtained

$$\mathbf{d}_i = \frac{1}{2a_i^*} \mathbf{e}_i, \quad \text{with} \quad i = 1 \dots 4 \quad \text{and} \quad \mathbf{d}_5 = \frac{1}{a_5^*} \begin{pmatrix} 0 \\ 0 \\ 1 \\ 0 \\ 0 \end{pmatrix}_V.$$

Without loss of generality c can be set to 1. The metric tensors G , G^* are of the type

$$\begin{pmatrix} A & 0 & 0 & 0 & 0 \\ 0 & A & 0 & 0 & 0 \\ 0 & 0 & A & 0 & 0 \\ 0 & 0 & 0 & A & 0 \\ 0 & 0 & 0 & 0 & B \end{pmatrix}$$

with $A = 2a_1^{*2}$, $B = a_5^{*2}$ and $A = 1/(2a_1^{*2})$, $B = 1/a_5^{*2}$ for the reciprocal and direct space, respectively. Thus we obtain $d_i^* = a_i^* \sqrt{2}$, $i = 1 \dots 4$, $d_5^* = a_5^*$, $\alpha_{ij}^* = 90^\circ$, $i, j = 1 \dots 5$ and $d_i = 1/(\sqrt{2}a_i^*)$, $i = 1 \dots 4$, $d_5 = 1/a_5^*$, $\alpha_{ij}^* = 90^\circ$, $i, j = 1 \dots 5$ for the magnitudes of the lattice parameters in reciprocal and direct space, respectively. The volume of the 5D unit cell amounts to $V = \sqrt{|G|} = 1/(4a_1^{*4}a_5^*)$.

3.3 Decagonal phases

An axial QC with decagonal diffraction symmetry is called decagonal phase. Its holohedral Laue symmetry group is $K = 10/mmm$. The set M^* of all vectors $\mathbf{H} \in M^*$ remains invariant under the action of the symmetry operators of the point group $10/mmm$ and its subgroups (Table 3-1). M^* is also invariant under scaling by τ^n ($n \in \mathbb{Z}$), with $\tau = 1/2(1 + \sqrt{5})$. All reciprocal space vectors $\mathbf{H} \in M^*$ can be represented as $\mathbf{H} = \sum_{i=1}^5 h_i \mathbf{a}_i^*$ on the basis (V-basis) $\mathbf{a}_i^* = a_i^* (\cos 2\pi i/5, \sin 2\pi i/5, 0)$, $i = 1, \dots, 4$ and $\mathbf{a}_5^* = a_5^* (0, 0, 1)$ (Fig. 3.1-1) (Setting I). Another possible choice (setting II) of basis vectors is $\mathbf{a}_i^* = a_i^* (\cos 2\pi i/10, \sin 2\pi i/10, 0)$, $i = 1, \dots, 4$ and $\mathbf{a}_5^* = a_5^* (0, 0, 1)$. The vector components refer to a Cartesian coordinate system in physical space.

In case of setting I, which we will use in the following, the reciprocal and direct bases in the 5D embedding space (D -space) and the scaling symmetry are the same as for the pentagonal case and coupling factor $k = 3$ (see chapter 3.1).

Indexing

There are several indexing schemes in use. Rarely employed are six-membered indices based on either a distorted icosahedral basis vector set derived from the icosahedral basis vector set or on a pentagonal-pyramidal basis vector set. For a comparative discussion see Choy, Fitz Gerald, Kalloniatis (1988) and references therein. Most frequently applied are the schemes of Yamamoto, Ishihara (1988), YI-scheme, and Steurer (1989), S-scheme, respectively. The reciprocal basis vectors are related by: $a_{YI}^* = \sqrt{5}/\tau a_S^*$ (for $a_i^* = a^*$, $i = 1, \dots, 4$), the coupling factors are $k_{YI} = 2$, $k_S = 3$, and the magnitudes of the physical space projections of the 5D reciprocal basis vectors amount to $\|\pi^\parallel(\mathbf{d}_i^*)\|_{YI} = a_{YI}^*/\sqrt{5}$ and $\|\pi^\parallel(\mathbf{d}_i^*)\|_S = a_S^*$, respectively. The transformation matrices for the indices are just the scaling matrices

$$\begin{pmatrix} 0 & 1 & 0 & -1 & 0 \\ 0 & 1 & 1 & -1 & 0 \\ -1 & 1 & 1 & 0 & 0 \\ -1 & 0 & 1 & 0 & 0 \\ 0 & 0 & 0 & 0 & 1 \end{pmatrix}_{S \Rightarrow YI} \quad \text{and}$$

$$\begin{pmatrix} -1 & 1 & 0 & -1 & 0 \\ 0 & 0 & 1 & -1 & 0 \\ -1 & 1 & 0 & 0 & 0 \\ -1 & 0 & 1 & -1 & 0 \\ 0 & 0 & 0 & 0 & 1 \end{pmatrix}_{YI \Rightarrow S}.$$

For instance, a^* and $a = 1/a^*$ amount to 0.26360 \AA^{-1} and 3.794 \AA in the S-scheme (Steurer, Haibach, Zhang, Kek,

Lück, 1993), and to 0.36429 \AA^{-1} and 2.745 \AA , respectively, in the YI-scheme (Yamamoto, Kato, Shibuya, Takeuchi, 1990).

Fung, Yang, Zhou, Zhao, Zhan, Shen (1986) named the two symmetrically inequivalent 2-fold axes D- and P-type. The SAED images perpendicular to a P-type axis (shortly P-pattern) contain systematic extinct reciprocal layer lines. The directions are denoted A2D, A2P and A10.

Approximants

Approximants in the wider sense of the word possess periodic crystal structures consisting of the same atomic clusters as QC. Rational approximants are the subset of structures that can geometrically be derived by a perpendicular-space shear of the QC in the higher-dimensional description (see Steurer, Haibach, 1999a; Ranganathan, Subramaniam, Ramakrishnan, 2001; Niizeki, 1991). Thereby, the irrational number τ is replaced by a rational number. According to the group/subgroup symmetry relationship between the d-phase and its approximants, the approximants may exhibit orthorhombic, monoclinic or triclinic symmetry. In the following, only the most frequent orthorhombic approximants will be discussed.

The lattice parameters of the general orthorhombic $\langle p/q, r/s \rangle$ -approximant are

$$a_1 = \frac{2(3-\tau)(\tau^2 p + q)}{5a^*}, \quad a_2 = \frac{\sqrt{3-\tau}(\tau r + s)}{5a^*}, \quad a_3 = a_5.$$

For the special case $p = F_{n+2}$, $q = -F_n$, $r = F_{n'+1}$, $s = F_{n'}$ we obtain the orthorhombic $\langle n, n' \rangle$ -approximants with lattice parameters

$$a_1 = \frac{2(3-\tau)}{5a^*} \tau^{n+2}, \quad a_2 = \frac{2\sqrt{3-\tau}}{5a^*} \tau^{n'+1}, \quad a_3 = a_5.$$

This corresponds to $a_1 = \tau^2 a_P$ and $a_2 = \tau a_D$ in the terminology a_P , a_D , used by Zhang, Kuo (1990). A few examples are given in Table 3.3-1. The orthorhombic unit cells are (110)-face centered if $n \bmod 3 = (n' + 1) \bmod 3$. The reciprocal space vectors $\mathbf{H}^{\parallel} = (h_1 h_2 h_3 h_4 h_5)$ are transformed by the perpendicular-space shear to $\mathbf{H}^{\parallel} = ([-p(h_2 + h_3) - q(h_1 + h_4)][r(h_1 - h_4) - s(h_2 + h_3)] h_5)$.

Table 3.3-1. Series of common rational $\langle n, n' \rangle$ -approximants of the d-phase. The reciprocal lattice parameter used is that of d-Al-Co-Ni, $a^* = 0.26352 \text{ \AA}^{-1}$ (Steurer, Haibach, Zhang, Kek, Lück, 1993).

n, n'	a_1	a_2
0	5.492	2.887
1	8.886	4.672
2	14.378	7.559
3	23.264	12.230
4	37.641	19.789
5	60.905	32.020
6	98.546	51.809
7	159.451	83.829

Periodic average structure (PAS)

The periodic average structure of a decagonal phase can be obtained by oblique projection of the five-dimensional hypercrystal structure (Steurer, Haibach, 1999b; Steurer, 2000). The lattice parameters of the most important side-face centered orthorhombic PAS (IMS-setting), which is closely related to the CsCl-type structure of the β -phase, can be calculated from

$$a_1^{\text{PAS}} = \frac{5a_r}{\tau^3}, \quad a_2^{\text{PAS}} = \frac{5a_r}{\tau^2 \sqrt{3-\tau}}, \quad a_3^{\text{PAS}} = a_5,$$

with $a_r = 2.456 \text{ \AA}$, the Penrose rhomb edge length in d-Al-Co-Ni, for instance. The PAS shows the correspondence between the atoms of a quasiperiodic structure and an underlying periodic structure. It can be very useful in understanding the geometry of continuous quasicrystal-to-crystal transformations. It may also help to discover structural relationships between QC and non-rational approximants such as the β -phase, for instance.

The geometrical relationship between the (110)-layer of the Al(Co, Ni) β -phase and the PAS of decagonal Al-Co-Ni (Steurer, Haibach, Zhan, Kek, Lück, 1993), for instance, is: the $[\bar{1}10]$ direction of the β -phase is parallel to the 10-fold axis, $[110]$ and $[111]$ are parallel to the two different 2-fold axes of the d-phase. Therefrom it follows for the PAS: $\mathbf{a}_1^{\text{PAS}} \parallel [001]$, $\mathbf{a}_2^{\text{PAS}} \parallel [110]$ and $\mathbf{a}_3^{\text{PAS}} \parallel [\bar{1}10]$. The translation period along $[001]$ amounts to 2.88 \AA , along $[110]$ and $[\bar{1}10]$ to 4.08 \AA for a lattice parameter of $a_\beta = 2.88 \text{ \AA}$ for the β -phase. This fits nicely to the periods in the respective directions of the PAS of d-Al-Co-Ni: $\mathbf{a}_1^{\text{PAS}} = 2.88 \text{ \AA}$, $\mathbf{a}_2^{\text{PAS}} = 3.99 \text{ \AA}$, $\mathbf{a}_3^{\text{PAS}} = 4.08 \text{ \AA}$.

3.4 Dodecagonal phases

An axial QC with dodecagonal diffraction symmetry is called dodecagonal phase (see also Gähler, 1988). Its holohedral Laue symmetry group is $K = 12/mmm$. The set M^* of all reciprocal space vectors \mathbf{H}^{\parallel} remains invariant under the action of the symmetry operators of the point group $12/mmm$ and its subgroups (Table 3-1). M^* is also invariant under scaling $\mathbf{S}^m M^* = s^m M^*$ with $s = (2 \pm \sqrt{3})/2$. The scaling matrix reads

$$\mathbf{S} = \begin{pmatrix} 1 & 1 & 0 & -1 & 0 \\ 1 & 1 & 1 & 0 & 0 \\ 0 & 1 & 1 & 1 & 0 \\ -1 & 0 & 1 & 1 & 0 \\ 0 & 0 & 0 & 0 & 1 \end{pmatrix}.$$

All vectors $\mathbf{H}^{\parallel} \in M^*$ can be represented as $\mathbf{H}^{\parallel} = \sum_{i=1}^5 h_i \mathbf{a}_i^*$ on a basis (V-basis) $\mathbf{a}_i^* = a_i^*(\cos 2\pi i/12, \sin 2\pi i/12, 0)$, $i = 1, \dots, 4$ and $\mathbf{a}_5^* = a_5^*(0, 0, 1)$ (Fig. 3.4-1). The vector components refer to a Cartesian coordinate system in physical space. The reciprocal basis $\mathbf{d}_i^* i = 1, \dots, 5$ in the 5D embedding space (D-space) reads

$$\mathbf{d}_i^* = a_i^* \mathbf{e}_i, \quad \text{with} \quad \mathbf{e}_i = \begin{pmatrix} \cos(2\pi i/12) \\ \sin(2\pi i/12) \\ 0 \\ c \cos(10\pi i/12) \\ c \sin(10\pi i/12) \end{pmatrix}_V,$$

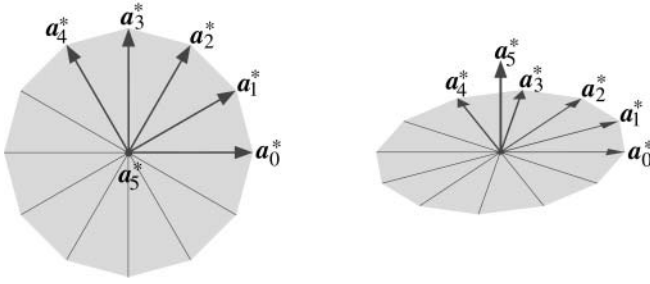


Fig. 3.4-1. Star of reciprocal basis vectors of the dodecagonal quasicrystal. At left, the projection along \mathbf{a}_5^* is shown, at right, a perspective view is given.

$$i = 1 \dots 4 \quad \text{and} \quad \mathbf{d}_5^* = \mathbf{a}_5^* \begin{pmatrix} 0 \\ 0 \\ 1 \\ 0 \\ 0 \end{pmatrix}_v.$$

The coupling factor amounts to $k = 5$. With the condition $\mathbf{d}_i \cdot \mathbf{d}_j^* = \delta_{ij}$ a basis in direct 5D space is obtained

$$\mathbf{d}_i = \frac{1}{3a_i^*} (2\mathbf{e}_i - \mathbf{e}_{(i+2) \bmod (4)}) \quad \text{with} \quad i = 1 \dots 4,$$

$$\text{and} \quad \mathbf{d}_5 = \frac{1}{a_5^*} \begin{pmatrix} 0 \\ 0 \\ 1 \\ 0 \\ 0 \end{pmatrix}_v.$$

Without loss of generality c can be set to 1. The metric tensors G, G^* are of the type

$$\begin{pmatrix} A & 0 & B & 0 & 0 \\ 0 & A & 0 & B & 0 \\ B & 0 & A & 0 & 0 \\ 0 & B & 0 & A & 0 \\ 0 & 0 & 0 & 0 & C \end{pmatrix}$$

with $A = 2a_1^{*2}$, $B = a_1^{*2}$, $C = a_5^{*2}$ and $A = 2/(3a_1^{*2})$, $B = -1/(3a_1^{*2})$, $C = 1/a_5^{*2}$ for the direct and reciprocal space, respectively. Thus we obtain for the lattice parameters in reciprocal space $d_i^* = a_i^* \sqrt{2}$, $i = 1 \dots 4$, $d_5^* = a_5^*$, $\alpha_{ij}^* = 60$, $\alpha_{i5}^* = 90$, $i, j = 1 \dots 4$ and for those in direct space $d_i = \sqrt{2}/(\sqrt{3} a_i^*)$, $i = 1 \dots 4$, $d_5 = 1/a_5^*$, $\alpha_{ij}^* = 120$, $\alpha_{i5}^* = 90$, $i, j = 1 \dots 4$. The volume of the 5D unit cell can be calculated to $V = \sqrt{|G|} = 1/(4a_1^{*4} a_5)$.

4 Limits and potentialities of methods for quasicrystal structure analysis

What do we want to know about the structure of a QC and what can we know employing the full potential of state-of-the-art methods? Why do we want to know that? How does this compare with the information we have about periodic structures from small molecule crystals to virus crystals?

Any real crystal, be it a periodic or an aperiodic one, is finite and has equilibrium and non-equilibrium defects such as thermal vacancies as well as dislocations and

grain boundaries, respectively. If it only has equilibrium defects it is called a perfect crystal otherwise an imperfect crystal. Beside defects a crystal may also show inherent structural disorder. A crystal is not a static arrangement of atoms or molecules. The atoms vibrate around their equilibrium positions due to the superposition of all thermally excited lattice vibrations (phonons). Consequently, the ideal structure of a crystal is just a simplified model of the real structure. To fully describe the real structure of a crystal one needs a model for the ideal structure as well as one describing the deviations from it (dynamics, disorder and defects). A real crystal is rarely in thermodynamic equilibrium. If crystallized from the melt, the actual structure at ambient conditions always is a kind of quenched metastable state. Thermodynamic equilibrium cannot be reached due to sluggish kinetics at lower temperature.

There is no doubt that regular crystals possess translationally periodic structures on time and space average. Nobody ever doubted that really and tried to prove this or even thought that it would make sense to prove it. In the case of QC the situation is different. At least on one single example it has to be demonstrated how an ideal QC structure looks like and what kind of disorder and defect structure is inherent or common. It is typical for X-ray diffraction patterns of QC that they show sharp Bragg reflections even if strong (phason) diffuse scattering is present. This indicates long correlation lengths (micrometers) of the space and time averaged structure. Thus, QC show long-range order accompanied by short-range disorder. This is preferentially random phason disorder and, in particular for pseudoternary QC, in addition chemical disorder.

There are, however, many problems making QC structure analysis extremely difficult. The most serious problem is that only very limited data sets are experimentally accessible, be it diffraction data or microscopic data. This makes it impossible to determine the “absolute order” of a macroscopic QC. A good fit to experimental data of a model is no proof that the global minimum was found and that the proposed model is the best possible one. Thus it is very difficult to find out whether a QC is quasiperiodic in the strict meaning of the word, only on average, or not at all; or to prove that a QC is energy or entropy stabilized, whether its structure can be described by an ordered tiling or rather by a random tiling. It will also be difficult to prove that QC modeling can be accurately done by the n D approach. Probably, final modeling has to be performed in 3D space to properly account for atomic relaxation and disorder. Therefore, it is essential to know at least the maximum error one can make by using the one or the other method. There is a couple of publications on the potential and limits of QC structure analysis (cf. Beeli, Steurer, 2000; Beeli, Nissen, 1993). In the following, the tools, techniques and methods most frequently employed in QC structure analysis are shortly commented.

Observation, interpretation, modeling

Theoreticians are eager to find confirmation of their ideal(ized) model systems in the “lowly spheres” of the experiment. Experimentalists like their role as pioneers who provide the proofs for important theories. Both of

them run the risk to use the experimental evidence somewhat selectively to support their points of view. Evidence for this can be found not only in the QC literature.

Theories are ideal because reality is too complex to be fully mapped into model systems and computing power is still too limited. Unfortunately, reality is imperfect, experimental resolution mostly too low, samples are not pure enough, annealing times too short, data finally too inaccurate, and funding never sufficient. It is particularly difficult to communicate experimental results to theoreticians and *vice versa*. There is a source of misunderstandings if a theoretician him/herself tries to interpret HRTEM images or electron density maps to find confirmation for his/her hypothesis; or, if an experimentalist looks to his/her data through the filter of the higher-dimensional description and wants to prove that a few ring contrasts on a HRTEM image are sufficient to prove strict quasiperiodicity.

There is also a problem in the interpretation of qualitative and quantitative structural information. It is state-of-the-art in structure research to describe a crystal structure quantitatively (coordinates, atomic displacement parameters, etc.). Due to the easy access to HRTEM images, structure solution is often reduced to a simplistic contrast interpretation of the projected structure. However, this should be only a first step to a quantitative structure description. A similar problem occurs in X-ray structure analysis, which always is the refinement of a globally averaged structure model. One never knows whether or not a better model does exist. This uncertainty should be considered in the discussion of the results.

The story of decagonal Al–Co–Ni (see chapter 5.2.1.4) is the perfect example for the long way scientists have to go in QC research until observation, interpretation, and modeling converge. Certainly, the end of this walk, fortunately not a random walk, is still out of sight. Looking back, however, real progress becomes visible.

Electron microscopy

General overviews of the application of electron microscopic methods to QC are given by Hiraga (2002) and Beeli (2000), and in general by Smith (1997), for instance.

SAED (selected area electron diffraction)

Due to multiple scattering and other interaction potentials, SAED patterns significantly differ from X-ray diffraction (XRD) patterns. The reflection intensities are not proportional to the squares of the structure amplitudes as it is the case if the kinematical theory applies. For SAED pattern calculation dynamical theory is needed, the powerful tools of X-ray structure analysis (direct methods, e.g.) do not work. However, the rapid progress in electron crystallography is going to change this situation (see Dorset, Gilmore, 2003). Multiple scattering generally leads to a relative enhancement of weak reflections and diffuse scattering. However, compared to X-ray diffraction, the SAED exposure time is usually much shorter, the intrinsic background much higher and the dynamical range of the SAED patterns much smaller (2–3 orders of magnitude). X-ray intensities may be quantitatively collected within a dynamical range of eight orders of magnitude. Diffraction symmetry (Laue class) as well as systematic extinctions

are imaged in the same way as in the case of X-ray and neutron diffraction.

There are some other reasons as well for the difference in SAED and XRD patterns. Due to the small penetration depth of the electron beam in the sample (<1000 Å) and its usually small diameter (500–5000 Å) (Tsuda, Nishida, Tanaka, Tsai, Inoue, Masumoto, 1996), scattering information of submicroscopic parts of a sample can be obtained only (the volume of a sample for XRD is larger by about nine orders of magnitude).

CBED (convergent beam electron diffraction)

By this method a very small area of the thinned (≈ 100 Å thickness) sample with 10–100 Å diameter is probed by the convergent electron beam. This method allows, for instance, deriving the full point group symmetry of the sample (Tanaka, 1994) instead of just the Laue class. One can even quantitatively refine the parameters of a trial structure model by fitting the line profiles of the high-order Laue-zone (HOLZ) reflections (see, for instance, Tsuda, Tanaka, 1995). Thus, by this method it is possible to determine the structure of a cluster, for instance.

HRTEM (high-resolution transmission electron microscopy)

The contrasts visible on electron micrographs are related to the projected structure (potential). They strongly depend on sample thickness (>50 Å) and defocus value. Their interpretation is not straightforward and contrast simulations should confirm the models derived. For instance, Tsuda, Nishida, Tanaka, Tsai, Inoue, Masumoto (1996) demonstrated by computer simulations that a pentagonal cluster model can produce HRTEM images with local pentagonal as well as decagonal symmetry depending on the accelerating voltage, 200 kV and 300 kV, respectively.

The lateral resolution of HRTEM experiments is approximately 1 to 2 Å depending on the acceleration voltage of the electrons. However, it is not always possible to work at highest resolution because even metallic samples may undergo structural changes under irradiation, in particular for voltages >400 kV (sometimes >250 kV).

An automated approach for the analysis of HRTEM images of QC was developed by Soltmann, Beeli (2001) based on previous work of Joseph, Ritsch, Beeli (1997). This technique should be used to match tilings to the observed contrasts in an unbiased way.

HAADF-STEM (high-angle annular detector dark-field scanning transmission electron microscopy) or Z-contrast method

The image is formed by electrons scattered incoherently at high angles (≈ 100 mrad) in a STEM. Dynamical effects and the influence of specimen thickness are less significant compared to SAED and HRTEM. By a finely focused electron beam (≈ 2 Å diameter) as probe the specimen is scanned illuminating atomic column by atomic column. The annular detector generates an intensity map of incoherently scattered electrons with atomic number (Z) contrast. Therefore, this method is also called 'Z-contrast method' (see Saitoh, Tsuda, Tanaka, Tsai, 2000, and references therein; Pennycook, 2002). Thus, in case of transition-metal aluminides it allows an easy differentiation

between contrasts originating from transition metal atoms or from aluminum atoms. Usually the contrast is reversed compared with HRTEM micrographs. Image deformation is possible due to the sample drift obscuring the symmetry (distortion of decagonal clusters, for instance).

Electron and Ion beam irradiation

By fast particle irradiation of a sample above a specific energy (20–30 eV) threshold radiolytic (ionization and bond breaking) or knock-on (collision and knocking out of atoms from their sites) damage can take place. Radiolytic effects predominantly occur at low energies, knock-on effects only at high-energies. The induced defects accelerate atomic diffusion considerably (Gittus, 1978; Smith, 1997). This may overcome the sluggish kinetics of low-temperature phase transformations. Irradiation by electrons in the electron microscope may induce structural defects already for energies >250 keV (Ritsch, Beeli, Nissen, Lück 1995).

XRD (X-ray diffraction) and Neutron diffraction (ND)

In both cases, the kinematical theory can be applied to describe the correspondence between structure and diffraction pattern of a sample. A very powerful toolbox of structure determination techniques has been developed during the past 80 years, which allow solving even virus structures in a more or less straightforward way. Some of these tools (Patterson analysis, least-squares refinement, method of entropy maximization etc.) have been modified for higher-dimensional structure analysis. XRD on polycrystalline materials is often used to characterize quasicrystalline samples and to check their quality. It has to be kept in mind, however, that a powder XRD pattern is just a projection of the full 3D reciprocal space information upon 1D. Superposition of Bragg peaks and levelling out of structured diffuse scattering is the rule. High-resolution powder XRD may be used as a fingerprint of a known QC or for the accurate determination of lattice parameters. It must not be used as the sole proof for quasiperiodicity or perfection of a QC.

Single-crystal XRD or elastic ND are the diffraction methods of choice. The Bragg reflections carry information about the globally averaged structure, the diffuse intensities about the pair correlation functions of local structural deviations from this average structure. A 3D resolution better than 0.001 Å can easily be obtained. XRD and ND are sometimes complimentary in scattering power. This can be used to distinguish, for instance, the ordering of Co and Ni. The different scattering power of different isotopes of an element can be used to calculate partial structure factors.

In case of an n D structure analysis, the long-range order of a QC structure is coded in the fine details of atomic surfaces (occupation domains, hyperatoms). Consequently, 5D structure analysis means determination of the detailed shape and internal structure of the atomic surfaces. Since the atomic surfaces are mainly extended in perpendicular space, reflections with large perpendicular space components of the diffraction vectors are particularly important in the refinement of their detailed structure (shapes of domains and subdomains, chemical composition, occupancy factors, parallel space shifts, mean square random displacement parameters in perpendicular and parallel

space). Unfortunately, this class of reflections is intrinsically weak. Since it is crucial to include in the n D refinements as much as possible information about weak reflections, no threshold value ($I > 3\sigma(I)$, for instance) should be set as it is often done in the course of standard structure analyses of periodic structures. It is also very important to check the results of an n D refinement not only by global reliability factors (R -factors) but also by $F(\text{obs})/F(\text{calc})$ -plots and statistical analysis (cf. Cervellino, Steurer, Haibach, 2002, for instance).

The potentialities and limits of XRD on QC have been discussed by Haibach, Cervellino, Estermann, Steurer (2000) with the focus on Bragg scattering and by Estermann, Lemster, Haibach, Steurer (2000) focusing on diffuse scattering. Those of ND have been outlined by de Boissieu (2000), Frey (2002) and Frey, Weidner (2003) with emphasis on Bragg and diffuse scattering, respectively.

Inelastic and quasielastic neutron scattering

The study of the dynamical properties of QC, i.e. the phonon and phason dynamics, can be performed in the usual way by inelastic and quasielastic NS, respectively (de Boissieu, 2000; Coddens, Lyonnard, Hennion, Calvayrac, 2000, and references therein).

Coherent X-ray diffraction

With the advent of third generation synchrotron sources (partly) coherent X-ray radiation became available. It can be particularly useful in the interpretation of the diffuse scattering. For instance, the study of the phason dynamics may profit from this technique (Letoublon, Yakhov, Livet, Bley, de Boissieu, Mancini, Caudron, Vettier, Gastaldi, 2001).

Higher-dimensional approach

This approach, first proposed by deWolff (1974) for incommensurately modulated structures, is very powerful in case of perfectly ordered quasiperiodic structures with dense atomic surfaces of polygonal shape (Yamamoto, 1996b; Steurer, Haibach, 2001; and references therein). It is also the only way to apply crystallographic tools such as the Patterson technique or direct methods. It allows 'lifting' atoms or clusters and refining easily infinite structures in a closed form. However, the n D approach does not work properly for (strongly) disordered structures and 'non-quasicrystallographical' degrees of freedom (continuous shifts instead of phason flips etc.). It also does not work properly in case of QC with random-tiling related structures (Henley, Elser, Mihalkovic, 2000).

Tiling decoration approach

This 3D approach (Mihalkovic, Mrafko, 1997, and references therein) is much more flexible than the n D approach, in particular if the tiling is not fixed and if beside vertex flips also continuous atomic shifts are possible. It allows modeling easily even tilings that possess fractal atomic surfaces in the n D description, which are common for maximum-density disk packings (Cockayne, 1995), for instance, or random tilings in the general meaning. The geometrical degrees of freedom of each atom can vary continuously in this approach contrary to the phason coordinate shifts in the n D description, for instance. To

get a physically and crystal-chemically reasonable model by the tiling decoration method, some constraints are needed. Joint refinements minimizing the differences between calculated and observed diffraction data and the energy of the system show promising results (Henley, Mihalkovic, Widom, 2002). A drawback is that only a rather limited “box of atoms” can be used as model.

Quasi-unit-cell approach

This term has been coined by Steinhardt, Jeong (1996). It refers to the description of quasiperiodic structures by coverings. In a covering, one single structure motif (cluster) is sufficient to build a quasiperiodic structure while for a tiling at least two different unit tiles are needed. How such a quasi-unit-cell (“monopteros”) and its overlaps could look like has already been shown for d-Al–Co–Ni by Steurer, Haibach, Zhang, Kek, Lück (1993). A decagon with overlap rules forcing a covering fully equivalent to a Penrose tiling was discovered by Gummelt (1996). Steinhardt, Jeong (1996) showed that the Penrose tiling contains the maximum possible number of these Gummelt-decagons. If it were decorated with an energetically favorable cluster, the quasiperiodic covering would have the lowest total energy. However, this is not always true. The density of pentagons in the approximant O_2 (Dong, Dubois, Song, Audier, 1992), for instance, is with 0.854 higher than in the pentagonal Penrose tiling where it amounts to $\tau/2 = 0.809$. Consequently, the total energy of a structure with energetically favorable pentagonal clusters would be lower for the approximant than for the quasicrystal.

Clusters

Most recent models of quasiperiodic structures are based on one or more unit clusters. However, the term ‘cluster’ is not always used with the same meaning. The classical definition distinguishes between ‘naked’ clusters as obtained and investigated in mass spectrometers, for example, and embedded clusters, like in metallorganic compounds. In both cases it is clearly defined which atom belongs to a cluster and which one does not. The chemical bond between an atom in the cluster to another atom in the same cluster clearly differs from the bond to an atom outside the cluster. In the QC community the term cluster is frequently used for “structure motif”, “structural unit”, “quasi-unit cell” or “coordination polyhedron”. For reviews on bare clusters see, for instance, Martin (1996), Wales, Munro, Doye (1996).

Tilings, coverings

Conventional crystal structures are crystallographically described by their (space group) symmetry and by the content of their unit cells. This has some analogies with the description of a QC structure in terms of a tiling or covering decorated by atoms or clusters (see Kramer, Papadopolos, 2003, and references therein). A quasiperiodic tiling can be built based on at least two unit tiles. The tiles are put together without any overlaps and gaps according to given matching rules (if there are any). The quasi-unit cell of a covering, for instance a decagon in case of decagonal structures, forms the structure by covering the plane (space) without gaps but with well-defined overlaps. The first time a decagonal cluster was used to

describe the structure of a decagonal phase by a covering was in the paper by Burkov (1992). He presented a model consisting of a random assembly of decagonal clusters.

From a crystal-chemical point of view, the structure may be seen as optimum packing of energetically favorable structural units such as coordination polyhedra. With other words, the optimization of interactions between atoms determines the type of coordination polyhedron and its way of packing. The problem of QC structure formation could then be reduced to the question why a quasiperiodic structure forms despite a large unit-cell approximant would locally have the same structure without sacrificing the benefits of periodicity.

Approximants

Crystalline approximants, i.e. phases with periodic structures that are locally similar to those of QC, play a key role for QC structure analysis. Their close relationship to QC can easily be seen on SAED patterns. The reciprocal lattice has basic vectors of characteristic length and the intensity distribution corresponds to the Fourier transform of the fundamental cluster building both the QC and the approximant. For reviews see, for instance, Goldman, Kelton (1993), Gratias, Katz, Quiquandon (1995), Tamura (1997).

Domain structures of approximants, resulting from a phase transformation from QC obey the usual twin laws. The lost symmetry elements relate approximant domains to each other (orientational twinning). Approximants often form nanodomain structures with coherent domain boundaries.

Disorder

Disorder related to short-range correlations within the quasiperiodic plane of a superperiod along the tenfold axis is discussed, for instance, by Tsai, Inoue, Masumoto (1995). For general reviews on diffuse scattering in QC see Steurer, Frey (1998) and Frey (2002). For modeling the short-range order in periodic crystal structures the Fourier transform of the cluster is multiplied by the Fourier transform of the finite crystal lattice. In case of a quasiperiodic structure, this has to be done in nD space using the cluster related atomic surfaces. In case of the Penrose tiling decorated with equal point atoms, for instance, the Fourier transform of the atomic surfaces (four pentagons) is only a function of the perpendicular space components of the reciprocal space.

5 The structure of axial quasicrystals

There are alternative descriptions of quasiperiodic structures possible either as incommensurately modulated phases or as composite crystals (Elcoro, Perez-Mato, 1996; Steurer, 2000). In these approaches, the special characteristics of QC such as scaling symmetry in reciprocal space, for instance, are just special cases.

In the case of octagonal and dodecagonal QC the alternative description as 2D incommensurately modulated structures may be more obvious than in the case of pentagonal or decagonal phases. The basic structures as well as the average structures are just tetragonal and hexagonal, respectively. This has important consequences. Firstly, in both cases a periodic average structure does exist. Secondly, the quasiperiodic structure can be described as 2D

modulation of a tetragonal and a hexagonal basic structure, respectively. By continuous variation of the length and orientation of the satellite vectors a transformation from the octagonal and dodecagonal structures to their tetragonal and hexagonal approximants, respectively, can be easily described. Thirdly, the finding that a dodecagonal QC can be nicely described as modulated phase (Uchida, Horiuchi, 1998a; 2000) is not an argument against the existence of the dodecagonal QC and its more appropriate, symmetry adapted description as quasicrystal.

In the following, the different classes of axial QC will be described in detail. The very few pentagonal QC known will be dealt together with decagonal phases.

5.1 Octagonal phases

A general introduction into simple octagonal tilings (Fig. 5.1-1), their generation and properties was given by Socolar (1989) and Ingalls (1993), for instance. The thermal and phason diffuse scattering for octagonal QC was discussed by Lei, Hu, Wang, Ding (1999). It is amazing that the only octagonal QC found ever were discovered within the two years 1987 and 1988 (Table 5.1-1).

Discovery

The first octagonal phase was discovered during the investigation of rapidly solidified samples of V–Ni–Si and Cr–Ni–Si alloys by SAED and HRTEM (Wang, Chen, Kuo, 1987). The contrasts resembled a square/rhomb octagonal tiling on a scale of several nanometers. The octagonal phase was found to coexist with an orientationally twinned approximant. This is a cubic phase with β -Mn structure type ($P4_132$, $a = 6.3 \text{ \AA}$) and pseudo-octagonal diffraction symmetry. The cube in the octagonal phase (i.e. the square in the octagonal tiling) has exactly the same size as the unit cell of the cubic phase, i.e. the edge lengths of the tiling is equal to the lattice parameter of the cubic phase.

HRTEM and SAED

A more perfect octagonal phase could be obtained in the system Mn–Si–Al (Wang, Fung, Kuo, 1988). Its symmetry was determined by CBED to $8/m$ or $8/mmm$. A qualitative comparison of 17 kinematically calculated and observed SAED reflection intensities (o-Cr–Ni–Si) was performed by Wang, Kuo (1988). The calculations were based on the canonical octagonal tiling (4D hypercubic lattice decorated by octagons).

A detailed structure model of o-Mn₈₀Si₁₅Al₅ was derived from HRTEM images based on the structure of

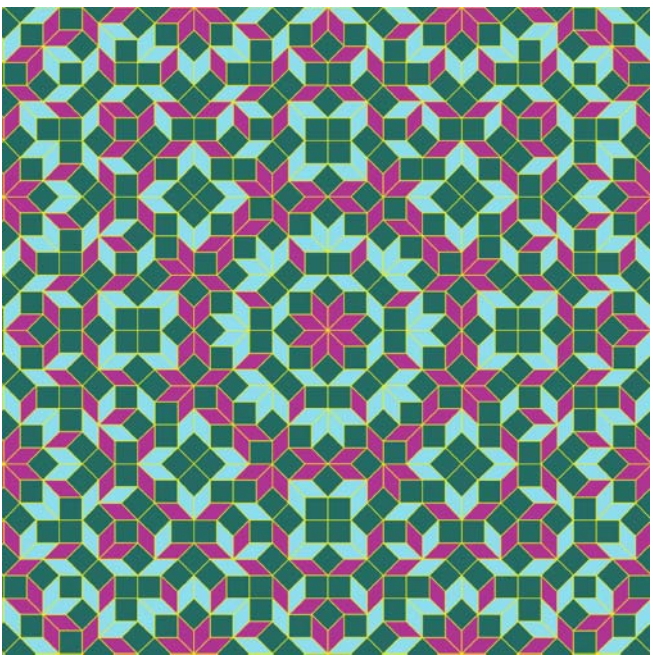


Fig. 5.1-1. Octagonal tiling generated by the dual-grid method using the JAVA applet *JTiling* (Weber, 1999).

β -Mn by Huang, Hovmöller (1991) and Jiang, Hovmöller, Zou (1995). The structure model consists of a stacking of four quasiperiodic layers with sequence $\dots ABAB' \dots$ and a period of 6.3 \AA . The layer A shows 8-fold symmetry while the layers B and B' are 4-fold symmetric only. B results by rotating layer B by 45° . Each layer corresponds to a quasiperiodic tiling built from 45 rhombs and squares with edge length $a_r = 8.2 \text{ \AA}$. These unit tiles can be further decomposed to tiles with an edge length $a'_r = 3.4 \text{ \AA}$, smaller by a factor $\sqrt{2} - 1$. The local symmetry is $8_4/mmc$. Based on this model, Ben-Abraham, Gähler (1999) developed a covering-cluster description. The octagonal QC has the highest density of this prismatic cluster. The authors also determined to $I8_4/mcm$ the 5D space group of the ideal structure obtained in this way.

A continuous change from metastable o-Cr–Ni–Si and o-Mn–Si–Al to the cubic phase with β -Mn structure type was observed by moving the SAED aperture successively from the octagonal to the cubic area of the samples (Wang, Kuo, 1990). The orientational relationship between the cubic and the octagonal phase resulted to

$$\begin{aligned} [001]_{\beta\text{-Mn}} &\parallel [00001]_{\text{octagonal}}, \\ [100]_{\beta\text{-Mn}} &\parallel [11000]_{\text{octagonal}}. \end{aligned}$$

The transformation was explained by gradual introduction of a phason strain field (Mai, Xu, Wang, Kuo, Jin, Cheng, 1989). A theoretical model based on the Schur rotation (i.e. a one-parameter rotation in the nD description) for this transition was published by Baake, Joseph, Kramer (1991). A theoretical analysis of the transformation of o-Mn–Si–Al to the β -Mn structure and to the Mn₃Si structure was performed by Xu, Wang, Lee, Fung (2000). The first transition takes place if the metastable octagonal phase is heated rapidly, and the other if it is heated slowly. The relationship between o-Mn–Si–Al and the β -Mn structure was described in more detail by Li, Cheng (1996).

Table 5.1-1. Timetable of the discovery of octagonal quasicrystals. All phases have been obtained by rapid solidification and all are metastable.

Year of discovery	Nominal Composition	Period along 8-fold axis	References
1987	o-V ₁₅ Ni ₁₀ Si	6.3 Å	Wang, Chen, Kuo (1987)
1988	o-Cr ₅ Ni ₃ Si ₂	6.3 Å	Wang, Chen, Kuo (1987)
1988	o-Mn ₄ Si	6.2 Å	Cao, Ye, Kuo (1988)
1988	o-Mn ₈₂ Si ₁₅ Al ₃	6.2 Å	Wang, Fung, Kuo (1988)
1988	o-Mn–Fe–Si		Wang, Kuo (1988)

5.2 Decagonal phases

Contrary to octagonal and dodecagonal phases, decagonal phases have been discovered more or less continuously over the last fifteen years (Tab. 5.2-1 and -2). There are many theoretical papers on tilings, which may serve as quasilat- tices of decagonal phases, the most famous one is the Penrose tiling (Fig. 5.2-1). More information on pentagonal and decagonal tilings can be found in Ingalls (1992) and Pavlovitch, Kleman (1987), for instance. There are only a few “quantitative” X-ray and neutron structure analyses of decagonal QC (Tab. 5.2-3) and approximants (Tab. 5.2-4) beside a huge number of “qualitative” electron microscopic (HRTEM, HAADF, ALCHEMI, SAED, CBED etc.) studies and quite a few spectroscopic (EXAFS, NMR, electron or ion channeling etc.) structural investigations. In the last few years, an increasing number of surface structural studies, most of them by STM or AFM, has been carried out.

The results of all these studies, i.e. in some way ideal- ized 3D and/or 5D structure models, indicate that at least some classes of QC posses rather well ordered quasiperi- odic structures with correlation lengths up to several micro- meters. There remain, however, many uncertainties since the amount of accessible experimental data is rather small compared to the complexity of the problem.

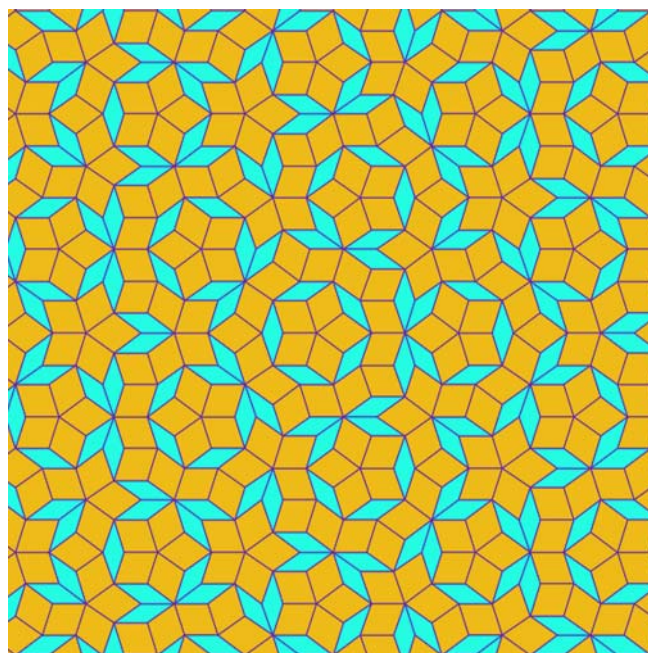


Fig. 5.2-1. Penrose tiling generated by the dual-grid method using the JAVA applet *JTiling* (Weber, 1999).

Table 5.2-1. Timetable of the discovery of stable decagonal quasicrystals. Only a few decagonal phases have been proved by differ- ent groups to be thermodynamically stable.

Year of discovery	Nominal alloy Composition	Period along 10-fold axis	References
1988	d-Al ₆₅ Cu ₂₀ Co ₁₅	4(8) Å	He, Zhang, Wu, Kuo (1988)
1989	d-Al ₇₀ Ni ₁₅ Me ₁₅ (Me = Co, Fe)	4(8) Å	Tsai, Inoue, Masumoto (1989a)
1989	d-Al ₆₅ Cu ₁₅ Rh ₂₀	4(8,12) Å	Tsai, Inoue, Masumoto (1989d)
1991	d-Al ₇₀ Pd ₁₅ Mn ₁₅	12 Å	Beeli, Nissen, Robadey (1991)
1991	d-Al ₇₅ Me ₁₀ Pd ₁₅ ^a (Me=Fe, Ru, Os)	16 Å	Tsai, Inoue, Masumoto (1991)
1992	d-Al ₇₂ Cu ₁₂ Cr ₁₆ ^b	37.8 Å	Okabe, Furihata, Morishita, Fujimori (1992)
1995	d-Al ₇₀ Ni ₂₀ Rh ₁₀	4(8) Å	Tsai, Inoue, Masumoto (1995)
1997	d-Ga ₃₃ Fe ₄₆ Cu ₃ Si ₁₈ ^c	12.5 Å	Ge, Kuo (1997)
	d-Ga ₄₃ Co ₄₇ Cu ₁₀ ^c	?	Ge, Kuo (1997)
	d-Ga ₃₅ V ₄₅ Ni ₆ Si ₁₄ ^c	?	Ge, Kuo (1997)
1997	d-Al ₄₀ Mn ₂₅ Fe ₁₅ Ge ₂₀ ^d	12 Å	Yokoyama, Yamada, Fukaura, Sunada, Inoue, Note (1997)
1997	d-Zn ₅₈ Mg ₄₀ Dy ₂	5.1 Å	Sato, Abe, Tsai (1997)
1997	d-Al ₆₅ Cu ₂₀ Ir ₁₅		Athanasiou (1997)
1998	d-Zn ₅₈ Mg ₄₀ RE ₂ (RE=Dy, Er, Ho, Lu, Tm, Y)	5.1 Å	Sato, Abe, Tsai (1998)
2000	d-Al ₇₀ Ni ₂₀ Ru ₁₀	16.7 Å	Sun, Hiraga (2000a)

a: sample seems to be stable at least for an annealing time of 48 h at 1100 K. At least, Al–Fe–Pd turned out to be unstable in later investigations (Balanetskyy et al., 2004).

b: sample is stable in a very small temperature range around 1000 °C at least for an annealing time of 100 h. However, according to Wu, Ma, Kuo (1996) it disappears after “long” annealing.

c: sample is stable in a small temperature range above around 800 °C at least for an annealing time of 48 h. It forms from the low-temperature crystalline approximant.

d: sample with decaprismatic morphology ($d > 0.1$ mm) is stable above around 798 K, for instance at 1050 K at least for an annealing time of 100 h and seems to be retained up to the melting temperature $T_m = 1070$ K.

Year of discovery	Nominal Alloy Composition	Period along 10-fold axis	References
1985	d-Al ₄ Mn	12.4 Å	Bendersky (1985)
1985	d-Al ₅ Ru	16 Å	Bancel, Heiney (1986)
1986	d-Al–Pd	16.5 Å	Bendersky (1986)
1986	d-Al–Pt ^a	16 Å	Bancel, Heiney (1986)
1986	d-Al _{4.5} Fe	16.4 Å	Fung, Yang, Zhou, Zhao, Zhan, Shen (1986)
1987	d-Al ₅ Os	16 Å	Kuo (1987)
1987	d-Al–Cr(–Si)	12 Å	Kuo (1987)
1987	d-V–Ni–Si		Kuo, Zhou, Li (1987)
1987	d-Al ₇₇ Co _{22.5}	16 Å	Dong, Li, Kuo (1987)
1987	d-Al ₇₉ Mn _{19.4} Fe _{2.6}		Ma, Stern (1987)
1988	d-Al ₅ Ir	16 Å	Ma, Wang, Kuo (1988)
1988	d-Al ₅ Rh	16 Å	Ma, Wang, Kuo (1988)
1988	d-Al ₄ Ni	4 Å	Li, Kuo (1988)
1988	d-Al ₆ Ni(Si)	16 Å	Li, Kuo (1988)
1988	d-Al ₆₅ Cu ₂₀ Mn ₁₅	12 Å	He, Wu, Kuo (1988)
1988	d-Al ₆₅ Cu ₂₀ Fe ₁₅	12 Å	He, Wu, Kuo (1988)
1988	d-Al ₆₅ Cu ₂₀ Co ₁₅	8, 12, 16 Å	He, Wu, Kuo (1988)
1988	d-Al ₇₅ Cu ₁₀ Ni ₁₅	4 Å	He, Wu, Kuo (1988)
1988	d-Al ₄₀ Cu ₁₀ Ge ₂₅ Mn ₂₅		Kimura, Inoue, Bizen, Masumoto, Chen (1988)
1989	d-Al–Cr–Si		Zhang, Wang, Kuo (1989)
1990	d-Al ₅ Os	4.2 Å	Wang, Gao, Kuo (1990)
1990	d-Al ₅ Ru	4.2 Å	Wang, Gao, Kuo (1990)
1990	d-Fe ₅₂ Nb ₄₈	4.7 Å	He, Yang, Ye (1990)
1990	d-Al ₇₈ Co ₂₀ Pd ₁₀	4 Å	Tsai, Yokoyama, Inoue, Masumoto (1990)
1993	d-Al ₇₂ Mg _x Pd _{28–x} , 5 ≤ x ≤ 10	16.57 Å	Koshikawa, Edagawa, Honda, Takeuchi (1993)
1995	d-Al ₇₀ Ni ₂₀ Ir ₁₀	4 Å	Tsai, Inoue, Masumoto (1995)
1995	d-Al ₇₂ Co ₂₈	8 Å	Tsai, Inoue, Masumoto (1995)
1995	d-Al ₇₀ Ni ₁₃ Ir ₁₇	16 Å	Tsai, Inoue, Masumoto (1995)
1997	d-Ga _{52–63} Mn _{48–37}	12.5 Å	Wu, Kuo (1997)
2000	d-Al ₇₀ Ni ₂₀ Ru ₁₀	4 Å	Sun, Hiraga (2000a,b)
2002	d-Co(Al,Ga) ₃ , x _{Ga} ≤ 0.1		Ellner, Meyer (2002)

a: Could not be confirmed by Ma, Kuo, Wang (1990)

Table 5.2-2. Timetable of the discovery of metastable decagonal quasicrystals obtained by rapid solidification.

Table 5.2-3. Quantitative X-ray structure analyses of d-Al–Co–Cu, d-Al–Co–Ni. Whether *R* factors are based on structure amplitudes or on intensities is unclear in most cases (intensity based *R* factors are approximately by a factor two larger than the structure amplitude based ones). *D_x* ... calculated density, PD ... point density, SG ... space group, PS ... Pearson symbol, *N_R* ... number of reflections, *N_V* ... number of variables. The quasilattice parameter listed is $a_i^y = \sqrt{5}/\tau a_i^y$ (a_i^y is defined in Steurer, Haibach, 1999a; a_i^y is defined in Yamamoto, Ishihara, 1988).

Nominal composition	SG PS	Lattice parameters	<i>D_x</i> PD	<i>N_R</i> <i>N_V</i>	<i>R</i> <i>wR</i>	Reference
d-Al ₆₅ Co ₁₅ Cu ₂₀	<i>P</i> 10 ₅ / <i>mmc</i>	$a_{1...4} = 3.765(3) \text{ Å}$ $a_5 = 4.1481(3) \text{ Å}$	4.4	259 11	0.167 0.098	Steurer, Kuo (1990a, b)
d-Al ₇₀ Co ₂₀ Ni ₁₀	<i>P</i> 10/ <i>mmm</i>	$a_{1...4} = 3.80 \text{ Å}$ $a_5 = 4.08 \text{ Å}$	0.0680	41 2	0.110	Yamamoto, Kato, Shibuya, Takeuchi (1990)
d-Al ₇₀ Co ₁₅ Ni ₁₅	<i>P</i> 10 ₅ / <i>mmc</i>	$a_{1...4} = 3.794(1) \text{ Å}$ $a_5 = 4.0807(3) \text{ Å}$	4.5 0.0741	253 21	0.091 0.078	Steurer, Haibach, Zhang, Kek, Lück (1993)
d-Al ₇₀ Co ₁₅ Ni ₁₅	<i>P</i> 10 ₅ / <i>mmc</i>	$a_{1...4} = 3.794(1) \text{ Å}$ $a_5 = 4.0807(3) \text{ Å}$	–	253 18	0.092 0.080	Elcoro, Perez-Mato (1995)
d-Al ₇₂ Co ₈ Ni ₂₀	<i>P</i> 10 ₅ / <i>mmc</i>	$a_{1...4} = 3.758 \text{ Å}$ $a_5 = 4.090 \text{ Å}$	3.94 0.0661	449 103	0.063 0.045	Takakura, Yamamoto, Tsai (2001)
d-Al _{70.6} Co _{6.7} Ni _{22.7}	<i>P</i> $\overline{1}0$	$a_{1...4} = 3.757(2) \text{ Å}$ $a_5 = 4.0855(1) \text{ Å}$	3.89 0.0644	2767 750	0.170 0.060	Cervellino, Haibach, Steurer (2002)

Table 5.2-4. Quantitative X-ray structure analyses of d-phase approximants. The pseudodecagonal axis is underlined. D_x ...calculated density, SG... space group, PS... Pearson symbol, N_R ... number of reflections, N_V ... number of variables.

Nominal composition	SG PS	Lattice parameters	D_x	N_R N_V	R wR	Reference
Co ₂ Al ₅ Al _{71.5} Co _{28.5}	<i>P6₃/mmc</i> <i>hP28</i>	$a = 7.6717(4) \text{ \AA}$ $c = 7.6052(5) \text{ \AA}$ $c/a = 0.9913$			0.072	Burkhardt, Ellner, Grin, Baumgartner (1998)
(Al,Cu) ₁₃ Co ₄ Al _{71.5} Co _{23.6} Cu _{4.9}	<i>Cm</i> <i>mC102</i>	$a = 15.2215(4) \text{ \AA}$ $b = 8.0849(2) \text{ \AA}$ $c = 12.3908(3) \text{ \AA}$ $\beta = 108.081(1)^\circ$			0.020	Freiburg, Grushko (1996)
Al ₁₁ Co ₄ Al _{73.24} Co _{26.76}	<i>P2</i> <i>mP52</i>	$a = 24.661(5) \text{ \AA}$ $b = 4.056(9) \text{ \AA}$ $c = 7.569(2) \text{ \AA}$ $\beta = 107.88(3)^\circ$	4.26	718 240	0.088	Li, Shi, Ma, Ma, Kuo (1995)
Co ₄ Al ₁₃ Al _{73.7} Co _{26.3}	<i>Cm</i> <i>mC102-5.2</i>	$a = 15.183(2) \text{ \AA}$ $b = 8.122(1) \text{ \AA}$ $c = 12.340(2) \text{ \AA}$ $\beta = 107.9(1)^\circ$	3.81		0.122 ^a 0.142 ^b	Hudd, Taylor (1962)
Co ₂ NiAl ₉ Al _{74.8} Co ₁₇ Ni _{8.2}	<i>Immm</i> <i>oI96</i>	$a = 12.0646(7) \text{ \AA}$ $b = 7.5553(7) \text{ \AA}$ $c = 15.353(1) \text{ \AA}$	3.98	437	0.112 0.117	Grin, Peters, Burkhardt, Gotzmann, Ellner (1998)
Al _{13-x} (Co _{1-y} Ni _y) ₄ Al _{75.2} (Co, Ni) _{24.8}	<i>C2/m</i> <i>mC34-1.8</i>	$a = 17.071(2) \text{ \AA}$ $b = 4.0993(6) \text{ \AA}$ $c = 7.4910(9) \text{ \AA}$ $\beta = 116.17(1)^\circ$	3.96	963 58	0.053 0.034	Zhang, Gramlich, Steurer (1995)
o-Co ₄ Al ₁₃ Al ₇₆ Co ₂₄	<i>Pmn2₁</i> <i>oP102</i>	$a = 8.158(1) \text{ \AA}$ $b = 12.342(1) \text{ \AA}$ $c = 14.452(2) \text{ \AA}$ $\beta = 107.9(1)^\circ$		839	0.062	Grin, Burkhardt, Ellner, Peters (1994b)

a: For [110] projections

b: For [010] projections

Most X-ray or neutron diffraction structure analyses of decagonal QC have been based on a ridiculously small number of Bragg reflections. Even for low-order rational approximants, much larger data sets have been used (see Tab. 5.2-3 and -4). How many reflections should be used and how many can be observed anyway? The total number of Bragg reflections n_{tot} we can expect for a diffraction experiment on a periodic crystal can be calculated from the formula $n_{\text{tot}} = (2\pi V)/(3d_{\text{min}}^3)$, with unit cell volume V and resolution $d_{\text{min}} = \lambda/(2 \sin(\theta_{\text{max}}))$. This number calculated for a high-order approximant gives also an estimate of the number of reflections, which should be observable in case of the related quasicrystal. One should keep in mind, however, that such a diffraction data set allows determining the structure of the QC only on a scale comparable to the approximant unit cell size. Most information about the type of quasiperiodic LRO is in the very weak reflections with large perpendicular-space components of the diffraction vectors. This would correspond to rational approximants with lattice parameters of the order of micrometers and billions of Bragg reflections.

The smallest observed distance between Bragg reflections of decagonal Al–Co–Ni amounts to $\approx 0.008 \text{ \AA}^{-1}$ (Beeli, Steurer, 2000; Steurer, Cervellino, Lemster, Ortelli, Estermann, 2001). In case of a cubic rational approximant, this would correspond to a lattice parameter of 125 Å. A

full data set would consist of $n_{\text{tot}} = 11\,464\,952$ Bragg reflections for standard resolution ($\text{MoK}\alpha$, $\theta_{\text{max}} = 30^\circ$). The number of unique reflections would amount to $n_{\text{tot}}/48 = 238\,853$. In case of a decagonal QC with 4.17 Å periodicity and 10/*mmm* Laue symmetry we would expect $n_{\text{tot}}/(30 \times 40) = 9554$ unique reflections. This is much more than what has been used in the structure analyses of decagonal phases published so far.

It is surprising, however, that we do not observe many more Bragg reflections for QC than for their low-order approximants. For instance, along reciprocal lattice lines of QC corresponding to net planes with Fibonacci sequence-like distances rarely more than 30 reflections are observed (dynamic range of $I_{\text{max}}/I_{\text{min}} \leq 10^6$, $0 \leq \sin(\theta/\lambda) \leq 0.8$). According to Steurer (1995) the expected number of reflections for this dynamic range would be 3940; and still 389 for a dynamic range of $I_{\text{max}}/I_{\text{min}} \leq 10^4$. This indicates a significant deviation from perfect quasiperiodic order and makes impossible an accurate structure solution solely by diffraction methods. Just for comparison, even such imperfect crystals as those of biological macromolecules exhibit often more than one million observable reflections. This finding may be explained by the fact that QC are usually annealed at high-temperatures and then rapidly quenched. By this procedure, a considerable amount of atomic disorder (correlated and random phason fluctua-

tions, thermal vacancies etc.) is frozen in to some extent. The diffraction experiment is performed on such a metastable sample that is in a partially relaxed but not very well-defined state. This is illustrated in Fig. 5.2.1.4-5 on the example of the temperature dependence of the diffuse interlayers in the diffraction pattern of decagonal $\text{Al}_{70}\text{Co}_{12}\text{Ni}_{18}$. In situ HT X-ray diffraction experiments show that the diffuse intensities become sharper with raising the temperature from RT to 800 °C.

The period along the decagonal axis results from the stacking of structural units. In all decagonal phases, the smallest structural unit is a pentagonal antiprism (PA) (i.e. an icosahedron without caps, or the period of a stack of interpenetrating icosahedra) (see, for instance Steurer, Haibach, Zhang, Kek, Lück, 1993). This PA is coordinated by a puckered decagon yielding a decoration of each one of the ten side planes by a tetrahedron. This structure motif is also common in approximants (Boström, Hövmöller, 2001).

5.2.1 4 Å and 8 Å periodicity

5.2.1.1 Al–Co

Discovery

Based on the similarity of the X-ray powder diffractogram of rapidly solidified $\text{Al}_{86}\text{Co}_{14}$ to that of d-Al–Mn, Dunlap, Dini (1986) concluded erroneously icosahedral quasicrystallinity of that sample. This was confirmed by a SAED study on $\text{Al}_{74}\text{Co}_{26}$ by which a metastable decagonal QC with ≈ 8 Å periodicity was identified (Suryanarayana, Menon, 1987). Menon, Suryarayana (1989) discuss the polytypism of this d-phase, which can exhibit ≈ 4 , ≈ 8 , ≈ 12 and ≈ 16 Å periodicity. After heating the rapidly solidified sample with ≈ 16 Å periodicity to above 450 K, a transformation to ≈ 12 Å periodicity was observed *in situ*. An *in situ* study of the formation of d-Al–Co in Al–Co multilayers with starting composition $\text{Al}_{13}\text{Co}_4$ was performed by Bergman, Joulaud, Capitan, Clugnet, Gas (2001). The formation of Al_9Co_2 takes place

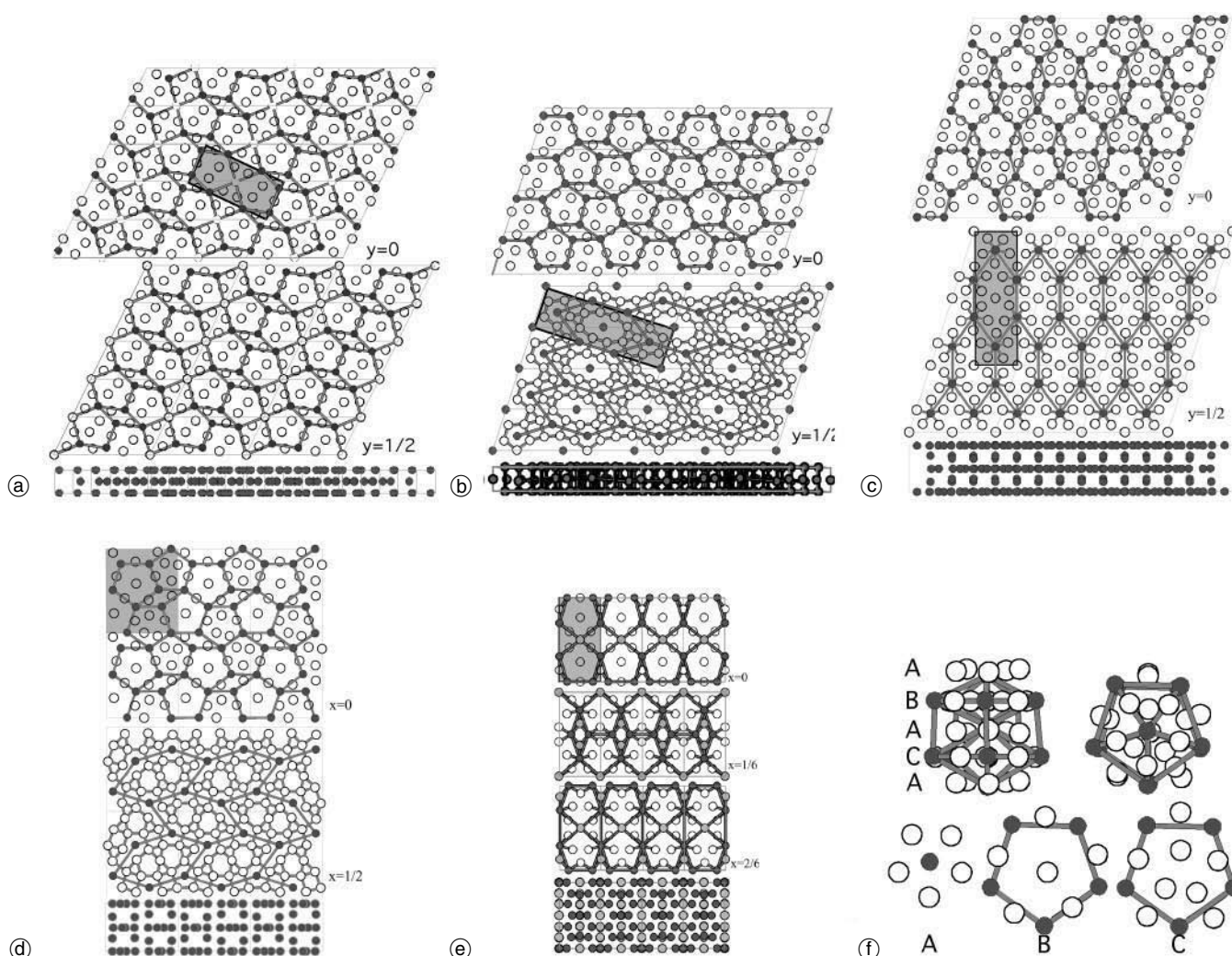


Fig. 5.2.1.1-1. Atomic layers and projected transition metal (TM) substructures of (a) $\text{Al}_{13}(\text{Co,Ni})_4$, (b) $\text{Al}_{11}\text{Co}_4$, (c) $m\text{-Al}_{13}\text{Co}_4$, (d) $o\text{-Al}_{13}\text{Co}_4$, (e) $\text{Al}_9\text{Co}_2\text{Ni}$. Flat pentagon-rhomb (PR-) layers alternate with puckered hexagon (H-) layers. The unit cell of the rational $\langle 2,2 \rangle$ -approximant is shown in (a) and (e), that of the $\langle 2,3 \rangle$ -approximant in (b) and (c), and that of the $\langle 3,2 \rangle$ -approximant is shown in (d), respectively. Five Al atoms pentagonally coordinate each TM atom of the H-layers. (TM atoms are represented by filled circles, Al

atoms by empty circles). (f) Example for a particular realization (in $o\text{-Al}_{13}\text{Co}_4$) of the fundamental cluster of decagonal Al–Co–Ni and its approximants: a pentagonal bipyramid (PBP) of TM atoms (black circles) is filled with Al atoms (empty circles). The number of Al atoms in a TM pentagon may vary between 1 and 5. The edge lengths of the slightly distorted PBPs vary between 4.5 and 4.9 Å. The double PBP shown has a period of approximately 8 Å along its axis.

in the first two steps, and then d-Al–Co is formed and remains stable up to the final temperature of 600°C. The growth of the d-phase seems not to be diffusion controlled but rather a consequence of easier nucleation with linear kinetics. The undercoolability and solidification of Al–Co melts with 72% and 74% Al was studied by Schroers, Holland-Moritz, Herlach, Grushko, Urban (1997). They found much larger values for the β -phase than for the d-phase. It was concluded that the interfacial energy of the d-phase should be much smaller than that of the β -phase due to icosahedral short-range order in the melt.

A SAED study was performed on slowly cooled samples with compositions $\text{Al}_{13-x}\text{Co}_4$ ($x = 0, 1, 1.5, 2, 2.5, 3$) (Ma, Kuo, 1992). Beside the d-phase, also a number of new approximants, such as primitive and centered monoclinic $\tau^2\text{-Al}_{13}\text{Co}_4$ ($a = 39.8$, $b = 8.1$, $c = 32.2$ Å, $\gamma = 108^\circ$) and o- $\text{Al}_{13}\text{Co}_4$ ($a = 12.5$, $b = 8.1$, $c = 14.6$ Å) have been identified. A detailed model (with atomic positions) of the structure of o- $\text{Al}_{13}\text{Co}_4$ based on HRTEM images was proposed by Li, Ma, Kuo (1994) and based on X-ray diffraction by Grin, Burkhardt, Ellner, Peters (1994b). The structure of an orthorhombic phase with composition $\text{Al}_{11}\text{Co}_4$ was determined by Li, Shi, Ma, Ma, Kuo (1995), however, no stable or metastable phase of this composition could be confirmed in the studies of the binary system Al–Co around the composition of the d- Al_3Co phase (Grushko, Holland-Moritz, Bickmann, 1996; Grushko, Holland-Moritz, 1997; Gödecke, 1997b; Gödecke, Ellner, 1996). According to Grushko, Freiburg, Bickmann, Wittenberg (1997) $\text{Al}_{11}\text{Co}_4$ may be just m- $\text{Al}_{13}\text{Co}_4$ in a non-standard setting (the calculated powder diffraction pattern of $\text{Al}_{11}\text{Co}_4$ fits well with the experimental for $\text{Al}_{13}\text{Co}_4$). Quantum-mechanical calculations also confirmed the instability of this phase (Widom, Moriarty (1998). $\tau^2\text{-Al}_{13}\text{Co}_4$ was studied in detail by electron microscopy by Ma, Li, Kuo (1995), Mo, Sui, Ma, Kuo (1998), Li, Hiraga (1998) as well as by Saitoh, Yokosawa, Tanaka, Tsai (1999).

Confirmed stable approximant phases in the binary system Al–Co are (Gödecke, Ellner, 1996): the high-temperature phase $\text{Al}_{13}\text{Co}_4(\text{h})$ with 75.25–76% Al (Zhang, Gramlich, Steurer, 1995), m- $\text{Al}_{13}\text{Co}_4$, o- $\text{Al}_{13}\text{Co}_4$, Al_3Co (i.e. $\tau^2\text{-Al}_{13}\text{Co}_4$) (see Table 5.2-4 and Fig. 5.2.1.1-1).

Modeling

A structure model of a phase with the lattice parameters of o- $\text{Al}_{13}\text{Co}_4$ with space group symmetry Pnmm was proposed by Widom, Phillips, Zou, Carlsson (1995) and its energetics determined. It consists of flat and puckered layers and has the lowest energy for a composition $\text{Al}_{73}\text{Co}_{27}$ (i.e. $\text{Al}_{11}\text{Co}_4$, see remark about its stability above) while o- $\text{Al}_{13}\text{Co}_4$ was found stable for a composition of $\approx \text{Al}_{75.8}\text{Co}_{24.2}$. Widom, Cockayne (1996) studied the energetics and atomic distribution function of Al–Co approximants. They point out the important role of pentagonal bipyramids (see Henley, 1993) as fundamental energetically favorable structure motifs. In a very comprehensive paper, Cockayne, Widom (1998a) study model structures and phason energetics of a 508-atom approximant of d-Al–Co with 8 Å periodicity by Monte Carlo simulations. The basic units, pentagonal bipyramids

(Fig. 5.2.1.1-f), decorate the vertices of an HBS-tiling with edge length ≈ 6.5 Å (similar to the model PB8 proposed by Henley, 1993). Simulations at 1000 K reveal some disorder of Co atoms uniquely associated with a HBS tiling with particular puckering. In the flat layers Al disorder is highest. Puckering disorder is likely to lead to an average structure with 4 Å periodicity and P10/mmm symmetry. A statistical description of atomic surfaces in the 5D description becomes necessary (e.g., Co occupying the middle part of a mixed Al/Co atomic surface; compare the experimental density shown in Steurer, Kuo, 1990b). Co mobility is highly dependent on the presence of Al vacancies. Two kinds of collective fluctuations of the pentagonal bipyramids are discussed: the more frequent ‘puckering flip’ shifts a column of clusters 4 Å along its axis; the ‘phason flip’ moves it and rotates it by 180° .

The atomic dynamics of $\text{Al}_{1-x}\text{TM}_x$ (TM = Co, Ni), $x = 0.3$, was studied by Mihalkovic, Elhor, Suck (2001) on the example of o- $\text{Al}_{13}\text{Co}_4$, h- Al_5Co_2 , o- $\text{Al}_9\text{Co}_2\text{Ni}$, o- Al_3Ni , d-Al–Co–Ni, using isotropic pair potentials for Al–Co (Ni was treated as Co). One of the most remarkable results is that the main stabilizing factor is the rigidity of the Co-subnetwork. The strongly oscillating tail of the Co–Co potential correlates the Co atoms far beyond the second-neighbor shells. Molecular dynamics annealing of the d-Al–Co–Ni model at 1000 K also showed the rather rigid Co-framework and highly mobile Al atoms (diffusive motion) as well.

5.2.1.2 Al–Ni

Discovery

In rapidly solidified samples of composition $\text{Al}_6\text{Ni}(\text{Si})$ and Al_4Ni d-phases with periodicities of ≈ 16 Å and ≈ 4 Å, respectively, have been found (Li, Kuo, 1988). In contrast to d-Al–Co, the formation by melt quenching of d-Al–Ni is quite difficult and only possible around 75% Al (Tsuda, Nishida, Saitoh, Tanaka, Tsai, Inoue, Masumoto, 1996; Grushko, Holland-Moritz, 1997). Vacancy-ordered Al–Ni–Cu τ -phases based on the CsCl-type, related to QC, are described by Chattopadhyay, Lele, Thangaraj, Ranganathan (1987).

Electron microscopy

By HAADF-STEM studies, the structure of rapidly solidified Al_3Ni was shown to be closely related to that of basic Ni-rich $\text{Al}_{72}\text{Co}_8\text{Ni}_{20}$ (Abe, Tsai, 2002). The authors point out that the low-symmetrical centers of the decagonal ≈ 20 Å clusters show a significant amount of disorder, more than in basic Ni-rich $\text{Al}_{72}\text{Co}_8\text{Ni}_{20}$. Indeed, there is some diffuse scattering visible on the SAED patterns, similar as on X-ray diffraction patterns of the HT-d-Al–Co–Ni phase (Steurer, Cervellino, Lemster, Ortelli, Estermann, 2001). This may support the model *AlCoNi-CHS-02* that locally each cluster has inherent ≈ 8 Å periodicity, which is averaged out by disorder along the columnar clusters. This kind of diffuse scattering becomes more intense during transformation to the orthorhombic equilibrium phase Al_3Ni (Pohla, Ryder, 1997). o- Al_3Ni , $a = 6.618(1)$ Å, $b = 7.368$ Å, $c = 4.814(1)$ Å, with Fe_3C -type structure

(Ellner, Kattner, Predel 1982), contains pentagonal structure units in the (110)-layers (Steurer, 2001, and references therein).

Approximants

Dong (1995) discusses the structural relationship to the d-phase of hexagonal Al_3Ni_2 , a vacancy ordered $1 \times 3 \times 3$ superstructure of the CsCl-type (with a homogeneity range from 57% to 62% Al). Its structure can be described by a six-layer stacking of (102)-planes that correspond to the CsCl-type (110)-plane or the quasiperiodic planes of the d-phase. Cubic Al_4Ni_3 , with homogeneity range from 54% to 56% Al, can also be seen as vacancy ordered $4 \times 4 \times 4$ superstructure of the CsCl-type (Ellner, Kek, Predel, 1989). The interactions between neighboring vacancies seems to be strongly repulsive.

Modeling

Based on first-principles interatomic potentials, the stability was calculated of aluminum rich intermetallics of composition $\text{Al}_{1-x}\text{TM}_x$ with $x < 0.3$ and $\text{TM} = \text{Co}, \text{Ni}$ (Widom, Moriarty (1998). One important result is that partially occupied Al positions stabilize phases such as m- and o- $\text{Al}_{13}\text{Co}_4$. Vacancies in these phases are only in the flat layers.

5.2.1.3 Al–Co–Cu

An overview about the most important structure models of d-Al–Co–Cu is given in Table 5.2.1.3-1.

Discovery

A stable decagonal phase with composition $\text{Al}_{65}\text{Co}_{15}\text{Cu}_{20}$ with different periodicities of ≈ 4 , ≈ 8 , ≈ 12 and ≈ 16 Å was reported by He, Zhang, Wu, Kuo (1988) and confirmed by Tsai, Inoue, Masumoto (1989b, c). Grushko, Urban (1991) studied the solidification behavior of d- $\text{Al}_{65}\text{Co}_{15}\text{Cu}_{20}$ and d- $\text{Al}_{65}\text{Co}_{20}\text{Cu}_{15}$ and found that the

d-phase melts incongruently. A B2 phase solidifies first, and then the d-phase is formed by reaction with the liquid. Significant coring was observed. The Al–Co–Cu phase diagram and the stability of the d-phase were studied in detail by Grushko (1992; 1993a, b, c). The existence of (1D quasiperiodically) vacancy ordered τ -phases (He, Li, Zhang, Kuo, 1988) was confirmed, and the stability range of the d-phase determined to be between d- $\text{Al}_{69}\text{Co}_{21}\text{Cu}_{10}$ and d- $\text{Al}_{62}\text{Co}_{14}\text{Cu}_{24}$. Vacancy-ordered derivatives of the CsCl-type structure are also known in binary LT- and HT-AlCu (El-Boragy, Szepean, Schubert, 1972; Sastry, Bariar, Chattopadhyay, Ramachandrarao, 1980). According to Daulton, Kelton, Song, Ryba (1992) the stability range is even smaller, centered on $\text{Al}_{65}\text{Co}_{15}\text{Cu}_{20}$. Higher Co/Cu ratio leads to approximants. D- $\text{Al}_{65}\text{Co}_{15}\text{Cu}_{20}$ can accommodate up to 2% of Si replacing Al (Grushko, Wittmann, Urban 1992). The mass density of d- $\text{Al}_{62}\text{Co}_{20}\text{Cu}_{15}\text{Si}_3$ ($a_{1-4} = 3.776(8)$, $a_5 = 4.1441(5)$) has been determined to $\rho_m = 4.53(3) \text{ Mg m}^{-3}$ (Kloess, Schetelich, Wittmann, Geist, 1994). The d-phase as well as m-(Al,Cu) $_{13}\text{Co}_4$ and the τ -phases lie on the connecting line between Al_3Co and the vacancy-ordered phase AlCu.

By high-energy ball milling a transformation of d- $\text{Al}_{65}\text{Co}_{20}\text{Cu}_{15}$ to a B2 (CsCl-type) phase was observed (Mukhopadhyay, Murthy, Murty, Weatherly, 2002). Even subsequent annealing at 600°C did not restore the d-phase, indicating instability of the d-phase at temperatures below 600°C. Features, which may be explained in terms of inclined netplanes (Steurer, Cervellino, 2001) have been observed in d-Al–Co–Cu (Saito, Saito, Sugawara, Guo, Tsai, Kamimura, Edagawa, 2002).

Spectroscopy

In an EXAFS study of d- $\text{Al}_{65}\text{Co}_{15}\text{Cu}_{20}$ was shown that the near-neighbor structures of Co and Cu atoms are very similar (Dong, Lu, Yang, Shan, 1991). Both of them are also very similar to that of Co in m- $\text{Al}_{13}\text{Co}_4$. By electron

Table 5.2.1.3-1. Structure models of d-Al–Co–Cu (for details see text).

<i>AlCuCo-SK-90</i>	XRD study of d- $\text{Al}_{65}\text{Co}_{15}\text{Cu}_{20}$. 5D structure model based on atomic surfaces derived from the 5D Patterson function; $P10_5/mmc$, $wR = 0.098$ for 259 reflections (Steurer, Kuo, 1990a, b). The structure was discussed in terms of pentagon tilings, one of the TM atoms with 4.7 Å edge length and another one of Al atoms with 2.9 Å edge length. The close resemblance to m- $\text{Al}_{13}\text{Co}_4$ was pointed out.
<i>AlCoCu-B-91</i>	Based on <i>AlCuCo-SK-90</i> and <i>AlCoNi-HSL-91</i> a model was proposed with symmetry $P10_5/mmc$, which can be considered as covering of the plane with decagonally shaped ≈ 20 Å clusters of pentagonal symmetry and mainly ≈ 12 Å linkages (Burkov, 1991).
<i>AlCuCo-DK-92</i>	Based on a SAED and CBED study on d- $\text{Al}_{65-x}\text{Co}_{20}\text{Cu}_{15}\text{Si}_x$ a general model was presented for d-phases with 4, 8, 12 and 16 Å periodicity. The basic columnar clusters were generated from differently deep interpenetrating distorted Mackay icosahedra (Daulton, Kelton, 1992).
<i>AlCoCu-B-93</i>	Based on the Tübingen-triangle tiling, a new model with symmetry $P10_5/m$, was proposed (Burkov, 1993). The tiling was no more decorated by clusters but by individual atoms.
<i>AlCoCu-SR-94</i>	Song, Ryba (1994) proposed a model for d-phase approximants based on two primary pentagonal polyhedral clusters derived from STM images by Kortan, Becker, Thiel, Chen (1990).
<i>AlCoCu-LSHZF-95</i>	Based on <i>AlCoCu-SK-90</i> , a 5D and a 3D structure model with composition $\text{Al}_{62.9}(\text{Co,Cu})_{37.1}$ was proposed by Li, Steurer, Haibach, Zhang, Frey (1995). The quasilattice was described as two-color Penrose-tiling with black and white H, C and S supertiles (edge length ≈ 6.5 Å).
<i>AlCoCu-Y-96</i>	Yamamoto (1996a) discussed the models <i>AlCoCu-B-91</i> , <i>AlCoNi-HSL-91</i> and <i>AlCoCu-SK-90</i> and presented a modified model fitting better the experimental data.
<i>AlCoCu-CW-98</i>	A ternary model of d- $\text{Al}_{64.8}\text{Co}_{19.6}\text{Cu}_{15.6}$, based on a 5D model similar to <i>AlCoCu-SK-90</i> , was studied by total energy calculations (Cockayne, Widom, 1998b). The model resulted to an HBS-tiling (edge length ≈ 6.38 Å) decorated with pentagonal clusters, all in the same orientation.

channeling the maximum corrugation of the atomic layers was determined in d-Al₆₅Co₁₅Cu₁₆Si₄ to 0.12 Å for Cu/Co and 0.28 for Al atoms and Si atoms midway between the layers (Nüchter, Sigle, 1994).

Electron microscopy

The first HRTEM study on an annealed sample (900 K) of d-Al₆₅Co₂₀Cu₁₅ was performed by Chen, Burkov, He, Poon, Shiflet (1990). Ring-like contrasts with ≈ 20 Å diameter were identified. Their distribution was related to a random tiling. A HRTEM study of d-Al₆₅Co₂₀Cu₁₅ quenched from 800 K and annealed at 550 K, respectively, showed the existence of a quasiperiodic (random) pentagon tiling for the former and of a rhomb tiling in crystalline nanodomains for the latter (Hiraga, Sun, Lincoln, 1991). In both cases the vertices of the tiling (≈ 20 Å edge length) were decorated with ring contrasts.

Based on a SAED and CBED study on d-Al_{65-x}Co₂₀·Cu₁₅Si_x a general model, *AlCuCo-DK-92* was presented for d-phases with 4, 8, 12 and 16 Å periodicity (Daulton, Kelton, 1992). The basic columnar clusters were generated by different interpenetration depths of distorted Mackay icosahedra. These clusters order randomly in the quasiperiodic plane. The ratio 2 of the diameters of the inner and outer icosahedra of their model is not in agreement with the electron density function of *AlCoCu-SK-90*, which shows a ratio of τ .

A first HRTEM study on d-Al₆₅Co₁₅Cu₂₀ showing one quasiperiodic and the periodic direction was performed by Reyes-Gasga, Lara, Riveros, Jose-Yacamán (1992). They also reported that irradiation of the d-phase with a 400 kV electron beam induced a structural transformation, which cannot be observed for beams with 100 kV, for instance. In a similar experiment, Zhang, Urban (1992) showed that d-Al₆₅Co₂₀Cu₁₅ and d-Al₆₂Co₁₅Cu₂₀Si₃ first transform into a bcc phase, which then reorders to a CsCl-type phase. The total time for the transformation was 15 min for an electron current density of 10^{23} electrons s⁻¹ m⁻². Lattice fringe images along A2D of Al₆₂Co₁₅Cu₂₀Si₃ before and after transformation are also given. The authors conclude that the transformation was not induced by electron beam heating ($\Delta T < 50$ °C) but by radiation damage, and that the major effect consisted in an enhancement of the rate at which the transformation occurred. The stable phase at room temperature should be the CsCl-type one. The orientation relationship between the d-phase and the cubic phase was as follows: A10 \parallel [110], A2D \parallel [$\bar{1}\bar{1}0$] or [$\bar{1}\bar{1}1$], A2P \parallel [001]. Song, Wang, Ryba (1993) observed in an as cast Al₆₅Co₁₅Cu₂₅ alloy lattices fringes, indicating a crystalline orientationally twinned nanodomain structure. Twinning was also visible in SAED patterns. After annealing 500 h at 800 °C the sample did not show any lattice fringes any more indicating a d-phase; the SAED pattern exhibited perfect tenfold symmetry.

A crystal to quasicrystal transformation was observed during electron beam irradiation of a slowly cooled sample with composition d-Al₆₃Co_{17.5}Cu_{17.5}Si₂ in the electron microscope (Audier, Robertson, 1991). The transformation from the microcrystalline to the quasiperiodic state takes place shortly before the sample begins to melt. Irradiation experiments carried out on microcrystalline Al₆₂Co₁₅Cu₂₀Si₃

with a 400 keV electron beam confirmed this sequence of phase transformations (Reyes-Gasga, Garcia, R., Jose-Yacamán, 1995).

The 5D space group of rapidly quenched Al₇₀Co_{30-x}Cu_x ($x = 4, 6, 8, 10, 12$), Al₆₅Co_{35-x}Cu_x ($x = 15, 20$) and Al₇₃Co₂₅ was determined by CBED to non-centrosymmetric $P10\bar{2}m2$ (Saitoh, Tsuda, Tanaka, Tsai, Inoue, Masumoto, 1994). d-Al₆₅Co₂₀Cu₁₅ and d-Al₆₅Co₁₅Cu₂₀ showed a poorer quality than d-Al₇₀Co_{30-x}Cu_x ($x = 4, 6, 8$) and d-Al₇₃Co₂₅ and no clear antiphase domain structure with phase shift of $c/2$ at the domain boundaries. HRTEM images of annealed (1050 °C, 3 h) d-Al₆₅Co₁₅Cu₂₀ show clearly only fivefold symmetry of the ≈ 20 Å clusters (Saitoh, Tsuda, Tanaka, Tsai, Inoue, Masumoto, 1996). The authors point out that the observation of tenfold symmetry can be an artifact, a function of accelerating voltage, defocus and convergence of the incident beam. As a function of temperature, samples originally showing symmetry $P10\bar{2}m2$ and inversion domains (100–1000 Å size) change to symmetry $P10_5/mmc$ and the domains shrink to a few nanometers. The authors present a model with a 10_5 axis between two columnar clusters instead in the center of the cluster. However, the way it is drawn in this paper corresponds to a 2_1 axis, a 10_5 axis would generate a bundle of 2×5 overlapping clusters around the axis.

X-ray and neutron diffraction

The first quantitative single-crystal X-ray structure analysis of the d-phase in the system Al–Co–Cu was performed on d-Al₆₅Co₁₅Cu₂₀ by Steurer, Kuo (1990a, b). The structure was solved by the 5D Patterson method, 11 parameters were refined against 259 reflections to $R = 0.098$ in the 5D space group $P10_5/mmc$. The structure was discussed in terms of pentagon tilings, *AlCoCu-SK-90*, one of the TM atoms with 4.7 Å edge length and another one of Al atoms with 2.9 Å edge length. The close resemblance to m-Al₁₃Co₄ was pointed out.

A stability study of d-Al₆₅Co_{17.5}Cu_{17.5} at RT and in the temperature range between 773 and 1083 K was performed by an *in situ* high-resolution powder neutron diffraction study (Dong, Dubois, de Boissieu, Janot, 1991). A stability range of the d-phase $973 < T < 1350$ K was found as well as a higher thermal expansion for the quasiperiodic plane than for the periodic direction. Some of the results of these authors were differently interpreted by Grushko, Wittmann, Urban (1992). The SAED patterns of an Al₆₂Co₁₄Cu₂₄ alloy annealed 1290 h at 700 °C and 3500 h at 550 °C were differed significantly from each other (Grushko, 1993c). The second one exhibited strong diffuse scattering connecting the Bragg reflections similar to a pentagon-decagon tiling. Alloys of composition Al₆₈Co₂₁Cu₁₁ annealed up to 700 h at 1000 °C showed a dense net of extra reflections overlapping the reflections observable on the as cast sample indicating formation of a metastable state (Grushko, Wittmann, Urban, 1994; 1993).

Approximants and twinning

By a combined HRTEM and single-crystal X-ray diffraction study of a sample with composition Al₆₃Co_{17.5}Cu_{17.5}Si₂ it was demonstrated that its tenfold symmetry resulted from an orientationally twinned crystalline microdomain struc-

ture rather than from a quasiperiodic structure (Launois, Audier, Denoyer, Dong, Dubois, Lambert, 1990). The lattice parameters of the monoclinic approximant were determined to $a = b = 51.58 \text{ \AA}$, $c = 8.4 \text{ \AA}$, $\gamma = 36^\circ$. This was a caveat for being more careful with the characterization of QC. The problem of pseudosymmetry and orientational twinning was also addressed in a study on $\text{Al}_{65}\text{Co}_{15}\text{Cu}_{20}$ (Song, Wang, Ryba, 1991). By TEM the size of the twin domains was found in a range between 200 and 5000 \AA . In large Bridgman-grown single crystals of composition $\text{Al}_{60}\text{Co}_{20}\text{Cu}_{18}\text{Si}_2$ even an orientationally twinned 1D QC was observed beside three different crystalline approximants (He, Lograsso, Goldman, 1992). Reflection splitting due to twinning was clearly visible on SAED patterns. A comprehensive synchrotron radiation diffraction study of the microcrystalline state of a slowly cooled sample with composition $\text{Al}_{63}\text{Co}_{17.5}\text{Cu}_{17.5}\text{Si}_2$ was performed by Fettweis, Launois, Denoyer, Reich, Lambert (1994). They discussed structure models of twinned approximants of the type $a = b = 51.58 \text{ \AA}$, $c = 8.4 \text{ \AA}$, $\gamma = 108^\circ$, as well as diffraction patterns which could be obtained from them. In an *in situ* high-temperature study on samples with the same composition a phase transformation between the microcrystalline state and the quasicrystalline state was found by single-crystal synchrotron radiation diffraction (Fettweis, Launois, Reich, Wittmann, Denoyer, 1995). The reversible transformation takes place at $\approx 750^\circ\text{C}$ and shows a hysteresis effect indicating that the transition is of first order. It is remarkable that no transient states (such as in a 'devils stair case' known from incommensurately modulated phases) have been observed.

A slowly cooled $\text{Al}_{63}\text{Co}_{17.5}\text{Cu}_{17.5}\text{Si}_2$ alloy was investigated by SAED and HRTEM and two approximant phases, O'_1 ($a = 38 \text{ \AA}$, $b = 4.1 \text{ \AA}$, $c = 52 \text{ \AA}$) and O'_2 ($a = 32 \text{ \AA}$, $b = 4.1 \text{ \AA}$, $c = 98 \text{ \AA}$), found (Dong, Dubois, Song, Audier, 1992). The authors point out that the approximant O'_1 has with 0.691 a lower pentagon packing density than O'_2 with 0.854, which is higher than that of the pentagonal Penrose tiling with 0.809 ($= \tau/2$) (see also Henley, 1986). The orientation relationship of the approximant phases with the CsCl-type phase is also discussed. The approximants can be considered as superstructures of the CsCl-type phase. This relationship is used to derive the atomic decoration of larger units of the Penrose tiling.

Further models

Based on the models *AlCoCu-SK-90* and *AlCoNi-HSL-91*, Burkov (1991, 1992) proposed a model, *AlCoCu-B-91*, with symmetry $P10_5/mmc$, which can be considered as covering of the plane with decagonally shaped clusters ($\approx 20 \text{ \AA}$ diameter) of pentagonal symmetry (Fig. 5.2.1.3-1). Yamamoto (1996a) discussed the models *AlCoCu-B-91*, *AlCoNi-HSL-91* and *AlCoCu-SK-90*. He pointed out that *AlCoCu-B-91* generates $\approx 20 \text{ \AA}$ clusters with mainly $\approx 12 \text{ \AA}$ linkages while the HRTEM images clearly show $\approx 20 \text{ \AA}$ linkages as the most frequent ones. A model, *AlCoCu-Y-96*, is presented which represents the experimental evidence in a better way. A new model, *AlCoCu-B-93*, with symmetry $P10_5/m$, was proposed by Burkov (1993) based on the Tübingen-triangle tiling. The tiling was no more decorated by clusters but by individual

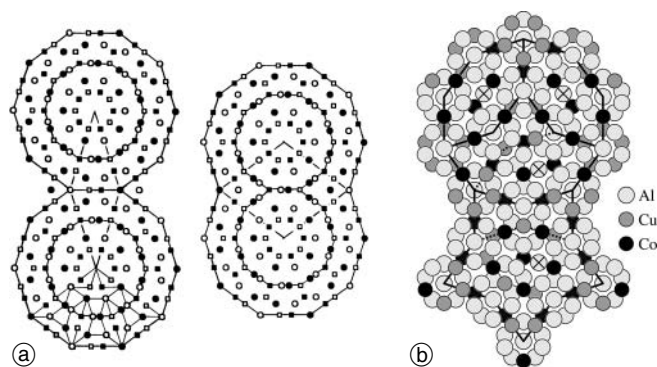


Fig. 5.2.1.3-1. (a) Unit tiles of the binary tiling based structure model *AlCoCu-B-91*. The vertices are decorated by a $\approx 20 \text{ \AA}$ decagonally shaped cluster with pentagonal symmetry. Circles, Al; squares, transition metal; open symbols $z = 0$; solid symbols, $z = 1/2$ layer (Burkov, 1991). (b) Tiling decoration model, *AlCoCu-CW-98*, based on Monte Carlo simulations. All atoms shown are at $z = 0.25$ or $z = 0.75$ except those on tile vertices and those marked X (Cockayne, Widom, 1998).

atoms. The stability of this model with different Co/Cu decorations was calculated by electronic calculations (Sabiryanov, Bose, Burkov, 1995). It was demonstrated that neither the original model *AlCoCu-B-93* nor the model suggested by Phillips, Widom (1993) have a minimum in the electronic density of states at the Fermi energy. These models may be entropically stabilized by disorder. First-principles calculations of the electronic structure of *AlCoCu-B-93* and several Co/Cu-ordered variants (Co–Co neighbors, no Cu–Cu contacts) demonstrated that this model explains better the experimental evidence than the older binary-tiling based model *AlCoCu-B-91* (Krajci, Hafner, Mihalkovic, 1997b). There are significant differences to d-Al–Co–Ni, where the attractive Ni–Ni and Co–Al interactions lead to high Ni–Ni and Co–Al coordination (Krajci, Hafner, Mihalkovic, 2000). The number of Ni–Co pairs is much lower than that of Cu–Co pairs. Just the opposite conclusions concerning the inner TM ring were drawn from the results of *ab initio* calculations on modified *AlCoCu-B-93* where 'Cu-tubules' with direct Cu–Cu contacts play an important role (Haerle, Kramer, 1998).

Song, Ryba (1994) proposed a model, *AlCoCu-SR-94*, for d-phase approximants based on two primary pentagonal polyhedral clusters derived from STM images by Kortan, Becker, Thiel, Chen (1990). Based on *AlCoCu-SK-90*, a 5D and a 3D structure model, *AlCoCu-LSHZF-95*, with composition $\text{Al}_{62.9}(\text{Co,Cu})_{37.1}$ was proposed by Li, Steurer, Haibach, Zhang, Frey (1995). The quasilattice was described as two-color Penrose-tiling with black and white H, C and S supertiles (edge length $\approx 6.5 \text{ \AA}$).

A ternary model of d- $\text{Al}_{64.8}\text{Co}_{19.6}\text{Cu}_{15.6}$, *AlCoCu-CW-98* (Fig. 5.2.1.3-1), based on a 5D model similar to *AlCoCu-SK-90*, was studied by total energy calculations (Cockayne, Widom, 1998). The model resulted to be an HBS-tiling (edge length $\approx 6.38 \text{ \AA}$) decorated with pentagonal 11-atom clusters, all in the same orientation in a given layer. The formation of Co–Cu zigzag chains (corresponding to a matching rule) resulted to be energetically more favorable than Co–Co or Cu–Cu chains. Co/Cu-ordering differs from that proposed in model *AlCoCu-B-93* (Burkov, 1993). Remarkably,

5.2.1.4 Al-Co-Ni

The structural modeling of the different modifications of the d-phase is converging. An overview of the most important structure models is given in Tab. 5.2.1.4-1 and Fig. 5.2.1.4-2. A fundamental decagonally shaped structure motif has been identified, a columnar ‘cluster’ with $\approx 20 \text{ \AA}$ diameter and with pentagonal or lower symmetry. This cluster decorates either a pentagonal tiling (Ni-rich HT-d-phase) or rhomb tilings (LT- and HT-pentagonal phase, 1D quasicrystal, Ni-rich LT-d-phase). The tilings are either quite perfectly quasiperiodically ordered or more randomly. Structural disorder, either substitutional or phasonic disorder, seems to play a stabilizing role by increasing the configurational entropy. Order/disorder transitions connect LT and HT modifications. Several stable approximants have been found such as m-, o- and τ^2 - $\text{Al}_{13}\text{Co}_4$, $\text{Al}_9\text{Co}_2\text{Ni}$ and W-Al-Co-Ni (composition and stability not yet confirmed).

The first ternary d-phase in the system Al–Co–Ni was prepared by rapid solidification of samples in a compositional range of 9% to 21% Co, and 9% to 16% Ni (Tsai, Inoue, Masumoto, 1989a). Shortly later, the stability range of the d-phase in this system was demarcated to 65% to 75% Al, 15% to 20% Co, and 10% to 15% Ni (Tsai, Inoue, Masumoto, 1989b). The d-phase found in samples of composition $\text{Al}_{70}\text{Co}_{15}\text{Ni}_{15}$ and $\text{Al}_{70}\text{Co}_{13}\text{Ni}_{17}$ was identified as fivefold superstructure ('superstructure type I', 'Edagawa-phase'; Edagawa, Ichihara, Suzuki, Takeuchi, 1992) of the basic d-phase, which was found later in a sample with composition $\text{Al}_{70}\text{Co}_8\text{Ni}_{22}$ (Edagawa, Sawa, Takeuchi, 1994). The reciprocal basis of the superstructure type I is related to that of the 'basic Ni-rich' d-phase by rotoresizing (rotation by 18° and scaling by a factor $\sqrt{3-\tau}$). The determinant of the transformation matrix equals five.

Stability ranges and phase equilibria of d-Al–Co–Ni and its modifications have been studied in great detail (Gödecke, 1997a; Gödecke, Ellner, 1996, 1997; Gödecke, Scheffer, Lück, Ritsch, Beeli, 1998; Scheffer, Gödecke, Lück, Ritsch, Beeli, 1998). Ritsch, Beeli, Nissen, Gödecke, Scheffer, Lück (1998) identified eight different structural modifications of the d-phase, which were called ‘basic Ni-rich’, ‘basic Co-rich’, ‘superstructure type I (S1 + S2)’, ‘superstructure type I (S1)’, ‘superstructure type II’, ‘1D quasicrystal’, ‘pentagonal phase’. The basic Ni-rich phase was seen as HT phase, its structure was

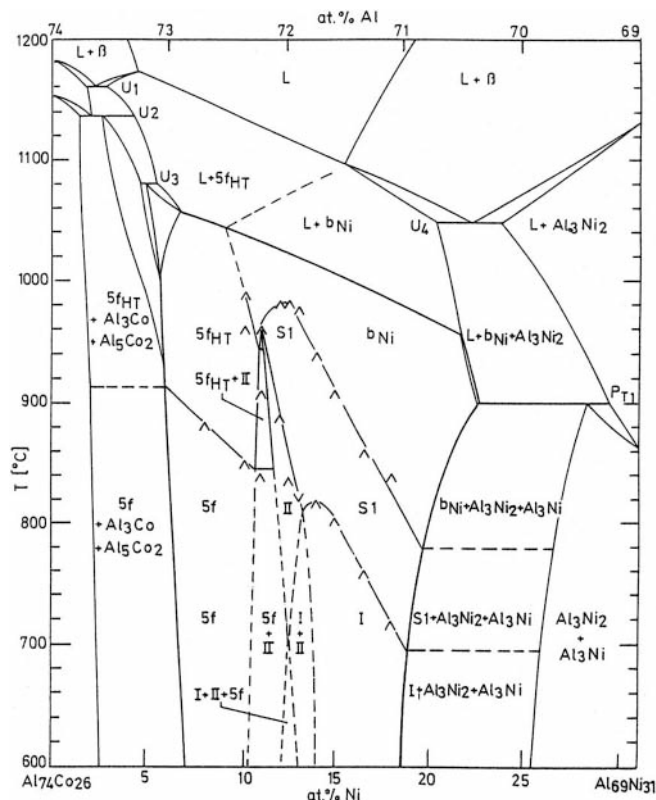


Fig. 5.2.1.4-1. Temperature concentration section $\text{Al}_{74}\text{Co}_{26}\text{-Al}_{69}\text{Ni}_{31}$. The transformations within the d-phase are determined by dilatometric measurements. The phase diagram is delineated assuming second order transformations between the d-phase modifications (Lück, Scheffer, Gödecke, Ritsch, Beeli, 1999). 5f ... basic Co-rich pentagonal phase with HT and LT modification; I, II ... superstructures type I, II; S1 ... superstructure type I with only first order superstructure reflections; b_{Ni} ... basic Ni-rich d-phase.

Table 5.2.1.4-1. Structure models of d-Al–Co–Ni (for details see text).

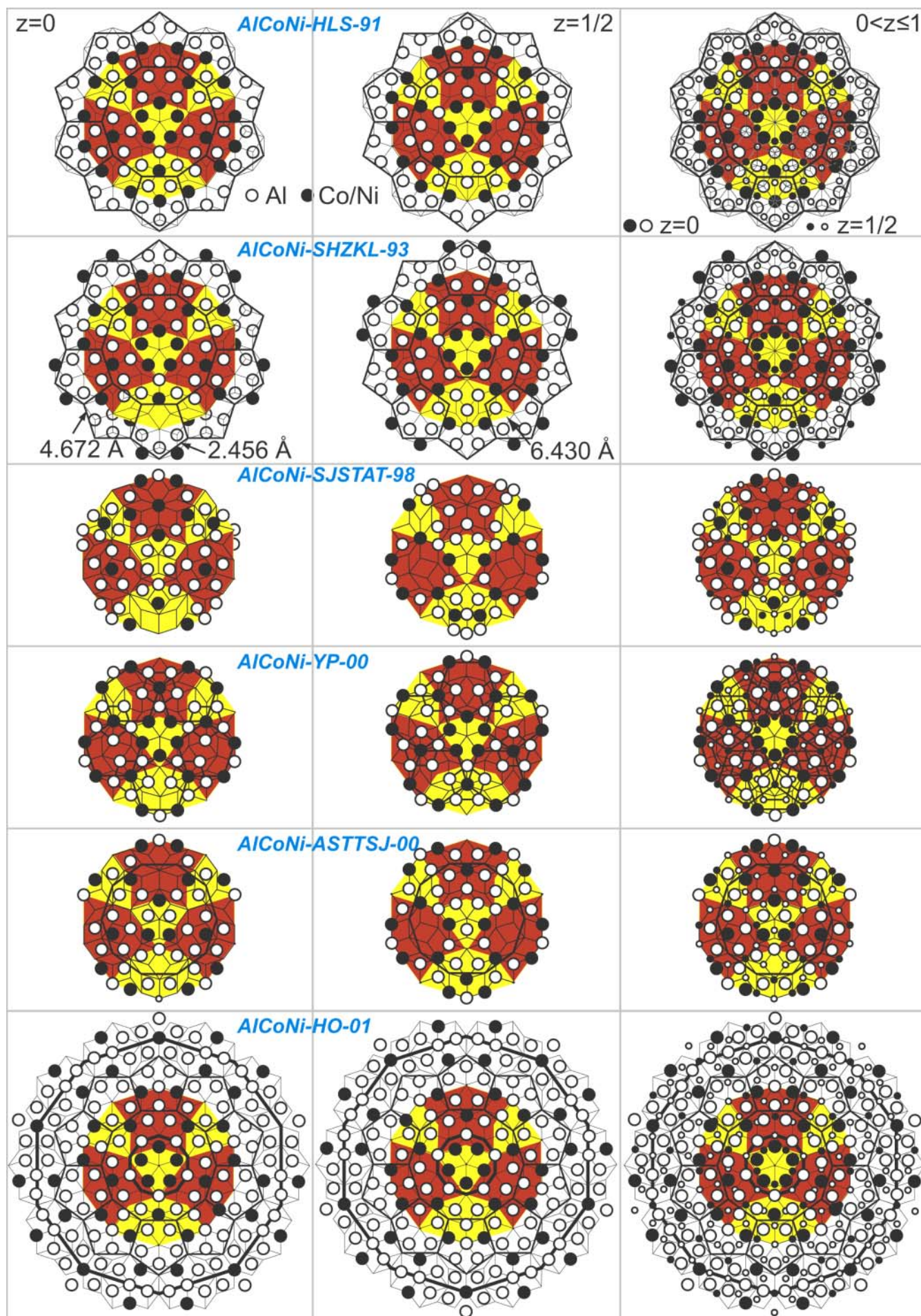
<i>AlCoNi-YKST-90</i>	XRD study of d-Al ₇₀ Co ₂₀ Ni ₁₀ . 5D structure model based on atomic surfaces derived from the structure of m-Al ₁₃ Fe ₄ ; <i>P10/mmm</i> , <i>R</i> = 0.11 for 41 reflections (Yamamoto, Kato, Shibuya, Takeuchi, 1990).
<i>AlCoNi-HLS-91</i>	HRTEM study of d-Al ₇₀ Co ₁₅ Ni ₁₅ . Random pentagon and rhomb tiling for HT (800 °C) and LT (550 °C) phase, respectively, decorated by ≈ 20 Å clusters (Hiraga, Lincoln, Sun, 1991).
<i>AlCoNi-SHZKL-93</i>	XRD study of d-Al ₇₀ Co ₁₅ Ni ₁₅ . 5D structure model based on atomic surfaces derived from the 5D Patterson function and MEM; <i>P10₅/mmc</i> , <i>wR</i> = 0.078 for 253 reflections (Steurer, Haibach, Zhang, Kek, Lück, 1993).
<i>AlCoNi-RBNL-95</i>	HRTEM study of d-Al ₇₀ Co ₁₅ Ni ₁₅ . Model of the type I superstructure: the fivefold symmetric cluster centers order antiparallel in case of ≈ 20 Å linkages and parallel for τ times larger distances (Ritsch, Beeli, Nissen, Lück, 1995).
<i>AlCoNi-EP-95</i>	5D structure refinement using symmetry-adapted functions based on data from <i>AlCoNi-SHZKL-93</i> ; <i>P10₅/mmc</i> , <i>wR</i> = 0.080 for 253 reflections (Elcoro, Perez-Mato, 1995).
<i>AlCoNi-YW-97</i>	5D structure model of the superstructure type I. The authors point out that the superstructure can be obtained essentially by phason flips of the fundamental cluster (Yamamoto, Weber, 1997a).
<i>AlCoNi-STT-98</i>	HAADF study of d-Al ₇₂ Co ₈ Ni ₂₀ . Model of the basic structure: ≈ 20 Å clusters with only mirror symmetry consist of subclusters (P,S) decorating a rhomb Penrose tiling and a HBS tiling, respectively (Saitoh, Tsuda, Tanaka, 1998).
<i>AlCoNi-YP-98</i>	HAADF study of d-Al ₇₂ Co ₈ Ni ₂₀ . Model of the basic structure: the intrinsic decagonal symmetry of the ≈ 20 Å clusters is broken by disorder \rightarrow entropy stabilization (Yan, Pennycook, Tsai, 1998).
<i>AlCoNi-SJSTAT-98</i>	HRTEM based study of d-Al ₇₂ Co ₈ Ni ₂₀ . Model of the basic structure: strictly ordered low-symmetry model of the ≈ 20 Å cluster with matching rules favouring a strictly quasiperiodic tiling (Steinhardt, Jeong, Saitoh, Tanaka, Abe, Tsai, 1998).
<i>AlCoNi-ASTTSJ-00</i>	HRTEM based study of d-Al ₇₂ Co ₈ Ni ₂₀ . Model of the basic structure: slightly modified version of <i>AlCoNi-SJSTAT-98</i> based on criticism by Yan, Pennycook, Tsai (1998) (Abe, Saitoh, Takakura, Tsai, Steinhardt, Jeong, 2000).
<i>AlCoNi-YP-00</i>	HAADF study of d-Al ₇₂ Co ₈ Ni ₂₀ . Model of the basic structure: the ≈ 20 Å clusters are composed of subclusters derived from τ^2 -Al ₁₃ Co ₄ ; still broken decagonal symmetry due to disorder (Yan, Pennycook, 2000a,b).
<i>AlCoNi-HON-00</i>	HAADF and HRTEM study of d-Al _{72.5} Co ₁₁ Ni _{16.5} . Model of the type I superstructure: The ≈ 20 Å clusters with pentagonal symmetry decorate two rhombic tilings with ≈ 32 Å edge length (Hiraga, Ohsuna, Nishimura, 2000).
<i>AlCoNi-YP-01</i>	HAADF study of d-Al ₇₂ Co ₈ Ni ₂₀ . Model of the basic structure: slightly modified based on results of first-principles calculations, features now also broken tenfold symmetry due to chemical order (Yan, Pennycook, 2001).
<i>AlCoNi-HO-01</i>	HRTEM study of d-Al ₇₂ Co ₈ Ni ₂₀ . Model of the basic structure: well-ordered pentagonal tiling (edge length ≈ 32 Å) decorated with a ≈ 32 Å cluster with full decagonal symmetry in the projection (Hiraga, Ohsuna, 2001a).
<i>AlCoNi-TYT-01</i>	XRD study of d-Al ₇₂ Co ₈ Ni ₂₀ . 5D structure model based on atomic surfaces derived from cluster models; <i>P10₅/mmc</i> , <i>wR</i> = 0.045 for 449 reflections (Takakura, Yamamoto, Tsai, 2001).
<i>AlCoNi-CHS-02</i>	XRD study of d-Al ₇₂ Co ₈ Ni ₂₀ . 5D structure model based on the atomic surfaces modelling method; <i>P$\overline{10}$</i> , <i>wR</i> = 0.060 for 2767 reflections (Cervellino, Haibach, Steurer, 2002).

described by a disordered cluster decorating a highly perfect pentagonal Penrose tiling, while all other d-phases could be better described by cluster-decorated random tilings (Joseph, Ritsch, Beeli, 1997). The order inside of the clusters of these d-phases appeared higher and a doubling of the period along the tenfold axis was indicated on SAED patterns by diffuse interlayer lines. Concerning the tiling analysis by Joseph, Ritsch, Beeli (1997) one has to keep in mind, however, that HRTEM images showing only 150–300 cluster ring contrasts leave some uncertainty about the significance of such an analysis to distinguish between different quasiperiodic tilings and to determine their degree of order. In the superstructures of type I and II, the pentagonal clusters were found to be ordered antiparallel along ≈ 20 Å linkages. The basic Co-rich phase was seen to be more related to the superstructures than to the basic Ni-rich phase. The structure contained domains of equally oriented pentagonal clusters. The pentagonal phase was characterized by a parallel orientation of all pentagonal clusters. The 1D quasicrystal, with periods ≈ 30.7 Å and ≈ 4.1 Å, also contained the pentagonal clusters in parallel orientation.

Grushko, Holland-Moritz, Wittmann, Wilde (1998) studied annealed (600–1000 °C, 70–5000 h) ingots of different compositions within or close to the stability field of d-Al–Co–Ni by SAED and powder XRD. Several high-

order approximant phases were identified and the complex transformation behavior studied. Remarkable results were that only the as-cast d-phase could be transformed into a LT approximant of same composition within the given time scale while the preannealed d-phase cannot. The approximant phase can quickly and irreversibly be transformed back to the d-phase. From my point of view these findings can be explained as follows. The as-cast phase is rich in defects and shows only medium-range correlation. Long-term annealing at low temperature transforms it into a crystalline approximant structure. Due to sluggish kinetics, however, the chemical order of the approximant may still show the characteristics of the original quasiperiodic order. Heating such an approximant with partial quasiperiodic chemical order induces a quick transition to the quasiperiodic state. After some HT annealing the perfection of the quasiperiodic phase hinders the transformation

Fig. 5.2.1.4-2. The most important models of the basic structure of d-Al–Co–Ni. In each row, the structure of the fundamental cluster (diameter ≈ 20 Å; only in the last row it is τ times larger) is shown for $z = 0$, $z = \frac{1}{2}$ and in projection. Open circles, Al; solid circles, transition metal; small (large) circles in the right column, $z = 0$ ($z = \frac{1}{2}$). The Gummelt decagon with ≈ 6.4 Å edge length and ≈ 20 Å diameter is drawn in. The model name code contains the reference where it was first published (first letter of the authors names and year of publication). For details see text.



back to the approximant at low temperatures. The energy differences are very small, long-range chemical reordering without defect-induced diffusion very slow.

According to Döblinger, Wittmann, Grushko (2001) the superstructure type II is not a d-phase but corresponds to an orientationally fivefold twinned nanodomain structure. According to several *in situ* HT X-ray diffraction studies (Baumgarte, Schreuer, Estermann, Steurer, 1997; Steurer, Cervellino, Lemster, Ortelli, Estermann, 2001), the HT-phase is a quasiperiodic phase without superstructure reflections. For Ni-rich compositions it shows decagonal diffraction symmetry, for Co-rich compositions the symmetry is only pentagonal. The temperature dependence of the 8 Å superstructure was studied by Frey, Weidner, Hradil, de Boissieu, Letoublon, McIntyre, Currat, Tsai (2002).

Electron microscopy – Ni rich d-phases

The first detailed HRTEM study of d-Al₇₀Co₁₅Ni₁₅ on annealed (800 °C, 5 h) and quenched as well as on only annealed (550 °C, 69 h) samples was performed by Hiraga, Lincoln, Sun (1991). The micrographs were interpreted by a random pentagonal tiling and a random rhomb tiling (with periodic nanodomains), respectively. The edge length of the tilings was determined to ≈ 20 Å, both tilings were found to be decorated by the same type of ≈ 20 Å clusters. A model, *AlCoNi-HLS-91* (Fig. 5.2.1.4-1), of the ≈ 20 Å cluster was proposed. It corresponds to a decorated Penrose rhomb tiling with edge length ≈ 2.5 Å. The two atomic layers per ≈ 4 Å period are related by a 10₅ screw axis.

A slightly modified model, *AlCoNi-HSY-94*, of the ≈ 20 Å columnar cluster was derived from HRTEM images of annealed (550 °C, 72 h) samples of d-Al₇₀Co₁₅Ni₁₅ (Hiraga, Sun, Yamamoto, 1994). The SAED pattern of the LT-sample resembles the superstructure found by Edagawa, Ichihara, Suzuki, Takeuchi (1992). Its HRTEM image was interpreted by a rhomb Penrose tiling with ≈ 20 Å edge length while the one of the HT-sample was found to be similar to a pentagonal Penrose tiling with the same edge length. The ≈ 20 Å cluster appeared to become slightly deformed by a rearrangement of just a few atoms.

The compositional and annealing-temperature dependence of SAED patterns and HRTEM images of the d-phase was investigated on samples with 10–22% Ni and 8–20% Co at annealing temperatures of 850 °C (4 h) and 650 °C (72 h) (Edagawa, Tamaru, Yamaguchi, Suzuki, Takeuchi, 1994). It was found that only the sample with composition d-Al₇₀Co₁₃Ni₁₇ annealed at 650 °C was in the fully ordered superstructure state while the sample d-Al₇₀Co₈Ni₂₂ annealed at 650 °C did not show any superstructure reflections and even no diffuse interlayer lines (related to a ≈ 8 Å superstructure) as it was always observed at more Co-rich compositions. The high order of the Ni-rich d-phase was confirmed by single-crystal X-ray diffraction studies of d-Al_{70.6}Co_{6.8}Ni_{22.6} (Zhang, 1995; Zhang, Estermann, Steurer, 1995, 1997). This is quite useful since despite the enhancement of weak diffraction effects by multiple scattering, standard electron diffraction never reaches the dynamic range (10^5 – 10^6) of state-of-the-art X-ray diffraction. Ritsch, Beeli, Nissen, Gödecke, Scheffer, Lück (1996) reported the existence of the basic

Ni-rich d-phase for a sample with composition Al₇₀Co₁₁Ni₁₉ after annealing at 1050 °C (12 h). After annealing at 900 °C (48 h), however, a d-phase with superstructure (S1) was formed, while annealing at 800 °C yielded decomposition into d-phase and Al₃Ni₂. The high quality of the basic Ni-rich phase was reflected in a SAED pattern with almost no diffuse background and in HRTEM images showing a highly perfect pentagon Penrose tiling decorated with ≈ 20 Å clusters with decagonal symmetry. In a narrow temperature range around 900 °C, the Ni-richest d-phase was found to be stable for a composition d-Al_{70.2}Co_{5.4}Ni_{24.4} (Grushko, Holland-Moritz, 1996). Quasilattice parameters were reported to increase with decreasing Ni-concentration (Al_{70.2}Co_{5.4}Ni_{24.4}: $a = 3.745$ Å; Al_{72.5}Co_{14.5}Ni₁₃: $a = 3.776$ Å; Al₇₃Co₂₇: $a = 3.825$ Å) while the lattice parameter along the tenfold axis increases less than 1% (Grushko, Holland-Moritz, 1997).

Ritsch, Beeli, Nissen, Lück (1995) found in a slowly cooled sample of composition Al₇₀Co₁₅Ni₁₅ decagonal SAED patterns with two different superstructures I and II. Type I, corresponds to the superstructure discovered by Edagawa, Ichihara, Suzuki, Takeuchi (1992), type II, characterized by reflections arranged in small (diffuse) pentagons was already described by Frey, Steurer (1993). As shown later by high-resolution XRD experiments, the existence of the type II superstructure is highly questionable anyway (Weidner, Hradil, Frey, de Boissieu, Letoublon, Morgenroth, Krane, Capitan, Tsai, 2000). HRTEM images were interpreted employing a rhomb tiling in case of type I and a pentagon tiling in case of type II, both with ≈ 20 Å edge length. The pentagon tiling appeared to be less ordered. A model was proposed for the type I superstructure (*AlCoNi-RBNL-95*): the fivefold symmetric cluster centers order antiparallel in case of ≈ 20 Å linkages and parallel for τ times larger distances. During irradiation with a 250 kV electron beam, due to radiation-induced diffusion of atoms, the superlattice reflections weakened and diffuse streaks between main and satellite reflections appeared in a transient stage. After 30 sec most of the superlattice reflections and also of the diffuse intensity disappeared (in the ≈ 8 Å related interlayers as well). The whole transformation to the basic d-phase was completed within 3–4 min.

The phase transformations of an annealed (627 °C, 24 h) sample with composition Al₇₀Co₁₅Ni₁₅ under irradiation with a 120 keV Ar⁺ ion beam were studied by SAED (Qin, Wang, Wang, Zhang, Pan, 1995). The following transformation sequence was observed as a function of the increasing dose: ordered d-phase \rightarrow disordered d-phase \rightarrow bcc phase \rightarrow CsCl-type phase \rightarrow bcc phase. First the increasing number of defects leads to an increase in disorder accompanied by diffusion of atoms to approach the equilibrium structure. Then due to the high concentration of defects thermal diffusion leads to an ordered (close to equilibrium) state. Finally, further irradiation destroys the ordered equilibrium phase again.

Phason-related disorder along the axis of the decagonal ≈ 20 Å cluster in annealed (850 °C, 3 d) d-Al₇₀Co₁₃Ni₁₇ was observed by Ritsch, Nissen, Beeli (1996). The authors emphasize that this kind of disorder may have been present in many samples studied by HRTEM biasing model-

ing of the structures. If in the squashed hexagon tiles no inner vertex can be defined, then this indicates the above-mentioned type of phason disorder.

In a study of annealed (1173 K, 47 h) samples with compositions $\text{Al}_{70}\text{Co}_x\text{Ni}_{30-x}$, $16 \leq x = 24$, the basic Ni-rich d-phase was identified for $x = 6$. Around $x = 12$ the type I superstructure was formed and around $x = 16$ the type II superstructure was found (Tsai, Fujiwara, Inoue, Masumoto, 1996). A comprehensive HRTEM, SAED and CBED study on melt-quenched as well as on annealed (800 °C, 48 h) samples of composition $\text{Al}_{70}\text{Co}_{15}\text{Ni}_{15}$, and on melt-quenched samples of other compositions was performed by Tsuda, Nishida, Saitoh, Tanaka, Tsai, Inoue, Masumoto (1996b). Contrary to melt-quenched d- $\text{Al}_{70}\text{Co}_{15}\text{Ni}_{15}$, the annealed sample showed superstructure type I reflections on the SAED patterns. The symmetry of melt-quenched $\text{Al}_{70}\text{Co}_{15}\text{Ni}_{15}$, $\text{Al}_{70}\text{Co}_{20}\text{Ni}_{10}$ and $\text{Al}_{75}\text{Ni}_{25}$ was determined to $P10_5/mmc$, while $P\bar{1}0m2$ was found for $\text{Al}_{70}\text{Co}_{27}\text{Ni}_3$ as well as for $\text{Al}_{70}\text{Co}_{27}$ (Saitoh, Tsuda, Tanaka, Tsai, Inoue, Masumoto, 1994). The symmetry of the ≈ 20 Å clusters appeared pentagonal for electron energies of 200 keV and decagonal for 300 or 400 keV. The observed decagonal symmetry was explained, and confirmed by contrast simulations, as artifact resulting from the strong contribution of the 1342-type reflections (*IY-indexing*) to the contrast transfer function.

The first 2D ALCHEMI (atom location by channeling-enhanced microanalysis) study on annealed d- $\text{Al}_{72}\text{Co}_8\text{Ni}_{20}$ (900 °C 47 h) showed that Al and TM atoms occupy different sets of sublattice sites while both Ni and Co occupy a similar set of sublattice sites, i.e. they are disordered as first simulations indicate (Saitoh, Tanaka, Tsai, Rossouw, 2000). Unfortunately no detailed discussion was given of the resolution of the experiment and on what scale they TM disorder takes place, on the scale of the basic pentagonal clusters or on that of the ≈ 20 Å columnar clusters or on that of the inversion the domains.

The first HAADF (100 and 200 kV) images on a d-phase in the system Al–Co–Ni were taken on annealed (900 °C, 47 h) $\text{Al}_{72}\text{Co}_8\text{Ni}_{20}$ (Saitoh, Tsuda, Tanaka, Kaneko, Tsai, 1997). The ≈ 20 Å cluster was found to have just mirror symmetry due to a triangular contrast in its center and to be composed of small pentagonal (P) and star-shaped (S) subclusters (Fig. 5.2.1.4-3). These clusters decorate a rhomb Penrose tiling and a HBS tiling, respectively. A detailed model, *AlCoNi-STT-98*, of the 5D atomic surfaces and 3D quasilattice obeying symmetry $P10_5/mmc$ was given by Saitoh, Tsuda, Tanaka (1998).

The local disorder in the fundamental ≈ 20 Å clusters was investigated by HAADF (300 kV) on annealed (900 °C, 47 h) d- $\text{Al}_{72}\text{Co}_8\text{Ni}_{20}$ (Yan, Pennycook, Tsai, 1998). Two types *a* and *b* of the fundamental cluster were observed with different atomic ordering on the innermost ring (*AlCoNi-YP-98*). In type *a*, it corresponds to a pure TM cluster, in type *b* rather to an Al/TM mixture contributing to the entropy of the system. The composition of this ring may vary from cluster to cluster. In the outermost ring, double contrasts are assigned to half-occupied TM columns yielding an ordered distribution of vacancies, crucial for the frequency of phason flips along the tenfold axis. In addition, three different decoration types of penta-

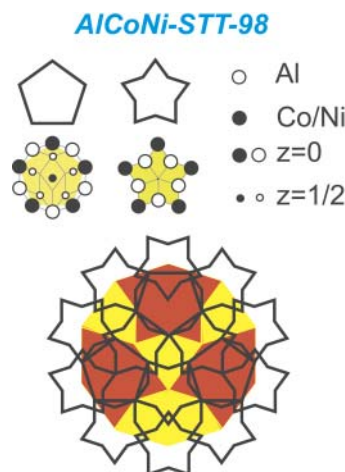


Fig. 5.2.1.4-3. Schematic structure model, *AlCoNi-STT-98*, of the fundamental ≈ 20 Å cluster in d-Al–Co–Ni with ≈ 4 Å (two atomic layers) periodicity along the tenfold axis. The two basic subclusters (≈ 8 Å diameter), a pentagonal (P) and a star-shaped one (S) are shown (Saitoh, Tsuda, Tanaka, 1998). The Gummelt decagon with ≈ 6.4 Å edge length and ≈ 20 Å diameter is drawn in. The model name code contains the reference where it was first published (first letter of the authors names and year of publication).

gons were identified on the perimeter of the outmost ring. This study agrees very well with the results of X-ray studies such as *AlCoNi-SHZKL-93* and *AlCoNi-CHS-02*, indicating a considerable amount of disorder in the clusters.

A ‘quasi-unit cell’ description (i.e. in terms of decorated Gummelt decagons) of the structure of d- $\text{Al}_{72}\text{Co}_8\text{Ni}_{20}$ was given by Steinhardt, Jeong, Saitoh, Tanaka, Abe, Tsai, (1998). The decoration of Gummelt-decagons was given with a mistake corrected later in Steinhardt, Jeong, Saitoh, Tanaka, Abe, Tsai (1999) (*AlCoNi-SJSTAT-98*, Fig. 5.2.1.4-1). This model was shown (Yan, Pennycook, 2000a, b) to have significant shortcomings. For instance, it did not fit to the HAADF images of Yan, Pennycook, Tsai (1998), which were taken with higher resolution than Saitoh, Tsuda, Tanaka, Kaneko, Tsai (1997) reached on samples that were prepared in the same way. Instead of the double columns clearly visible on the images, the model has only single columns. However, the crucial difference between both models lies in the symmetry. *AlCoNi-YP-98* possesses intrinsic decagonal symmetry that is broken by disorder. The consequence is a random tiling model for the d-phase indicating entropy stabilization. Contrary to that, *AlCoNi-SJSTAT-98* is a strictly ordered low-symmetry model with matching rules favoring a strictly quasiperiodic tiling, which could be a ground state. Based on the criticism by Yan, Pennycook (2000a) and new experimental evidence (HRTEM 400 kV), Steinhardt, Jeong, Saitoh, Tanaka, Abe, Tsai (2000) and Abe, Saitoh, Takakura, Tsai, Steinhardt, Jeong (2000) modified their model to *AlCoNi-ASTTSJ-00* (Fig. 5.2.1.4-1). One of their arguments, however, is rather poor. In contrast to the findings of Ritsch, Beeli, Nissen, Gödecke, Scheffer, Lück (1998), they consider d- $\text{Al}_{72}\text{Co}_8\text{Ni}_{20}$ as perfectly ordered phase although it is a HT-phase. They state ‘if the structure could tolerate sufficient disorder ... to transform all or nearly all decagonal clusters to tenfold symmetry breaking clusters, then one would expect that the single phase region would extend to a wider composition range (at high temperature) than an

order of a few atomic percent, but it evidently does not.' This assumption is wrong as can be seen, for instance, from the HT studies of Baumgarte, Schreuer, Estermann, Steurer (1997) where a very wide existence range of this phase was found.

A modified model, *AlCoNi-YP-00* (Fig. 5.2.1.4-1), consisting of pentagonal subclusters was proposed by Yan, Pennycook (2000a, b). The proposed structure of the subclusters was based on the structure of τ^2 -Al₁₃Co₄, with ≈ 8 Å periodicity along the pseudo-tenfold axis being an approximant of the more Co-rich d-phase. Like in their previous model, *AlCoNi-YP-98*, disorder in the innermost ring of TM atoms is responsible for the observed broken symmetry. Depending on the degree of disorder, however, a random tiling would be observed in contrast to the observations of Ritsch, Beeli, Nissen, Gödecke, Scheffer, Lück (1998) who confirm the existence of disorder inside the clusters but found almost perfect quasiperiodic order in the pentagonal tiling. Consequently, the next model, *AlCoNi-YP-01*, slightly modified based on results of first-principles calculations, features now also broken tenfold symmetry due to chemical order, however, only in the innermost ring (Yan, Pennycook, 2001).

A HRTEM (400 kV) and HAADF (200 kV) study was carried out on annealed (950 °C, 65 h) d-Al₇₂Co₈Ni₂₀ (Hiraga, Ohsuna, 2001a). A description of the structure was presented in form of a well-ordered pentagonal tiling (edge length ≈ 32 Å) decorated with $a \approx 32$ Å cluster with full decagonal symmetry in the projection, *AlCoNi-HO-01*. The authors argue that former observations have overlooked this τ -times larger fundamental cluster due to irradiation damage. One has to keep in mind that the sample of this study was annealed 65 h at 950 °C compared to 47 h at 900 °C for the samples used by the other groups that performed HAADF experiments.

A local thermal vibration anomaly by phason related atomic fluctuations was observed *in situ* at 1100 K on annealed (1100 K) d-Al₇₂Co₈Ni₂₀ by HAADF (200 kV and 300 kV) (Abe, Pennycook, Tsai, 2003). The main changes are observed on the innermost ring of the ≈ 20 Å cluster. At 1100 K this ring appears enhanced compared to the quenched sample. The (non-perfect) pentagon tiling (≈ 20 Å edge length) appears greatly enhanced at 1100 K as well.

The type I superstructure was studied on an annealed (900 °C, 120 h) sample with composition d-Al_{72.5}Co₁₁Ni_{16.5} by HAADF (200 kV) and HRTEM (400 kV) (Hiraga, Ohsuna, Nishimura, 2000). Three types of atom clusters were identified, two oppositely oriented with pentagonal symmetry and one with triangular contrast in the center. The clusters decorate two rhombic tilings (superlattices of a pentagonal tiling with 20 Å edge length) with ≈ 32 Å edge length. A similar order was found in d-Al–Ni–Ru (Sun, Ohsuna, Hiraga, 2000). A model of the cluster with pentagonal symmetry was proposed, *AlCoNi-HON-00*, a modified variant of *AlCoNi-HLS-91* with different TM atom distribution.

Electron microscopy – Co rich d-phases

Annealed (1050 °C, 12 h) samples from the Co-rich part of the assumed stability region of the d-phase with compositions Al_{72.5}Co₂₀Ni_{7.5} and Al_{72.5}Co₁₉Ni_{8.5} exhibit SAED

patterns with only fivefold symmetry and strong diffuse (interlayer) scattering related to ≈ 8 Å periodicity (Ritsch, Beeli, Nissen, 1996). Despite the fact that the pentagon tiling on the micrographs resembles rather a nanodomain structure than a quasiperiodic one, the authors interpreted it as a quasiperiodic phase with pentagonal symmetry (5f). Similar observations were made in annealed (1160 °C, 2 h) and quenched samples with composition Al_{71.5}Co_{25.5}Ni₃, which can rather be seen as Ni stabilized d-Al–Co (Ritsch, Beeli, Lück, Hiraga, 1999). The tenfold SAED patterns show S1 and S2 reflections and strong diffuse scattering underneath and close to the main and S2 reflections. By analysis of HRTEM images employing the method of Joseph, Ritsch, Beeli (1997) a random rhomb tiling state was found decorated by parallel ordered pentagons. The superstructure reflections are caused just by the rhomb tiling, which can be seen as superstructure of a pentagon tiling (Niizeki, 1994).

The 1D QC studied quantitatively by high-resolution X-ray diffraction (Kalning, Kek, Krane, Dorna, Press, Steurer, 1997) was also investigated by Ritsch, Radulescu, Beeli, Warrington, Lück, Hiraga (2000). From SAED and HRTEM (1250 kV) images taken on annealed (1050 °C 20 h; 950 °C, 4 d, 900 °C, 4 d) samples of composition 71–71.5% Al and 18–22% Co as well as on Al₇₁Co₁₉Ni₁₀ (1100 °C 11 h; 1080 °C 17 h), they concluded the existence of a stable 1D QC with lattice parameters ≈ 61 Å and ≈ 8.1 Å. The ≈ 20 Å clusters show a LSLS... sequence along the ≈ 61 Å axis, with $L = 19.82$ Å based on a rhomb tiling with edge length $a_r = 2.46$ Å (the same values for a_r and L , just more accurate, were already obtained for the ≈ 20 Å cluster and the underlying rhomb tiling by Steurer, Haibach, Zhang, Kek, Lück, 1993).

The pentagonal QC with composition d-Al_{71.5}Co_{25.5}Ni₃ (1160 °C, 3 h) was also investigated by HAADF (200 kV) (Hiraga, Ohsuna, Nishimura, 2001a). Clusters with ≈ 20 Å diameter and pentagonal symmetry were found to decorate a rhomb tiling all with the same orientation. A model of the cluster, different from that proposed by Ritsch, Beeli, Lück, Hiraga (1999) was given by Hiraga, Ohsuna, Nishimura (2000). A HAADF (200 kV) study of an annealed (900 °C, 40 h) sample with composition d-Al_{72.5}Co_{17.5}Ni₁₀ yielded that the so-called basic Co-rich phase (Ritsch, Beeli, Nissen, Gödecke, Scheffer, Lück, 1998) is just the pentagonal QC without superstructure reflections in a not very well ordered state (Hiraga, Sun, Ohsuna, 2001). Thus its structure can be described by a pentagonal tiling decorated with ≈ 20 clusters with pentagonal symmetry all oriented in the same way.

The structure of an annealed (900 °C, 72 h) sample with composition Al_{71.5}Co₁₆Ni_{12.5} (superstructure type II) was studied by HAADF (200 kV) and HRTEM (400 kV) (Hiraga, Ohsuna, Nishimura, 2001c). A rather disordered tiling was identified on the micrographs, which contained translational parts of pentagon decorated squashed hexagons as well as a rhomb tiling. Both types of tilings can be derived from a 5D hypercubic NaCl-type structure. The vertices are all decorated by the same ≈ 20 Å cluster with pentagonal symmetry that was found in all other phases in the Al–Co–Ni system with the exception of the basic Ni-rich phase.

Hiraga, Ohsuna, Nishimura (2001b) studied by HAADF (200 kV) and HRTEM (400 kV) a sample with the same composition $\text{Al}_{71.5}\text{Co}_{16}\text{Ni}_{12.5}$, which had been longer annealed (900 °C, 120 h), however. It resulted to be the orthorhombic PD_{3c} approximant, $Pmn2_1$, $a \approx 52$ Å, $b \approx 4$ Å, $c \approx 37$ Å, (Grushko, Holland-Moritz, Wittmann, 1998), which is related to the type I superstructure. A structure model was presented using the same clusters with pentagonal symmetry that were also found in the superstructure type I. The linking of the clusters is the L-type linkage already shown in Steurer, Haibach, Zhang, Kek, Lück (1993).

A continuous transformation between quasicrystalline and crystalline state was observed by SAED and HRTEM (200 kV) investigations of differently long annealed (1120–1370 K, 40–1370 h) samples with composition $\text{Al}_{72.7}\text{Co}_{19}\text{Ni}_{8.3}$ (Döblinger, Wittmann, Gerthsen, Grushko, 2002). After 40 h annealing time at 1300 K a d-phase with S1 superstructure was identified. By prolonged annealing the d-phase was transformed into a 1D QC and finally to a non-rational approximant, $a \approx 50.8$ Å, $b \approx 8.25$ Å, $c \approx 32.2$ Å (a simple tiling structure model was proposed).

The transformation behavior of a homogenized (1290 K, 43 h) and annealed (1140 K, 384 h, 1125 h, 2718 h) sample with composition $\text{Al}_{72.5}\text{Co}_{15.5}\text{Ni}_{12}$ was studied by SAED and HRTEM (200 kV) (Döblinger, Wittmann, Grushko, 2001). It was found that a homogenous d-phase (superstructure type S1) of this composition transforms via intermediate states (such as ‘superstructure type II’, which resulted to show first a fivefold twinned 1D QC and then a twinned $\langle 4,6 \rangle$ -approximant) to a mixture of the monoclinic X-phase and a d-phase (superstructure type I, unfinished transition probably due to not equilibrated chemical order) after 2718 h at 1140 K. This kind of transformation has been predicted by Steurer (1999, 2000) and Honal, Haibach, Steurer (1998). The transition from nanodomain structures (NDS) to approximants was studied on another annealed (1270 K, 69 h) sample with composition $\text{Al}_{71.3}\text{Co}_{17.4}\text{Ni}_{11.3}$ (Döblinger, Wittmann, Gerthsen, Grushko, 2003). The starting material consisted of NDS embedded in domains of disordered 1D QC, which transformed via intermediate structures two different approximants. The orientationally twinned NDS and 1D QC of the starting material must have been formed from a d-phase at higher temperature.

X-ray diffraction and neutron scattering

The first single-crystal X-ray structure analysis on a d-phase in the system Al–Co–Ni was performed on slowly cooled d- $\text{Al}_{70}\text{Co}_{20}\text{Ni}_{10}$ (Yamamoto, Kato, Shibuya, Takeuchi, 1990). The 5D structure model refined was based on atomic surfaces derived from the structure of m- $\text{Al}_{13}\text{Fe}_4$. However, only models with two-layer periodicity of 4.08 Å were studied. For the refinement of the final model (2 parameters), *AlCoNi-YKST-90*, only the strongest 41 reflections out of the 1400 unique collected intensities were used, and $R = 0.11$ was obtained employing the 5D space group $P10/mmm$. Another model with symmetry $P10mc$ was refined to $R = 0.134$. No detailed information about diffraction data collection was given.

Another single-crystal X-ray structure analysis was performed on annealed (1123 K, 24 h) and quenched d- $\text{Al}_{70}\text{Co}_{15}\text{Ni}_{15}$ (Steurer, Haibach, Zhang, Kek, Lück, 1993). The 5D model was refined in space group $P10_5/mmc$ to $wR = 0.078$ (253 reflections, 21 variables). The final electron density maps were calculated employing for the first time the maximum-entropy method (MEM) in QC structure analysis to get truncation error free data. The structure model, *AlCoNi-SHZKL-93*, derived from the electron density maps consists of ≈ 20 Å columnar clusters decorating the vertices of a rhomb Penrose tiling with edge length 19.79(1) Å and additionally the body-diagonals of the fat rhombs. This could also be seen as Robinson triangle tiling of same edge length. The structure was also discussed in terms of an HBS-tiling (called ‘network of icosagonal rings’ and ‘Y-like strips’) with 6.430 Å edge length and decorated with pentagonal antiprismatic clusters of ≈ 6.4 Å diameter (Fig. 5.2.1.4-1). The cluster model differs from *AlCoNi-HLS-91* mainly in the occupation of the centers of the outmost ring of pentagons. Full crystallographic data and refinement information were given.

The structure of annealed (1373 K, 1 h; 1173 K, 60 h) d- $\text{Al}_{72}\text{Co}_8\text{Ni}_{20}$ was determined by single-crystal X-ray diffraction and refined in 5D space group $P10_5/mmc$ to $wR = 0.045$ for 449 reflections and 103 parameters (Takakura, Yamamoto, Tsai, 2001). The resulting structure model, *AlCoNi-TYT-01*, resembles *AlCoNi-CW-98* (Cockayne, Widom, 1998b). From the results it is concluded that the structure consists of an HBS-tiling with 6.36 Å edge length decorated by ≈ 20 Å clusters with inherently lower than tenfold symmetry. For comparison, the model *AlCoCu-B-91* (Burkov, 1991) was refined by the authors to $wR = 0.161$ for 55 parameters.

The most recent single-crystal X-ray diffraction structure analysis was performed on slowly solidified and quenched (800 °C) d- $\text{Al}_{70.6}\text{Co}_{6.7}\text{Ni}_{22.7}$ (Cervellino, Haibach, Steurer, 2002). By the atomic surfaces modeling method a four-layer structure model projected on two layers was refined in 5D space group $P\bar{1}0$ to $wR = 0.060$ for 2767 reflections and 749 parameters. The resulting structure, *AlCoNi-CHS-02*, can be described in terms of a disordered Gummelt cluster with broken tenfold symmetry decorating a pentagonal Penrose tiling. The projected electron density agrees quite well with typical HAADF images (Fig. 5.2.1.4-4).

The temperature dependence of the intensities of main reflections and first and second-order superstructure reflections was measured by X-ray diffraction on annealed single-crystalline samples of composition $\text{Al}_{70}\text{Co}_{13}\text{Ni}_{17}$ (Edagawa, Sawa, Takeuchi, 1994). An X-ray single crystal study on a series of decaprisymmetric crystals of compositions $\text{Al}_{65-77}\text{Co}_{3-22}\text{Ni}_{3-22}$, quenched from 800 °C, was performed as function of composition and temperature (Zhang, 1995; Zhang, Estermann, Steurer, 1997; Baumgarte, Schreuer, Estermann, Steurer, 1997). The sample with composition $\text{Al}_{73.5}\text{Co}_{21.7}\text{Ni}_{4.8}$ could be clearly identified as twinned nanodomain structure. $\text{Al}_{70.7}\text{Co}_{19.0}\text{Ni}_{10.3}$ and $\text{Al}_{71.0}\text{Co}_{17.7}\text{Ni}_{11.3}$ did not show reflection splitting in the low-resolution X-ray precession photographs but “satellite reflections” which have been shown to be related to

twinned domain structures of 1D QC (Kalning, Kek, Burandt, Press, Steurer, 1994; Kalning, Press, Kek, 1995; Kalning, Kek, Krane, Dorna, Press, Steurer 1997). $\text{Al}_{72.7}\text{Co}_{11.6}\text{Ni}_{15.7}$ was superstructure I and $\text{Al}_{70.6}\text{Co}_{6.8}\text{Ni}_{22.6}$ the basic Ni-rich d-phase. The same single crystals were used for an *in situ* high-temperature X-ray diffraction study Baumgarte, Schreuer, Estermann, Steurer (1997). There was a mistake in temperature calibration, the nominal temperatures given in the publication are ≈ 200 K too high (e.g., 1520 K should read 1320 K). The main result was that at all the above given compositions a basic quasi-periodic phase with ≈ 4 Å periodicity existed at temperatures close to the peritectic decomposition into melt and β -phase.

Phason hopping was studied *in situ* by time-of-flight quasielastic neutron scattering on isotopic powder samples with compositions $\text{Al}_{71}\text{Co}_{12}\text{Ni}_{17}$ for natural Ni, and $\text{Al}_{71.5}\text{Co}_{13}\text{Ni}_{15.5}$ for the pure isotopes Ni^{58} and Ni^{60} (Coddens, Steurer, 1999). Since the fast hopping process is local, there is a continuous dependence of the quasielastic parameters in the whole temperature range between 500 °C and 940 °C despite the transformations, which the superstructure of type I undergoes in this temperature range. There were no indications of TM hopping.

A Patterson space analysis was performed based on X-ray diffraction data of d- $\text{Al}_{71}\text{Co}_{13}\text{Ni}_{16}$ to derive the proper basis of the superstructure I (Haibach, Cervellino, Estermann, Steurer, 1999). Its relationship to the reciprocal bases of Edagawa, Ichihara, Suzuki, Takeuchi et al. (1992) and Yamamoto and Weber (1997a) was given.

By multiple-beam single-crystal X-ray diffraction studies on annealed samples of d- $\text{Al}_{68}\text{Co}_{21}\text{Cu}_{11}$ (1000 °C, 133 h), $\text{Al}_{71}\text{Fe}_5\text{Ni}_{24}$ (910 °C, 120 h), $\text{Al}_{72.5}\text{Co}_{11}\text{Ni}_{16.5}$ (910 °C, 120 h), for all of three types of d-phases non-centrosymmetry was found (Eisenhower, Colella, Grushko, 1998).

The atomic short-range order (SRO) of (annealed?) d- $\text{Al}_{72}\text{Co}_8\text{Ni}_{20}$ was studied by anomalous-X-ray scattering by the three-wavelength method (Abe, Matsuo, Saitoh, Kusawake, Ohshima, Nakao, 2000). The sample did not show any H^\perp dependence of the FWHM of Bragg reflections. The contribution to diffuse scattering from Ni–Co ordering was largest. The correlation length of the SRO related to the width of diffuse maxima amounts to approximately the ≈ 20 Å cluster diameter. In another experiment the diffuse scattering of annealed (1073 K, 1 d) d- $\text{Al}_{72}\text{Co}_8\text{Ni}_{20}$ was studied *in situ* in the temperature range $965 \leq T \leq 1116$ K (Abe, Saitoh, Ueno, Nakao, Matsuo, Ohshima, Matsumoto, 2003). The quenched (from 1073 K) sample shows diffuse peaks at the locations of S1 superstructure reflections, which become sharper at 965 K and disappear at 1002 K ($= T_c + 10$ K).

An *in-situ* high-temperature X-ray diffraction study on d- $\text{Al}_{70}\text{Co}_{12}\text{Ni}_{18}$, quenched from 900 °C, was performed by Steurer, Cervellino, Lemster, Ortelli, Estermann (2001). Reconstructed reciprocal space sections (perpendicular and parallel to the tenfold axis; Bragg layers as well as diffuse interlayers) are shown as a function of temperature (Fig. 5.2.1.4-5). It is remarkable that between 800 and 850 °C the correlation length related to the diffuse interlayers is drastically decreased and the S2 superstructure

reflections (called 1st order satellites) become weaker. The S1 reflections and the main reflections with large perpendicular space component, however, even increase their intensities within a certain temperature range supporting the random tiling picture. From the difference Patterson map calculated from the satellite reflections alone, one sees positive and negative correlations indicating Al/TM ordering between atoms of different clusters.

Approximants

The high-temperature phase m- $\text{Al}_{13}\text{Co}_4(\text{h})$ can be stabilized to lower temperatures by substituting 2–3% Co by Ni (Gödecke, Ellner, 1996). Its structure was determined by Zhang, Gramlich, Steurer (1995). The structure of $\text{Al}_9\text{Co}_2\text{Ni}$ (Y2-phase) was determined by Grin, Peters, Burkhardt, Gotzmann, Ellner (1998). The crystal structure of the approximant W-Al–Co–Ni (*Cm*, $a = 39.668(3)$ Å, $b = 8.158(1)$ Å, $c = 23.392$ Å) was studied on an annealed (950 °C, 0–20 d) sample with composition $\text{Al}_{72.5}\text{Co}_{20}\text{Ni}_{7.5}$ by HAADF (200 kV) and HRTEM (400 kV) (Hiraga, Ohsuna, Nishimura, 2001b) as well as by single-crystal X-ray diffraction (Sugiyama, Nishimura, Hiraga, 2002). Unfortunately, only a qualitative picture was given, no quantitative crystallographic data were reported. The comparison of SAED and HAADF images with those of the pentagonal QC (Hiraga, Ohsuna, Yubuta, Nishimura, 2001), $\text{Al}_{71.5}\text{Co}_{25.5}\text{Ni}_3$ (1160 °C, 2 h), indicated close structural similarity. Consequently, W- $\text{Al}_{72.5}\text{Co}_{20}\text{Ni}_{7.5}$ can be seen as approximant of the pentagonal quasicrystal.

High-resolution XRD studies have been performed on samples with composition $\text{Al}_{70}\text{Co}_{15}\text{Ni}_{15}$ with different thermal history: ACN1 slowly (1 K min^{−1}) cooled from 800 °C, ACN2 rapidly cooled from 800 °C after annealing, ACN3 slowly (10 K min^{−1}) cooled from 1200 °C (Kalning, Kek, Burandt, Press, Steurer, 1994; Kalning, Press, Kek, 1995). In sample ACN1 a twinned nanodomain structures was observed of the monoclinic $\langle 5,7 \rangle$ -approximant, $a = 51.911(5)$ Å, $b = 51.907(5)$ Å, $c = 4.0799(5)$ Å, $\gamma = 108.00(1)^\circ$ (the same type of approximant was also observed in Al–Co–Cu samples by Song, Wang, Ryba, 1991; Fettweis, Launois, Denoyer, Reich, Godard, Lambert, 1993; Fettweis, Launois, Denoyer, Reich, Lambert 1994; Fettweis, Launois, Reich, Wittmann, Denoyer, 1995). Sample ACN2 seemed to be in a kind of intermediate state between QC and approximant, ACN3 was a decagonal phase with sharp but weak satellite reflections (satellite vector of 30.5 Å). The results on ACN1 have been revisited and based on these data and newly measured ones, the authors concluded that the data can be better interpreted by a twinned 1D quasi-crystal (decagonal phase with strong linear phason strain) than with the above mentioned approximant (Kalning, Kek, Krane, Dorna, Press, Steurer, 1997). Indeed, based on a simulation of a $8000 \text{ Å} \times 8000 \text{ Å} \times 4 \text{ Å}$ nanodomain structure of a 1D QC obtained by linear phason strain from d-Al–Co–Ni, the observed reflection splitting could be nicely reproduced (Honal, Haibach, Steurer, 1998).

The temperature dependence of the interlayer-diffuse scattering was studied by *in-situ* X-ray and neutron diffraction on samples with composition $\text{Al}_{72}\text{Co}_{16}\text{Ni}_{12}$ (Frey, Weidner, Hradil, de Boissieu, Letoublon, McIntyre, Currat,

Tsai, 2002). Above 800 °C the peaked diffuse scattering becomes more diffuse, at 950 °C the homogenous part disappeared while residual density was observed for the peaked part. For the decay of diffuse scattering with temperature a power law $I(T) \approx (T - T_c)^{2\beta}$, with $\beta \approx 0.11$ and $T_c \approx 910$ °C, was found.

A very accurate *in-situ* HT study ($290 \leq T \leq 1100$ K) by dilatometry and powder XRD was performed on annealed (1220 K, 4 d; 1070 K, 7 d; 1000 K, 7 d) d-Al_{71.2}Co_{12.8}Ni₁₆ (Soltmann, Beeli, Lück, Gander, 2003). The type I \leftrightarrow S1 phase transition was identified to be of second order with an onset temperature of 1007 K and a finishing temperature of 1042 K. It is accompanied by an elongation of coordination polyhedra along the tenfold axis and a contraction perpendicular to it. Thermal expansion was found to be isotropic at temperatures up to 900 K. The mobility of atoms was estimated based on diffusion coefficient data; the diffusion lengths within 100 sec are for Co and Al: 0.8 Å and 20 Å at 670 K, 18 Å and 350 Å at 770 K, respectively.

A low-temperature study was performed on slowly cooled d-Al_{70.7}Co_{13.3}Ni_{16.0}, milled 2 min in a ball mill (Kupsch, Meyer, Gille, Paufler, 2002). Powder diffractograms were taken *in situ* in the temperature range $100 \leq T \leq 200$ K. At ≈ 150 K additional reflections appeared. The phase transition was found to be reversible but subjected to fatigue. The authors assumed a milling

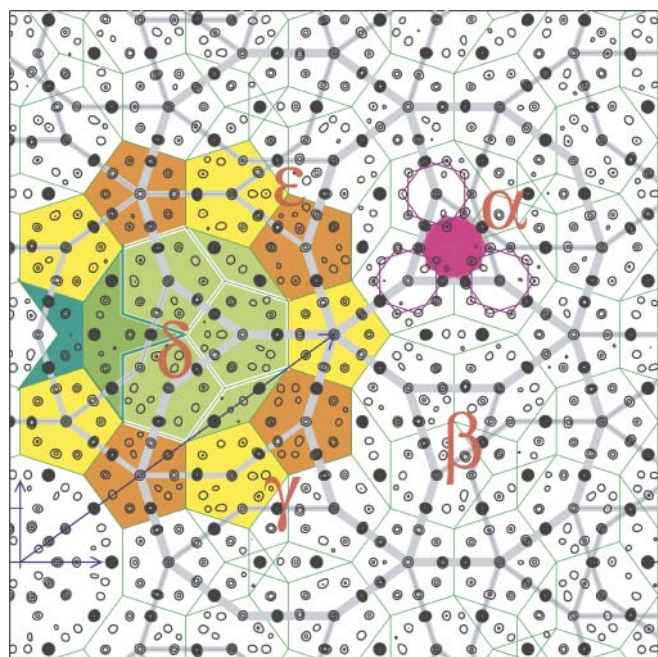
induced defect structure giving rise to the observed structural changes since no transition was observed on single crystals yet.

Further models

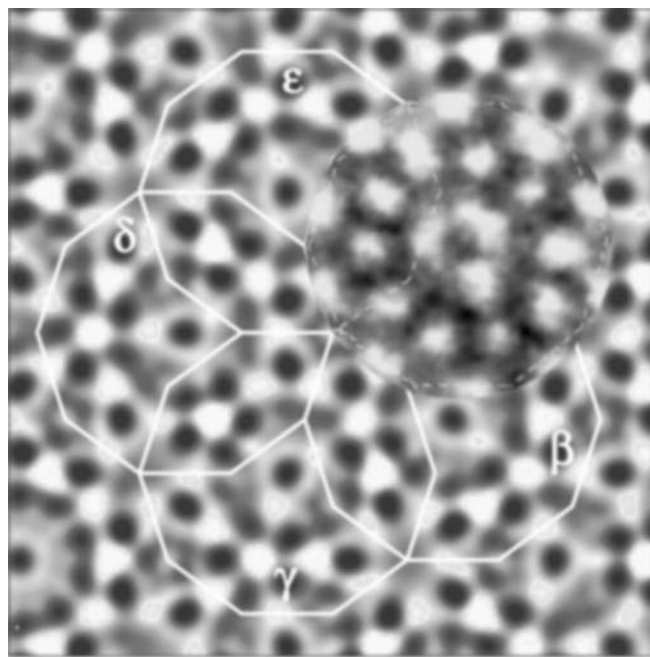
Based on the diffraction data of model *AlCoNi-SHZKL-93*, a 5D structure refinement was performed in 5D space group $P10_5/mmc$ employing symmetry-adapted functions to describe the atomic surfaces (*AlCoNi-EP-95*; Elcoro, Perez-Mato, 1995). The final reliability factors reached ($R = 0.092$, $wR = 0.080$, for 253 reflections and 18 parameters) almost the same values as in the refinement by Steurer, Haibach, Zhang, Kek, Lück (1993) with 23 parameters. The electron density maps also showed great similarity.

Saitoh, Tsuda, Tanaka (1997) presented a series of models (atomic surfaces and projected structures) for d-phases with 4 Å periodicity (d-Al–Ni–Co, d-Al–Ni–Fe, d-Al–Co–Cu) and symmetries $P10_5/mmc$ and $P\bar{1}0m2$, which have pentagonal clusters. The models are modifications of a model already discussed by Yamamoto (1996a).

A 5D model, *AlCoNi-YW-97*, of the type I superstructure was discussed by Yamamoto, Weber (1997a). Atomic surfaces of the 5-fold supercell were designed and a 3D projection of the structure shown. The authors point out that the superstructure can be obtained essentially by phason flips of the fundamental cluster (accompanied by diffusion to restore chemical order inside the clusters).

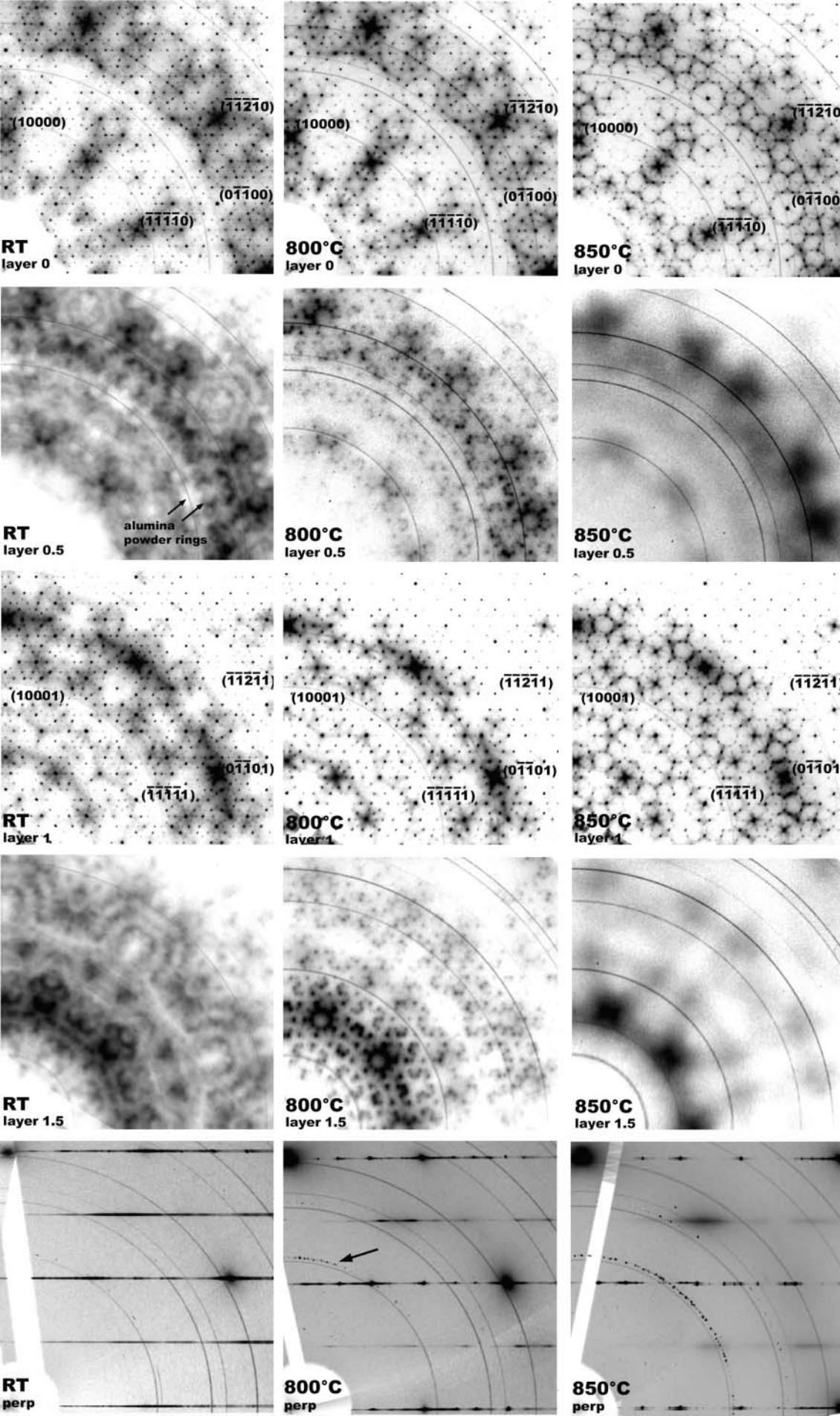


(a)



(b)

Fig. 5.2.1.4-4. (a) The projected electron density is shown in a $45 \text{ Å} \times 45 \text{ Å}$ contour plot. A pentagonal Penrose tiling modified according to Niizeki (1993) is shown with green lines (edge length $a_t = 4.625 \text{ Å}$). A group of five Gummelt decagonal clusters with 20.600 Å diameters is drawn in, labeled by Greek letters. Note that the centres of the clusters α , γ , δ , appear clearly asymmetric, while clusters β , ϵ appear approximately decagonal (compare with HAADF images of Yan, Pennycook, Tsai, 1998). The centres of the Gummelt decagons are located on a τ^2 -inflated version of the pentagon tiling. Note the Y configuration of three pentagons in the centre of each Gummelt decagon; on their intersection a small decagon of atoms with an empty centre is formed. On cluster α this configuration is marked in pink. Each decagon corresponds to a pair of inverted pentagons belonging to different atomic layers. The double tiling introduced by Hiraga, Sun, Yamamoto (1994) and Yamamoto (1996a) is marked on Gummelt decagon δ . The green star corresponds to the 'ejection' of the tenth surrounded pentagon observed by Hiraga. The tile symmetry should match the decorations symmetry, however, this is not the case. On clusters β and ϵ this is less evident. (b) The projected electron density on a resolution comparable to that of the HAADF image (from a sample with composition $\text{Al}_{72}\text{Co}_8\text{Ni}_{20}$ studied by Abe, Tsai (2001) copied upon the place of Gummelt decagon α . Black corresponds to zero density, white to maximum density. The qualitative agreement between the distribution of TM related contrasts is easily seen.



A structural model for the phase transformation of a decagonal QC to its approximant was discussed by Honal, Haibach, Steurer (1998). The authors propose a mechanism based on the periodic average structure common to the d-phase and the approximant (Steurer, Haibach, 1999b). Simulations of the scattering of a $8000 \times 8000 \times 4 \text{ \AA}^3$ sized model of the resulting nanodomain structures was compared with experimental data (Kalning, Kek, Burandt, Press, Steurer, 1994; Kalning, Kek, Krane, Dorna, Press, Steurer, 1997; Kalning, Press, Kek, 1995). A pentagon-tiling-flip based simulation of this transformation was performed in a Monte-Carlo study by Honal, Welberry (2002). It was not possible by this method to get full quasicrystal-to-crystal transformation or *vice versa*. The average structure remained quasiperiodic as shown by the calculation of the Fourier transform.

The atomic and electronic structure of $d\text{-Al}_{\approx 70}\text{Co}_{\approx 15}\text{Ni}_{\approx 15}$ was studied by quantum-mechanical calculations as well as by single-crystal X-ray data (data set of Steurer, Haibach, Zhang, Kek, Lück, 1993) based structure refinements (Krajci, Hafner, Mihalkovic, 2000). A comparison of different models showed that the $\approx 20 \text{ \AA}$ clusters are essential to obtain a satisfactory agreement of measured and calculated photoemission data. One important contribution came from TM–TM interactions such as pentagonal antiprismatic TM clusters in the center of the $\approx 20 \text{ \AA}$ clusters. The best (but still not perfect) agreement was obtained for the pure Ni inner-core model and a high Co coordination by Al (as already proposed by Steurer, Haibach, Zhang, Kek, Lück, 1993). The outer part of the cluster was assumed to have some disorder in the decoration. Significant differences to $d\text{-Al-Co-Cu}$ were found, where strongly repulsive Cu–Cu interactions are avoided. In $d\text{-Al-Co-Ni}$ the attractive Ni–Ni and Co–Al interactions leads to high Ni–Ni and Co–Al coordination. The number of Ni–Co pairs is much lower than that of Cu–Co pairs.

Total-energy calculations based on GPT (generalized pseudopotential theory) pair potentials were used to study binary and ternary phases in the systems Al–Co–Cu and Al–Co–Ni (Widom, AlLehyani, Moriarty, 2000). The pair potentials showed that Al–Al interactions below $\approx 3 \text{ \AA}$ are strongly disfavoured compared to Al–Ni or Al–Co and less strongly to Al–Cu interactions. At low TM concentration this tends to maximize their Al coordination number. It is remarkable that the deep minimum in the Co–Co pair potential matches the frequent Co–Co distance of 4.5 \AA and 6.5 \AA found in the d-phase structure related to the TM pentagonal network.

A total-energy-based structure prediction for $d\text{-Al}_{70}\text{Co}_9\text{Ni}_{21}$ by Monte-Carlo simulation as well as by Molecular dynamics calculations was performed by

Henley, Mihalkovic, Widom (2002) and Mihalkovic, Al-Lehyani, Cockayne, Henley, Moghadam, Moriarty, Wang, Widom (2002) based on a 3D tiling-decoration model. Their model has great similarity with both more recent electron microscopy images as well as with results of X-ray structure refinements. In particular, they found the $\approx 20 \text{ \AA}$ cluster with triangular symmetry in the center. The authors pointed out the special role each type of atom has in its site in this d-phase. Due to the pair potentials employed, the minimum-energy structure must maximize the number of Al–TM bonds, each Co atom must have only Al neighbours (this is possible only up to $\approx 10\%$ Co, explaining why a superstructure is needed for higher Co content), and all TM–TM neighbours have to be Ni–Ni.

From a comparative study of structures of approximants and d-phases, Steurer (2001) concluded that the fundamental building unit of approximants and d-phases in the system Al–Co–Ni is the pentagonal double-bipyramid (Fig. 5.2.2.1-1(f)). It has an inherent 8 \AA periodicity, and in projection it exhibits pentagonal symmetry in agreement with HAADF observations (see, for instance, Hiraga, 2002). It should be kept in mind that the pentagonal bipyramid possesses a rather high packing density since it consists of five, only slightly distorted tetrahedra.

5.2.1.5 Al–Co–Pd

Discovery

Metastable $d\text{-Al}_{70}\text{Co}_{20}\text{Pd}_{10}$, with $\approx 4 \text{ \AA}$ periodicity, was obtained by melt spinning (Tsai, Yokoyama, Inoue, Masumoto, 1990). While the SAED image in this work resembles that of basic Ni-rich $d\text{-Al-Co-Ni}$, the images of $d\text{-Al}_{73}\text{Co}_{22}\text{Pd}_5$ taken by Yubuta, Sun, Hiraga (1997) clearly show a (somewhat disordered) superstructure with $\approx 8 \text{ \AA}$ periodicity. As expected (Ni and Pd are in the same column of the periodic table), $d\text{-Al-Co-Pd}$ seems to order similar to $d\text{-Al-Co-Ni}$. Non-centrosymmetric symmetry was assigned to $d\text{-Al}_{73}\text{Co}_{22}\text{Pd}_5$.

Approximants

A close approximant of the d-phase, $W\text{-Al-Co-Pd}$, was discovered in as cast alloys as well as in rapidly solidified samples (Yubuta, Sun, Hiraga, 1997). From SAED patterns, the space group $Pmm2_1$ and the lattice parameters $a = 8.2 \text{ \AA}$, $b = 20.6 \text{ \AA}$, $c = 23.5 \text{ \AA}$ were determined. A comparison of the SAED images of the approximant and the d-phase (Fig. 2 of Yubuta, Sun, Hiraga, 1997) clearly shows that the 8 \AA superstructure, which is ordered in the approximant, is disordered in a similar way as known from $d\text{-Al-Co-Ni}$.

Yubuta, Sun, Hiraga (1997) proposed a tentative model, $AlCoPd\text{-YSH-97}$, for the structure of $W\text{-Al}_{73.8}\text{Co}_{23.3}\text{Pd}_{3.5}$ based on HRTEM images and on the structure model $AlCo\text{-Ni-HLS-91}$. The framework is built up of pentagonal and decagonal structural units with edge length 4.8 \AA . The four atomic layers are packed with a sequence ABA'B (A and A' are mirror planes differing by Pd/Co order; B layers do not contain any Pd). The d-phase is assumed to consist of the same structure motif packed quasiperiodically.

The phase diagram of Al–Co–Pd for 50–100% Al was studied by Yurechko, Grushko (2000) and Yurechko,

◀ **Fig. 5.2.1.4-5.** Series of reciprocal space sections of $d\text{-Al}_{70}\text{Co}_{12}\text{Ni}_{18}$ reconstructed from 360 image plate scanner frames at each temperature (*marresearch* 345, wavelength $\lambda = 0.7000 \text{ \AA}$, oscillation angle $\Delta\varphi = 0.5^\circ$, Swiss-Norwegian Beam Lines/ESRF, Grenoble). In the first column, sections of the reciprocal space layers $h_1h_2h_3h_4h_5$ with $h_5 = 0, 1/2, 1, 1.5$ and of the section $h_1h_2h_2h_1h_5$ perpendicular to them, all taken at room temperature, are shown. The second and the third column contain the sections collected at 800°C and 850°C , respectively. The reference basis of Steurer, Haibach, Zhang, Kek, Lück (1993) was used for indexing.

Grushko, Velikanova, Urban (2002). They confirmed the stability of the approximant W-Al–Co–Pd at 1050 °C in a small compositional range around $\text{Al}_{72.0}\text{Co}_{23.7}\text{Pd}_{4.3}$. The Al–Pd ε -phase region was found to extend up to 16.1% Co. The ε_n -phases are orthorhombic approximant phases where $n = 1$, the index of the strong (001) reflection related to a netplane distance of ≈ 2 Å. This means, for instance, $\text{Y-Al}_3\text{Pd}$ (Matsuo, Hiraga, 1994), $a = 23.5$ Å, $b = 16.8$ Å, $c = 12.3$ Å is denoted ε_6 ; the ε -phases with $a = 23.5$ Å, $b = 16.8$ Å, $c = 57.0$ Å and $a = 23.5$ Å, $b = 16.8$ Å, $c = 70.1$ Å are denoted ε_{28} and ε_{34} , respectively (Yurechko, Grushko, Velikanova, Urban, 2002).

5.2.1.6 Al–Fe–Ni

Discovery

D-Al–Fe–Ni was discovered by rapid solidification as metastable QC of high quality and 4 Å periodicity (Tsai, Inoue, Masumoto, 1989a). Lemmerz, Grushko, Freiburg, Jansen (1994) identified the unknown stable phase $\text{Al}_{10}\text{FeNi}_3$, discovered in a study of the phase diagram Al–Fe–Ni (Khaidar, Allibert, Driole, 1982), as decagonal phase. The stability range resulted to be rather narrow around $\text{Al}_{71}\text{Fe}_5\text{Ni}_{24}$ at temperatures between 1120 and 1200 K. The quasilattice parameter was determined to $a = 3.78$ Å, the periodicity to 4.11 Å. Below 1120 K, the d-phase decomposes to a mixture of $\text{Al}_{13}(\text{Fe},\text{Ni})_4$, $\text{Al}_3\text{Ni}_2(\text{Fe})$ and $\text{Al}_3\text{Ni}(\text{Fe})$ (Grushko, Lemmerz, Fischer, Freiburg, 1996). The transformation is diffusion driven. Neither intermediate states with continuously increasing phason strain nor nanodomain structures of high-order approximants were observed in *in-situ* experiments (Döblinger, Wittmann, Grushko, 2003).

Electron microscopy

Based on a CBED study, the space group symmetry of $\text{d-Al}_{70}\text{Fe}_{15}\text{Ni}_{15}$ was determined to $P\overline{1}0m2$ (Saito, Tanaka, Tsai, Inoue, Masumoto, 1992). The authors found it remarkable that a metastable phase was the first d-phase that survived a CBED symmetry examination. They also discussed the diffuse interlayers that indicate a twofold superstructure (≈ 8 Å) with short correlation length. A further CBED study on melt quenched samples of $\text{Al}_{70}\text{Fe}_{20-x}\text{Ni}_{10+x}$ ($0 \leq x \leq 10$) yielded the space group $P\overline{1}0m2$ for $0 \leq x \leq 7$ and $P10/mmm$ for $7 \leq x \leq 10$ (Tanaka, Tsuda, Terauchi, Fujiwara, Tsai, Inoue, Masumoto, 1993). Detailed dark-field electron microscopic studies showed that non-centrosymmetric anti-phase domains (≈ 300 nm diameter) exist in the sample with $x \leq 7$ (Tanaka, Tsuda, Terauchi, Fujiwara, Tsai, Inoue, Masumoto, 1993; Tsuda, Saito, Terauchi, Tanaka, Tsai, Inoue, Masumoto, 1993). The domains are related by an inversion center, this is equivalent to a $c/2$ translation. With increasing x , the size of the domains decreases drastically to a few nanometers, i.e. almost to the size of the ≈ 2 nm unit clusters. Since the homogenous distribution of these nanodomains obeys the symmetry $P10/mmm$ it makes sense to consider a centrosymmetric structure instead of a nano-anti-phase domain structure. Lemmerz, Grushko, Freiburg, Jansen (1994) point out, that this composition range corresponds to the stability region of $\text{m-Al}_{13}(\text{Fe},\text{Ni})_4$, and that

the metastable d-phase is just an intermediate state between the liquid and $\text{m-Al}_{13}(\text{Fe},\text{Ni})_4$.

A first structure model, *AlFeNi-HYP-96*, based on HRTEM investigations on $\text{d-Al}_{71.6}\text{Fe}_{4.7}\text{Ni}_{23.7}$ and in analogy to the model *AlCoNi-HLS-91* was proposed by Hiraga, Yubuta, Park (1996). The fundamental structural unit was found to be a columnar cluster with ≈ 12 Å diameter (by a factor $1/\tau$ smaller than the cluster in d-Al-Co-Ni). These clusters decorate the vertices of a pentagonal Penrose tiling. However, this clusters size could not be confirmed in later studies.

Three kinds of ≈ 20 Å clusters, 1, 1' and 2, were found in the first HAADF-STEM study of melt-quenched $\text{d-Al}_{70}\text{Fe}_{15}\text{Ni}_{15}$, and a structure model, *AlFeNi-STTT-99*, was proposed based on the structure of $\tau^2\text{-Al}_{13}\text{Co}_4$ (Saitoh, Tsuda, Tanaka, Tsai, 1999). The three clusters are linked in a similar way as in $\tau^2\text{-Al}_{13}\text{Co}_4$ (Saitoh, Yokosawa, Tanaka, Tsai, 1999) and decorate a pentagonal Penrose tiling. The authors also imaged the anti-phase shift between the columnar clusters.

Annealed (920 °C) $\text{d-Al}_{73}\text{Fe}_5\text{Ni}_{22}$ was studied by HAADF and a structure model, *AlFeNi-STT-01*, proposed based on symmetry $P10_5/mmc$ (Saitoh, Tanaka, Tsai, 2001). The authors identified two different ≈ 20 Å clusters; one, called *m*, with mirror symmetry (90%), another one, *f*, with fivefold symmetry (10% of all clusters). The mirror symmetric cluster *m* can be decomposed into two ≈ 4 Å subclusters, P and S. According to the authors, the clusters of type *f* are responsible for disorder (diffuse interlayer lines). The global structure of the d-phase can be described by a pentagonal Penrose tiling decorated in an ordered way with the two types of ≈ 20 Å clusters.

Hiraga, Ohsuna (2001b) presented a new model, *AlFeNi-HO-01*, with a ≈ 32 Å cluster based on HAADF studies of annealed (900 °C) $\text{d-Al}_{71.6}\text{Fe}_{4.7}\text{Ni}_{23.7}$ and the results of comparable studies of d-Al-Co-Ni and d-Al-Cu-Rh phases. The cluster symmetry is $10_5/mmc$, the atoms decorate the vertices of a Penrose rhomb tiling with 2.5 Å edge length. They do not discuss why they now obtain such a large cluster. However, in his review article on electron microscopic studies of QC, Hiraga (2002) points out that under electron radiation the ≈ 32 Å cluster contrasts disappear. He concludes that most QC undergo extensive structural changes by irradiation damage.

The SAED patterns of most studies published (with the exception of Fig. 4 of Grushko, Urban, 1994) show weak diffuse interlayer scattering indicating $a \approx 8$ Å translation period with weak lateral correlation resembling d-Al-Co-Cu or d-Al-Co-Ni .

X-ray diffraction

The anisotropic diffuse scattering around Bragg reflections was studied with synchrotron radiation on annealed (900 °C) $\text{d-Al}_{71.5}\text{Fe}_5\text{Ni}_{23.5}$ by Weidner, Lei, Frey, Wang, Grushko (2002). The authors interpret the observations with thermal diffuse scattering and, additionally, defect caused Huang scattering.

Further structure models

A higher-dimensional model, *AlFeNi-YW-97*, based on the SAED and CBED study by Saito, Tanaka, Tsai, Inoue,

Masumoto (1992) was suggested by Yamamoto, Weber (1997b). They use the 5D color symmetry space group $P_{2c}10\bar{2}m'(5mm')$ to describe the ≈ 8 Å superstructure along the tenfold direction. This space group includes two mirror planes m perpendicular to the tenfold axis at $c/8$ and $5c/8$, and two antisymmetric mirror planes m' at $3c/8$ and $7c/8$. All atomic surfaces are located on one of these mirror planes. The 3D structure can be described as decoration of a pentagonal Penrose tiling with the ≈ 20 Å columnar clusters.

5.2.1.7 Al–Me1–Me2 (Me1 = Cu, Ni, Me2 = Rh, Ir)

Discovery

The existence of stable d-Al₆₅Cu₁₅Rh₂₀ in an annealed sample (1200 K) was reported by Tsai, Inoue, Masumoto (1989 d) based on powder X-ray diffraction patterns. The SAED pattern showed two diffuse layer lines between the Bragg layers, related to the ≈ 4 Å structure, indicating ≈ 12 Å periodicity with short correlation length (Li, Hiraga, Yubuta, 1996). This may be due to the coexistence of the d-phase with an i-phase of composition Al_{66.1}Cu_{12.3}Rh_{21.5} (Li, Park, Sugiyama, Hiraga, 1998) since d-phases with 12 Å periodicity show a strong icosahedral pseudosymmetry. A detailed investigation of a part of the phase diagram confirmed the stability of the d-phase in a narrow range around Al_{64.5}Cu_{16.8}Rh_{18.7} at 900 °C, and Al_{64.0}Cu_{18.0}Rh_{18.0} at 800 °C (Grushko, Gwozdz, Yurechko, 2000). The authors observed only very weak diffuse interlayer lines. Consequently, d-Al–Cu–Rh seems to be one of the more perfect d-phases comparable to basic Ni-rich d-Al–Co–Ni.

Decagonal phases have been obtained by rapid solidification at compositions Al₇₀Ni_{10+x}Me_{20-x} (Me = Ir, Rh), $x = 0, 5$ (Tsai, Inoue, Masumoto, 1995). Samples with low Ir content showed 4 Å periodicity, those with high Ir content 16 Å. All melt-quenched samples with composition Al₇₀Ni₂₀Rh₁₀ and Al₇₀Ni_xIr_{30-x}, $x = 15, 17, 20$, exhibited 4 Å periodicity without any diffuse interlayers (Tsuda, Nishida, Tanaka, Tsai, Inoue, Masumoto, 1996). The 5D space group was determined by CBED for all compositions to $P10_5/mmc$. From HRTEM images a structure model was proposed based on a pentagonal Penrose tiling decorated with ≈ 20 Å decagonal clusters. Grushko, Mi (2003) confirmed the stability of d-Al–Ni–Rh in a small compositional range around Al_{70.5}Ni_{15.5}Rh₁₄ at 1100 °C. Their SAED patterns exhibit diffuse interlayer lines and other diffuse diffraction phenomena.

A decagonal phase has been found in the system Al–Cu–Ir for compositions Al₆₅Cu₂₀Ir₁₅ and Al_{72.5}Cu₂₀Ir_{7.5} (Athanasios, 1997). In this system also an i-phase exists. D-Al₆₅Cu₂₀Ir₁₅, spontaneously grown in large (≈ 1 mm) decaprismatic crystals, shows high thermal stability and was regarded as stable d-phase.

Electron microscopy

A first structure model, AlCuRh-LHY-96, based on an electron microscopic investigation of annealed (950 °C) d-Al₆₃Cu_{18.5}Rh_{18.5} and the structure model AlCuCo-SK-90 was proposed by Li, Hiraga, Yubuta (1996). The structure was described as two-colour Penrose tiling consisting of three kinds of subunits H(exagon), C(rown = boat), and S(tar) with edge length 6.5 Å. A more detailed model, AlCuRh-LHY-97, based on the close resemblance of the

electron micrographs to those of d-Al–Co–Ni, was published one year later by Li, Hiraga, Yubuta (1997) and Li, Hiraga (1997).

The atomic decoration of the H, C, S subunits, which are arranged according to a two-colour Penrose tiling, was derived from models AlCoNi-HLS-91 and AlCoNi-SHZ-93. As well a decoration for a D(ecagon) subunit was suggested despite it was not observed in d-Al–Cu–Rh. On the contrary, in d-Al–Co–Ni the D subunit is found most frequently. This model was also described in the higher-dimensional approach and shapes for the atomic surfaces, compatible with the 5D space group $P10_5/mmc$, suggested (AlCuRh-LH-97; Li, Hiraga, 1997).

A new model, AlCuRh-HOP-01, based on HAADF and HRTEM studies proposed $a \approx 32$ Å cluster located at the vertices of a pentagonal Penrose tiling (Hiraga, Ohsumi, Park, 2001). The cluster itself is seen as decorated variant of the rhombic Penrose tiling with edge length 2.5 Å.

5.2.1.8 Zn–Mg–RE (RE = Y, Dy, Ho, Er, Tm, Lu)

Discovery

A stable decagonal phase was found in an annealed sample of composition d-Zn₇₀Mg₂₀Dy₁₀ (Sato, Abe, Tsai, 1997). Later, the actual stoichiometry was determined to Zn₅₈Mg₄₀Dy₂ (Sato, Abe, Tsai, 1998). It was the first stable decagonal QC belonging to the pentagonal Frank-Kasper-type (close packing of tetrahedra in the form of icosahedral chains; e.g., Zr₃Al₄ or MgCu₂ structure types).

Electron microscopy

A comparative SAED and HRTEM study of d-Zn₅₈Mg₄₀Dy₂ and d-Al₇₀Ni₂₄Co₆ was performed by Abe, Sato, Tsai (1998). It was pointed out that the ratios of the characteristic distances differ significantly, which are related to the reciprocal lattice vectors 00002 and 10010 (setting of Steurer, Haibach, Zhang, Kek, Lück, 1993), for d-Al–Ni–Co (1.03) and d-Zn–Mg–Dy (1.17). Based on a comparative analysis of the rather similar SAED patterns, the authors suggest a slightly modified pentagonal cluster for d-Zn–Mg–Dy. The pentagonal cluster in d-Al–Ni–Co can be considered as pentagonal antiprismatic column. In case of d-Zn–Mg–Dy, one atom is placed between adjacent pentagons. This leads to a cap-sharing chain of pentagonal bipyramids stacked in anti-configuration (ZnMgDy-AST-98). This structural unit was also used to model the d-phase in terms of a Gummelt-decagon with ≈ 23 Å diameter (ZnMgDy-AST-99; Abe, Sato, Tsai, 1999). Strangely, the authors discuss the idea of a “stable cluster” decorating a quasiperiodic tiling and of an energetically favourable “quasi-unit cell” (i.e. the Gummelt decagon) as contradictory. Of course, the same structural unit can be described in either approach.

Sato, Abe, Tsai. (1998) investigated the homologous series of rare earth homologues of composition d-Zn₅₈Mg₄₀RE₂ and found stable d-phases for RE = Dy, Er, Ho, Lu, Tm, Y. The atomic diameters for these elements all are ≤ 3.55 Å. For the larger rare earth elements crystalline phases are formed. The valence electron concentration amounts to $el/a = 2.02$ compared to a value of 2.1–2.2 found for FK-type icosahedral QC.

Approximants

Orthorhombic τ -Zn₅₈Mg₄₀Dy₂, $a = 39.2$ Å, $b = 5.1$ Å, $c = 25.0$ Å, was found to coexist with the d-phase (Abe, Tsai, 2000). The τ -phase was considered as an intermediate phase during the transformation from monoclinic Zn₇Mg₄ to the d-phase. A structure model was proposed based on two unit tiles, R and H, with edge length 4.5 Å. The R(homb) tile corresponds to the fat Penrose rhomb, the H(exagon) tile to the union of one fat and two skinny Penrose rhombs. The tiling is decorated with the pentagonal columns of model ZnMgDy-AST-98 (Abe, Sato, Tsai, 1998).

5.2.2 12 Å periodicity

5.2.2.1 d-Al–Mn

An overview of the most important structure models of d-Al–Mn is given in Table 5.2.2.1-1. Metastable d-Al–Mn is of interest because it was the first decagonal phase identified; it took three years more before the first stable decagonal phase, d-Al–Co–Cu, was discovered (He, Wu, Kuo, 1988); with higher cooling rate an amorphous (a) or an icosahedral (i) phase can be formed; it can be stabilized by replacing mainly Al by Pd. The updated binary phase diagram of Al–Mn, as part of the ternary phase diagram Al–Mn–Pd, is discussed by Gödecke, Lück (1995).

Discovery

The first decagonal quasicrystal, an intermetallic phase with a structure being quasiperiodic in two dimensions only, was identified in rapidly solidified Al–Mn alloys independently by Chattopadhyay, Ranganathan, Subbanna, Thangaraj (1985), Chattopadhyay, Lele, Ranganathan, Subbanna, Thangaraj (1985) and Bendersky (1985). The former authors interpreted the diffraction patterns of this metastable phase by a periodic stacking of quasiperiodic layers and point out that it could be described as periodic structure in 5D space. The latter author determined its symmetry to $10/m$ or $10/mmm$ by convergent beam electron diffraction (CBED) and coined the term *decagonal phase*. Both groups discussed the origin of the strong dif-

fuse scattering indicating disorder within the quasiperiodic layers. The space group $P10_5/m$ was suggested by Bendersky (1986), $P10_5/mc1$ by Fitz Gerald, Withers, Stewart, Calka (1988). By annealing 2 h at 873 K, d-Al–Mn transforms into π -Al₄Mn (Li, Kuo, 1992).

Electron microscopy

The first HRTEM image of the twofold plane was published by Pérez-Ramírez, Pérez, Gomez, Cota-Araiza, Martínez, Herrera, José-Yacamán (1987) showing an arrangement of twisted chains along the tenfold axis. This supported an interpretation of the decagonal phase rather as a quasiperiodic packing of columnar clusters than as a periodic stacking of quasiperiodic layers.

Spectroscopy

In the first extended X-ray absorption fine-structure (EXAFS) study on d-Al–Mn, a smaller coordination number of 8 Al atoms for Mn compared to ten for i-Al–Mn was found (Bridges, Boyce, Dimino, Giessen, 1987). The authors proposed a pentagonal six-layer structure model of the building elements, columnar clusters. Two years later, a more detailed EXAFS study was performed on the a-, d- and i-phases as well as on several crystalline phases in the systems Al–Mn and Al–Cr–Fe (Sadoc, Dubois, 1989). In contrast to Bridges, Boyce, Dimino, Giessen (1987), a very similar short-range order in the first coordination shell was found for the d-, i- and a-phases. The second and third coordination shells look somewhat different, in particular, the Mn–Mn pairs at 4.47 Å, which also occur in the crystalline phases o-Al₆Mn and cubic α -Al–Mn–Si. This indicates a layer structure perpendicular to the tenfold axis.

Neutron diffraction

Dubois, Janot (1988) performed a neutron diffraction study on five polycrystalline decagonal Al₈₀Mn_{1-x}(FeCr)_x samples. By the contrast-variation method the partial pair distribution functions were calculated and compared to those of cubic α -Al–Mn–Si, an approximant of i-Al–Mn. The structures resulted to be very similar up to distances of 15 Å.

X-ray structure analysis

The first single crystal X-ray diffraction study of a decagonal phase was performed on d-Al₇₈₍₂₎Mn₂₂₍₂₎ (Steurer, Mayer, 1989; Steurer, 1989, 1991) (Table 5.2.2.1-2). The “single crystal” of this metastable phase was an almost perfectly parallel intergrowth of tiny needles with a resulting total mosaic spread of almost 5°. Despite the low quality of the sample 1807 reflections could be collected, which were merged to 332 unique reflections (233 reflections $> 2\sigma_1$). The 5D refinements were performed in the centrosymmetric superspace group $P10_5/mmc$. Due to the small number of Bragg reflections the atomic surfaces were not modelled in great detail. The focus was on the calculation of electron density maps of the six layers. The structural relationship to monoclinic Al₁₃Fe₄ (Black, 1955a, b) as well as the similarity to HRTEM images of d-Al–Mn (Fig. 8 of Hiraga, Hirabayashi, Inoue, Masumoto, 1987) was pointed out.

Table 5.2.2.1-1. Structure models of d-Al–Mn (for details see text).

AlMn-KSA-86	Theoretical study of d-Al–Mn and d-Al–Fe based on the structure of the approximants Al ₆ Mn, δ -Al ₁₁ Mn ₄ , Al ₁₃ Fe ₄ . Decorated pentagon Penrose tiling; two types of layers (Kumar, Sahoo, Athithan, 1986).
AlMn-YI-88	Theoretical 5D study of d-Al–Mn and d-Al–Fe. Penrose tiling based structure model (Yamamoto, Ishihara, 1988).
AlMn-S-91	5D X-ray structure analysis of d-Al ₇₈ Mn ₂₂ . $R = 0.305$, $wR = 0.144$ for 233 reflections (Steurer, 1991).
AlMn-N-93	Theoretical study of d-Al–Mn. Pentagon tiling and HBS-tiling based description of the layers (Niizeki, 1993).
AlMn-LK-92	Theoretical study of d-Al–Mn based on the structure of the approximant π -Al ₄ Mn and on the structure model AlMn-S-91. Two sets of Penrose tiles with decoration derived from approximants (Li, Kuo, 1992).
AlMn-L-95	Theoretical study of d-Al–Mn based on the structure of the approximant Al ₃ Mn, on HRTEM data, and on the structure model AlMn-S-91. HBS-tiling model and its 5D description (Li, 1995; Li, Frey, 1995).

Table 5.2.2.1-2. Quantitative X-ray structure analyses of d-Al–Mn and its approximants. Whether R factors are based on structure amplitudes or on intensities is unclear in most cases (intensity based R factors are approximately by a factor two larger than the structure amplitude based ones). D_x ... calculated density, PD ... point density, SG ... space group, PS ... Pearson symbol, N_R ... number of reflections, N_V ... number of variables.

Nominal composition	SG PS	Lattice parameters	D_x PD	N_R N_V	R wR	Reference
d-Al ₇₈ Mn ₂₂	$P10_5/mmc$	$a_{1..4} = 3.912(1) \text{ \AA}$ $a_5 = 12.399(7) \text{ \AA}$	3.6	233 18	0.305 0.144	Steurer (1989, 1991)
Y-Al ₃ Mn (HT-Al ₁₁ Mn ₄) (Al _{72.1} Mn _{27.9})	$Pn2_1a$ $oP156$	$a = 14.837(4) \text{ \AA}$ $b = 12.457(2) \text{ \AA}$ $c = 12.505(2) \text{ \AA}$	3.90	2539 164	0.131 0.119	Shi, Li, Ma, Kuo (1994); Pavlyuk, Yanson, Bodak, Cerny, Gladyshevskii, Yvon (1995)
μ -Al _{4.12} Mn (Al _{80.5} Mn _{19.5})	$P6_3/mmc$ $hP563$	$a = 19.98(1) \text{ \AA}$ $c = 24.673(4) \text{ \AA}$	3.56	2824 127	0.139 0.079	Shoemaker, Keszler, Shoemaker (1989)
δ -Al ₁₁ Mn ₄ (Al _{80.5} Mn _{19.5})	$P\bar{1}$ $aP15$	$a = 5.095(4) \text{ \AA}$ $b = 8.879(8) \text{ \AA}$ $c = 5.051(4) \text{ \AA}$ $\alpha = 89.35(7)^\circ$ $\beta = 100.47(5)^\circ$ $\gamma = 105.08(6)^\circ$	3.88	1180 78	0.067 0.068	Kontio, Stevens, Coppens (1980)
λ -Al ₄ Mn (Al _{81.2} Mn _{18.8})	$P6_3/m$ $hP568.1$	$a = 28.382(9) \text{ \AA}$ $c = 12.389(2) \text{ \AA}$	3.52	2508 228	0.092 0.059	Kreiner, Franzen (1997)
π -Al ₄ Mn	isostructural to the R-phase Al ₆₀ Mn ₁₁ Ni ₄					Li, Kuo (1992)
Al ₆₀ Mn ₁₁ Ni ₄ (R-phase)	$Bbmm$ $oB156$	$a = 23.8 \text{ \AA}$ $b = 12.5 \text{ \AA}$ $c = 7.55 \text{ \AA}$	3.62			Robinson (1954)
Al ₆ Mn	$Cmcm$ $oC24$	$a = 7.5551(4) \text{ \AA}$ $b = 6.4994(3) \text{ \AA}$ $c = 8.8724(17) \text{ \AA}$	3.31	530 11	0.021 0.029	Kontio, Coppens (1981)
Al _{68.8} Mn _{17.5} Zn _{13.7} (T ₃ -Al-Mn-Zn)	$Cmcm$ $oC152$	$a = 7.78 \text{ \AA}$ $b = 12.6 \text{ \AA}$ $c = 23.8 \text{ \AA}$	3.97	265 35	0.170	Damjanovic (1961)

On the example of this structure, its decagrammatical symmetry and the properties of the infinite point groups consistent with a self-similar decagramma in general, were discussed in detail (Janner, 1992). The structural similarities between d-Al–Mn and the crystalline approximant μ -MnAl_{4.12} were discussed in detail by Shoemaker (1993). The authors critically discuss the models by Steurer (1991), Li, Kuo (1992), Daulton, Kelton, Gibbons (1992), and suggest a modification of the model by Steurer (1991). A comparative study of series of approximants is reviewed by Kuo (1993).

Approximants

Close to the composition of d-Al–Mn, several stable approximants are known (Table 5.2.2.1-2). These are Al₁₁Mn₄ (a rational $\langle 3,2 \rangle$ -approximant according to Zhang, Kuo, 1990), hexagonal μ -MnAl_{4.12} (Shoemaker, Keszler, Shoemaker, 1989) and λ -Al₄Mn (Kreiner, Franzen, 1997), and orthorhombic Y-Al₃Mn (Shi, Li, Ma, Kuo, 1994; Pavlyuk, Yanson, Bodak, Cerny, Gladyshevskii, Yvon, 1995). The structure of Y-Al₃Mn can be seen as a squashed-hexagon (H) tiling decorated with edge-sharing pentagons. Each pentagon is filled with a pentagonal columnar cluster. The same type of structure motifs is found in d-Al–Mn. Several more probably metastable approximants such as π -Al₄Mn (Li, Kuo, 1992), isostructural to the R-phase, have been described as well. An interesting aspect offers the description of some approximants in terms of a ‘wheel cluster’ (Boström, Hovmöller, 2001),

which has already been identified eight years before in d-Al–Co–Ni (Steurer, Haibach, Zhang, Kek, Lück, 1993).

Further structure models

A first structure model, *AlMn-KSA-86*, based on an approximant-based decoration of the Penrose tiling was proposed by Kumar, Sahoo, Athithan (1986). A pentagon-rectangle-triangle subtiling of the Penrose tiling was used which turned out to resemble rather the d-Al–Co–Ni (Steurer, Zhang, Kek, Lück, 1993) than the d-Al–Mn structure (Steurer, 1991). Takeuchi, Kimura (1987) proposed another detailed structure model of d-Al_{76.4}Mn_{23.6} as a decorated Penrose tiling with edge length $a_r = 4.29 \text{ \AA}$ (derived from the experimentally obtained value $a_r^* = 0.416(3) \text{ \AA}^{-1}$). The density of the model amounts to 3.7 Mg m^{-3} . The first 5D structure model, *AlMn-YI-88*, was proposed by Yamamoto, Ishihara (1988) and qualitatively compared with selected area electron diffraction (SAED) data. Based on the structure of orthorhombic Al₃Mn (Hiraga, Kaneko, Matsuo, Hashimoto, 1993) and d-Al–Mn (Steurer, 1991), an idealized 5D structure model for the d-phase, *AlMn-N-93*, was proposed (Niizeki, 1993). The polygonal atomic surfaces obey the closeness condition and are in good agreement with the results by Steurer (1991). A detailed structure model of d-Al–Mn, *AlMn-L-95*, based on the structure of the Y-Al₃Mn approximant was derived in terms of a hexagon-boat-star (HBS) two-color Penrose tiling by Li (1995) (Fig. 5.2.2.1-1). In

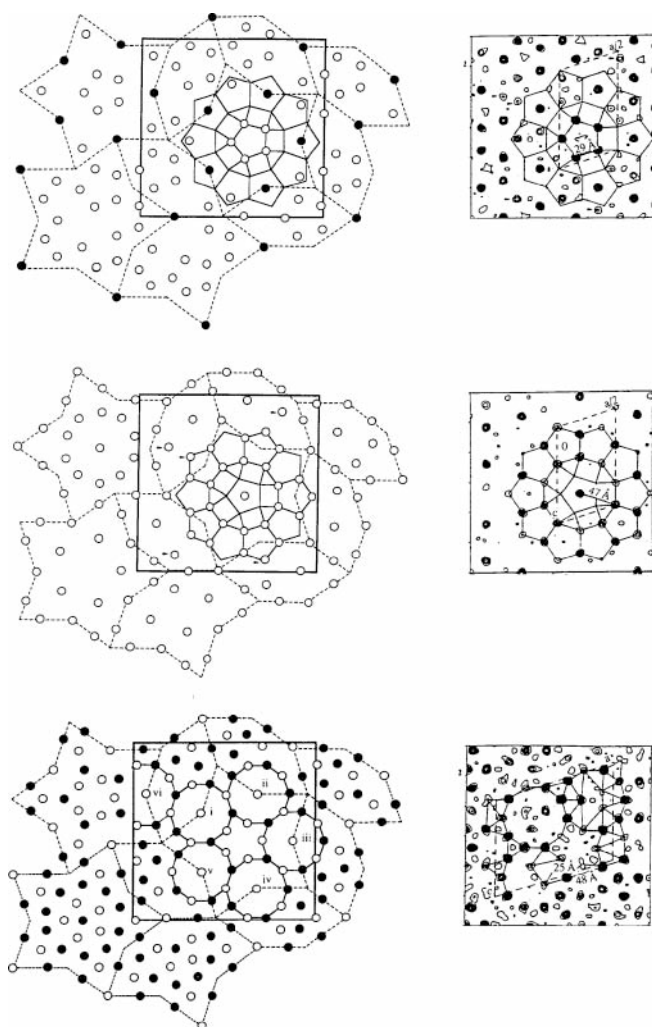


Fig. 5.2.2.1-1. Model *AlMn-L-95* of d-AlMn (Li, 1995) compared with the electron density maps of *AM-S-91* (Steurer, 1991). The decoration of the hexagon, boat, and star unit tiles is based on the structures of the approximants $Y-Al_3Mn$ and $\pi-Al_4Mn$ and the two-colour Penrose tiling (Al empty circle, Mn filled circles).

its major parts it is consistent with the electron density distribution function resulting from the 5D structure analysis by Steurer (1991). This 3D model was also shown in the corresponding 5D description (Fig. 5.2.2.1-2; Li & Frey, 1995) and compared to Niizekis model, *AlMn-N-93*.

5.2.2.2 d-Al–Mn–Pd

There exist metastable binary decagonal phases in the boundary systems Al–Mn (with ≈ 12 Å period, i.e. six layers) and Al–Pd (with ≈ 16 Å period, i.e. eight layers). Stable d- $Al_{70.5}Mn_{16.5}Pd_{13}$ with ≈ 12 Å period (Beeli, Nissen, Robadey, 1991) can be seen as Pd-stabilized d-Al–Mn. Metastable d- $Al_{70}Mn_5Pd_{25}$ with ≈ 16 Å period (Tsai, Yokoyama, Inoue, Masumoto, 1991), however, is just a solid solution of Mn in d-Al–Pd. It was shown that only decagonal QC formed by a solid/solid transformation from the icosahedral phase can be prepared almost free of linear phason strain (Sun, Hiraga, 1995; Beeli, Stadelmann, P., Lück, R., Gödecke, 1996). Samples without decaprismatic facetting directly grown from the melt consist of a twinned nano-domain structure of an approximant (D_h) with B-centred orthorhombic unit cell, $a = 20.3$ Å,

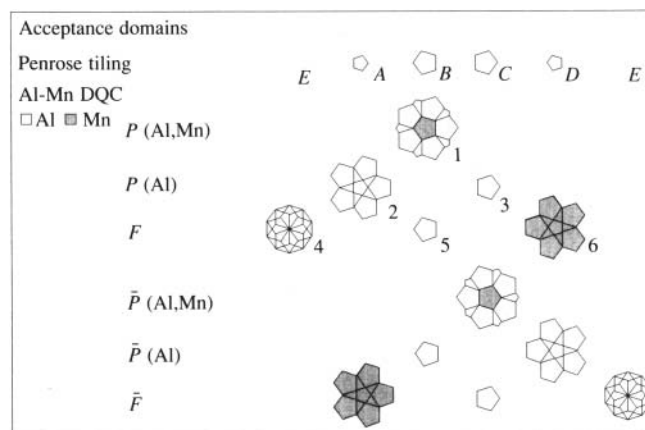


Fig. 5.2.2.1-2. Model *AlMn-L-95* in the 5D description (Li, Frey, 1995). The atomic surfaces are shown generating the different layers of d-Al–Mn compared to those of the Penrose tiling.

$b = 12.5$ Å, $c = 62.5$ Å, which seems to be stable above 865 °C (Beeli, Nissen, 1993). This approximant was called τ^2 -R phase by Krajci, Hafner, Mihalkovic (1997a) since its lattice parameters a and c are scaled by a factor of τ^2 compared to the Robinson-phase $Al_{60}Mn_{11}Ni_4$ (Robinson, 1954). It is almost impossible to transform this sample to a decagonal phase without phason strain by annealing at 800 °C on the time scale of weeks. Samples crystallized in decaprisms, on the other side, can be considered as decagonal QC with strong linear phason strain, however. The phase diagram of Al–Mn–Pd has been studied in great detail in the Al-rich corner by Gödecke & Lück (1995). The formation of the d-phase was investigated as a function of composition and the tiling structure of the differently ordered phases studied (Sun, Hiraga, 1996a, b; 1997). An overview of the most important structure models of d-Al–Mn–Pd is given in Table 5.2.2.2-1.

Discovery

During a SAED and HRTEM study of slowly cooled (or water-quenched) $Al_{70}Mn_{15}Pd_{15}$, annealed at different temperatures up to one week, a decagonal quasicrystalline phase was discovered (Beeli, Nissen, Robadey, 1991) in coexistence with the already known icosahedral phase (Tsai, Inoue, Yokoyama, Masumoto, 1990). The authors described the structure of the d-phase by a cluster-decorated random-pentagon tiling with ≈ 21 Å edge length. Al–Mn–Pd was the first system known with both a stable decagonal phase, d- $Al_{70.5}Mn_{16.5}Pd_{13}$, and a stable icosahedral phase, fci- $Al_{70.5}Mn_{8.5}Pd_{21}$.

Electron microscopy

The (annealed and water-quenched) sample studied by Hiraga, Sun, Lincoln, Kaneko, Matsuo (1991) showed regions with a phason strained decagonal phase and crystalline nanodomains. The image perpendicular to the quasiperiodic plane exhibited quite a perfect stacking sequence along the tenfold axis. The distribution of ring contrasts within the quasiperiodic plane could be interpreted by a (growth, not equilibrium) random tiling of unit tiles with linkages $S = 20$ Å and $L = \tau S$. The unit tiles were later called decagon (D), pentagonal star (P), and squashed hexagon (H) (Hiraga, Sun, 1993a). A model,

Table 5.2.2.2-1. Structure models of d-Al–Mn–Pd (for details see text).

<i>AlMnPd-HS-93</i>	HRTEM study of d-Al _{70.5} Mn _{16.5} Pd ₁₃ . Model, based on AlMn-S91 and o-Al ₃ Mn: decagon, star, hexagon tiling decorated by two types of pentagonal clusters (Hiraga, Sun, 1993a, b).
<i>AlMnPd-BH-94</i>	HRTEM study of d-Al _{70.5} Mn _{16.5} Pd ₁₃ . Chemically partially ordered model with ≈ 20 Å decagon clusters based on AlMn-S-91 and T ₃ -Al–Mn–Zn (Beeli, Horiuchi, 1994).
<i>AlMnPd-SHZBN-94</i>	XRD study of d-Al _{70.5} Mn _{16.5} Pd ₁₃ . 5D structure model based on atomic surfaces derived from the 5D Patterson function; $P10_5/mmc$, $wR = 0.214$ for 476 reflections (Steurer, Haibach, Zhang, Beeli, Nissen, 1994).
<i>AlMnPd-LD-94</i>	Theoretical study of d-Al _{70.5} Mn _{16.5} Pd ₁₃ . Model based on <i>AlMnPd-SHZBN-94</i> and T ₃ -Al–Mn–Zn: Tiling of large hexagon, crown (= boat), star subunits (Li, Dubois, 1994).
<i>AlMnPd-KHM-96</i>	Theoretical study of d-Al _{70.5} Mn _{16.5} Pd ₁₃ . Model based on <i>AlMnPd-HS-93</i> and the approximant structures of Al ₃ Mn and Al ₆₀ Ni ₄ Mn ₁₁ . Pentagonal columnar clusters are the structure stabilizing units (Krajci, Hafner, Mihalkovic, 1997a).
<i>AlMnPd-MM-97</i>	3D X-ray structure analysis of d-Al _{70.5} Mn _{16.5} Pd ₁₃ based on <i>AlMnPd-SHZBN-94</i> X-ray data. $wR = 0.067$ for 476 reflections (Mihalkovic, Mrafko, 1997).
<i>AlMnPd-MKYKSH97</i>	X-ray structure analysis of o-Al ₇₅ Mn ₂₀ Pd ₅ . Structure model for the d-phase from its ($1/1$, $1/1$)-approximant and <i>AlMnPd-HS93</i> (Matsuo, Kaneko, Yamanoi, Kaji, Sugiyama, Hiraga, 1997).
<i>AlMnPd-WY97</i>	5D X-ray structure analysis of d-Al _{70.5} Mn _{16.5} Pd ₁₃ based on <i>AlMnPd-HS-93</i> . $wR = 0.129$ for 1428 reflections (Weber, Yamamoto, 1997).
<i>AlMnPd-WY98</i>	5D X-ray structure analysis of d-Al _{70.5} Mn _{16.5} Pd ₁₃ based on <i>AlMnPd-WY-97</i> . $wR = 0.119$ for 1428 reflections (Weber, Yamamoto, 1998).

AlMnPd-HS-93, for the detailed atomic arrangement of a cluster decorated DPH-tiling was derived from HRTEM images (Hiraga, Sun, 1993b) using structure information from the approximant Al₃Mn (Hiraga, Kaneko, Matsuo, Hashimoto, 1993) and the structure of d-Al–Mn (Steurer, 1991) (Fig. 5.2.2.2-1). Since the approximant Al₃Mn can only be considered as decorated H-tiling, the model for the D- and P-tiles had to be assembled from information contained in *AlMn-S-91*.

The close resemblance between the structures of d-Al–Mn–Pd and d-Al–Mn is shown by a comparison of a HRTEM image of d-Al–Mn–Pd and the X-ray data based projected electron density function of d-Al–Mn (Fig. 3 of Beeli, Nissen, 1993). A thorough 800-kV HRTEM study of d-Al_{70.5}Mn_{16.5}Pd₁₃ found that the sub-clusters ('monopteros piles') have triangular centers, which can only be explained by slight atomic relaxations (Beeli, Horiuchi, 1994). This is also seen on the electron density maps (Fig. 5.2.2.2-2a and -3) of the X-ray structure analyses (Steurer, Haibach, Zhang, Beeli, Nissen, 1994; Weber, Yamamoto, 1997; 1998). On D-type HRTEM images a typical sequence SLLSL of columnar-cluster distances was identified ($L = 12.5$ Å) (Beeli, Horiuchi, 1994). This 52.5 Å long sequence was occasionally disturbed by the short sequence SL. A chemically partially ordered model with 20 Å clusters on a pentagonal tiling is

proposed (*AlMnPd-BH-94*) based on Steurers structure solution (Steurer, Haibach, Zhang, Beeli, Nissen, 1994). The authors point out that thin layers (< 50 Å) of QC are not stable under electron irradiation and transform easily to vacancy-rich CsCl-type structures (displacive transformation).

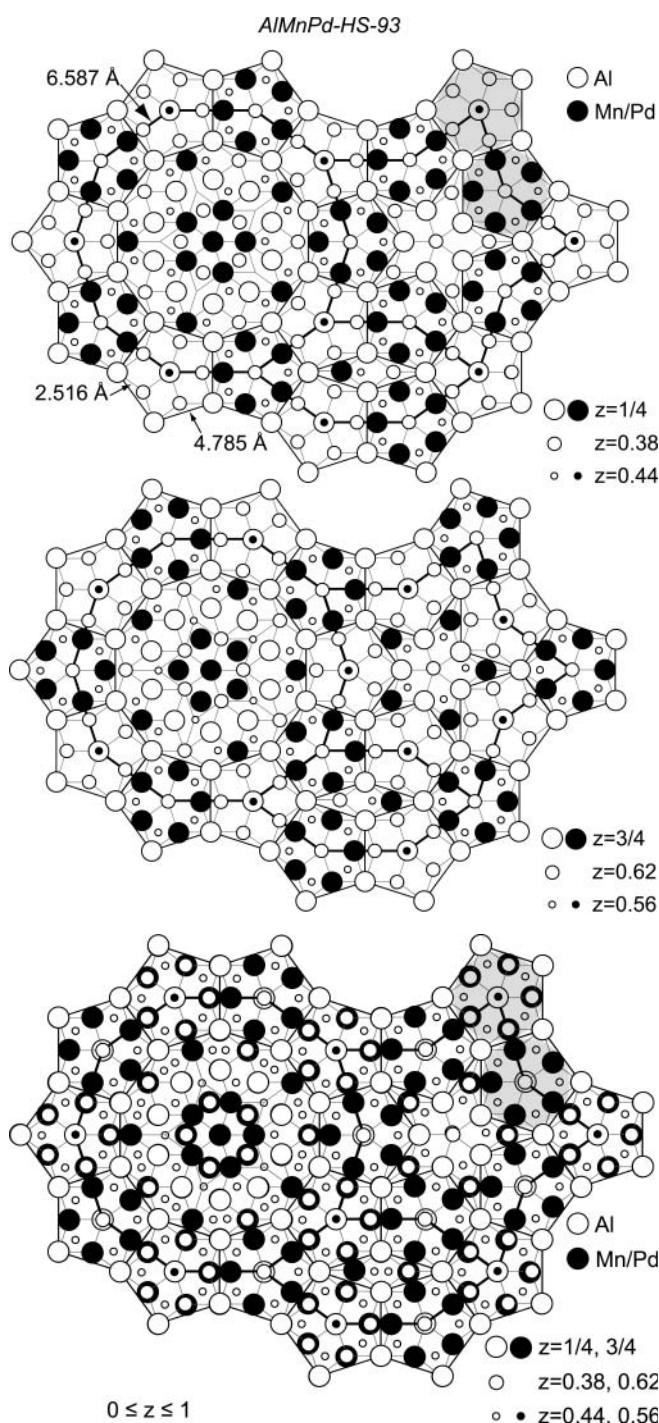


Fig. 5.2.2.2-1. Model *AlMnPd-HS-93* derived from HRTEM images (Hiraga, Sun, 1993b) using structure information from the approximant Al₃Mn (Hiraga, Kaneko, Matsuo, Hashimoto, 1993) and the structure of d-Al–Mn (Steurer, 1991). The edge length of the underlying rhomb Penrose Tiling is 2.516 Å, of the pentagonal subunits 4.785 Å and of the large decagon, star, hexagon tiles 6.587 Å (distances refer to the lattice parameters of Al_{74.7}Mn_{20.9}Pd_{4.4}; Matsuo, Kaneko, Yamanoi, Kaji, Sugiyama, Hiraga, 1997). The grey shaded regions mark two neighbouring pentagonal atomic columns considered as characteristic structural elements. The columns are related by a rotation of π and a shift of $c/2$ (2_1 -screw axis).

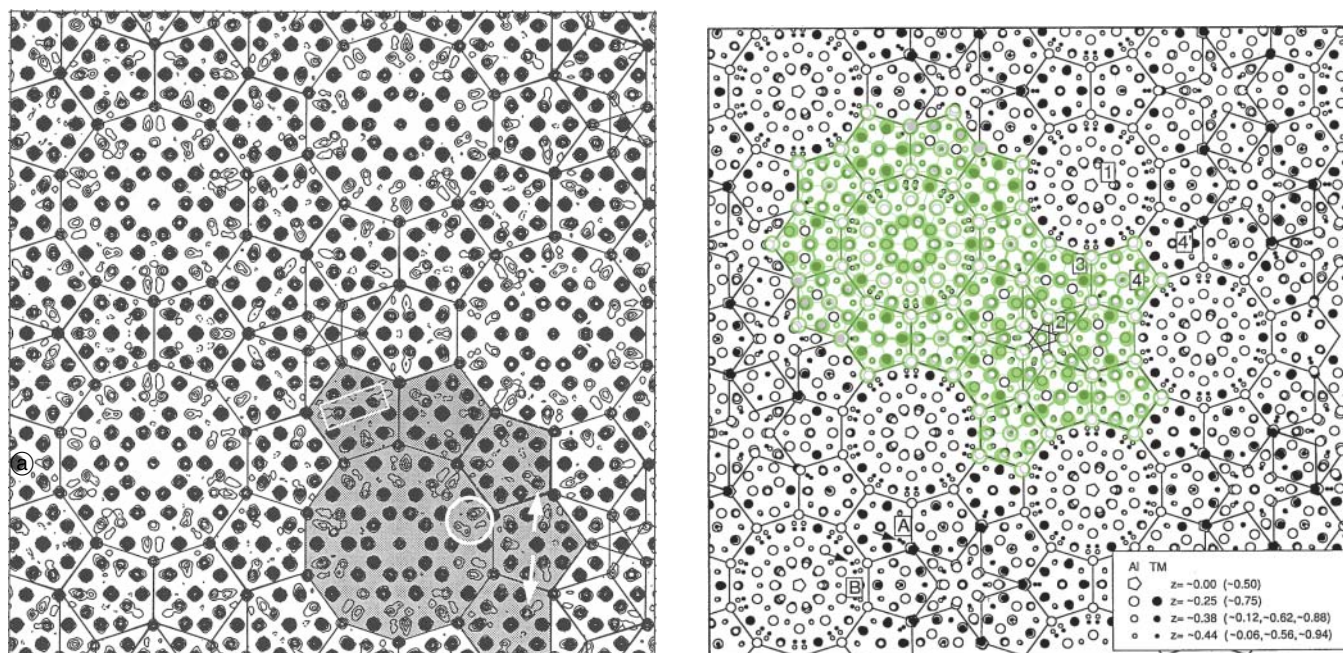


Fig. 5.2.2.2-2. (a) 50 Å × 50 Å projected MEM electron density map of d-Al₇₀Mn₁₇Pd₁₃ (Fig. 24 of Weber, 1997). The edge length of the outlined pentagon tiling is 4.65 Å. (b) Projected structure of the model refined in the 5D space group *P10₅/mc*. For comparison, the projected model *AlMnPd-HS-93* (Hiraga, Sun, 1993b) is superposed in green.

X-ray structure analysis

An overview of quantitative structure analyses of d-Al–Mn–Pd and its approximants is shown in Table 5.2.2.2-2. The first quantitative structure analysis of d-Al_{70.5}Mn_{16.5}Pd₁₃ was performed by Steurer, Haibach, Zhang, Beeli, Nissen (1994) (*AlMnPd-SHZBN-94*). The structure was solved by the 5D Patterson method, 33 parameters were refined against 476 reflections in the 5D space group *P10₅/mmc* to *R* = 0.214. The maximum-entropy method (MEM) (cf. Haibach, Steurer, 1996), which was first employed in a QC structure determination by Steurer, Haibach, Zhang, Kek, Lück (1993), was used to modify the nD model and to calculate a truncation-effect free electron density map (Fig. 5.2.2.2-3). Geometrically,

the resulting structure can be described as periodic stacking of two different quasiperiodic layers A (puckered ±0.3 Å) and B (planar) with sequence ABAaba (a, b correspond to layers A, B rotated by $\pi/5$). In terms of the physically more reasonable cluster model, it was described by 20 Å columnar clusters decorating the vertices of a disordered Robinson triangle tiling. The packing of clusters was shown with overlap rules for each of the layers. The tiling was selected based on a qualitative interpretation of the diffuse scattering. From the similarities in the respective (model free) projected 3D Patterson functions of the d-phase and Al₃Mn (Hiraga, Kaneko, Matsuo, Hashimoto, 1993) the similarity of their projected local structures (for interatomic distances <12 Å) was demonstrated. It is

AlMnPd-HS-93 and AlMnPd-SHZBN-94

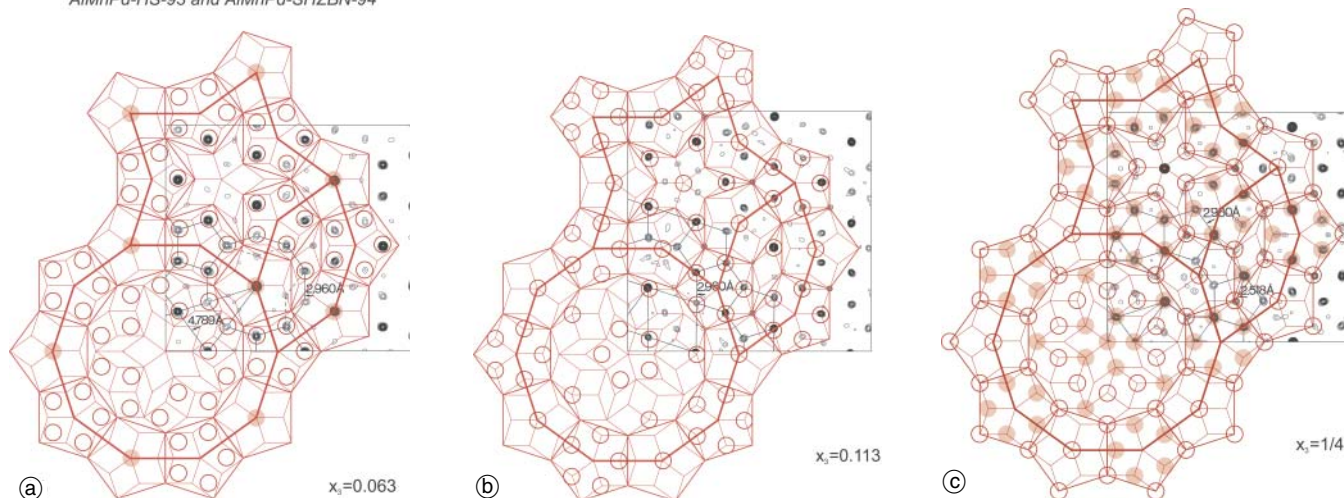


Fig. 5.2.2.2-3. 23.4 Å by 23.4 Å parallel space (11000) electron density maps of d-Al_{70.5}Mn_{16.5}Pd₁₃ (Steurer, Haibach, Zhang, Beeli, Nissen, 1994) with the *AlMnPd-HS-93* (Hiraga, Sun, 1993b) model (red drawing; Al...empty circles, Mn/Pd...full circles) superposed. Sections correspond to (a) $x_3 = 0.063$, (b) $x_3 = 0.113$ (puckered layers), (c) $x_3 = 0.25$ (flat layer on mirror plane).

Table 5.2.2.2-2. Quantitative X-ray structure analyses of d-Al–Mn–Pd and its approximants. Whether R factors are based on structure amplitudes or on intensities is unclear in most cases (intensity based R factors are approximately by a factor two larger than the structure amplitude based ones). D_x ... calculated density, PD ... point density, SG ... space group, PS ... Pearson symbol, N_R ... number of reflections, N_V ... number of variables.

Nominal composition	SG PS	Lattice parameters	D_x PD	N_R N_V	R wR	Reference
d-Al _{70.5} Mn _{16.5} Pd ₁₃	$P10_5/mmc$	$a_{1...4} = 3.891(1) \text{ \AA}$ $a_5 = 12.557(4) \text{ \AA}$	4.59 0.066	476 33	0.249 0.214	Steurer, Haibach, Zhang, Beeli, Nissen (1994)
d-Al ₇₀ Mn ₁₇ Pd ₁₃	$P10_5/mmc$	$a_{1...4} = 3.49 \text{ \AA}$ $a_5 = 12.06 \text{ \AA}$	4.86 0.070	1311 72	0.270 0.186	Yamamoto, Matsuo, Yamanoi, Tsai, Hiraga, Masumoto (1995)
d-Al _{70.5} Mn _{16.5} Pd ₁₃	$P10_5/mmc$	$a_{1...4} = 3.891(1) \text{ \AA}$ $a_5 = 12.557(4) \text{ \AA}$	4.66 0.067	476 97	0.084 0.067	Mihalkovic, Mrafsko (1997)
d-Al ₇₀ Mn ₁₇ Pd ₁₃	$P10_5/mmc$	$a_{1...4} = 3.49 \text{ \AA}$ $a_5 = 12.06 \text{ \AA}$	4.73 0.068	1428 121	0.234 0.129	Weber, Yamamoto (1997)
d-Al ₇₀ Mn ₁₇ Pd ₁₃	$P10_5mc$	$a_{1...4} = 3.49 \text{ \AA}$ $a_5 = 12.06 \text{ \AA}$	4.73 0.068	1428 217	0.167 0.119	Weber, Yamamoto (1998)
Al ₇₅ Mn ₂₀ Pd ₅ (Al ₃ Mn-type)	$Pnma$ $oP156$	$a = 14.727(3) \text{ \AA}$ $b = 12.509(3) \text{ \AA}$ $c = 12.600(3) \text{ \AA}$		2197 96	0.062	Matsuo, Kaneko, Yamanoi, Kaji, Sugiyama, Hiraga (1997)

remarkable that the projected electron densities of d-Al_{70.5}Mn_{16.5}Pd₁₃ and i-Al_{68.7}Mn_{9.6}Pd_{21.7} (Boudard, de Boissieu, Janot, Heger, Beeli, Nissen, Vincent, Ibberson, Audier, Dubois, 1992) agree quite well. Even the atomic sites on the layers A, B have their counterparts in the icosahedral phase. Thus the d-phase, which has pseudo-icosahedral symmetry like other d-phases with 12 Å period, is an approximant of the i-phase. Of course, there is also a close resemblance between the structures of d-Al–Mn–Pd and d-Al–Mn.

Weber, Yamamoto (1997) refined the structure of d-Al₇₀Mn₁₇Pd₁₃ against an X-ray data set of 1428 reflections to a final $R = 0.234$. The model (*AlMnPd-WY-97*) refined was based on the 20 Å cluster (*AlMnPd-HS-93*) proposed by Hiraga, Sun (1993a). 5D MEM was used to modify the starting model and to find small atomic surfaces. Displacements of the atoms from their ideal positions (physical-space shifts) were crucial for the refinement. The structure is built up from 20 Å columnar clusters decorating the vertices of a subset of the pentagonal Penrose tiling (Fig. 5.2.2.2-4) (Niizeki, 1991). The projected structure is similar to that shown by Steurer, Haibach, Zhang, Beeli, Nissen (1994). The main difference is due to the number and shape of the atomic surfaces. This is plausible since Steurer, Haibach, Zhang, Beeli, Nissen (1994) used the nD refinement mainly to get accurate phases as starting values for the calculation of the electron density function by MEM. The structure contains one more pentagonal cluster in the pentagonal subunits besides the two symmetry related clusters in *AlMnPd-HS-93* (Hiraga, Sun, 1993a).

By removing the mirror planes perpendicular to the 10₅-axis, Weber, Yamamoto (1998) got the starting model for the refinement in the non-centrosymmetric 5D space group $P10_5mc$. For 217 parameters and 1428 reflections it converged to $R = 0.167$. The R -factor improvement resulted mainly from a better fit of the large number of weak reflections due to a more realistic assignment of chemical species to former mirror-related atomic sites (*AlMnPd-WY-98*, Fig. 5.2.2.2-2b). The authors also discuss the symmetry breaking in the subclusters (marked A and

B in their Fig. 4). This symmetry breaking, called ‘triangular centers of the subclusters’, has also been identified by Beeli, Horiuchi (1994).

A 3D DPH-tiling-decoration model based on *AlMnPd-HS-93* was refined against the X-ray diffraction data of Steurer, Haibach, Zhang, Beeli, Nissen (1994) by Mihalkovic, Mrafsko (1997). The model had at least 10% of guessed, uncertain positions. The authors point out that a hypothesis about the physically relevant degrees of freedom assigned to each atomic site has to be part of a QC model. The main goal of their refinement was a physically plausible model with unique atomic decoration and without too short atomic distances. Therefore, the refined model was modified to meet these goals at the cost of the quality of the fit to the X-ray data and the reliability of the model ($R = 0.084$ increased to $R = 0.147$). However, the authors did not take into account that Bragg intensity data can only provide information of the average structure so the modification was quite arbitrary. For a reliable fit the diffracted intensities of a large number of different realisations of the structure had to be incoherently summed up.

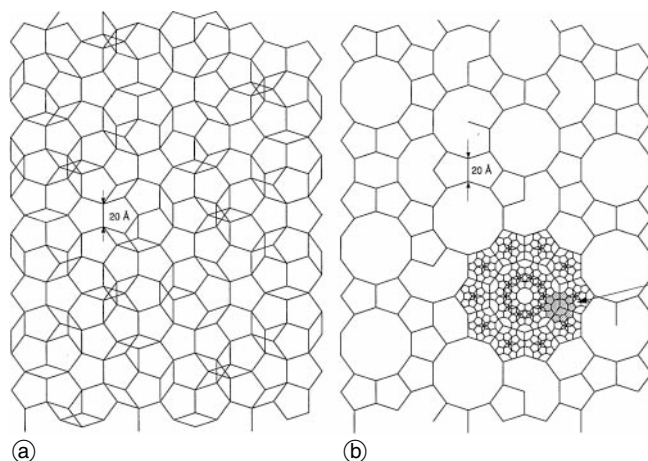


Fig. 5.2.2.2-4. (b) Subset of the (a) pentagonal Penrose tiling used in the refinements (Fig. 15 of Weber, 1997). The edge length of the tiling corresponds to the cluster diameter of $\approx 20 \text{ \AA}$. One cluster (shaded area) is marked by an arrow in (b).

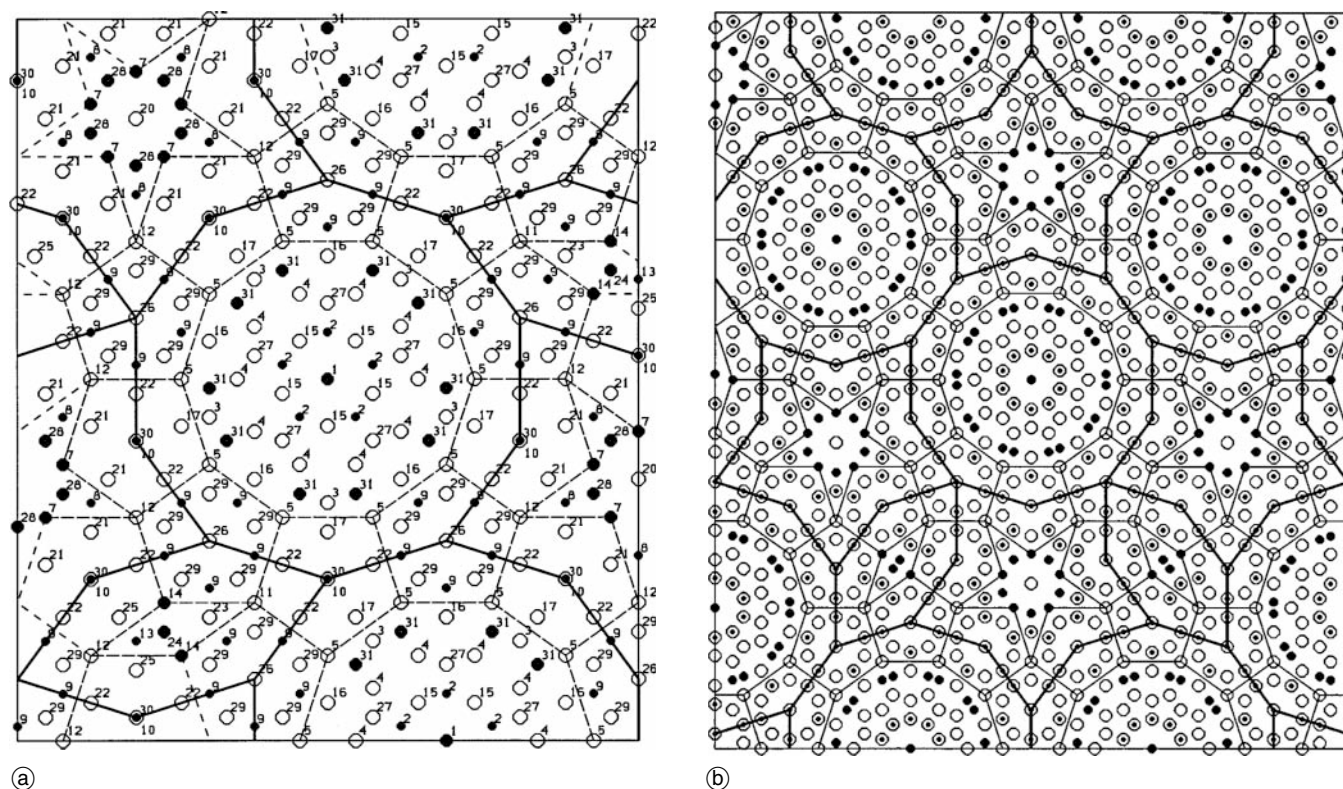


Fig. 5.2.2.2-5. (a) Structure model of the τ^2 -T phase according to *AlMnPdKHM-97*. The atoms of one half of the unit cell along the pseudofold direction are projected (Fig. 8 of Krajci, Hafner, Mihalkovic, 1997a). (b) Projected structure of the τ^3 -T approximant according to *AlMnPdKHM-97* (Fig. 2 of Krajci, Hafner, Mihalkovic, 1997a). Open circles mark Al atoms, large (small) closed circles Pd (Mn) atoms.

Approximants

A series of one stable and three metastable orthorhombic rational approximants was found by SAED in annealed samples (3d, 800 °C) of composition $\text{Al}_{70}\text{Mn}_{15}\text{Pd}_{15}$ in co-existence with the d- as well as the i-phase (Li, Kuo, 1994). Structure models of these approximants were presented by Li, Li, Frey, Steurer, Kuo (1995). The structure of the $(1/1, 1/1)$ -approximant $\text{Al}_{74.7}\text{Mn}_{20.9}\text{Pd}_{4.4}$ was determined by single-crystal X-ray diffraction and a model for the unit tiles of the d-phase proposed (*AlMnPd-MKYKSH-97*; Matsuo, Kaneko, Yamanoi, Kaji, Sugiyama, Hiraga, 1997). This model is based on *AlMnPd-HS-93* and contains Pd atom positions taken from the approximant structure. However, there are mistakes in the model leading to too short distances of 1.626 Å.

Further models

An interesting model (*AlMnPd-LD-94*) mainly based on the structure analysis of Steurer, Haibach, Zhang, Beeli, Nissen (1994) and on the structure of the approximant $\text{T}_3\text{-Al-Mn-Zn}$ (Damjanovic, 1961) was presented by Li, Dubois (1994) and Li, Frey, Kuo (1995). It agrees quite well qualitatively with structural information based on X-ray studies as well as on HRTEM images. The authors also found that the structure of d-Al-Mn can be described by a cluster decorated HCS-tiling (C... crown unit tile equivalent to B... boat unit tile; S... star unit tile equivalent to P... pentagonal star unit tile) while d-Al-Mn-Pd corresponds to a HSD tiling. The existence of D-tiles is attributed to the replacement of Al atoms by Pd. The edge lengths of the d-Al-Mn-Pd unit tiles are larger by a factor τ^2 than those of d-Al-Mn (inflation/deflation rule related).

By a self-consistent real-space tight-binding-linear-muffin-tin-orbital (TB-LMTO) formalism the atomic and electronic structure of DPH-tiling based approximants were studied (Krajci, Hafner, Mihalkovic, 1997a). The models used were based on DPH-tilings as proposed by Hiraga, Sun (1993a, b) modified in some way (two distinct decorations of the pentagonal subunits; splitting each puckered layer into four sublayers to increase the rather short distances of *AlMnPd-HS-93*). The largest approximant studied was the τ^3 -T phase with 2771 atoms per unit cell ($a = 53.233$ Å, $b = 62.579$ Å, $c = 12.43$ Å). The Al/Mn/Pd-decoration of the model structures was optimized based on the results of the electronic-structure calculations (Fig. 5.2.2.2-5; *AlMnPd-KHM-97*). It was found that the small pentagonal Al-Mn clusters dominate the stability of the whole structure. Pd atoms are located mostly inside the D-tiles. The *AlMnPd-KHM-97* model is certainly the most reliable of the idealized models for the local structure of d-AlMnPd. One has to keep in mind, however, that it cannot give information about the origin and kind of the quasiperiodic long-range order of this phase.

5.2.3 16 Å periodicity

There are a couple of metastable and a few possibly stable d-phases known with 16 Å (eight-layer) periodicity. The most important class of this type of d-phases is the Al-Pd based ones (Table 5.2.3-1). They can be seen as transition-metal stabilized d-Al-Pd QC. Recently, another stable d-phase with 16 Å periodicity was discovered in the system Al-Ni-Ru.

Table 5.2.3-1. Quantitative X-ray structure analyses of d-Al–Me–Pd quasicrystals and their approximants. Whether R factors are based on structure amplitudes or on intensities is unclear in most cases (intensity based R factors are approximately by a factor two larger than the structure amplitude based ones). RASrational approximant, D_x ... calculated density, PD ... point density, SG ... space group, PS ... Pearson symbol, N_R ... number of reflections, N_V ... number of variables.

Nominal composition	SG PS	Lattice parameters	D_x PD	N_R N_V	R wR	Reference
d-Al ₇₅ Os ₁₀ Pd ₁₅	$P10_5/mmc$	$a_{1...4} = 3.8986(3) \text{ \AA}$ $a_5 = 16.750(3) \text{ \AA}$	5.36	1738 14	— 0.140	Cervellino (2002)
Al ₃ Pd (Al _{72.5} Pd _{27.5}) ($2/1, 1/1$)-RAS	$Pna2_1$ $oP280$	$a = 23.36 \text{ \AA}$ $b = 12.32 \text{ \AA}$ $c = 16.59 \text{ \AA}$		2348 98	0.072	Matsuo, Hiraga (1994)
Al ₇₅ Pd ₁₃ Ru ₁₂ ($3/2, 2/1$)-RAS	— oC	$a = 23.889(3) \text{ \AA}$ $b = 32.802(3) \text{ \AA}$ $c = 16.692(1) \text{ \AA}$				Zhang, Li, Steurer, Schneider, Frey (1995)

5.2.3.1 d-Al–Pd

Discovery

Metastable d-Al–Pd with 16 Å periodicity along the 10-fold axis was obtained by rapid solidification independently by different groups (Bancel, Heiney, 1986; Bendersky, 1986; Sastry, Suryanarayana, 1986). The phase diagram of Al–Pd was recently revised by Yurechko, Fattah, Velikanova, Grushko (2001).

Electron microscopy

A comprehensive study of d-Al₃Pd and its structural transitions as a function of temperature was performed by Ma, Kuo, Wang (1990). On heating to 600 °C several hours, the d-phase gradually transforms into decagonally twinned orthorhombic Al₃Pd and into τ -phases. A detailed study was performed by Saito, Hiraga (2002) on the intermediate phases locally appearing during this transformation. These phases can structurally be described by rearrangements of the decagonal clusters ($\approx 7.6 \text{ \AA}$ diameter) building the d-phase.

Approximants

The rational ($2/1, 1/1$)-approximant Al₃Pd was studied by SAED in great detail and its orientational relationship (as well as the intensity distribution) to the d-phase discussed (Ma, Kuo, Wang, 1990). The same authors as well studied the CsCl-structure-type based τ -phases (τ_3, τ_5), which also are transformation products of the d-phase above 600 °C. The τ -phases are characterized by a quasiperiodic ordering of structural vacancies along the [111] direction. The orientation relationships between d-Al₃Pd and its transformation products are as follows

[00001] parallel [010]_{Al₃Pd} parallel [1 $\bar{1}$ 0]_{CsCl},

[10000] parallel [100]_{Al₃Pd} parallel [001]_{CsCl},

[11 $\bar{1}$ 10] parallel [001]_{Al₃Pd} parallel [110]_{CsCl}.

The structure of orthorhombic Al₃Pd was determined by Matsuo, Hiraga (1994). It can be seen as a squashed-hexagon (H) tiling decorated with edge-sharing decagons. The decagons, of the same size as in Y-Al₃Mn, are each filled

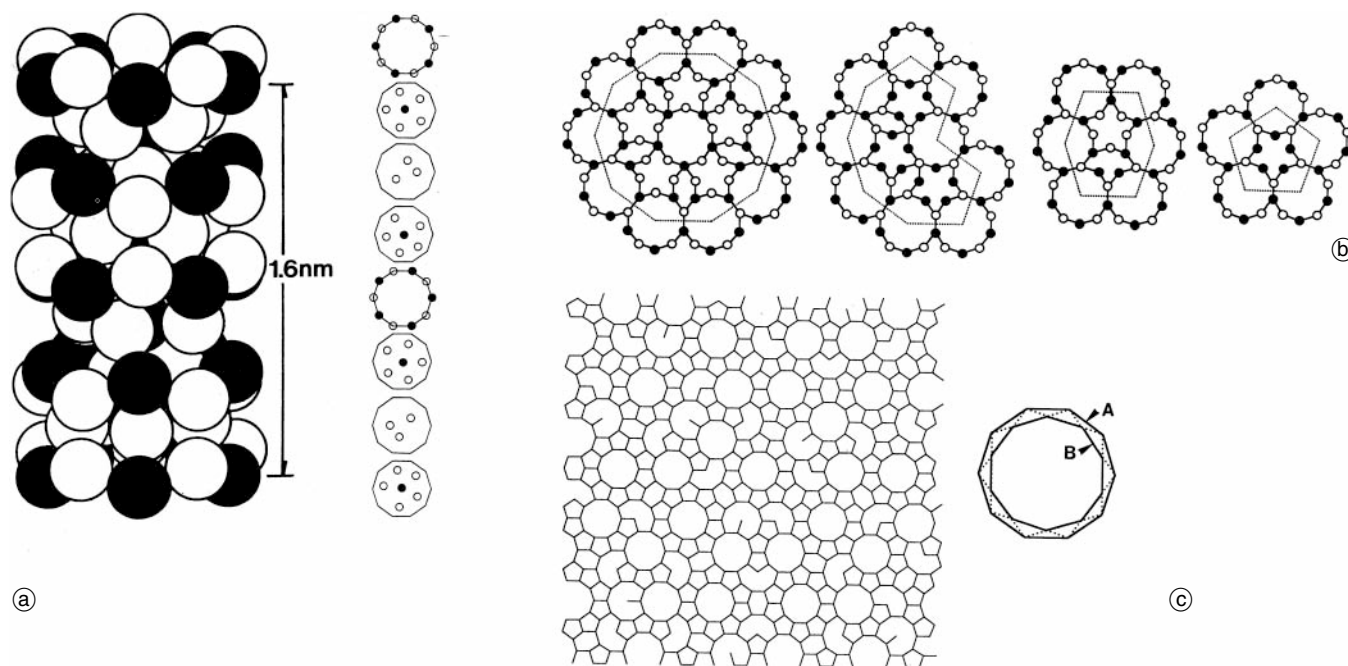


Fig. 5.2.3.1-1. Characteristic structure elements of d-Al–Pd according to the model AP-HAM-94 (Hiraga, Abe, Matsuo, 1994). The decagonal columnar cluster is shown in (a). (b) The polygons are pictured forming the tiling shown in (c). (c) This tiling is suggested as a model quasitilattice for the structure of d-Al–Pd. It results from employing window B in the nD description.

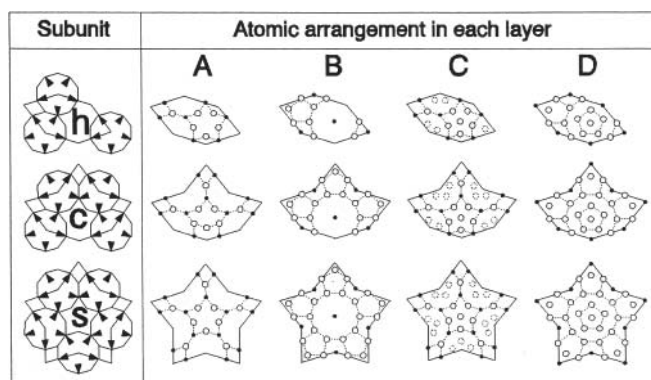


Fig. 5.2.3.1-2. The basic structural subunits h, c and s in the layers A, B, C and D, respectively, of d-Al–Pd according to the model *AP-LSF-96* (Li, Steurer, Frey, 1996). Open circles: Al, full circles Pd atoms.

with one pentagonal columnar cluster. Al_3Pd served as a model structure for the description of the d-phase with 16 Å periodicity. Depending on stoichiometry several orthorhombic phases (ϵ -phases) were found around the composition Al_3Pd and its ternary extensions with a third element ($x_{\text{Co}} < 16.5\%$, $x_{\text{Fe}} < 10\%$, $x_{\text{Mn}} < 5\%$) (Yurechko, Grushko, Velikanova, Urban, 2003).

Structure Models

A first structure model of d-Al–Pd, *AP-HAM-94* (Fig. 5.2.3.1-1) was based on the structure of the $(\frac{2}{1}, \frac{1}{1})$ -approximant Al_3Pd (Hiraga, Abe, Matsuo, 1994). Li, Steurer, Frey (1996) derived another Al_3Pd -based model, *AP-LSF-96* (Fig. 5.2.3.1-2), which can be seen as a packing of crown shaped unit tiles. The two other unit tiles (star, squashed hexagon) needed for the construction of the decagonal structure were derived from the crown tile. The authors suggested an ideal as well as a random packing of these subunits for models of the d-phase.

5.2.3.2 Al–Fe

Discovery

The decagonal phase in the system Al–Fe was discovered by Fung, Yang, Zhou, Zhao, Zhan, Shen (1986). The microstructural characteristics of d-Al–Fe with ≈ 16 Å periodicity along the 10-fold axis and of related crystalline phases was investigated by Kim, Cantor (1994). From the similarity of SAED patterns taken in different orientation they concluded that monoclinic $\text{Al}_{13}\text{Fe}_4$ and tetragonal Al_4Fe are approximants of the d-phase. d-Al–Fe is the only d-phase known where the diffuse streaks are parallel to the tenfold axis and not perpendicular to it.

Electron microscopy

TEM studies of rapidly solidified Al–Fe showed coexisting d-Al–Fe and tenfold orientationally twinned monoclinic $\text{Al}_{13}\text{Fe}_4$ (Fung, Zou, Yang, 1987). The authors observed by heating in the electron microscope an in situ transformation of the d-phase ($T > 500$ °C) into the monoclinic $\text{Al}_{13}\text{Fe}_4$ phase keeping a well defined orientation relationship (Fung, Zou, Yang, 1987; Zou, Fung, Kuo, 1987).

Approximants

The structure of monoclinic $\text{Al}_{13}\text{Fe}_4$, first studied by Black (1955a, b) was redetermined by Grin, Burkhardt, Ellner, Perters (1994a). Barbier, Tamura, Verger-Gaugry (1993) demonstrated that $\text{Al}_{13}\text{Fe}_4$ is an approximant for both the decagonal phase as well as for the icosahedral phase Al–Cu–Fe.

5.2.3.3 d-Al–Me–Pd (*Me* = Fe, Mg, Mn, Os, Ru)

Discovery

Metastable d- $\text{Al}_{70}\text{Mn}_5\text{Pd}_{25}$ with 16 Å periodicity along the 10-fold axis can be obtained by rapid solidification (Tsai, Inoue, Masumoto, 1991). It can be considered as solid solution of Mn in metastable d-Al–Pd. Another metastable d-phase was found in the system Al–Fe–Pd for compositions $\text{Al}_{75}\text{Fe}_{10}\text{Pd}_{15}$, $\text{Al}_{75}\text{Fe}_{15}\text{Pd}_{10}$ and $\text{Al}_{72}\text{Fe}_3\text{Pd}_{25}$, coexisting with a fci-i-phase (Tsai, Inoue, Masumoto, 1993). The SAED patterns of the Fe-rich samples showed reflection broadening compared to the Fe-poor one, which may be just a solid solution of Fe in d-Al–Pd. After annealing d- $\text{Al}_{75}\text{Fe}_{10}\text{Pd}_{15}$ transformed into a 1D quasiperiodic phase, which may be an intermediate state on the way to a stable crystalline phase (Tsai, Matsumoto, Yamamoto, 1992). The stability of all these phases is not quite clear yet. The same is true for d- $\text{Al}_{75}\text{Os}_{10}\text{Pd}_{15}$ and d- $\text{Al}_{75}\text{Ru}_{10}\text{Pd}_{15}$, discovered by Tsai, Inoue, Masumoto (1991).

Metastable d- $\text{Al}_{72}\text{Mg}_x\text{Pd}_{28-x}$, $5 \leq x \leq 10$ was found in a rapidly solidified sample coexisting with a Frank-Kasper-type and a Mackay-type icosahedral phase (Koshikawa, Edagawa, Honda, 1993; Koshikawa, Edagawa, Takeuchi, 1994). It can be seen as an extension of binary d-Al–Pd into the ternary system.

Electron microscopy

A comprehensive study of the structure of metastable d- $\text{Al}_{70}\text{Mn}_5\text{Pd}_{25}$ with 16 Å periodicity was performed by Sun, Hiraga (1996b). The ring contrasts on the images are similar to those of the approximant Al_3Pd (Matsuo, Hiraga, 1994). The main structural difference to d-Al–Mn–Pd with 12 Å period is that the fundamental pentagons (each one containing a small pentagonal cluster) are linked via vertices instead of sharing edges and that the underlying tiling is by a factor of τ^2 smaller. This means, that they are of the same size as those building d-Al–Pd. The sample showed a linear phason strain as demonstrated by lifting centers of clusters into the 5D space. By annealing d- $\text{Al}_{70}\text{Mn}_5\text{Pd}_{25}$ transformed into a crystalline phase.

X-ray structure analysis

A single-crystal X-ray diffraction study of d-Al–Os–Pd was performed by Cervellino (2002). It was based on a data set collected by Haibach, Kek, Honal, Edler, Mahne, Steurer (1996), which consisted of 6543 reflections merged in the Laue group $10/mmm$ to 1738 unique reflections (455 with $I > 3\sigma_I$). However, the quality of the data set was not sufficient (large mosaic spread) to perform a high-quality structure refinement with detailed atomic surface modelling. Consequently, the refinement was only used to get a starting set of phases for 3D physical-space MEM modelling (Hai-

AlOsPd-C-00

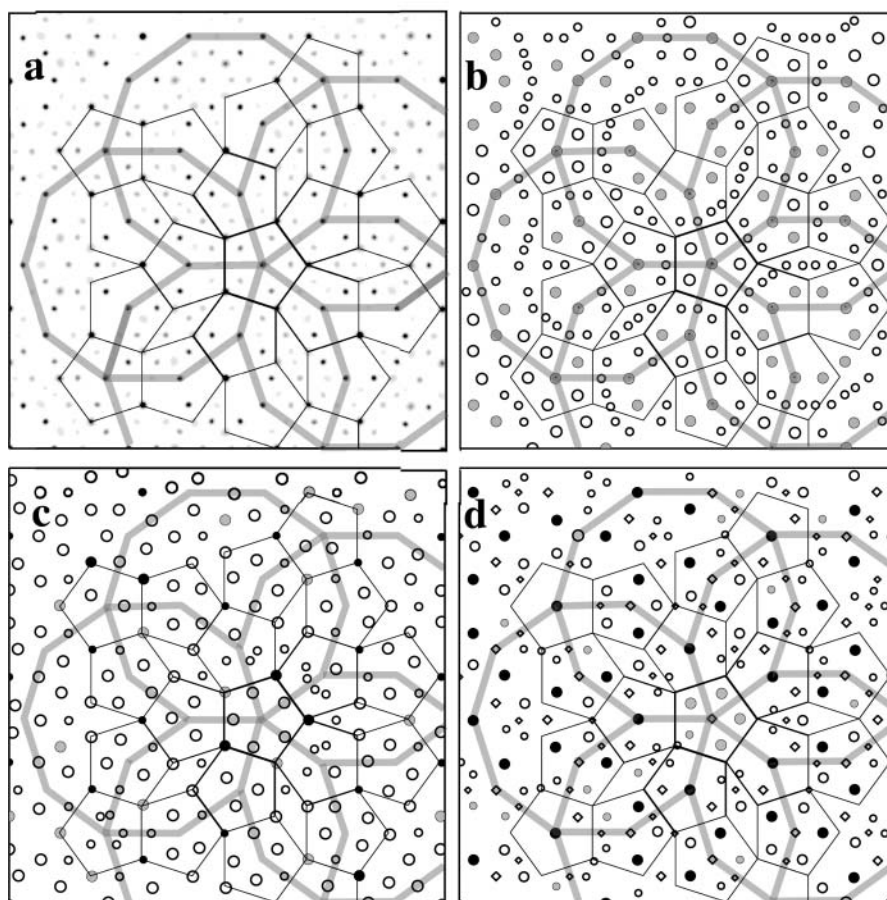


Fig. 5.2.3.3-1. (a) Projected MEM electron density map ($39 \text{ \AA} \times 39 \text{ \AA}$) of $d\text{-Al}_{75}\text{Os}_{10}\text{Pd}_{15}$ ($0 = z = 1/4$). The reconstructed structures of the layers are shown for (b) 0 , (c) $z = 1/8$, (d) $z = 1/4$. Empty circles are Al, full grey circles are Pd, black full circles are Os (size is proportional to the occupancy of the site); diamonds (only in $z = 1/4$) are Al atoms shifted from the mirror plane (split position). Pentagon tiling and HBS-supertiling are shown (Cervellino, 2002).

bach, Steurer, 1996). The evaluation of the large-scale electron density maps (cf. Haibach, Cervellino, Estermann, Steurer, 2000, and references therein) resulted in a first structure model (AOP-C-00). In physical space, a pentagonal Penrose tiling is obtained with edge length 4.799 \AA . It is the basis for a dual HBS-supertiling (edge length 6.605 \AA) decorated appropriately by decagonal clusters with 21.378 \AA diameter (Fig. 5.2.3.3-1). In perpendicular space, the atomic surfaces could be nicely reconstructed by fitting

the MEM electron density maxima to 3D Gaussians and lifting to 5D space (Fig. 5.2.3.3-2).

Approximants

Several approximants, Al_3Pd , the base-centred orthorhombic R-phase and the monoclinic T-phase, have been found to co-exist with $d\text{-Al}_{70}\text{Mn}_5\text{Pd}_{25}$ (Sun, Hiraga, 1996b). The building principles are similar to the above-mentioned ones for the d-phase. A rational $(3/2, 2/1)$ -approximant with composition

AlOsPd-C-00

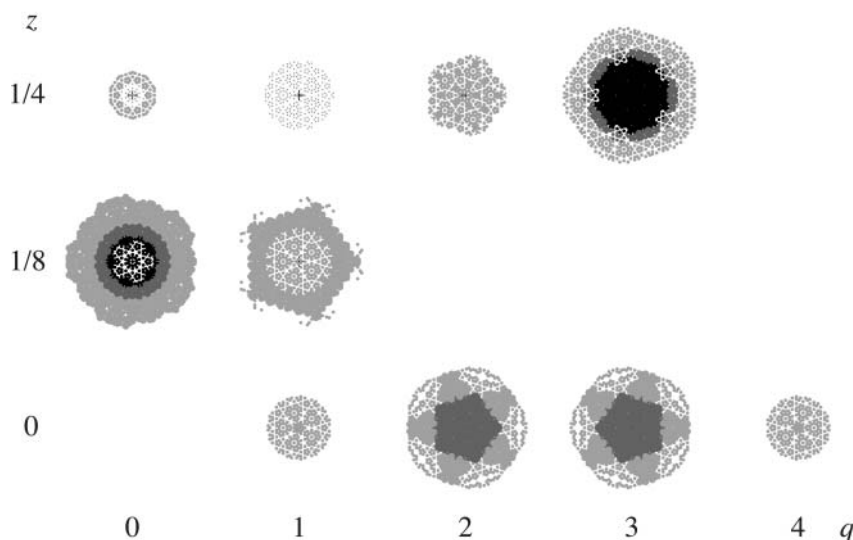


Fig. 5.2.3.3-2. Reconstructed atomic surfaces of $d\text{-Al}_{75}\text{Os}_{10}\text{Pd}_{15}$ for layers $z = 0$, $z = 1/8$ and $z = 1/4$ (Cervellino, 2002). The surfaces show displacements along z . The numbers q refer to the positions of the atomic surfaces on the diagonal in the 5D unit cell. Black dots represent Os, dark grey Pd, light grey Al atoms (dot size is proportional to occupancy of the site in physical space).

$\text{Al}_{75}\text{Pd}_{13}\text{Ru}_{12}$ and a structure built up from crown and hexagon tiles (of the structure of d-Al–Pd), was discovered by Zhang, Li, Steurer, Schneider, Frey (1995). Fivefold orientational twinning occurred frequently in the samples studied.

5.2.3.4 d-Al–Ni–Ru

Discovery

Two decagonal phases, one with 4 Å and one with 16 Å translation period were found in the system Al–Ni–Ru after slow cooling (Sun, Hiraga, 2000a). After annealing at 900 °C samples with compositions $\text{Al}_{75}\text{Ni}_{15}\text{Ru}_{10}$, $\text{Al}_{70}\text{Ni}_{20}\text{Ru}_{10}$, $\text{Al}_{70}\text{Ni}_{22}\text{Ru}_8$, the 16 Å d-phase became the major phase and the 4 Å d-phase disappeared. Later studies confirmed the stability of the 16 Å d-phase at temperatures below 1057 °C (Mi, Grushko, Dong, Urban, 2003a, b; Mandal, Hashimoto, Suzuki, Hosono, Kamimura, Edagawa, 2003). The stability range at 1000 °C is around $\text{Al}_{73.1}\text{Ni}_{15.7}\text{Ru}_{11.2}$, at 700 °C it is shifted by $\approx 1\%$. Beside the two decagonal phases, also a metastable fci-phase was found in slowly as well as rapidly cooled samples for low Ru contents (Sun, Hiraga, 2002a).

Electron microscopy

By detailed analysis of HRTEM as well as of HAADF-STEM images a model, *AlNiRu-SOH-01*, was derived for the short-range order of the basic structural units (Sun, Ohsuna, Hiraga, 2001) and the underlying tiling (Sun, Hiraga, 2000b; 2001; 2002b). The basic structural unit is a columnar cluster, which is by a factor τ^2 larger than in d-Al–Pd. This cluster decorates a pentagonal tiling. Its quasiperiodicity on a scale of $1400 \times 1000 \text{ Å}^2$ could be demonstrated by lifting it into the perpendicular space. The window occupied by the lifted points corresponds to a decagon rotated $\pi/10$ and scaled by a factor $\cos(\pi/5)/\cos(\pi/10)$ compared to the window of the original pentagonal Penrose tiling (Sun, Hiraga, 2002b).

The SAED diffraction pattern of d- $\text{Al}_{70}\text{Ni}_{20}\text{Ru}_{10}$ as well as the of the type I superstructure in the system Al–Co–Ni can be derived from a 5D CsCl-type hypercubic structure (Ohsuna, Sun, Hiraga, 2000). In 3D direct space such a structure is related to an ordered decoration of a rhomb tiling with clusters with pentagonal symmetry in two different orientations.

X-ray diffraction

The quasilattice constant was determined by X-ray powder diffraction to $a_r = 2.49 \text{ Å}$ and the periodicity to 16.7 Å , respectively (Mandal, Hashimoto, Suzuki, Hosono, Kamimura, Edagawa, 2003). No peak shifts or broadening, indications for linear or random phason strain, respectively, could be observed. A single-crystal X-ray diffraction study found quasilattice parameter of $a_i = 3.8361(5) \text{ Å}$, $a_5 = 16.539(3) \text{ Å}$ and $a_r = 2.4838(4) \text{ Å}$ (Scholpp, 2002). The amount of diffuse scattering was much less than in other stable d-phases.

5.2.4 High-pressure experiments on decagonal phases

Only a few high-pressure experiments have been performed on decagonal QC. The first study was performed on polycrystalline d- $\text{Al}_{71}\text{Co}_{10}\text{Ni}_{17}$ at hydrostatic pressures

up to 40 GPa (Zhou, Che, Zhang, 1996). Almost isotropic behaviour and no indication of a phase transformation were found. These findings were essentially confirmed by a study on d- $\text{Al}_{72}\text{Co}_8\text{Ni}_{20}$ up to pressures of 67 GPa (Hasegawa, Tsai, Yagi, 1999). Most peaks broadened considerably after compression. The bulk modulus and its pressure derivative resulted to $B_0 = 120 \text{ GPa}$ and $B'_0 = 5 \text{ GPa}$. The strain behaviour is anisotropic, i.e. the structure within the quasiperiodic plane is more easily distorted than along the tenfold axis.

High-pressure experiments on polycrystalline QC usually image a few Bragg reflections only (3 to 10). Only single-crystal experiments also allow the observation of weak Bragg reflections, and much more important of changes in symmetry. If additionally an area detector is used also diffuse scattering can be imaged. The disadvantage of this method is that the pressures that can be reached are smaller by one order of magnitude.

The first experiment of this type was performed by Krauss, Miletich, Steurer (2003) on d- $\text{Al}_{70}\text{Co}_{12}\text{Ni}_{18}$ at pressure up to 10.7 GPa. The earlier findings could be confirmed, $B_0 = 121(8) \text{ GPa}$ and its pressure derivative $B' = 3.5(1.4)$. No changes could be observed in position and intensity of Bragg as well as diffuse scattering.

It is still an open question whether these observations confirm the stability of d-phases under pressure or the transformation to a crystalline phase is just too sluggish to be observed on the time scale of the experiment.

5.2.5 Surface studies of decagonal phases

A comprehensive review on low-energy electron diffraction (LEED) from QC surfaces was published by Diehl, Ledieu, Ferralis, Szmodis, McGrath (2003). A topical review on QC surfaces investigated by scanning-tunneling microscopy (STM) was written by McGrath, Ledieu, Cox, Diehl (2002).

The first surface study of a QC was performed by STM on d- $\text{Al}_{65}\text{Co}_{20}\text{Cu}_{15}$ (Kortan, Becker, Thiel, Chen, 1990). The high-resolution images clearly show a quasiperiodic structure similar to a pentagon Penrose tiling and gave no indication for a reconstruction of the surface structure. A model for the 8 Å structure of the unit cluster was proposed. LEED experiments on twofold and tenfold surfaces of a sample with the same composition were performed *in situ* as function of temperature in the range $300 \leq T \leq 800 \text{ K}$ (McRae, Malic, Lalonde, Thiel, Chen, Kortan, 1990). At $T = 715(5) \text{ K}$ a second order transition into a disordered surface structure was observed on the tenfold surface. No reflection broadening was observed.

Secondary-electron imaging was used to study the decagonal surface of d- $\text{Al}_{70}\text{Co}_{15}\text{Ni}_{15}$ (Zurkirch, Bolliger, Erbudak, Kortan, 1998). It was shown that the Al depletion caused by 1.5-keV Ar^+ -ion bombardment leads to a phase transformation into a disordered B2-phase. There are five domains related by fivefold symmetry. One of the [110]-directions is parallel to the tenfold axis of the d-phase, another one parallel to the twofold direction A2P. Annealing at 700 K restores the equilibrium Al composition of the surface and the original quasiperiodic structure. These

results could be confirmed by reflection high-energy electron diffraction (RHEED) and X-ray photoelectron diffraction (XPD) on d-Al₇₂Co₁₆Ni₁₂ (Shimoda, Guo, Sato, Tsai, 2000).

A spot profile analysis low-energy electron diffraction (SPA-LEED) study performed on d-Al_{72.1}Co_{16.4}Ni_{11.5} revealed that the surface structure should be similar to that of the bulk (Gierer, Mikkelsen, Graber, Gille, Moritz, 2000). From the existence of broad features in the diffraction pattern the authors conclude that significant disorder should be present on the scale of inter-cluster distances of more than 30 Å. A He atom diffraction experiment on the twofold (001 $\bar{1}0$) surface of d-Al_{71.8}Co_{13.4}Ni_{14.8} was carried out by Sharma, Theis, Gille, Rieder (2002). All five reciprocal basis vectors related to the bulk structure were clearly identified to form also the basis of the surface structure. The surface consisted of (10000)-terraces with a width of approximately 100 Å indicating the higher stability of the (10000)-growth facets.

The first STM study on the tenfold as well as on the twofold surface of d-Al₇₂Co₁₆Ni₁₂ was performed by Kishida, Kamimura, Tamura, Edagawa, Takeuchi, Sato, Yokoyama, Guo, Tsai (2002). In the quasiperiodic layer they found atomically flat terraces with a step height of 2.2(4) Å. The pentagonal-star shaped motifs all have the same orientation within a terrace and the opposite orientation in adjacent terraces. The step heights of the terraces parallel to the twofold surface amount to 8.0(4) and 5.0(4) Å. Two-, four- and six-layer periodicities of the columnar clusters along the periodic direction were identified.

The structure of tenfold cleavage surfaces of d-Al_{72.4}Co_{11.8}Ni_{15.8} was investigated by scanning electron microscopy (SEM) as well as by STM with much lower resolution (Ebert, Kluge, Yurechko, Grushko, Urban, 2003). Only features with diameters of 10 to 20 Å which form aggregates of 30 to 60 Å size ("cluster-subcluster" structure) could be resolved. The surface showed a rather high roughness of 4 to 8 Å. According to the authors, the "cluster-subcluster" structure directly reflects the architecture of the d-phase, which is considered a quasiperiodic packing of 20 Å columnar clusters. One shortcoming of this interpretation is, however, that the distribution of features in the STM images is not quasiperiodic (this could be easily shown by the calculation of the autocorrelation function) as it should be. The cleavage surface is rather a random cut through the cluster structure, i.e. there are no particularly preferred crack propagation directions through such a cluster or an arrangement of clusters. There is no difference in the strength of bonds within a cluster or between clusters. The picture of strongly bonded low energy clusters in a matrix with weaker bonds does not apply to decagonal QC. Firstly, there are no matrix atoms at all. All atoms of the structure are part of at least one cluster. Secondly, all clusters are partially overlapping each other. Thirdly, by flipping a small subset of atoms clusters can flip. This fact alone shows that cluster boundaries do not have a particular meaning for the mechanical stability of a decagonal quasicrystal.

SEM investigation of samples annealed 1 h at 790(30) °C showed roughening of the surface due to the

formation of very small pits due to bulk vacancy diffusion and agglomeration (Ebert, Kluge, Yurechko, Grushko, Urban, 2003). Heat treatment at 824(30) °C resulted in surface melting (bulk melting temperature $T_m \approx 880$ °C according to Scheffer, Gödecke, Lück, Ritsch, Beeli, 1998).

5.3 Dodecagonal phases

A general introduction into simple dodecagonal (dd) tilings (Fig. 5.3-1), their generation and properties is given by Socolar (1989). The generation of dd-tilings by the dual grid method is discussed in detail by Häussler, Nissen, Lück (1994). Gähler, Lück, Ben-Abraham, Gummelt (2001) and Ben-Abraham, Gummelt, Lück, Gähler (2001) demonstrated that the Socolar tiling corresponds to the unique twelvefold tiling which is maximally covered by a suitable pair of clusters (dodecagon and butterfly cluster). Of course, this result can be transferred to all other tilings, which are mutually locally derivable or locally equivalent with the Socolar tiling (Baake, Klitzing, Schlottmann, 1992). The thermal and phason diffuse scattering for dodecagonal QC were discussed by Lei, Wang, Hu, Ding (2000). An overview of dd-phases discovered so far is given in Table 5.3-1, and some quantitative information on the (stable?) dd-phase and its approximant is listed in Table 5.3-2.

Discovery

The first (metastable) dodecagonal phase has been discovered by Ishimasa, Nissen, Fukano (1985) in the system Ni–Cr. Small particles (≤ 100 nm) of the dd-phase were prepared by evaporating a Ni_{70.6}Cr_{29.4} alloy in Xe gas and investigated by SAED and HRTEM. The contrasts of a nanometer-sized part of the sample formed the vertices of a dodecagonal tiling. The triangles and squares of the tiling (edge length 4.58 Å) were found to be decorated by one half of the unit cell of the Zr₄Al₃ and one unit cell of

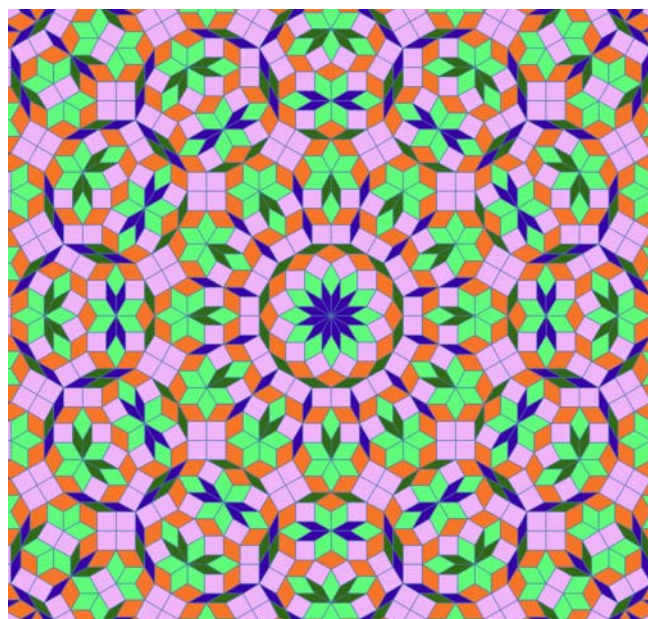


Fig. 5.3-1. Dodecagonal tiling generated by the dual-grid method using the JAVA applet *JTiling* (Weber, 1999).

Table 5.3-1. Timetable of the discovery of dodecagonal (dd) quasicrystals. Probably stable phases are marked by *.

Year of discovery	Nominal Alloy Composition	Period along 12-fold axis [Å]	References
1985	dd-Ni _{70.6} Cr _{29.4}		Ishimasa, Nissen, Fukano (1985)
1988	dd-V ₃ Ni ₂	4.5	Chen, Li, Kuo (1988)
1988	dd-V ₁₅ Ni ₁₀ Si	4.5	Chen, Li, Kuo (1988)
1988	dd-Bi–Mn		Yoshida, Yamada (1988)
1994	*dd-Ta _{1.6} Te	20.79(9)	Krumeich, Conrad, Harbrecht (1994)

the Cr₃Si structure typ, respectively. The outer regions of the particle consisted of twinned nanodomains with σ -phase structure and common c -axis.

A first discussion of a dodecagonal quasilattice as a model lattice of the dd-Ni–Cr phase was given by Yang, Wei (1987). They applied the projection method (6D to 2D) to obtain a suitable quasilattice and to index several Bragg reflections. They suggest a structure model consisting of dodecagonal prismatic clusters with a period of four layers along the 12-fold axis. A dd-phase with slightly different structure, based on a square-triangle tiling without rhombi, was found in the system V–Ni(–Si) (Chen, Li, Kuo, 1988).

A growth model of dodecagonal QC was proposed by Kuo, Feng, Chen (1988). It consists of hexagonal antiprisms on a square and triangle tessellation based on the structure of the σ -phase. Depending on given correlation rules structures close to randomness, periodic order or dodecagonal order resulted.

The first dodecagonal phase that could be prepared by slow cooling in macroscopic amounts was found in the system Ta–Te by Krumeich, Conrad, Harbrecht (1994). It was shown later that Ta can be partially substituted by V to a certain amount dd-(Ta_{1–x}V_x)_{1.6}Te, $0 \leq x \leq 0.28$ (Reich, Conrad, Krumeich, Harbrecht, 1999). With increasing V content the quasilattice parameter shrinks due to the smaller diameter of V compared to that of Ta, and the period along the twelvefold axis is halved.

An alternative description of dd-Ta₆₂Te₃₈ as incommensurately modulated structure (IMS) was suggested by Uchida, Horiuchi (1997; 1998a; 2000). They found at the same composition the dd-phase as well as a high-order approximant. They demonstrate that both phases can be described as IMS with slightly different modulation vectors and that their structure is composed of two incommensurate layers rotated by 30° against each other. The origin of the modulation should be the same as for the well-known IMS TaTe₄. It

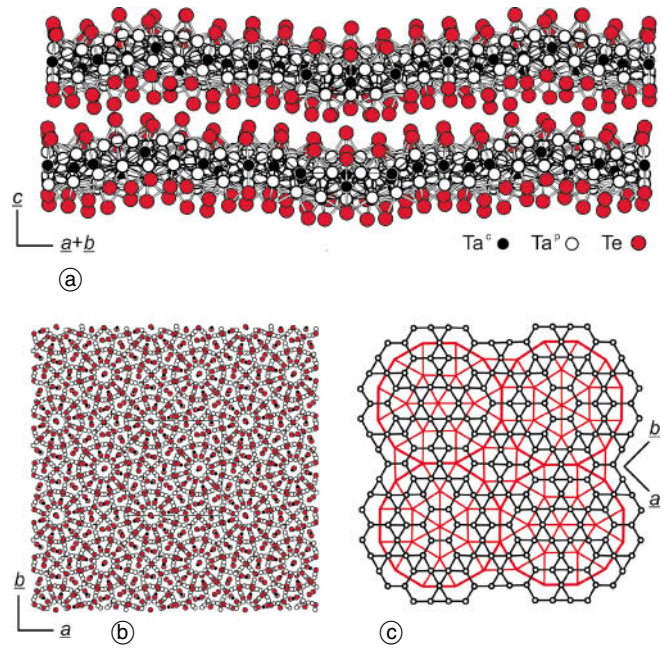


Fig. 5.3-2. (a) The three chemically distinct coordination types for Ta in the d-phase approximant Ta₉₇Te₆₀. (b) Projection onto (001) and (c) side view of two partially overlapping vaulted Ta₁₅₁ units composed of 19 concentrically fused hexagonal antiprismatic TaTa₁₂ clusters covered by Te atoms (red circles) in (b) (Fig. 3 of Conrad, Harbrecht, 2002).

should result from periodic lattice distortions and vacancy ordering due to charge-density waves.

Due to the low quality of the dd-phase, which possesses contrary to all other axial QC a real layer structure, no accurate structure analysis could be performed so far. Therefore, it is still not clear whether or not this phase can be better described by a quasiperiodic structure, a random tiling, a modulated structure or an orientationally twinned domain structure of one of its approximants.

Structure of dd-(Ta_{1–x}V_x)_{1.6}Te, $0 \leq x \leq 0.28$

Contrary to the quite well ordered approximants Ta₉₇Te₆₀ and Ta₈₃V₁₄Te₆₀ (see Fig. 1 of Reich, Conrad, Krumeich, Harbrecht, 1999), the dodecagonal phase appears to be strongly disordered. The SAED along the periodic direction indicates strong disorder within the quasiperiodic plane as well as disorder and a rather short correlation length in the stacking of quasiperiodic planes (see Fig. 3 of Krumeich, Reich, Conrad, Harbrecht, 2000 and Fig. 5 of Reich, Conrad, Krumeich, Harbrecht, 1999). A more detailed tiling-based analysis of a large HRTEM image of a rather disordered dd-Ta_{1.6}Te has been performed by Krumeich, Conrad, Nissen, Harbrecht (1998). Several weeks of thermal annealing of dd-Ta_{1.6}Te causes no struc-

Table 5.3-2. Quantitative structural information on the dodecagonal (dd) quasicrystal and one of its approximants. Whether R factors are based on structure amplitudes or on intensities is unclear in most cases (intensity based R factors are approximately by a factor two larger than the structure amplitude based ones). D_x ... calculated density, PD ... point density, SG ... space group, PS ... Pearson symbol, N_R ... number of reflections, N_V ... number of variables.

Nominal composition	SG PS	Lattice parameters	D_x PD	N_R N_V	R wR	Reference
dd-Ta _{1.6} Te		$a_{1...4} = 3.8171(6) \text{ \AA}$ $a_5 = 20.79(9) \text{ \AA}$				Conrad, Krumeich, Harbrecht (1998)
Ta ₉₇ Te ₆₀	$P2_12_12_1$ $oP628$	$a = 27.672(2) \text{ \AA}$ $b = 27.672(2) \text{ \AA}$ $c = 20.613(2) \text{ \AA}$		30458 1415	0.059 0.129	Conrad, Harbrecht (2002)

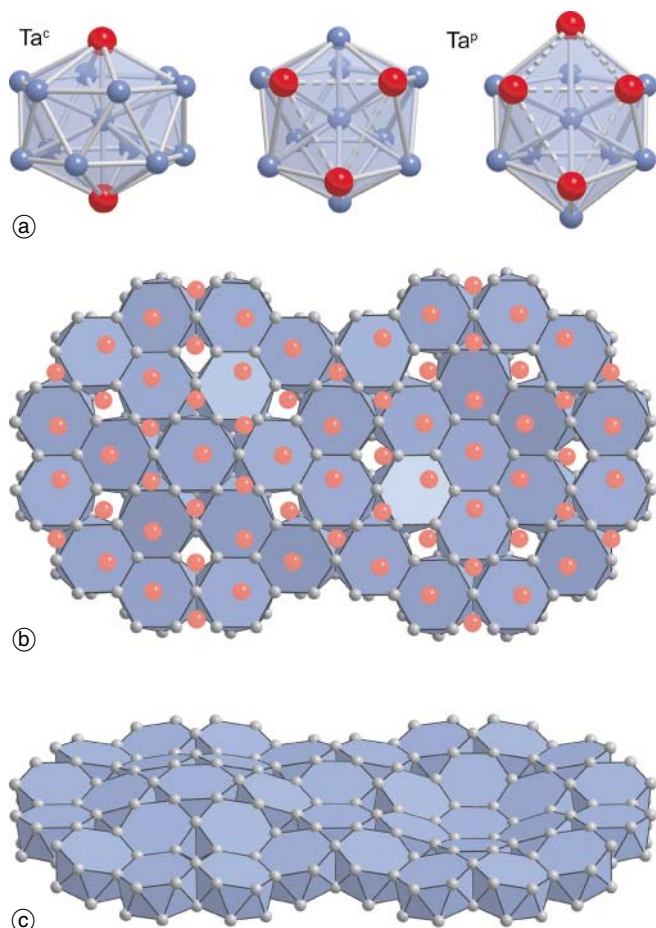


Fig. 5.3-3 (a) Projection of a suitable section of the crystal structure of the dd-phase approximant $\text{Ta}_{97}\text{Te}_{60}$ onto (110) with emphasis on the corrugation of the lamellae. (b) Projection of the lamella onto (001). (c) Network presentation of the Ta partial structure. The Ta^{P} atoms are arranged in layers corresponding to an irregular hexagon/triangle net (black). The Ta^{C} atoms form an irregular square triangle net (red). (Fig. 2 of Conrad, Harbrecht, 2002).

tural changes, which can be observed by standard X-ray diffraction experiments while annealing above 1870 K induces a transition into crystalline phases (Conrad, Krummeich, Harbrecht, 1998).

Approximants

The determination of the structure of $\text{Ta}_{97}\text{Te}_{60}$, an orthorhombic approximant to the dd-phase, gives a good estimate how the structure of the dd-phase may look like locally (Conrad, Harbrecht, 2002). The basic building unit is a Ta-centered and Te-capped hexagonal antiprismatic $\text{TaTa}_{12}\text{Te}_2$ cluster ($d_{\text{Ta-Te}} \approx 3.05 \text{ \AA}$, $d_{\text{Ta-Ta}} \approx 2.95 \text{ \AA}$). Nineteen condensed basic clusters of this kind form a vaulted $\text{Ta}_{151}\text{Te}_{74}$ -supercluster with dodecagonal shape and $\approx 25 \text{ \AA}$ diameter (Fig. 5.3-2). Along the pseudo dodecagonal c-axis approximately 10 \AA thick slabs of this supercluster are stacked with a period of two slabs and related by a 2_1 -screw axis. Each slab consists of five corrugated atomic layers, the outer ones are just Te layers ... Te-Ta-Ta-Ta-Te ... Consequently, the slabs are bonded just by weak Te-Te interactions ($d_{\text{Te-Te}} \leq 3.34 \text{ \AA}$), which are responsible for the lubricant-like properties of this material. The superclusters occupy the vertices of a square tiling with edge length 19.52 \AA (same edge

length as found for dd- $\text{Ta}_{1.6}\text{Te}$ from HRTEM images) (Fig. 5.3-3). The ideal stoichiometry of a dd-quasicrystal based on this supercluster results to $\text{Ta}_3 + 2\sqrt{3}\text{Te}_4$. It is remarkable that the Ta substructure of the slabs corresponds just to a tetrahedral close packing. Therefore, the dd-phase shows close structural similarities to some Frank-Kasper phases like the σ -phase (Bergman, Shoemaker, 1954). Strictly seen, however, dd- $\text{Ta}_{1.6}\text{Te}$ is not a Frank-Kasper phase, since the Te atoms are not tetrahedrally close packed.

6 Conclusions

Quantitative QC structure analysis in the strict sense is a never-ending story. However, it soon will reach the turning point when we know enough to answer the fundamental questions about structure and stability of quasiperiodic phases. Probably it will never become a routine tool in the suite of structure determination methods since the number of QC structures to be determined is too small and the technique too complex and specific. QC structure analysis, however, will certainly contribute to the solution of complex intermetallic phases in general.

Acknowledgments. I want to thank B. Grushko, K. H. Kuo for useful comments and B. Harbrecht for helpful discussions and providing some pictures.

References

- Abe, H.; Matsuo, Y.; Saitoh, H.; Kusawake, T.; Ohshima, K.; Nakao, H.: Atomic short-range order in an $\text{Al}_{72}\text{Ni}_{20}\text{Co}_8$ decagonal quasicrystal by anomalous-X-ray scattering. *J. J. Appl. Phys.* **39** (2000a) L1111–L1114.
- Abe, E.; Pennycook, S. J.; Tsai, A. P.: Direct observation of a local thermal vibration anomaly in a quasicrystal. *Nature* **421** (2003) 347–350.
- Abe, E.; Sato, T. J.; Tsai, A. P.: The structure of a Frank-Kasper decagonal quasicrystal in the Zn–Mg–Dy system: comparison with the Al–Ni–Co system. *Philos. Mag. Lett.* **77** (1998) 205–211.
- Abe, E.; Sato, T. J.; Tsai, A. P.: Structure of a quasicrystal without atomic clusters. *Phys. Rev. Lett.* **82** (1999) 5269–5272.
- Abe, E.; Saitoh, K.; Takakura, H.; Tsai, A. P.; Steinhardt, P. J.; Jeong, H. C.: Quasi-unit-cell model for an Al–Ni–Co ideal quasicrystal based on clusters with broken tenfold symmetry. *Phys. Rev. Lett.* **84** (2000) 4609–4612.
- Abe, H.; Saitoh, H.; Ueno, T.; Nakao, H.; Matsuo, Y.; Ohshima, K.; Matsumoto, H.: Diffuse scattering from an $\text{Al}_{72}\text{Ni}_{20}\text{Co}_8$ decagonal quasicrystal on an order-disorder transformation. *J. Phys.-Condens. Matter* **15** (2003) 1665–1676.
- Abe, E.; Tsai, A. P.: Orthorhombic τ -Zn–Mg–Dy phase related to a Frank Kasper type decagonal quasicrystal. *Acta Crystallogr.* **B56** (2000) 915–917.
- Abe, E.; Tsai, A. P.: Structure of quasicrystals studied by atomic-resolution electron microscopy. *JEOL News* **36** (2001) 18–21.
- Abe, E.; Tsai, A. P.: Structure of a metastable Al_3Ni decagonal quasicrystal: comparison with a highly perfect $\text{Al}_{72}\text{Ni}_{20}\text{Co}_8$. *J. Alloys Comp.* **342** (2002) 96–100.
- Al-Lehyani, I.; Widom, M.: Tile Hamiltonian for decagonal AlCoCu derived from first principles. *Phys. Rev.* **B6701** (2003) art. no. 014204.
- Athanasiou, N. S.: Formation, characterization and magnetic properties of some ternary Al–Cu–M (M equals transition metal) quasicrystals prepared by conventional solidification. *Intern. J. Modern Physics* **B11** (1997) 2443–2464.

- Audier, M.; Robertson, B.: Crystalline to Quasi-Crystalline Transformation in an AlCoCuSi Alloy – Characteristics of the Observed Decagonal Quasi-Lattice. *Philos. Mag. Lett.* **64** (1991) 401–409.
- Axel, F.; Denoyer, F.; Gazeau, J. P. (eds.): From Quasicrystals to more Complex Systems. Centre de Physique des Houches Series No 13. Springer-Verlag Berlin and EDP Sciences Les Ulis 1999.
- Axel, F.; Gratias, D. (eds.): Beyond Quasicrystals. Centre de Physique des Houches Series No 3. Springer-Verlag Berlin and EDP Sciences Les Ulis 1995.
- Baake, M.; Klitzing, R.; Schlottmann, M.: Fractally Shaped Acceptance Domains of Quasiperiodic Square Triangle Tilings with Dodecagonal Symmetry. *Physica A* **191** (1992) 554–558.
- Baake, M.; Joseph, D.; Kramer, P.: The Schur Rotation as a Simple Approach to the Transition Between Quasiperiodic and Periodic Phases. *J. Phys. (London)*. **A24** (1991) L961–L967.
- Baake, M.; Moody, R. V. (eds.): Directions in mathematical Quasicrystals. CRM Monograph Series 13, American Mathematical Society, Providence, Rhode Island 2000.
- Balanetskyy, S.; Grushko, B.; Kowalska-Strzeciwlk, E.; Velikanova, T. Ya.; Urban, K.: An investigation of the Al–Pd–Re phase diagram between 50 and 100 at% Al: phase equilibria at 900–1020 °C. *J. Alloys Comp.* **364** (2004) 164–170.
- Ball, M. D.; Lloyd, D. J.: Particles apparently exhibiting fivefold symmetry in Al–Cu–Li–Mg alloys. *Scr. Met.* **19** (1985) 1065–1068.
- Bancel, P. A.; Heiney, P. A.: Icosahedral aluminum-transition-metal alloys. *Phys. Rev.* **B33** (1986) 7917–7922.
- Barbier, J. N.; Tamura, N.; Verger-Gaugry, J. L.: Monoclinic Al₁₃Fe₄ Approximant Phase – a Link between Icosahedral and Decagonal Phases. *J. Non-Cryst. Solids* **153** (1993) 126–131.
- Baumgarte, A.; Schreuer, J.; Estermann, M. A.; Steurer, W.: X-ray diffraction study of decapristmatic Al–Co–Ni crystals as a function of composition and temperature. *Phil. Mag.* **A75** (1997) 1665–75.
- Beeli, C.: Quasicrystal structures studied by high-resolution transmission electron microscopy. *Z. Kristallogr.* **215** (2000) 606–617.
- Beeli, C.; Horiuchi, S.: The Structure and Its Reconstruction in the Decagonal Al₇₀Mn₁₇Pd₁₃ Quasi-Crystal. *Philos. Mag.* **B70** (1994) 215–240.
- Beeli, C.; Nissen, H. U.: Stable Decagonal Al₇₀Mn₁₇Pd₁₃ Quasi-Crystal. *J. Non-Cryst. Solids* **153** (1993) 463–467.
- Beeli, C.; Nissen, H. U.; Robadey, J.: Stable Al–Mn–Pd Quasi-Crystals. *Philos. Mag. Lett.* **63** (1991) 87–95.
- Beeli, C.; Stadelmann, P.; Lück, R.; Gödecke, T.: Decagonal quasicrystal free of linear phason strain. Proceedings of the 5th International Conference on Quasicrystals (ICQ5), Avignon, France. Eds.: C. Janot & R. Mosseri, pp. 680–687. World Scientific, Singapore 1996.
- Beeli, C.; Steurer, W. (Eds.): Proceedings of the Workshop on Quasicrystal Structure Analysis – A Satellite Meeting to ICQ7. *Z. Kristallogr.* **215** (2000) 553–626.
- Belin-Ferré, E.; Berger, C.; Quiquandon, M.; Sadoc, A. (eds.): Quasicrystals – Current Topics. World Scientific, Singapore 2000.
- Ben-Abraham, S. I.; Gähler, F.: Covering cluster description of octagonal MnSiAl quasicrystals. *Phys. Rev.* **B60** (1999) 860–864.
- Ben-Abraham, S. I.; Gummelt, P.; Lück, R.; Gähler, F.: Dodecagonal tilings almost covered by a single cluster. *Ferroelectrics* **250** (2001) 313–316.
- Bendersky, L.: Quasicrystal with One-Dimensional Translational Symmetry and a Tenfold Rotation Axis. *Phys. Rev. Lett.* **55** (1985) 1461–1463.
- Bendersky, L.: Decagonal Phase. *J. De Physique* **47** (1986) C3-457–C3-464.
- Bergman, C.; Joulaud, J. L.; Capitan, M.; Clugnet, G.; Gas, P.: In situ real-time analysis of the formation of a quasicrystalline phase in Al–Co multilayers by solid-state reaction. *J. Non-Crystall. Solids* **287** (2001) 193–196.
- Bergman, G.; Shoemaker, P.: The determination of the crystal structure of the σ -phase in the iron-chromium and iron-molybdenum systems. *Acta Crystallogr.* **7** (1954) 857–865.
- Black, P. J.: The Structure of FeAl₃.1. *Acta Crystallogr.* **8** (1955) 43–48.
- Black, P. J.: The Structure of FeAl₃.2. *Acta Crystallogr.* **8** (1955) 175–182.
- Boström, M.; Hövmöller, S.: A pentagonal cluster in certain approximants to decagonal quasicrystals. *Acta Crystallogr.* **B57** (2001) 646–651.
- Boudard, M.; de Boissieu, M.; Janot, C.; Heger, G.; Beeli, C.; Nissen, H. U.; Vincent, H.; Ibberson, R.; Audier, M.; Dubois, J. M.: Neutron and X-ray single-crystal study of the AlPdMn icosahedral phase. *J. Phys.: Condens. Matter* **4** (1992) 10149–10168.
- Bradley, A. J.; Goldschmidt, H. J.: An X-ray study of slowly-cooled iron-copper-aluminium alloys. Part II-Alloys rich in aluminium. *J. Inst. Met.* **65** (1939) 195–210.
- Bridges, F.; Boyce, J. B.; Dimino, G. M.; Giessen, B. C.: Mn Local-Structure in the Decagonal Phase of Al–Mn Alloys. *Phys. Rev.* **B36** (1987) 8973–8978.
- Bruzzzone, G.: The Ca–Cd and Ba–Cd systems. *Gazz. Chim. Ital.* **102** (1971) 234–242.
- Burkhardt, U.; Ellner, M.; Grin Yu.; Baumgartner, B.: Powder diffraction refinement of the Co₂Al₅ structure. *Powder Diffraction* **13** 159–162 (1998).
- Burkov, S. E.: Structure Model of the Al–Cu–Co Decagonal Quasicrystal. *Phys. Rev. Lett.* **67** (1991) 614–617.
- Burkov, S. E.: Modeling Decagonal Quasi-Crystals – Random Assembly of Interpenetrating Decagonal Clusters. *J. Physique* **I2** (1992) 695–706.
- Burkov, S. E.: Enforcement of Matching Rules by Chemical Ordering in the Decagonal AlCuCo Quasi-Crystal. *Phys. Rev.* **B47** (1993) 12325–12328.
- Cao, W.; Ye, H. Q.; Kuo, K. H.: A New Octagonal Quasicrystal and Related Crystalline Phases in Rapidly Solidified Mn₄Si. *Phys. Stat. Solidi A* **107** (1988) 511–519.
- Cervellino, A.: Higher-dimensional modelling of decagonal quasicrystal structures. ETH Zurich Thesis No. 14023 (2002).
- Cervellino, A.; Haibach, T.; Steurer, W.: Derivation of the proper basis of quasicrystals. *Phys. Rev.* **B57** (1998) 11223–11231.
- Cervellino, A.; Haibach, T.; Steurer, W.: Structure solution of the basic decagonal Al–Co–Ni phase by atomic surface modelling method. *Acta Crystallogr.* **B58** (2002) 8–33.
- Cervellino, A.; Steurer, W.: General periodic average structures of decagonal quasicrystals. *Acta Crystallogr.* **A58** (2002) 180–184.
- Chattopadhyay, K.; Lele, S.; Thangaraj, N.; Ranganathan, S.: Vacancy Ordered Phases and One-Dimensional Quasiperiodicity. *Acta Metall.* **35** (1987) 727–733.
- Chattopadhyay, K.; Ranganathan, S.; Subbanna, G. N.; Thangaraj, N.: Electron Microscopy of Quasi-Crystals in Rapidly Solidified Al–14% Mn Alloys. *Scr. Metall.* **19** (1985) 767–771.
- Chattopadhyay, K.; Lele, S.; Ranganathan, S.; Subbanna, G. N.; Thangaraj, N.: Electron Microscopy of Quasi-Crystals and Related Structures. *Curr. Sci.* **54** (1985) 895–903.
- Chen, H.; Burkov, S. E.; He, Y.; Poon, S. J.; Shiflet, G. J.: High-Resolution Electron-Microscopy Study and Structure Modeling of the Stable Decagonal Al–Cu–Co Quasicrystal. *Phys. Rev. Lett.* **65** (1990) 72–75.
- Chen, H. S.; Inoue, A.: Formation and structure of new quasicrystals of Ga₁₆Mg₃₂Zn₅₂ and Al₆₀Si₂₀Cr₂₀. *Scr. Metall.* **21** (1987) 527–530.
- Chen, H.; Li, D. X.; Kuo, K. H.: New Type of Two-Dimensional Quasicrystal with Twelfold Rotational Symmetry. *Phys. Rev. Lett.* **60** (1988) 1645–1648.
- Choy, T. C.; Fitz Gerald, J. D.; Kalloniatis, A. C.: The Al–Mn Decagonal Phase. Part. 3. Diffraction Pattern Simulation Based on a New Index Scheme. *Philos. Mag.* **B58** (1988) 35–46.
- Cockayne, E.: Dense quasiperiodic decagonal disc packing. *Phys. Rev.* **B51** (1995) 14958–14961.
- Cockayne, E.; Widom, M.: Structure and phason energetics of Al–Co decagonal phases. *Philos. Mag.* **A77** (1998a) 593–619.
- Cockayne, E.; Widom, M.: Ternary model of an Al–Cu–Co decagonal quasicrystal. *Phys. Rev. Lett.* **81** (1998b) 598–601.
- Coddens, G.; Lyonard, S.; Hennion, B.; Calvayrac, Y.: Triple-axis neutron-scattering study of phason dynamics in Al–Mn–Pd quasicrystals. *Phys. Rev.* **B62** (2000) 6268–6295.
- Coddens, G.; Steurer, W.: A time-of-flight neutron-scattering study of phason hopping in decagonal Al–Co–Ni quasicrystals. *Phys. Rev.* **B60** (1999) 270–6.
- Conrad, M.; Harbrecht, B.: Ta₉₇Te₆₀: A crystalline approximant of a tantalum telluride quasicrystal with twelfold rotational symmetry. *Chem.-Eur. J.* **8** (2002) 3094–3102.
- Conrad, M.; Krumeich, F.; Harbrecht, B.: A dodecagonal quasicrystalline chalcogenide. *Angew. Chem.-Int. Edit.* **37** (1998) 1384–1386.

- Damjanovic, A.: The structure analysis of the T3(AlMnZn) compound. *Acta Crystallogr.* **14** (1961) 982–987.
- Daulton, T. L., Kelton, K. F.: The Decagonal Phase in (Al,Si)₆₅Co₂₀Cu₁₅ Alloys. *Philos. Mag. B* **66** (1992) 37–61.
- Daulton, T. L.; Kelton, K. F.; Gibbons, P. C.: Construction of Al–Mn Decagonal Zone Axes from Distorted Icosahedra. *Philos. Mag. B* **66** (1992) 311–330.
- Daulton, T. L.; Kelton, K. F.; Song, S.; Ryba, E. : Decagonal and Decagonal Approximant Formation as a Function of Composition in Ternary Al–Co–Cu Alloys. *Philos. Mag. Lett.* **65** (1992) 55–65.
- De Boissieu, M.: Structure determination of quasicrystals and neutron scattering. *Z. Kristallogr.* **215** (2000) 597–605.
- De Bruijn, X.: Algebraic theory of Penrose's non-periodic tilings of the plane. I. *Kon. Nederl. Akad. Wetensch. Proc. Series A* **84** (1981) 39–52.
- DeWolff, P. M.: The pseudosymmetry of modulated crystal structures. *Acta Crystallogr.* **A30** (1974) 777–785.
- Diehl, R. D.; Ledieu, J.; Ferralis, N.; Szmodis, A. W.; McGrath, R.: Low-energy electron diffraction from quasicrystal surfaces. *J. Phys.: Condens. Matter* **15** (2003) R63–R81.
- Döblinger, M.; Wittmann, R.; Gerthsen, D.; Grushko, B.: Continuous transition between decagonal quasicrystal and approximant by formation and ordering of out-of-phase domains. *Phys. Rev. B* **65** (2002) art. no.-224201.
- Döblinger, M.; Wittmann, R.; Gerthsen, D.; Grushko, B.: Intermediate stages of a transformation between a quasicrystal and an approximant including nanodomain structures in the Al–Ni–Co system. *Philos. Mag.* **83** (2003) 1059–1074.
- Döblinger, M.; Wittmann, R.; Grushko, B.: Metastable transformation states of decagonal Al–Co–Ni due to inhibited decomposition. *Phys. Rev. B* **64** (2001) art. no.-134208.
- Döblinger, M.; Wittmann, R.; Grushko, B.: Initial stages of the decomposition of the decagonal phase in the system Al–Ni–Fe. *J. Alloys Comp.* **360** (2003) 162–167.
- Dong, C.: The Al₃Ni₂ structure as approximant of quasicrystals. *J. Phys. I France* **5** (1995) 1625–1634.
- Dong, C.; Dubois, J. M.: The Reversible Transition from Decagonal to Orthorhombic Approximant Phase. *Phase Transitions* **32** (1991) 119–124.
- Dong, C.; Dubois, J. M.; de Boissieu, M.; Janot, C.: Phase-Transformations and Structure Characteristics of the Al₆₅Cu_{17.5}Co_{17.5} Decagonal Phase. *J. Phys.-Condens. Matter* **3** (1991) 1665–1673.
- Dong, C. A.; Dubois, J. M.; Song, S. K.; Audier, M.: The Orthorhombic Approximant Phases of the Decagonal Phase. *Philos. Mag. B* **65** (1992) 107–126.
- Dong, C.; Li, G. B.; Kuo, K. H.: Decagonal Phase in Rapidly Solidified Al₆Co Alloy. *J. Phys. F* **17** (1987) L189–L192.
- Dong, J.; Lu, K. Q.; Yang, H.; Shan, Q.: Extended X-Ray Absorption Fine-Structure Study of the Local Structure of Quasi-Crystalline Al₆₅Cu₂₀Co₁₅ in the Decagonal Phase. *Philos. Mag. B* **64** (1991) 599–609.
- Donnadieu, P.; Su, H. L.; Proult, A.; Harmelin, M.; Effenberg, G.; Aldinger, F.: From modulated phases to a quasiperiodic structure with a cubic point group and inflation symmetry. *J. Physique I* **6** (1996) 1153–1164.
- Donnadieu, P.; Harmelin, M.; Su, H. L.; Seifert, H. J.; Effenberg, G.; Aldinger, F.: A quasicrystal with inflation symmetry and no forbidden symmetry axes in a rapidly solidified Mg–Al alloy. *Z. Metallkd.* **88** (1997) 33–37.
- Dorset, D. L.; Gilmore, C. J. (Eds.): Special issue on Electron Crystallography. *Z. Kristallogr.* **218** (2003) 237–319.
- Dubois, J. M.; Janot, C.: Chemical Isomorphism and Partial Pair Distribution Functions in Decagonal Al–Mn. *Europhys. Lett.* **5** (1988) 235–240.
- Dubois, J.-M.; P. A. Thiel, Tsai, A.-P.; Urban, K. (eds.): *Quasicrystals*. MRS Proceedings **553**, Materials Research Society, Warrendale Pennsylvania 1999.
- Dunlap, R. A.; Dini, K.: Amorphization of Rapidly Quenched Quasicrystalline Al–Transition Metal Alloys by the Addition of Si. *J. Mater. Res.* **1** (1986) 415–419.
- Ebert, P.; Kluge, F.; Yurechko, M.; Grushko, B.; Urban, K.: Structure and composition of cleaved and heat-treated tenfold surfaces of decagonal Al–Ni–Co quasicrystals. *Surface Science* **523** (2003) 298–306.
- Edagawa, K.; Ichihara, M.; Suzuki, K.; Takeuchi, S.: New Type of Decagonal Quasi-Crystal with Superlattice Order in Al–Ni–Co Alloy. *Philos. Mag. Lett.* **66** (1992) 19–25.
- Edagawa, K.; Sawa, H.; Takeuchi, S.: Order-Disorder Transformation in an Al–Ni–Co Decagonal Quasi-Crystal. *Philos. Mag. Lett.* **69** (1994) 227–234.
- Edagawa, K.; Tamaru, H.; Yamaguchi, S.; Suzuki, K.; Takeuchi, S.: Ordered and disordered phases in Al–Ni–Co decagonal quasicrystals. *Phys. Rev. B* **50** (1994) 12413–12420.
- Eisenhower, R.; Colella, R.; Grushko, B.: Multiple-beam x-ray-diffraction studies of decagonal quasicrystals. *Phys. Rev. B* **57** (1998) 8218–8222.
- El-Boragy, M.; Szepan, R.; Schubert, K.: Crystal structure of Cu₃Al₂ (H) and CuAl (R). *J. Less-Common Met.* **29** (1972) 133–140.
- Elcoro, L.; Perez-Mato, J. M.: Structural analysis of the decagonal quasicrystal Al₇₀Ni₁₅Co₁₅ using symmetry-adapted functions. *J. Physique I France* **5** (1995) 729–745.
- Elcoro, L.; Perez-Mato, J. M.: Superspace description of quasiperiodic structures and the nonuniqueness of superspace embedding. *Phys. Rev. B* **54** (1996) 12115–12124.
- Ellner, M.; Kattner, U.; Predel, B.: Konstitutionelle und strukturelle Untersuchungen im aluminiumreichen Teil der Systeme Ni–Al und Pt–Al. *J. Less-Comm. Metals* **87** (1982) 305–325.
- Ellner, M.; Kek, S.; Predel, B.: Ni₃Al₄ – a phase with ordered vacancies isotypic to Ni₃Ga₄. *J. Less-Comm. Metals* **154** (1989) 207–215.
- Ellner, M.; Meyer, H.: Structure of the ternary phase Co₃Al₈Ga and formation of the gallium-containing decagonal phase d-Co(Al, Ga)(3)(M). *J. Alloys Comp.* **340** (2002) 118–121.
- Erbudak, M.; Hochstrasser, M.; Wetli, E.; Zurkirch, M.: Investigation of symmetry properties of surfaces by means of backscattered electrons. *Surf. Rev. Lett.* **4** (1997) 179–196.
- Estermann, M. A.; Haibach, T.; Steurer, W.: Quasicrystal Versus Twinned Approximant – A Quantitative Analysis with Decagonal Al₇₀Co₁₅Ni₁₅. *Philos. Mag. Lett.* **70** (1994) 379–384.
- Estermann, M.A.; Lemster, K.; Haibach, T.; Steurer, W.: Towards the real structure of quasicrystals and approximants by analysing diffuse scattering and deconvolving the Patterson. *Z. Kristallogr.* **215** (2000) 584–596.
- Fang, A. H.; Zou, H. M.; Yu, F. M.; Wang, R. H.; Duan, X. F.: Structure refinement of the icosahedral AlPdMn quasicrystal using quantitative convergent beam electron diffraction and symmetry-adapted parameters. *J. Phys.-Condens. Matter* **15** (2003) 4947–4960.
- Feng, Y. C.; Lu, G.; Ye, H. Q.; Kuo, K. H.; Withers, R. L.; van Tendeloo, G.: Experimental evidence for and a projection model of a cubic quasi-crystal. *J. Phys.: Condens. Matter* **2** (1990) 9749–9755.
- Fettweis, M.; Launois, P.; Denoyer, F.; Reich, R.; Godard, J.M.; Lambert, M.: Diffraction Patterns of Al–Cu–Co(Si) – Microcrystalline or Quasicrystalline Phases? *J. Non-Crystall. Solids* **153** (1993) 24–27.
- Fettweis, M.; Launois, P.; Denoyer, F.; Reich, R.; Lambert, M.: Decagonal Quasi-Crystalline or Microcrystalline Structures – the Specific Case of Al–Cu–Co(Si). *Phys. Rev. B* **49** (1994) 15573–15587.
- Fettweis, M.; Launois, P.; Reich, R.; Wittmann, R.; Denoyer, F.: Evidence of a reversible microcrystal quasicrystal phase transition in decagonal Al–Cu–Co(Si). *Phys. Rev. B* **51** (1995) 6700–6703.
- Fitz Gerald, J. D.; Withers, R. L.; Stewart, A. M.; Calka, A.: The Al–Mn Decagonal Phase. I. A Re-Evaluation of Some Diffraction Effects. 2. Relationship to Crystalline Phases. *Philos. Mag. B* **58** (1988) 15–33.
- Freiburg, C.; Grushko, B.; Wittenberg, R.; Reichert, W. (1996) Once more about monoclinic Al₁₃Co₄. *Proc. Of the European Powder Diffraction Conference, EPDIC 4*, TransTech Publications, Leerdam, Switzerland, p. 583–585.
- Frey, F.: Disorder Diffuse Scattering of Crystals and Quasicrystals. In: *Particle Scattering, X-ray diffraction and Microstructure of Solids and Liquids* (Eds: M. Ristig & K. Gernoth) pp. 133–166 (2002) Lecture notes in Physics, Springer.
- Frey, F.; Steurer, W.: Disorder Diffuse Scattering from Decagonal Phase Alloys. *J. Non-Crystalline Solids* **153/154** (1993) 600–605.

- Frey, F.; Weidner, E.: Disorder in Decagonal Quasicrystals. *Z. Kristallogr.* **218** (2003) 160–169.
- Frey, F.; Weidner, E.; Hradil, K.; de Boissieu, M.; Letoublon, A.; McIntyre, G.; Currat, R.; Tsai, A. P.: Temperature dependence of the 8-Ångström superstructure in decagonal Al–Co–Ni. *J. Alloys Comp.* **342** (2002) 57–64.
- Fung, K. K.; Yang, C. Y.; Zhou, Y. Q.; Zhao, J. G.; Zhan, W. S.; Shen, B. G.: Icosahedrally Related Decagonal Quasicrystal in Rapidly Cooled Al–14 at% Fe Alloy. *Phys. Rev. Lett.* **56** (1986) 2060–2063.
- Fung, K. K.; Zou, X. D.; Yang, C. Y.: Transmission electron study of Al₁₃Fe₄ tenfold twins in rapidly cooled Al–Fe alloys. *Philos. Mag. Lett.* **55** (1987) 27–32.
- Gähler, F.: Crystallography of Dodecagonal Quasicrystals. In: *Quasicrystalline Materials. Proceedings*. Janot, C.; Dubois, J. M. (Eds.) World Scientific, Singapore: 1988, pp. 272–284.
- Gähler, F.; Lück, R.; Ben-Abraham, S.I.; Gummelt, P.: Dodecagonal tilings as maximal cluster coverings. *Ferroelectrics* **250** (2001) 335–338.
- Ge, S. P.; Kuo, K. H.: Icosahedral and stable decagonal quasicrystals in Ga₄₆Fe₂₃Cu₂₃Si₈, Ga₅₀Co₂₅Cu₂₅ and Ga₄₆V₂₃Ni₂₃Si₈. *Phil. Mag. Lett.* **75** (1997) 245–253.
- Gierer, M.; Over, H.: Complex surface structures studied by low-energy electron diffraction. *Z. Kristallogr.* **214** (1999) 14–56.
- Gierer, M.; Mikkelsen, A.; Graber, M.; Gille, P.; Moritz, W.: Quasicrystalline surface order on decagonal Al_{72.1}Ni_{11.5}Co_{16.4}: An investigation with spot profile analysis LEED. *Surface Science* **463** (SEP 10 2000) L654–L660.
- Gittus, J.: Irradiation effects in crystalline solids, Applied Science London 1978.
- Gödecke, T.: Liquidus projection surface and phase equilibria with liquid of the Al–AlCo–AlNi ternary subsystem. *Z. Metallkd.* **88** (1997a) 557–569.
- Gödecke, T.: Stable and metastable states in the Al–AlCo binary system. *Z. Metallkd.* **88** (1997b) 904–910.
- Gödecke, T.; Ellner, M.: Phase equilibria in the aluminum-rich portion of the binary system Co–Al and in the cobalt/aluminum-rich portion of the ternary system Co–Ni–Al. *Z. Metallkd.* **87** (1996) 854–864.
- Gödecke, T.; Ellner, M.: Phase equilibria in the Al-rich portion of the ternary system Co–Ni–Al at 75 and 78 at% Al. *Z. Metallkd.* **88** (1997) 382–389.
- Gödecke, T.; Lück, R.: The Aluminium-Palladium-Manganese System in the Range from 60 to 100 at% Al. *Z. Metallkd.* **86** (1995) 109–121.
- Gödecke, T.; Scheffer, M.; Lück, R.; Ritsch, S.; Beeli, C.: Isothermal sections of phase equilibria in the Al–AlCo–AlNi system. *Z. Metallkd.* **89** (1998) 687–698.
- Goldman, A. I.; Kelton, K. F.: Quasi-Crystals and Crystalline Approximants. *Rev. Mod. Phys.* **65** (1993) 213–230.
- Goldman, A. I.; Sordet, D. J.; Thiel, P. A.; Dubois, J. M. (eds.): *New Horizons in Quasicrystals. Research and Applications*. World Scientific, Singapore 1997.
- Gratias, D.; Katz, A.; Quiquandon, M.: Geometry of approximant structures in quasicrystals. *J. Phys. Cond. Matter* **7** (1995) 9101–9125.
- Grin, Yu.; Burkhardt, U.; Ellner, M.; Peters, K.: Refinement of the Fe₄Al₁₃ Structure and Its Relationship to the Quasi-Homological Homeotypical Structures. *Z. Kristallogr.* **209** (1994a) 479–487.
- Grin, J.; Burkhardt, U.; Ellner, M.; Peters, K.: Crystal-Structure of Orthorhombic Co₄Al₁₃. *J. Alloys Comp.* **206** (1994b) 243–247.
- Grin, Yu.; Peters, K.; Burkhardt, U.; Gotzmann, K.; Ellner, M.: The structure of the ternary phase Co₂NiAl₉ (Y₂). *Z. Kristallogr.* **213** (1998) 364–368.
- Grushko, B.: The Composition of the Decagonal Quasicrystalline Phase in the Al–Cu–Co Alloy System. *Philos. Mag. Lett.* **66** (1992) 151–157.
- Grushko, B.: Phase Equilibrium and Transformation of Stable Quasicrystals – Decagonal Al–Cu–Co Phase. *Mater. Trans.; JIM.* **34** (1993a) 116–121.
- Grushko, B.: A study of the Al–Cu–Co phase diagram and the solidification of alloys containing decagonal phase. *Phase Transitions* **44** (1993b) 99–110.
- Grushko, B.: A Study of the High-Cu Al–Cu–Co Decagonal Phase. *J. Mater. Res.* **8** (1993c) 1473–1476.
- Grushko, B.; Döblinger, M.; Wittmann, R.; Holland-Moritz, D.: A study of high-Co Al–Ni–Co decagonal phase. *J. Alloys Comp.* **342** (2002) 30–34.
- Grushko, B.; Freiburg, C.; Bickmann, K.; Wittenberg, R.: Discussion of the Al–Co phase diagram. *Z. Metallkd.* **88** (1997) 379–381.
- Grushko, B.; Gwozdz, J.; Yurechko, M.: Investigation of the Al–Cu–Rh phase diagram in the vicinity of the decagonal phase. *J. Alloys Comp.* **305** (2000) 219–224.
- Grushko, B.; Holland-Moritz, D.: High-Ni Al–Ni–Co decagonal phase. *Scr. Mater.* **35** (1996b) 1141–1146.
- Grushko, B.; Holland-Moritz, D.: Decagonal quasicrystals in Al–Co, Al–Ni and in their ternary alloys. *Mater. Sci. Eng. A226* (1997) 999–1003.
- Grushko, B.; Holland-Moritz, D.; Bickmann, K.: Decagonal quasicrystals in Al–Co and ternary alloys containing Cu and Ni. *J. Alloys Comp.* **236** (1996a) 243–252.
- Grushko, B.; Holland-Moritz, D.; Wittmann, R.: Transition between periodic and quasiperiodic structures in Al₇₁Ni_{14.5}Co_{14.5}. In: *Proceedings of the International Conference on Aperiodic Crystals APERIODIC 97*. Singapore – World Scientific (1998) p. 569–574.
- Grushko, B.; Holland-Moritz, D.; Wittmann, R.; Wilde, G.: Transition between periodic and quasiperiodic structures in Al–Ni–Co. *J. Alloys Comp.* **280** (1998) 215–230.
- Grushko, B.; Lemmerz, U.; Fischer, K.; Freiburg, C.: The low-temperature instability of the decagonal phase in Al–Ni–Fe. *Phys. Stat. Solidi A155* (1996) 17–30.
- Grushko, B.; Mi, S.: Stable Al–Ni–Rh decagonal phase. *Z. Kristallogr.* **218** (2003) 389–391.
- Grushko, B.; Urban, K.: Solidification of Al₆₅Cu₂₀Co₁₅ and Al₆₅Cu₁₅Co₂₀ Alloys. *J. Mater. Res.* **6** (1991) 2629–2636.
- Grushko, B.; Urban, K.: A Comparative-Study of Decagonal quasicrystalline Phases. *Philos. Mag.* **B70** (1994) 1063–1075.
- Grushko, B.; Wittenberg, R.; Bickmann, K.; Freiburg, C.: The constitution of aluminum-cobalt alloys between Al₅Co₂ and Al₉Co₂. *J. Alloys Comp.* **233** (1996) 279–287.
- Grushko, B.; Wittmann, R.; Urban, K.: On the Solidification of Al₆₂Cu₂₀Co₁₅Si₃ and Al₆₁Cu_{19.5}Co_{14.5}Si₅ Alloys. *J. Mater. Res.* **7** (1992) 2713–2723.
- Grushko, B.; Wittmann, R.; Urban, K.: Investigation of the Al–Cu–Co Decagonal Phase with a Low Copper Content. *Philos. Mag. Lett.* **67** (1993) 25–33.
- Grushko, B.; Wittmann, R.; Urban, K.: Structural Variations and Transformation Behavior of the Al₆₈Cu₁₁Co₂₁ Decagonal Phase. *J. Mater. Res.* **9** (1994) 2899–2906.
- Gummelt, P.: Penrose tilings as coverings of congruent decagons. *Geom. Dedic.* **62** (1996) 1–17.
- Guo, J. Q.; Abe, E.; Tsai, A. P.: Stable icosahedral quasicrystals in binary Cd–Ca and Cd–Yb systems. *Phys. Rev.* **B62** (2000b) R14605–R14608.
- Haerle, R.; Kramer, P.: Copper tubules and local origin of a pseudogap in d-AlCuCo from *ab initio* calculations. *Phys. Rev.* **B58** (1998) 716–720.
- Haibach, T.; Cervellino, A.; Estermann, M. A.; Steurer, W.: The decagonal superstructure Al₇₁Co₁₃Ni₃₆ and its relation to the basic decagonal phase Al₇₁Co₇Ni₂₂. *Phil. Mag.* **A42** (1999), 933–42.
- Haibach, T.; Cervellino, A.; Estermann, M. A.; Steurer, W.: X-ray structure determination of quasicrystals – limits and potentiality. *Z. Kristallogr.* **215** (2000) 569–583.
- Haibach, T.; Kek, S.; Honal, M.; Edler, F.; Mahne, S.; Steurer, W.: High-resolution synchrotron measurement of decagonal Al₇₅Os₁₀Pd₁₅ optimised for atomic surface determination. *HASYLAB Annual report I* (1996) 668–669.
- Haibach, T.; Steurer, W.: Five-dimensional Symmetry Minimum Function and Maximum Entropy Method for *ab initio* Solution of decagonal Structures. *Acta Crystallogr.* **A52** (1996) 277–286.
- Hardy, H. K.; Silcock, J. M.: The phase sections at 500 °C and 350 °C of aluminium-rich aluminium-copper-lithium alloys. *J. Inst. Met.* **84** (1956) 423–428.
- Hasegawa, M.; Tsai, A. P.; Yagi, T.: Stability and strain of decagonal Al–Ni–Co quasicrystal under high pressure up to 70 GPa. *Phil. Mag. Lett.* **79** (1999) 691–698.
- Häussler, D.; Nissen, H. U.; Lück, R.: Dodecagonal Tilings Derived as Duals from Quasi-Periodic Ammann-Grids. *Phys. Status Solidi A146* (1994) 425–435.

- He, L. X.; Li, X. Z.; Zhang, Z.; Kuo, K. H.: One-Dimensional Quasi-crystal in Rapidly Solidified Alloys. *Phys. Rev. Lett.* **61** (1988) 1116–1118.
- He, L. X.; Lograsso, T.; Goldman, A. I.: Twinned One-Dimensional Quasi-Crystals in Bridgman-Grown Al–Si–Cu–Co Alloys. *Phys. Rev. B* **46** (1992) 115–119.
- He, L. X.; Wu, Y. K.; Kuo, K. H.: Decagonal quasicrystals with different periodicities along the tenfold axis in rapidly solidified $\text{Al}_{65}\text{Cu}_{20}\text{M}_{15}$ (M=Mn, Fe, Co or Ni). *J. Mater. Sci. Lett.* **7** (1988) 1284–1286.
- He, A. Q.; Yang, Q. B.; Ye, H. Q.: The Fe–Nb Decagonal Phase and Its Structure Model. *Phil. Mag. Lett.* **61** (1990) 69–75.
- He, L. X.; Zhang, Z.; Wu, Y. K.; Kuo, K. H.: Stable decagonal quasicrystals with different periodicities along the tenfold axis in $\text{Al}_{65}\text{Cu}_{20}\text{Co}_{15}$. *Inst. Phys. Conf. Ser. No. 93: Vol. 2, Chapter 13, Conf. EUREM* (1988) 501–502.
- Henley, C. L.: Sphere Packings and Local Environments in Penrose Tilings. *Phys. Rev. B* **34** (1986) 797–816.
- Henley, C. L.: Current Models of Decagonal Atomic-Structure. *J. Non-Cryst. Solids* **153** (1993) 172–176.
- Henley, C. L.; Elser, V.; Mihalkovic, M.: Structure determinations for random-tiling quasicrystals. *Z. Kristallogr.* **215** (2000) 553–568.
- Henley, C. L.; Mihalkovic, M.; Widom, M.: Total-energy-based structure prediction for d(AlNiCo). *J. Alloys. Comp.* **342** (2002) 221–227.
- Hiraga, K.: The structure of quasicrystals studied by atomic-scale observations of transmission electron microscopy. *Adv. Imag. Electron Phys.* **122** (2002) 1–86.
- Hiraga, K.; Abe, E.; Matsuo, Y.: The Structure of an Al–Pd Decagonal Quasicrystal Studied by High-Resolution Electron Microscopy. *Philos. Mag. Lett.* **70** (1994) 163–168.
- Hiraga, K.; Hirabayashi, M.; Inoue, A.; Masumoto, T.: High-resolution electron microscopy of Al–Mn–Si icosahedral and Al–Mn decagonal quasicrystals. *J. Microscopy* **146** (1987) 245–260.
- Hiraga, K.; Kaneko, M.; Matsuo, Y.; Hashimoto, S.: The Structure of Al_3Mn – Close Relationship to Decagonal Quasi-Crystals. *Philos. Mag.* **B67** (1993) 193–205.
- Hiraga, K.; Lincoln, F. J.; Sun, W.: Structure and Structural-Change of Al–Ni–Co Decagonal Quasi-Crystal by High-Resolution Electron-Microscopy. *Mater. Trans. JIM* **32** (1991) 308–314.
- Hiraga, K.; Ohsuna, T.: The structure of an Al–Ni–Co decagonal quasicrystal studied by atomic-scale electron microscopic observations. *Mater. Trans. JIM* **42** (2001a) 509–513.
- Hiraga, K.; Ohsuna, T.: The structure of an Al–Ni–Fe decagonal quasicrystal studied by high-angle annular detector dark-field scanning transmission electron microscopy. *Mater. Trans. JIM* **42** (2001b) 894–896.
- Hiraga, K.; Ohsuna, T.; Nishimura, S.: An ordered arrangement of atom columnar clusters in a pentagonal quasiperiodic lattice of an Al–Ni–Co decagonal quasicrystal. *Philos. Mag. Lett.* **80** (2000) 653–659.
- Hiraga, K.; Ohsuna, T.; Nishimura, S.: The structure of an Al–Ni–Co pentagonal quasicrystal studied by high-angle annular detector dark-field electron microscopy. *Philos. Mag. Lett.* **81** (2001a) 123–127.
- Hiraga, K.; Ohsuna, T.; Nishimura, S.: A new crystalline phase related to an Al–Ni–Co decagonal phase. *J. Alloys Comp.* **325** (2001b) 145–150.
- Hiraga, K.; Ohsuna, T.; Nishimura, S.: The structure of type-II Al–Ni–Co decagonal quasicrystal studied by atomic-scale electron microscopic observations. *Mater. Trans. JIM* **42** (2001c) 1081–1084.
- Hiraga, K.; Ohsuna, T.; Park, K. T.: A large columnar cluster of atoms in an Al–Cu–Rh decagonal quasicrystal studied by atomic-scale electron microscopy observations. *Philos. Mag. Lett.* **81** (2001) 117–122.
- Hiraga, K.; Ohsuna, T.; Yubuta, K.; Nishimura, S.: The structure of an Al–Co–Ni crystalline approximant with an ordered arrangement of atomic clusters with pentagonal symmetry. *Mater. Trans. JIM* **42** (2001) 897–900.
- Hiraga, K.; Sun, W.: The Atomic Arrangement of an Al–Pd–Mn Decagonal Quasicrystal Studied by High-Resolution Electron Microscopy. *Philos. Mag. Lett.* **67** (1993a) 117–123.
- Hiraga, K.; Sun, W.: Tiling in Al–Pd–Mn Decagonal Quasi-Crystal, Studied by High-Resolution Electron-Microscopy. *J. Phys. Soc. Jpn.* **62** (1993b) 1833–1836.
- Hiraga, K.; Sun, W.; Lincoln, F. J.: Structural-Change of Al–Cu–Co Decagonal Quasi-Crystal Studied by High-Resolution Electron-Microscopy. *Jpn. J. Appl. Phys.* **30** (1991) L302–L305.
- Hiraga, K.; Sun, W.; Lincoln, F. J.; Kaneko, M.; Matsuo, Y.: Formation of Decagonal Quasi-Crystal in the Al–Pd–Mn System and Its Structure. *Jpn. J. Appl. Phys.* **30** (1991) 2028–2034.
- Hiraga, K.; Sun, W.; Ohsuna, T.: Structure of a pentagonal quasicrystal in $\text{Al}_{72.5}\text{Co}_{17.5}\text{Ni}_{10}$ studied by high-angle annular detector dark-field scanning transmission electron microscopy. *Mater. Trans. JIM* **42** (2001) 1146–1148.
- Hiraga, K.; Sun, W.; Yamamoto, A.: Structures of Two Types of Al–Ni–Co Decagonal Quasi-Crystals Studied by High-Resolution Electron-Microscopy. *Mater. Trans. JIM* **35** (1994) 657–662.
- Hiraga, K.; Yubuta, K.; Park, K. T.: High-resolution electron microscopy of Al–Ni–Fe decagonal quasicrystal. *J. Mater. Res.* **11** (1996) 1702–1705.
- Honal, M.; Haibach, T.; Steurer, W.: Mechanism of the phase transformation of decagonal Al–Co–Ni to its periodic approximant. *Acta Crystallogr. A* **54** (1998) 374–87.
- Honal, M.; Welberry, T. R.: Monte Carlo study of the quasicrystal-to-crystal transformation using an approach based on the Gummelt covering. *Z. Kristallogr.* **217** (2002) 109–118.
- Huang, Z.; Hovmöller, S.: An Octagonal Quasi-Crystal Structure Model with 8_3 Screw Axes. *Phil. Mag. Lett.* **64** (1991) 83–88.
- Hudd, R. C.; Taylor, W. H.: Structure of Co_4Al_3 . *Acta Crystallogr.* **15** (1962) 441–442.
- Ingalls, R.: Octagonal Quasi-Crystal Tilings. *J. Non-Cryst. Solids* **153** (1993) 177–180.
- Ingalls, R.: Decagonal Quasi-Crystal Tilings. *Acta Crystallogr. A* **48** (1992) 533–541.
- Ishimasa, T.; Nissen, H. U.; Fukano, Y.: New Ordered State between Crystalline and Amorphous in Ni–Cr Particles. *Phys. Rev. Lett.* **55** (1985) 511–513.
- Janner, A.: Decagrammatic Symmetry of Decagonal $\text{Al}_{78}\text{Mn}_{22}$ Quasi-Crystal. *Acta Crystallogr. A* **48** (1992) 884–901.
- Janssen, T.: Aperiodic Crystals. A Contradictio in Terminis. *Phys. Rep.* **168** (1988) 55–113.
- Jiang, J. C.; Hovmöller, S.; Zou, X. D.: A 3-Dimensional Structure Model of 8-Fold Quasicrystals Obtained by High-Resolution Electron Microscopy. *Phil. Mag. Lett.* **71** (1995) 123–129.
- Joseph, D.; Ritsch, S.; Beeli, C.: Distinguishing quasiperiodic from random order in high-resolution TEM images. *Phys. Rev. B* **55** (1997) 8175–8183.
- Kalning, M.; Kek, S.; Burandt, B.; Press, W.; Steurer, W.: An Examination of a Multiple-Twinned Periodic Approximant of the Decagonal Phase $\text{Al}_{70}\text{Co}_{15}\text{Ni}_{15}$. *J. Phys.: Condens. Matter* **6** (1994) 6177–6187.
- Kalning, M.; Press, W.; Kek, S.: Investigation of a decagonal $\text{Al}_{70}\text{Co}_{15}\text{Ni}_{15}$ single crystal by means of high-resolution synchrotron X-ray diffraction. *Philos. Mag. Lett.* **71** (1995) 341–349.
- Kalning, M.; Kek, S.; Krane, H. G.; Dorna, V.; Press, W.; Steurer, W.: Phason-strain analysis of the twinned approximant to the decagonal quasicrystal $\text{Al}_{70}\text{Co}_{15}\text{Ni}_{15}$: Evidence for a one-dimensional quasicrystal. *Phys. Rev. B* **55** (1997) 187–192.
- Khaidar, M.; Allibert, C. H.; Driole, J.: Phase equilibria of the Fe–Ni–Al system for Al content above 50 at% and crystal structures of some ternary phases. *Z. Metallkde.* **73** (1982) 433–438.
- Kim, D. H.; & Cantor, B.: Quasicrystalline and related phases in rapidly solidified Al–Fe alloys. *Philos. Mag. A* **69** (1994) 45–55.
- Kimura, H. M.; Inoue, A.; Bizen, Y.; Masumoto, T.; Chen, H. S.: New Quasi-Crystalline and Amorphous Phases in Rapidly Quenched Al–Ge–(Cr, Mn) and Al–Si–(Cr, Mn) Alloys With High Metalloid Concentrations. *Mater. Sci. Eng.* **99** (1988) 449–452.
- Kishida, M.; Kamimura, Y.; Tamura, R.; Edagawa, K.; Takeuchi, S.; Sato, T.; Yokoyama, Y.; Guo, J. Q.; Tsai, A. P.: Scanning tunneling microscopy of an Al–Ni–Co decagonal quasicrystal. *Phys. Rev. B* **65** (2002) art. no.-094208.
- Kloess, G.; Schetelich, C.; Wittmann, R.; Geist, V.: Mass Density and Perfection of Decagonal Quasicrystals with Nominal Composition $\text{Al}_{62}\text{Cu}_{20}\text{Co}_{15}\text{Si}_3$. *Phys. Stat. Sol. A* **144** (1994) K5–K9.

- Kontio, A.; Coppens, P.: New study of the structure of Al_6Mn . *Acta Crystallogr.* **B37** (1981) 433–435.
- Kontio, A.; Stevens, E.D.; Coppens, P.: New investigation of the structure of $\text{Mn}_4\text{Al}_{11}$. *Acta Crystallogr.* **B36** (1980) 435–436.
- Kortan, A. R.; Becker, R. S.; Thiel, F. A.; Chen, H. S.: Real-Space Atomic Structure of a Two-Dimensional Decagonal Quasicrystal. *Phys. Rev. Lett.* **64** (1990) 200–203.
- Koshikawa, N.; Edagawa, K.; Honda, Y.; Takeuchi, S.: Formation of three types of quasicrystal in the Al–Pd–Mg System. *Philos. Mag. Lett.* **68** (1993) 123–129.
- Koshikawa, N.; Edagawa, K.; Takeuchi, S.: Icosahedral and Decagonal Quasi-Crystals in the Al–Pd–Mg System. *Mater. Sci. Eng.* **A182** (1994) 811–814.
- Krajci, M.; Hafner, J.; Mihalkovic, M.: Atomic and electronic structure of decagonal Al–Pd–Mn alloys and approximant phases. *Phys. Rev.* **B55** (1997a) 843–855.
- Krajci, M.; Hafner, J.; Mihalkovic, M.: Electronic structure and transport properties of decagonal Al–Cu–Co alloys. *Phys. Rev.* **B56** (1997b) 3072–3085.
- Krajci, M.; Hafner, J.; Mihalkovic, M.: Atomic and electronic structure of decagonal Al–Ni–Co alloys and approximant phases. *Phys. Rev.* **B62** (2000) 243–255.
- Kramer, P.; Papadopolos, Z. (eds.): *Coverings of Discrete Quasiperiodic Sets*, Springer Tracts in Modern Physics 180, Springer-Verlag Berlin 2003.
- Krauss, G.; Miletich, R.; Steurer, W.: Reciprocal space imaging and the use of a diamond anvil cell – the first single-crystal high-pressure study of a quasicrystal up to 10.7 GPa. *Philos. Mag. Lett.* **83** (2003) 525–531.
- Kreiner, G.; Franzen, H. F.: The crystal structure of $\lambda\text{-Al}_4\text{Mn}$. *J. Alloys Comp.* **261** (1997) 83–104.
- Krumeich, F.; Conrad, M.; Harbrecht, B.: TEM Study of dodecagonal tantalum telluride and two tetragonal approximants. *Proc. 13th Int. Congr. Electron Microscopy. ICEM 1994* **2A** (1994) 751–752. Les Editions de Physique: Paris.
- Krumeich, F.; Conrad, M.; Nissen, H. U.; Harbrecht, B.: The mesoscopic structure of disordered dodecagonal tantalum telluride: a high-resolution transmission electron microscopy study. *Phil. Mag. Lett.* **78** (1998) 357–367.
- Krumeich, F.; Reich, C.; Conrad, M.; Harbrecht, B.: Periodic and aperiodic arrangements of dodecagonal $(\text{Ta,V})_{151}\text{Te}_{74}$ clusters studied by transmission electron microscopy. The methods merits and limitations. *Mater. Sci. Eng.* **A294–296** (2000) 152–155.
- Kuhn, T.: *The Structure of Scientific Revolutions*. University of Chicago Press, 1962.
- Kumar, V.; Sahoo, D.; Athithan, G.: Characterization and Decoration of the Two-Dimensional Penrose Lattice. *Phys. Rev.* **B34** (1986) 6924–6932.
- Kuo, K. H.: Some New Icosahedral and Decagonal Quasicrystals. *Mater. Sci. Forum* **22–24** (1987) 131–140.
- Kuo, K. H.: Decagonal Approximants. *J. Non-Cryst. Solids* **153** (1993) 40–44.
- Kuo, K. H.; Feng, Y. C.; Chen, H.: Growth-Model of Dodecagonal Quasicrystal Based on Correlated Tiling of Squares and Equilateral Triangles. *Phys. Rev. Lett.* **61** (1988) 1740–1743.
- Kuo, K. H.; Zhou, D. S.; Li, D. X.: Quasi-Crystalline and Frank-Kasper Phases in a Rapidly Solidified $\text{V}_{41}\text{Ni}_{36}\text{Si}_{23}$ Alloy. *Philos. Mag. Lett.* **55** (1987) 33–39.
- Kupsch, A.; Meyer, D. C.; Gille, P.; Paufler, P.: Evidence of phase transition in decagonal Al–Co–Ni at low temperatures. *J. Alloys Comp.* **336** (2002) 154–158.
- Launois, P.; Audier, M.; Denoyer, F.; Dong, C.; Dubois, J. M.; Lambert, M.: Decagonal Phases: Non-Quasi-Crystalline Microcrystalline State in an Al–Cu–Co–Si Alloy. *Europhys. Lett.* **13** (1990) 629–634.
- Lei, J. L.; Hu, C. Z.; Wang, R. H.; Ding, D. H.: Diffuse scattering from octagonal quasicrystals. *J. Phys.: Condens. Matter* **11** (1999) 1211–1223.
- Lei, J. L.; Wang, R. H.; Hu, C. Z.; Ding, D. H.: Diffuse scattering from dodecagonal quasicrystals. *Eur. Phys. J.* **B13** (2000) 21–30.
- Lemmerz, U.; Grushko, B.; Freiburg, C.; Jansen, M.: Study of decagonal phase formation in the Al–Ni–Fe alloy system. *Phil. Mag. Lett.* **69** (1994) 141–146.
- Letoublon, A.; Yakhou, F.; Livet, F.; Bley, F.; de Boissieu, M.; Mancini, L.; Caudron, R.; Vettier, C.; Gastaldi, J.: Coherent X-ray diffraction and phason fluctuations in quasicrystals. *Europhys. Lett.* **54** (2001) 753–759.
- Li, X. Z.: Structure of Al–Mn Decagonal Quasi-Crystal. 1. A Unit-Cell Approach. *Acta Crystallogr.* **B51** (1995) 265–270.
- Li, F. H.; Cheng, Y. F.: Relationship between octagonal quasicrystal and $\beta\text{-Mn}$ type crystal in cut description. *Chin. Phys. Lett.* **13** (1996) 199–202.
- Li, X. Z.; Dubois, J. M.: Structural Sub-Units of the Al–Mn–Pd Decagonal Quasicrystal Derived From the Structure of the T3 Al–Mn–Zn-Phase. *J. Phys. Condens. Matter* **6** (1994) 1653–1662.
- Li, X. Z.; Frey, F.: Structure of Al–Mn Decagonal Quasi-Crystal. 2. A High-Dimensional Description. *Acta Crystallogr.* **B51** (1995) 271–275.
- Li, X. Z.; Frey, F.; Kuo, K. H.: Aperiodic Tilings Related to the Al–Mn–Pd Decagonal Quasi-Crystal. *Philos. Mag. Lett.* **71** (1995) 237–242.
- Li, X. Z.; Hiraga, K.: Structure of the Al–Rh–Cu decagonal quasicrystal: II. A higher-dimensional description. *Physica* **B240** (1997) 338–342.
- Li, X. Z.; Hiraga, K.: High-resolution electron microscopy of the $\epsilon\text{-Al}_3\text{Co}$, a monoclinic approximant of the Al–Co decagonal quasicrystal. *J. Alloys Comp.* **269** (1998) L13–L16.
- Li, X. Z.; Hiraga, K.; Yubuta, K.: Structure of the Al–Rh–Cu decagonal quasicrystal studied by high-resolution electron microscopy. *Phil. Mag. Lett.* **74** (1996) 247–252.
- Li, X. Z.; Hiraga, K.; Yubuta, K.: Structure of the Al–Rh–Cu decagonal quasicrystal: I. A unit-cell approach. *Physica* **B240** (1997) 330–337.
- Li, H. L.; Kuo, K. H.: Some New Crystalline Approximants of Al–Pd–Mn Quasi-Crystals. *Philos. Mag. Lett.* **70** (1994) 55–62.
- Li, X. Z.; Kuo, K. H.: Decagonal Quasicrystals with Different Periodicities Along the Tenfold Axis in Rapidly Solidified Al–Ni Alloys. *Philos. Mag. Lett.* **58** (1988) 167–171.
- Li, X. Z.; Kuo, K. H.: The Structural Model of Al–Mn Decagonal Quasi-Crystal Based on a New Al–Mn Approximant. *Philos. Mag.* **B65** (1992) 525–533.
- Li, X. Z.; Li, H. L.; Frey, F.; Steurer, W.; Kuo, K. H.: Structural models of high-order approximants of the Al–Mn–Pd decagonal quasicrystal. *Philosophical Magazine* **B71** (1995) 1101–1110.
- Li, X. Z.; Ma, X. L.; Kuo, K. H.: A Structural Model of the Orthorhombic Al_3Co Derived from the Monoclinic $\text{Al}_{13}\text{Co}_4$ by High-Resolution Electron-Microscopy. *Philos. Mag. Lett.* **70** (1994) 221–229.
- Li, X. Z.; Park, K. T.; Sugiyama, K.; Hiraga, K.: F-type icosahedral phase and a related cubic phase in the Al–Rh–Cu system. *Metall. Trans.* **A29** (1998) 1559–1563.
- Li, X. Z.; Shi, N. C.; Ma, Z. S.; Ma, X. L.; Kuo, K. H.: Structure of $\text{Al}_{11}\text{Co}_4$, a new monoclinic approximant of the Al–Co decagonal quasicrystal. *Philos. Mag. Lett.* **72** (1995) 79–86.
- Li, X. Z.; Steurer, W.; Frey, F.: Structural model of the Al–Pd decagonal quasicrystal. *Philos. Mag.* **A74** (1996) 299–305.
- Li, X. Z.; Steurer, W.; Haibach, T.; Zhang, B.; Frey, F.: Color quasilattice in decagonal $\text{Al}_{65}\text{Cu}_{20}\text{Co}_{15}$ phase. *Z. Kristallogr.* **210** (1995) 509–512.
- Lord, E. A.: Indexing schemes for quasilattices. *Philos. Mag.* **83** (2003) 3283–3307.
- Lu, X. S.; Li, F. H.: The crystal structure of $(\text{Ni},\text{Co})_3\text{Al}_4$ – a new vacancy controlled phase. *Acta Physica Sinica* **29** (1980) 182–198.
- Lück, R.; Scheffer, M.; Gödecke, T.; Ritsch, S.; Beeli, C.: Phase diagram determination for modifications of the d-phase in the Al–AlCo–AlNi system. *Mater. Res. Soc. Symp. Proc.* Vol. **553** (1999) 25–36.
- Luo, Z.; Zhang, S.; Tang, Y.; Zhao, D.: Quasicrystals in as-cast Mg–Zn–RE alloys. *Scr. Met. Mater.* **28** (1993) 1513–1518.
- Ma, X. L.; Kuo, K. H.: Decagonal Quasi-Crystal and Related Crystalline Phases in Slowly Solidified Al–Co Alloys. *Metall. Trans.* **A23** (1992) 1121–1128.
- Ma, L.; Kuo, K. H.; Wang, R.: Quasicrystals in Rapidly Solidified Alloys of Al–Pt Group Metals – IV. Quasicrystals in Rapidly Solidified Al–Pd and Al–Pt Alloys. *J. Less-Common Met.* **163** (1990) 37–49.
- Ma, X. L.; Li, X. Z.; Kuo, K. H.: A Family of τ -Inflated Monoclinic $\text{Al}_{13}\text{Co}_4$ Phases. *Acta Crystallogr.* **B51** (1995) 36–43.

- Ma, L.; Wang, R.; Kuo, K. H.: Decagonal Quasicrystals and Related Crystalline Phases in Rapidly Solidified Al-Ir, Al-Pd and Al-Pt. *Scr. Metall.* **22** (1988) 1791–1796.
- Ma, Y.; Stern, E. A.: Fe and Mn sites in noncrystallographic alloy phases of Al–Mn–Fe and Al–Mn–Fe–Si. *Phys. Rev.* **B35** (1987) 2678–2681.
- Mai, Z. H. I.; Xu, L.; Wang, N.; Kuo, K. H.; Jin, Z. C.; Cheng, G.: Effect of Phason Strain on the Transition of an Octagonal Quasicrystal to a β -Mn-Type Structure. *Phys. Rev.* **B40** (1989) 12183–12186.
- Mandal, P.; Hashimoto, T.; Suzuki, K.; Hosono, K.; Kamimura, Y.; Edagawa, K.: Formation of decagonal and approximant phases in the Al–Ni–Ru system. *Philos. Mag. Lett.* **83** (2003) 315–323.
- Martin, T. P.: Shells of atoms. *Phys. Rep.* **273** (1996) 199–241.
- Matsuo, Y.; Hiraga, K.: The Structure of Al_3Pd – Close Relationship to Decagonal Quasi-Crystals. *Philos. Mag. Lett.* **70** (1994) 155–161.
- Matsuo, Y.; Kaneko, M.; Yamanoi, T.; Kaji, N.; Sugiyama, K.; Hiraga, K.: The structure of an Al_3Mn -type $\text{Al}_3(\text{Mn}, \text{Pd})$ crystal studied by single-crystal X-ray diffraction analysis. *Philos. Mag. Lett.* **76** (1997) 357–362.
- McGrath, R.; Ledieu, J.; Cox, E. J.; Diehl, R. D.: Quasicrystal surfaces: structure and potential as templates. *J. Phys.: Condens. Matter* **14** (2002) R119–R144.
- McRae, E. G.; Malic, R. A.; Lalonde, T. H.; Thiel, F. A.; Chen, H. S.; Kortan, A. R.: Observation of Quasicrystal Surface Order and Disorder by Low-Energy Electron Diffraction. *Phys. Rev. Lett.* **65** (1990) 883–886.
- Menon, J.; Suryanarayana, C.; Singh, G.: Polytypism in a Decagonal Quasicrystalline Al–Co Phase. *J. Crystallography* **22** (1989) 96–99.
- Mi, S.; Grushko, B.; Dong, C.; Urban, K.: Ternary Al–Ni–Ru phases. *J. Alloys Comp.* **351** (2003a) L1–L5.
- Mi, S.; Grushko, B.; Dong, C.; Urban, K.: Isothermal sections of the Al-rich part of the Al–Ni–Ru phase diagram. *J. Alloys Comp.* **359** (2003b) 193–197.
- Mihalkovic, M.; Al-Lehyani, I.; Cockayne, E.; Henley, C. L.; Moghadam, N.; Moriarty, J. A.; Wang, Y.; Widom, M.: Total-energy-based prediction of a quasicrystal structure. *Phys. Rev.* **B65** (2002) art. no.-104205.
- Mihalkovic, M.; Elhor, H.; Suck, J. B.: Atomic dynamics in Al-rich Al–Co alloys near the composition of the decagonal quasicrystal. *Phys. Rev.* **B63** (2001) art. no. 214301.
- Mihalkovic, M.; Mrafko, P.: Quasicrystal structure modelling. *Mater. Sci. Eng.* **A226** (1997) 961–966.
- Mo, Z. M.; Sui, H. X.; Ma, X. L.; Kuo, K. H.: Structural models of τ^2 -inflated monoclinic and orthorhombic Al–Co phases. *Metall. Mater. Trans.* **A29** (1998) 1565–1572.
- Mukhopadhyay, Lord, E. A.: Least path criterion (LPC) for unique indexing in a two-dimensional decagonal quasilattice. *Acta Crystallogr.* **A58** (2002) 424–428.
- Mukhopadhyay, N. K.; Murthy, G. V. S.; Murty, B. S.; Weatherly, G. C.: Transformation of the decagonal quasicrystalline phase to a B2 crystalline phase in the Al–Cu–Co system by high-energy ball milling. *Philos. Mag. Lett.* **82** (2002) 383–392.
- Niizeki, K.: A classification of the space groups of approximant lattices to a decagonal quasilattice. *J. Phys. A* **24** (1991) 3641–3654.
- Niizeki, K.: Model Quasi-Lattice for Al–Mn Decagonal Quasi-Crystal. *Mater. Trans. JIM* **34** (1993) 109–115.
- Niizeki, K.: The diffraction pattern of a non-Bravais-type quasicrystal with application to a decagonal quasicrystal. *J. Phys. Soc. Jpn.* **63** (1994) 4035–4043.
- Nüchter, W.; Sigle, W.: The Structure of Decagonal Al–Cu–Co–Si: an Electron Channeling Study. *Philos. Mag. Lett.* **70** (1994) 103–109.
- Ohsuna, T.; Sun, W.; Hiraga, K.: Decagonal quasicrystal with ordered body-centred (CsCl-type) hypercubic lattice. *Philos. Mag. Lett.* **80** (2000) 577–583.
- Okabe, T.; Furihata, J. I.; Morishita, K.; Fujimori, H.: Decagonal Phase and Pseudo-Decagonal Phase in the Al–Cu–Cr System. *Phil. Mag. Lett.* **66** (1992) 259–264.
- Padezhnova, E. M.; Melnik, E. V.; Miliyevskiy, R. A.; Dobatkina, T. V.; Kinzhbalo, V. V.: Investigation of the Zn–Mg–Y system. *Russ. Metall. (Engl. Transl.)* **3** (1982) 185–188.
- Palenzona, A.: The Ytterbium-Cadmium system. *J. Less-Common Met.* **25** (1971) 367–372.
- Pavlovitch, A.; Kleman, M.: Generalised 2d Penrose Tilings. *Structural Properties. J. Phys.; A (London). Math. Gen.* **20** (1987) 687–702.
- Pavlyuk, V. V.; Yanson, T. I.; Bodak, O. I.; Cerny, R.; Gladyshevskii, R. E.; Yvon, K.: Structure Refinement of Orthorhombic MnAl_3 . *Acta Crystallogr.* **C51** (1995) 792–794.
- Pennycook, S. J.: Structure determination through Z-contrast microscopy. *Adv. Imag. Elect. Phys.* **123** (2002) 173–206.
- Pérez-Ramirez, J. G.; Pérez, R.; Gomez, A.; Cota-Araiza, L.; Martinez, L.; Herrera, R.; José-Yacaman, M.: An Investigation of the $\text{Al}_{86}\text{Mn}_{14}$ Alloy and Its Quasicrystalline Phases. *J. Mater. Res.* **2** (1987) 153–162.
- Phillips, R.; Widom, M.: Total Energies of Decagonal Models for Quasi-Crystals. *J. Non-Cryst. Solids* **153** (1993) 416–419.
- Pohla, C.; Ryder, P. L.: Crystalline and quasicrystalline phases in rapidly solidified Al–Ni alloys. *Acta Mater.* **45** (1997) 2155–2166.
- Qin, Y. L.; Wang, R. H.; Wang, Q. L.; Zhang, Y. M.; Pan, C. X.: Ar⁺-Ion-Irradiation-Induced Phase Transformations in an $\text{Al}_{70}\text{Co}_{15}\text{Ni}_{15}$ Decagonal Quasicrystal. *Philos. Mag. Lett.* **71** (1995) 83–90.
- Rabson, D. A.; Mermin, N. D.; Rokhsar, D. S.; Wright, D. C.: The Space-Groups of Axial Crystals and Quasi-Crystals. *Reviews of Modern Physics* **63** (1991) 699–733.
- Raghavan, V.: Phase Diagrams of Quaternary Iron Alloys, The Indian Institute of Metals: Calcutta 1996.
- Ranganathan, S.; Chattopadhyay, K.; Singh, A.; Kelton, K. F.: Decagonal quasicrystals. *Prog. Mater. Sci.* **41** (1997) 195–240.
- Ranganathan, S.; Subramaniam, A.; Ramakrishnan, K.: Rational approximant structures to decagonal quasicrystals. *Mater. Sci. Eng.* **A304–306** (2001) 888–891.
- Reich, C.; Conrad, M.; Krumeich, F.; Harbrecht, B.: The dodecagonal quasicrystalline telluride $(\text{Ta,V})_{16}\text{Te}$ and its crystalline approximant $(\text{Ta,V})_{97}\text{Te}_{60}$. *MRS Proceedings* **553** (1999) 83–94.
- Reyes-Gasca, J.; Garcia, R.; Jose-Yacaman, M.: Electron-Beam-Induced Structure Transformation of the Quasicrystalline Phases of the $\text{Al}_{62}\text{Cu}_{20}\text{Co}_{15}\text{Si}_3$ Alloy. *Radiat. Phys. Chem.* **45** (1995) 283–291.
- Reyes-Gasca, J.; Lara, A.; Riveros, H.; Jose-Yacaman, M.: Characterization of the Decagonal Quasi-Crystalline Phase of the $\text{Al}_{62}\text{Co}_{20}\text{Cu}_{15}\text{Si}_3$ Alloy by TEM. *Mater. Sci. Eng.* **A150** (1992) 87–99.
- Ritsch, S.; Beeli, C.; Lück, R.; Hiraga, K.: Pentagonal Al–Co–Ni quasicrystal with a superstructure. *Philos. Mag. Lett.* **79** (1999) 225–232.
- Ritsch, S.; Beeli, C.; Nissen, H. U.: One-dimensionally periodic five-fold Al–Co–Ni quasicrystals. *Philos. Mag. Lett.* **74** (1996) 203–209.
- Ritsch, S.; Beeli, C.; Nissen, H. U.; Godecke, T.; Scheffer, M.; Lück, R.: Highly-perfect decagonal Al–Co–Ni quasicrystals. *Philos. Mag. Lett.* **74** (1996) 99–106.
- Ritsch, S.; Beeli, C.; Nissen, H. U.; Godecke, T.; Scheffer, M.; Lück, R.: The existence regions of structural modifications in decagonal Al–Co–Ni. *Philos. Mag. Lett.* **78** (1998) 67–75.
- Ritsch, S.; Beeli, C.; Nissen, H. U.; Lück, R.: Two Different Superstructures of the Decagonal Al–Co–Ni Quasi-Crystal. *Philos. Mag.* **A71** (1995) 671–685.
- Ritsch, S.; Nissen, H. U.; Beeli, C.: Phason related stacking disorder in decagonal Al–Co–Ni. *Phys. Rev. Lett.* **76** (1996) 2507–2510.
- Ritsch, S.; Radulescu, O.; Beeli, C.; Warrington, D. H.; Lück, R.; Hiraga, K.: A stable one-dimensional quasicrystal related to decagonal Al–Co–Ni. *Philos. Mag. Lett.* **80** (2000) 107–118.
- Robinson, K.: The determination of the crystal structure of $\text{Ni}_4\text{Mn}_{11}\text{Al}_4$. *Acta Crystallogr.* **7** (1954) 494–497.
- Sabiryanov, R. F.; Bose, S. K.; Burkov, S. E.: Electronic structure and stability of a model of the decagonal quasicrystal Al–Cu–Co. *J. Phys.: Condens. Matter* **7** (1995) 5437–5459.
- Sadoc, A. L.; Dubois, J. M.: Structural Relationships Between Non-Crystalline Phases in AlMn and AlFeCr Systems Through EXAFS Measurements. *J. Phys. Condens. Matter* **1** (1989) 4283–4296.
- Saintfort, P.; Dubost, B.; Dubus, A.: “Quasi-Crystalline Precipitation From Solid Solutions of the Al–Li–Cu–Mg System. C. R. Seances Acad. Sci.; Ser. II, **301** (1985) 689–692.

- Saito, K.; Hiraga, K.: Local structures appearing in an intermediate state of transformation from Al–Pd decagonal to Al_3Pd crystalline phases. *J. Alloys Comp.* **342** (2002) 126–129.
- Saito, K.; Saito, Y.; Sugawara, S.; Guo, J. Q.; Tsai, A. P.; Kamimura, Y.; Edagawa, K.: Dissolution patterns caused by etching of low-indexed surfaces of Al–Pd–Mn icosahedral and Al–Cu–Co decagonal quasicrystals. *J. Alloys Comp.* **342** (2002) 45–48.
- Saito, M.; Tanaka, M.; Tsai, A. P.; Inoue, A.; Masumoto, T.: Space Group Determination of Decagonal Quasi-Crystals of an $\text{Al}_{70}\text{Ni}_{15}\text{Fe}_{15}$ Alloy Using Convergent-Beam Electron-Diffraction. *Jpn. J. Appl. Phys.* **31** (1992) L109–L112.
- Saitoh, K.; Tanaka, M.; Tsai, A. P.: Structural study of an $\text{Al}_{73}\text{Ni}_{22}\text{Fe}_5$ decagonal quasicrystal by high-angle annular dark-field scanning transmission electron microscopy. *J. Electron Microsc.* **50** (2001) 197–203.
- Saitoh, K.; Tanaka, M.; Tsai, A. P.; Rossouw, C. J.: ALCHEMI study of an $\text{Al}_{72}\text{Ni}_{20}\text{Co}_8$ decagonal quasicrystal. *J. Phys. Soc. Jpn.* **69** (2000) 2379–2382.
- Saitoh, K.; Tsuda, K.; Tanaka, M.: Structural models for decagonal quasicrystals with pentagonal atom-cluster columns. *Philos. Mag.* **A76** (1997) 135–150.
- Saitoh, K.; Tsuda, K.; Tanaka, M.: New structural model of an $\text{Al}_{72}\text{Ni}_{20}\text{Co}_8$ decagonal quasicrystal. *J. Phys. Soc. Jpn.* **67** (1998) 2578–2581.
- Saitoh, K.; Tsuda, K.; Tanaka, M.; Kaneko, K.; Tsai, A. P.: Structural study of an $\text{Al}_{72}\text{Ni}_{20}\text{Co}_8$ decagonal quasicrystal using the high-angle annular dark-field method. *Jpn. J. Appl. Phys.* **36** (1997) L1400–L1402.
- Saitoh, K.; Tsuda, K.; Tanaka, M.; Tsai, A. P.: Structural study of an $\text{Al}_{70}\text{Ni}_{15}\text{Fe}_{15}$ decagonal quasicrystal using high-angle annular dark-field scanning transmission electron microscopy. *Jpn. J. Appl. Phys.* **38** (1999) L671–L674.
- Saitoh, K.; Tsuda, K.; Tanaka, M.; Tsai, A. P.: Structural studies on decagonal quasicrystals using the HAADF-STEM and CBED methods. *Z. Kristallogr.* **215** (2000) 618–626.
- Saitoh, K.; Tsuda, K.; Tanaka, M.; Tsai, A. P.; Inoue, A.; Masumoto, T.: Convergent-Beam Electron-Diffraction and Electron-Microscope Study on Decagonal Quasi-Crystals of Al–Cu–Co and Al–Co Alloys. *Mater. Sci. Eng.* **A182** (1994) 805–810.
- Saitoh, K.; Tsuda, K.; Tanaka, M.; Tsai, A. P.; Inoue, A.; Masumoto, T.: Electron microscope study of the symmetry of the basic atom cluster and a structural change of decagonal quasicrystals of Al–Cu–Co alloys. *Philos. Mag.* **A73** (1996) 387–398.
- Saitoh, K.; Yokosawa, T.; Tanaka, M.; Tsai, A. P.: Structural studies of monoclinic approximants of $\text{Al}_{13}\text{Fe}_4$ and τ^2 -inflated $\text{Al}_{13}\text{Co}_4$ by the high-angle annular dark-field method. *J. Electron Microsc.* **48** (1999) 105–114.
- Sastry, G. V. S.; Bariar, K. K.; Chattopadhyay, K.; Ramachandrarao, P.: Vacancy Ordered Phases in Rapidly Solidified Aluminum-Copper Alloys. *Z. Metallkd.* **71** (1980) 756–759.
- Sastry, G. V. S.; Suryanarayana, C.: A Comparison of the Decagonal Phase in Rapidly Solidified Al–Mn and Al–Pd Alloys. *Scr. Metall.* **20** (1986) 1359–1360.
- Sato, T. J.; Abe, E.; Tsai, A. P.: A novel decagonal quasicrystal in Zn–Mg–Dy system. *Jpn. J. Appl. Phys.* **36** (1997) L1038–L1039.
- Sato, T. J.; Abe, E.; Tsai, A. P.: Composition and stability of decagonal quasicrystals in the Zn–Mg–rare-earth systems. *Phil. Mag. Lett.* **77** (1998) 213–219.
- Scheffer, M.; Gödecke, T.; Lück, R.; Ritsch, S.; Beeli, C.: Phase equilibria of the decagonal AlCoNi phase. *Z. Metallkd.* **89** (1998) 270–278.
- Scholpp, T.: Dekagonale Quasikristalle und Approximanten in den Systemen Al–Ni–Co, Al–Cu–Co und Al–Ni–Ru. ETH Zurich Thesis No. 14292 (2002).
- Schroers, J.; Holland-Moritz, D.; Herlach, D.M.; Grushko, B.; Urban, K.: Undercooling and solidification behaviour of a metastable decagonal quasicrystalline phase and crystalline phases in Al–Co. *Mater. Sci. Eng.* **A226** (1997) 990–994.
- Sharma, H. R.; Theis, W.; Gille, P.; Rieder, K. H.: Faceting of the two-fold decagonal $\text{Al}_{71.8}\text{Ni}_{14.8}\text{Co}_{13.4}(00110)$ surface studied by He diffraction. *Surface Science* **511** (2002) 387–391.
- Shechtman, D.; Blech, I. A.; Gratias, D.; Cahn, J.: Metallic phase with long-range orientational order and no translational symmetry. *Phys. Rev. Lett.* **52** (1984) 1951–1953.
- Shi, N. C.; Li, X. Z.; Ma, Z. S.; Kuo, K. H.: Crystalline Phases Related to a Decagonal Quasi-Crystal .1. A Single-Crystal X-Ray-Diffraction Study of the Orthorhombic Al_3Mn Phase. *Acta Crystallogr.* **B50** (1994) 22–30.
- Shimoda, M.; Guo, J. Q.; Sato, T. J.; Tsai, A. P.: Surface structure and structural transition of decagonal Al–Ni–Co quasicrystal. *Surface Science* **454** (2000) 11–15.
- Shoemaker, C. B.: On the Relationship between $\mu\text{-MnAl}_{4.12}$ and the Decagonal Mn–Al Phase. *Philos. Mag.* **B67** (1993) 869–881.
- Shoemaker, C. B.; Keszler, D. A.; Shoemaker, D. P.: Structure of $\mu\text{-MnAl}_4$ with composition close to that of quasicrystal phases. *Acta Crystallogr.* **B45** (1989) 13–20.
- Smith, D. J.: The realization of atomic resolution with the electron microscope. *Rep. Prog. Phys.* **60** (1997) 1513–1580.
- Socolar, J. E. S.: Simple Octagonal and Dodecagonal Quasicrystals. *Phys. Rev.* **B39** (1989) 10519–10551.
- Soltmann, C.; Beeli, C.: Structure analysis of two-dimensional quasicrystals. *Philos. Mag. Lett.* **81** (2001) 877–884.
- Soltmann, C.; Beeli, C.; Lück, R.; Gander, W.: In situ high-temperature powder diffraction study of reversible phase transitions in decagonal $\text{Al}_{71.2}\text{Co}_{12.8}\text{Ni}_{16}$. *J. Appl. Crystallogr.* **36** (2003) 1030–1039.
- Song, S. G.; Ryba, E. R.: Structure of the Al–Co–Cu Decagonal Phase and Its Crystalline Approximants. *Philos. Mag.* **B69** (1994) 707–724.
- Song, S. H.; Wang, L. C.; Ryba, E. R.: Twinning in the Structure of the Decagonal Phase $\text{Al}_{65}\text{Cu}_{20}\text{Co}_{15}$. *Philos. Mag. Lett.* **63** (1991) 335–344.
- Song, S. H.; Wang, L.; Ryba, E. R.: Observation of Lattice Fringes in an Approximant to the Al–Co–Cu Decagonal Phase. *J. Mater. Sci. Lett.* **12** (1993) 80–83.
- Stadnik, Z. M. (Ed.): *Physical Properties of Quasicrystals*, Springer Series in Solid-State Sciences, Springer-Verlag Berlin 1999.
- Steinhardt, P. J.; Jeong, H. C.: A simpler approach to Penrose tiling with implications for quasicrystal formation. *Nature* **382** (1996) 431–433.
- Steinhardt, P. J.; Jeong, H. C.; Saitoh, K.; Tanaka, M.; Abe, E.; Tsai, A. P.: Experimental verification of the quasi-unit-cell model of quasicrystal structure. *Nature* **396** (1998) 55–57.
- Steinhardt, P. J.; Jeong, H. C.; Saitoh, K.; Tanaka, M.; Abe, E.; Tsai, A. P.: Experimental verification of the quasi-unit-cell model of quasicrystal structure (vol. 396, p. 55, 1998). *Nature* **399** (1999) 84–84.
- Steinhardt, P. J.; Jeong, H. C.; Saitoh, K.; Tanaka, M.; Abe, E.; Tsai, A. P.: Alloys – Atomic structure of the quasicrystal $\text{Al}_{72}\text{Ni}_{20}\text{Co}_8$ – Reply. *Nature* **403** (2000) 267–267.
- Steurer, W.: Five-Dimensional Patterson-Analysis of the Decagonal Phase of the System Al–Mn. *Acta Crystallogr.* **B45** (1989) 534–542.
- Steurer, W.: The structure of quasicrystals. *Z. Kristallogr.* **190** (1990) 179–234.
- Steurer, W.: Five-dimensional Structure Refinement of decagonal $\text{Al}_{78}\text{Mn}_{22}$. *J. Phys.: Condens. Matter* **3** (1991) 3397–410.
- Steurer, W.: Experimental aspects of the structure analysis of aperiodic materials. In: *Beyond Quasicrystals* (Eds: F. Axel & D. Gratias) pp. 203–28 (1995) Les Editions de Physique – Springer.
- Steurer, W.: Phase Transitions of Decagonal Quasicrystals. *MRS Proceedings* **553** (1999) 159–70.
- Steurer, W.: The quasicrystal-to-crystal transformation. I. Geometrical principles. *Z. Kristallogr.* **215** (2000) 323–334.
- Steurer, W.: Approximants – the key to the structure of quasicrystals. *MRS Proceedings* **643** (2001) K3.2.1–12.
- Steurer, W.; Cervellino, A.: Quasiperiodicity in decagonal phases forced by inclined netplanes? *Acta Crystallogr.* **A57** (2001) 333–340.
- Steurer, W.; Cervellino, A.; Lemster, K.; Ortelli, S.; Estermann, M. A.: Ordering principles in decagonal Al–Co–Ni Quasicrystals. *Chimia* **55** (2001) 528–33.
- Steurer, W.; Frey, F.: Disorder diffuse scattering from quasicrystals. *Phase transitions* **67** (1998) 319–361.
- Steurer, W.; Haibach, T.: Crystallography of Quasicrystals. In: *Physical properties of Quasicrystals* (ed. Z. Stadnik), Springer, Heidelberg-New York (1999a) 51–90.

- Steurer, W.; Haibach, T.: The periodic average structure of particular quasicrystals. *Acta Crystallogr.* **A55** (1999b) 48–57.
- Steurer, W.; Haibach, T.: Reciprocal space images of aperiodic crystals. In: *International Tables for Crystallography*. Vol. **B**, Ed. U. Shmueli, Kluwer Academic Publishers: Dordrecht. (2001) 486–518.
- Steurer, W.; Haibach, T.; Zhang, B.; Beeli, C.; Nissen, H. U.: The structure of decagonal $\text{Al}_{70.5}\text{Mn}_{16.5}\text{Pd}_{13}$. *J. Phys.: Condens. Matter* **6** (1994) 613–632.
- Steurer, W.; Haibach, T.; Zhang, B.; Kek, S.; Lück, R.: The Structure of Decagonal $\text{Al}_{70}\text{Ni}_{15}\text{Co}_{15}$. *Acta Crystallogr.* **B49** (1993) 661–675.
- Steurer, W.; Kuo, K. H.: Five-dimensional structure refinement of decagonal $\text{Al}_{65}\text{Cu}_{20}\text{Co}_{15}$. *Philos. Mag. Lett.* **62** (1990a) 175–182.
- Steurer, W.; Kuo, K. H.: 5-Dimensional Structure Analysis of Decagonal $\text{Al}_{65}\text{Cu}_{20}\text{Co}_{15}$. *Acta Crystallogr.* **B46** (1990b) 703–712.
- Steurer, W.; Mayer, J.: Single Crystal X-ray Study of the Decagonal Phase of the System Al–Mn. *Acta Crystallogr.* **B45** (1989) 355–359.
- Suck, J. B.; Schreiber, M.; Häussler, P. (eds.), *Quasicrystals. An Introduction to Structure, Physical properties, and Applications*, Springer Series in Materials Science, Springer-Verlag Berlin 2002.
- Sugiyama, K.; Nishimura, S.; Hiraga, K.: Structure of a W-(AlCoNi) crystalline phase related to Al–Co–Ni decagonal quasicrystals, studied by single crystal X-ray diffraction. *J. Alloys Comp.* **342** (2002) 65–71.
- Sun, W.; Hiraga, K.: The Decagonal Quasi-Crystal Formed from an Al–Pd–Mn Icosahedral Quasi-Crystal. *J. Mater. Res.* **10** (1995) 1146–1153.
- Sun, W.; Hiraga, K.: High-resolution electron microscopy study of the early stage of formation of a Al–Pd–Mn decagonal quasi-crystal from its crystalline approximant. *Philos. Mag. Lett.* **73** (1996a) 395–404.
- Sun, W.; Hiraga, K.: High-resolution transmission electron microscopy of the Al–Pd–Mn decagonal quasicrystal with 1.6 nm periodicity and its crystalline approximants. *Philos. Mag.* **A73** (1996b) 951–971.
- Sun, W.; Hiraga, K.: Al–Pd–Mn decagonal quasicrystals formed with different tiling structures. *Philos. Mag.* **A76** (1997) 509–526.
- Sun, W.; Hiraga, K.: Formation and structures of decagonal quasicrystals in the Al–Ni–Ru system. *Mater. Sci. Eng.* **A294** (2000a) 147–151.
- Sun, W.; Hiraga, K.: A new highly ordered Al–Ni–Ru decagonal quasicrystal with 1.6 nm periodicity. *Philos. Mag. Lett.* **80** (2000b) 157–164.
- Sun, W.; Hiraga, K.: Structural study of a superlattice Al–Ni–Ru decagonal quasicrystal using high-resolution electron microscopy and a high-angle annular dark-field technique. *Philos. Mag. Lett.* **81** (2001) 187–195.
- Sun, W.; Hiraga, K.: A new icosahedral quasicrystal coexisting with decagonal quasicrystals in the Al–Ni–Ru system. *J. Alloys Comp.* **347** (2002a) 110–114.
- Sun, W.; Hiraga, K.: Long-range tiling structures in a highly ordered Al–Ni–Ru decagonal quasicrystal with 1.6 nm periodicity and its closely related approximant. *Physica B* **324** (2002b) 352–359.
- Sun, W.; Ohsuna, T.; Hiraga, K.: Quasiperiodic superstructure with an ordered arrangement of atom columnar clusters in an Al–Ni–Ru decagonal quasicrystal with 0.4 nm periodicity. *J. Phys. Soc. Jpn.* **69** (2000) 2383–2386.
- Sun, W.; Ohsuna, T.; Hiraga, K.: Structural characteristics of a high-quality Al–Ni–Ru decagonal quasicrystal with 1.6 nm periodicity, studied by atomic-scale electron microscopy observations. *Philos. Mag. Lett.* **81** (2001) 425–431.
- Suryanarayana, C.; Menon, J.: An Electron-Microscopic Study of the Decagonal Phase in a Melt-Spun Al-26 Wt-Percent Co Alloy. *Scr. Metallurg.* **21** (1987) 459–460.
- Takakura, H.; Yamamoto, A.; Tsai, A. P.: The structure of a decagonal $\text{Al}_{72}\text{Ni}_{20}\text{Co}_8$ quasicrystal. *Acta Crystallogr.* **A57** (2001) 576–585.
- Takeuchi, S.; Kimura, K.: Structure of Al_4Mn Decagonal Phase as a Penrose-Type Lattice. *J. Phys. Soc. Jpn.* **56** (1987) 982–988.
- Tamura, N.: The concept of crystalline approximants for decagonal and icosahedral quasicrystals. *Philos. Mag.* **A76** (1997) 337–356.
- Tanaka, M.: Convergent-Beam Electron-Diffraction. *Acta Crystallogr.* **A50** (1994) 261–286.
- Tanaka, M.; Tsuda, K.; Terauchi, M.; Fujiwara, A.; Tsai, A. P.; Inoue, A.; Masumoto, T.: Electron-Diffraction and Electron-Microscope Study on Decagonal Quasi-Crystals on Al–Ni–Fe Alloys. *J. Non-Cryst. Solids* **153** (1993) 98–102.
- Trebin, H. R. (ed.), *Quasicrystals. Structure and Physical properties*, Wiley-VCH, Weinheim 2003.
- Tsai, A. P.: “Back to the future” – an account discovery of stable quasicrystals. *Acc. Chem. Res.* **36** (2003) 31–38.
- Tsai, A. P.; Fujiwara, A.; Inoue, A.; Masumoto, T.: Structural variation and phase transformations of decagonal quasicrystals in the Al–Ni–Co system. *Philos. Mag. Lett.* **74** (1996) 233–240.
- Tsai, A. P.; Guo, J. Q.; Abe, E.; Takakura, H.; Sato, T. J.: A stable binary quasicrystal. *Nature* **408** (2000) 537–538.
- Tsai, A. P.; Inoue, A.; Masumoto, T.: New Decagonal Al–Ni–Fe and Al–Ni–Co Alloys Prepared by Liquid Quenching. *Mater. Trans. JIM* **30** (1989a) 150–154.
- Tsai, A. P.; Inoue, A.; Masumoto, T.: A Stable Decagonal Quasicrystal in the Al–Cu–Co System. *Mater. Trans. JIM* **30** (1989b) 300–304.
- Tsai, A. P.; Inoue, A.; Masumoto, T.: Stable decagonal Al–Co–Ni and Al–Co–Cu quasicrystals. *Mater. Trans. JIM.* **30** (1989c) 463–473.
- Tsai, A. P.; Inoue, A.; Masumoto, T.: Icosahedral, Decagonal and Amorphous Phases in Al–Cu–M (M = Transition Metal) Systems. *Mater. Trans. JIM* **30** (1989d) 666–676.
- Tsai, A. P.; Inoue, A.; Masumoto, T.: Stable Decagonal Quasicrystals With a Periodicity of 1.6 nm in Al–Pd–(Fe, Ru or Os) Alloys. *Philos. Mag. Lett.* **64** (1991) 163–167.
- Tsai, A. P.; Inoue, A.; Masumoto, T.: Quasicrystalline and Related Crystalline Phases in Al–Pd–Fe System. *Mater. Trans. JIM* **34** (1993) 155–161.
- Tsai, A. P.; Inoue, A.; Masumoto, T.: Chemical Effects on Periodicity and Structure of Decagonal Phases in Al–Ni–Based and Al–Co–Based Alloys. *Philos. Mag. Lett.* **71** (1995) 161–167.
- Tsai, A. P.; Inoue, A.; Yokoyama, Y.; Masumoto, T.: Stable icosahedral Al–Pd–Mn and Al–Pd–Re alloys. *Mater. Trans. JIM.* **31** (1990) 98–103.
- Tsai, A. P.; Matsumoto, T.; Yamamoto, A.: Stable One-Dimensional Quasicrystals in Al–Pd–Fe Alloys. *Philos. Mag. Lett.* **66** (1992) 203–208.
- Tsai, A. P.; Yokoyama, Y.; Inoue, A.; Masumoto, T.: Quasicrystals in Al–Pd–TM (TM = Transition Metal) Systems Prepared by Rapid Solidification. *Jpn. J. Appl. Phys.* **29** (1990) 1161–1164.
- Tsai, A. P.; Yokoyama, Y.; Inoue, A.; Masumoto, T.: Formation, Microstructure, Chemical Long-Range Order, and Stability of Quasicrystals in Al–Pd–Mn Alloys. *J. Mater. Res.* **6** (1991) 2646–2652.
- Tsuda, K.; Nishida, Y.; Tanaka, M.; Tsai, A. P.; Inoue, A.; Masumoto, T.: Convergent-beam electron diffraction and electron microscopy study of decagonal quasicrystals of Al–Ni–Rh and Al–Ni–Ir. *Philos. Mag. Lett.* **73** (1996) 271–278.
- Tsuda, K.; Nishida, Y.; Saitoh, K.; Tanaka, M.; Tsai, A. P.; Inoue, A.; Masumoto, T.: Structure of Al–Ni–Co decagonal quasicrystals. *Philos. Mag.* **A74** (1996) 697–708.
- Tsuda, K.; Saito, M.; Terauchi, M.; Tanaka, M.; Tsai, A. P.; Inoue, A.; Masumoto, T.: Electron-Microscope Study of Decagonal Quasi-Crystals of $\text{Al}_{70}\text{Ni}_{15}\text{Fe}_{15}$. *Jpn. J. Appl. Phys.* **32** (1993) 129–134.
- Tsuda, K.; Tanaka, M.: Refinement of Crystal-Structure Parameters Using Convergent-Beam Electron-Diffraction – the Low-Temperature Phase of SrTiO_3 . *Acta Crystallogr.* **A51** (1995) 7–19.
- Uchida, M.; Horiuchi, S.: $\text{Ta}_{62}\text{Te}_{38}$ twelvefold quasicrystal synthesized by non-equilibrium solid state reactions. *Jpn. J. Appl. Phys.* **36** (1997) L1523–L1524.
- Uchida, M.; Horiuchi, S.: Modulated-crystal model for the twelvefold quasicrystal $\text{Ta}_{62}\text{Te}_{38}$. *J. Appl. Crystallogr.* **31** (1998a) 634–637.
- Uchida, M.; Horiuchi, S.: New approximant of twelvefold quasicrystal in Ta–Te: Electron diffraction study. *Jpn. J. Appl. Phys.* **37** (1998b) L531–L532.
- Uchida, M.; Horiuchi, S.: Twelve-fold quasicrystal and its approximant of $\text{Ta}_{62}\text{Te}_{38}$ interpreted as modulated crystals. *Micron* **31** (2000) 493–497.

- Wales, D. J.; Munro, L. J.; Doye, J. P. K.: What can calculations employing empirical potentials teach us about bare transition-metal clusters. *J. Chem. Soc.; Dalton Trans.* (1996) 611–623.
- Wang, N.; Chen, H.; Kuo, K. H.: Two-Dimensional Quasicrystal With Eightfold Rotational Symmetry. *Phys. Rev. Lett.* **59** (1987) 1010–1013.
- Wang, N.; Fung, K. K.; Kuo, K. H.: Symmetry Study of the Mn–Si–Al Octagonal Quasicrystal by Convergent Beam Electron-Diffraction. *Appl. Phys. Lett.* **52** (1988) 2120–2121.
- Wang, Z. M.; Gao, Y. Q.; Kuo, K. H.: Quasi-Crystals of Rapidly Solidified Alloys of Al–Pt Group Metals – II. Quasi-Crystals in Rapidly Solidified Al–Ru and Al–Os Alloys. *J. Less-Common Met.* **163** (1990) 19–26.
- Wang, Z. M.; Kuo, K. H.: The Octagonal Quasilattice and Electron-Diffraction Patterns of the Octagonal Phase. *Acta Crystallogr. A* **44** (1988) 857–863.
- Wang, N.; Kuo, K. H.: Transformation of the Octagonal Quasicrystal Into the β -Mn-Type Crystalline Structure. *Phil. Mag. Lett.* **61** (1990) 63–68.
- Weber, S.: Steffen Webers Home Page (1999) <http://jcrystal.com/steffenweber/>
- Weber, S.: Application of the five-dimensional MEM method to the structure refinement of decagonal Al–Mn–Pd quasicrystal. University of Tsukuba, Thesis Roll No.-945587 (1997).
- Weber, S.; Yamamoto, A.: Application of the five-dimensional maximum-entropy method to the structure refinement of decagonal Al₇₀Mn₁₇Pd₁₃. *Philos. Mag.* **A76** (1997) 85–106.
- Weber, S.; Yamamoto, A.: Noncentrosymmetric structure of a decagonal Al₇₀Mn₁₇Pd₁₃ quasicrystal. *Acta Crystallogr. A* **54** (1998) 997–1005.
- Weidner, E.; Hradil, K.; Frey, F.; de Boissieu, M.; Letoublon, A.; Morgenroth, W.; Krane, H.-G.; Capitan, M.; Tsai, A.-P.: High-resolution X-ray and Neutron Diffraction of Super- and Disorder in Al–Co–Ni. *Mat. Sci. Eng.* **294–296** (2000) 308–314.
- Weidner, E.; Lei, J. L.; Frey, F.; Wang, R.; Grushko, B.: Diffuse scattering in decagonal Al–Ni–Fe. *J. Alloys Comp.* **342** (2002) 156–158.
- Widom, M.; AlLehyani, I.; Moriarty, J.A.: First-principles interatomic potentials for transition-metal aluminides. III. Extension to ternary phase diagrams. *Phys. Rev. B* **62** (2000) 3648–3657.
- Widom, M.; Cockayne, E.: Atomic correlations in AlCo decagonal approximant phases. *Physica* **A232** (1996) 713–722.
- Widom, M.; Moriarty, J. A.: First-principles interatomic potentials for transition-metal aluminides. II. Application to Al–Co and Al–Ni phase diagrams. *Phys. Rev. B* **58** (1998) 8967–8979.
- Widom, M.; Phillips, R.; Zou, J.; Carlsson, A. E.: Structural Model of Orthorhombic Al₃Co. *Philos. Mag.* **B71** (1995) 397–406.
- Wu, J. S.; Kuo, K. H.: Decagonal quasicrystal and related crystalline phases in Mn–Ga alloys with 52 to 63 at. % Ga. *Metall. Mater. Trans. A* **28** (1997) 729–742.
- Wu, J. S.; Ma, X. L.; Kuo, K. H.: Decagonal quasicrystals (periodicity of 1.24 nm and 3.72 nm) and their orthorhombic approximants in Al₆₇Cr₁₅Cu₁₈. *Philos. Mag. Lett.* **73** (1996) 1663–171.
- Xu, L.; Wang, N.; Lee, S. T.; Fung, K. K.: Electron diffraction study of octagonal-cubic phase transitions in Mn–Si–Al. *Phys. Rev. B* **62** (2000) 3078–3082.
- Yokoyama, Y.; Yamada, Y.; Fukaura, K.; Sunada, H.; Inoue, A.; Note, R.: Stable decagonal quasicrystal in an Al–Mn–Fe–Ge system. *Jap. J. Appl. Phys. Part 1* **36** (1997) 6470–6474.
- Yamamoto, A.: Structure of decagonal Al₆₅Cu₂₀Co₁₅ quasicrystals. *Sci. Rep. RITU* **A42** (1996a) 207–212.
- Yamamoto, A.: Crystallography of quasicrystals. *Acta Crystallogr. A* **52** (1996b) 509–560.
- Yamamoto, A.; Ishihara, K. N.: Penrose Patterns and Related Structures. 2. Decagonal Quasicrystals. *Acta Crystallogr. A* **44** (1988) 707–714.
- Yamamoto, A.; Kato, K.; Shibuya, T.; Takeuchi, S.: Atomic Structure of a Decagonal Al–Co–Ni Quasicrystal. *Phys. Rev. Lett.* **65** (1990) 1603–1606.
- Yamamoto, A.; Matsuo, Y.; Yamanoi, T.; Tsai, A. P.; Hiraga, K.; Masumoto, T.: Structure refinement of quasicrystals. In: *Proc. of APERIODIC94* (Eds. G. Chapuis and W. Paciorek), pp. 393–398, World Scientific, Singapore, 1995.
- Yamamoto, A.; Weber, S.: Five-dimensional superstructure model of decagonal Al–Ni–Co quasicrystals. *Phys. Rev. Lett.* **78** (1997a) 4430–4433.
- Yamamoto, A.; Weber, S.: Superstructure and color symmetry in quasicrystals. *Phys. Rev. Lett.* **79** (1997b) 861–864.
- Yan, Y. F.; Pennycook, S. J.: Alloys – Atomic structure of the quasicrystal Al₇₂Ni₂₀Co₈. *Nature* **403** (2000a) 266–267.
- Yan, Y. F.; Pennycook, S. J.: Structural model for the Al₇₂Ni₂₀Co₈ decagonal quasicrystals. *Phys. Rev. B* **61** (2000b) 14291–14294.
- Yan, Y. F.; Pennycook, S. J.: Chemical ordering in Al₇₂Ni₂₀Co₈ decagonal quasicrystals. *Phys. Rev. Lett.* **86** (2001) 1542–1545.
- Yan, Y.; Pennycook, S. J.; Tsai, A. P.: Direct imaging of local chemical disorder and columnar vacancies in ideal decagonal Al–Ni–Co quasicrystals. *Phys. Rev. Lett.* **81** (1998) 5145–5148.
- Yang, Q. B.; Wei, W. D.: Description of the Dodecagonal Quasicrystal by a Projection Method. *Phys. Rev. Lett.* **58** (1987) 1020–1023.
- Yokoyama, Y.; Yamada, Y.; Fukaura, K.; Sunada, H.; Inoue, A.; Note, R.: Stable decagonal quasicrystal in an Al–Mn–Fe–Ge system. *Jpn. J. Appl. Phys. Part 1*, **36** (1997) 6470–6474.
- Yoshida, K.; Yamada, T.: Non-equilibrium alloy phases in Bi–Mn thin films prepared by vacuum depositions, a metastable Mn₃Bi and other long period crystal lattices. In: *Proc. of JIMIS-5: Non-Equilibrium Solid Phases of Metals and Alloys. Suppl. Trans. JIM* **29** (1988) 135–138.
- Yubuta, K.; Sun, W.; Hiraga, K.: A new crystalline phase related to decagonal quasicrystals with non-central symmetry in Al–Co–Pd alloys. *Phil. Mag.* **A75** (1997) 273–284.
- Yurechko, M.; Fattah, A.; Velikanova, T.; Grushko, B.: A contribution to the Al–Pd phase diagram. *J. Alloys Comp.* **329** (2001) 173–181.
- Yurechko, M.; Grushko, B.: A study of the Al–Pd–Co alloy system. *Mater. Sci. Eng. A* **294** (2000) 139–142.
- Yurechko, M.; Grushko, B.; Velikanova, T.; Urban, K.: Isothermal sections of the Al–Pd–Co alloy system for 50–100 at% Al. *J. Alloys Comp.* **337** (2002) 172–181.
- Yurechko, M.; Grushko, B.; Velikanova, T.; Urban, K.: Orthorhombic “Al₃Pd” and its ternary extensions in Al–Pd–Mn (Fe,Co). *J. Noncryst. Sol.* (2003) preprint.
- Zhang, B.: Characterization of decagonal Al–Co–Ni and its crystalline approximants. Thesis ETH No. 11439 (1995).
- Zhang, B.; Estermann, M. A.; Steurer, W.: Compositional dependence of the ordering phenomena in decaprisymmetric Al–Co–Ni single crystals. *Z. Kristallogr. Suppl.* **10** (1995) 120.
- Zhang, B.; Estermann, M.; Steurer, W.: The growth of decagonal Al–Co–Ni single crystals as a function of composition. *J. Mater. Res.* **12** (1997) 714–723.
- Zhang, B.; Gramlich, V.; Steurer, W.: Al_{13–x}(Co_{1–y}Ni_y)₄, a new approximant of the decagonal quasicrystal in the Al–Co–Ni system. *Z. Kristallogr.* **210** (1995) 498–503.
- Zhang, H.; Kuo, K. H.: Giant Al–M (M = Transitional Metal) Crystals as Penrose-Tiling Approximants of the Decagonal Quasicrystal. *Phys. Rev. B* **42** (1990) 8907–8914.
- Zhang, B.; Li, X. Z.; Steurer, W.; Schneider, J.; Frey, F.: New crystalline approximant of the decagonal quasicrystal in Al–Pd–Ru alloy. *Philos. Mag. Lett.* **72** (1995) 239–244.
- Zhang, H.; Urban, K.: Radiation-Induced Transformation from the Decagonal Quasi-Crystalline Phase to a CsCl-Type Phase in Al–Cu–Co(–Si). *Philos. Mag. Lett.* **66** (1992) 209–215.
- Zhang, H.; Wang, D. H.; Kuo, K. H.: Icosahedral and Decagonal Quasicrystals, Crystalline Phases, and Multiple Twins in Rapidly Solidified Al₁₃Cr₄Si₄. *J. Mater. Sci.* **24** (1989) 2981–2986.
- Zhou, L.; Che, R.; Zhang, D.: High-pressure X-ray diffraction of Al–Ni–Co quasicrystal using synchrotron radiation. *Proceedings of ICQ5*, Avignon, 22–26. May 1995, ed. C. Janot, R. Mosseri, World Scientific, Singapore 1996.
- Zou, X. D.; Fung, K. K.; Kuo, K. H.: Orientation relationship of decagonal quasicrystal and tenfold twins in rapidly cooled Al–Fe alloy. *Phys. Rev. B* **35** (1987) 4526–4528.
- Zurkirch, M.; Bolliger, B.; Erbudak, M.; Kortan, A. R.: Structural transformations at the surface of the decagonal quasicrystal Al₇₀Co₁₅Ni₁₅. *Phys. Rev. B* **58** (1998) 14113–14116.